ISBN - 0 - 7743 - 8797 -1

STANDARDS DEVELOPMENT BRANCH OMOE
3 6936 00000 2419

PROCEEDINGS

TECHNOLOGY TRANSFER CONFERENCE No.5

November 27 & 28 , 1984

Part 2

Air Pollution Research

Organized By

The RESEARCH ADVISORY COMMITTEE

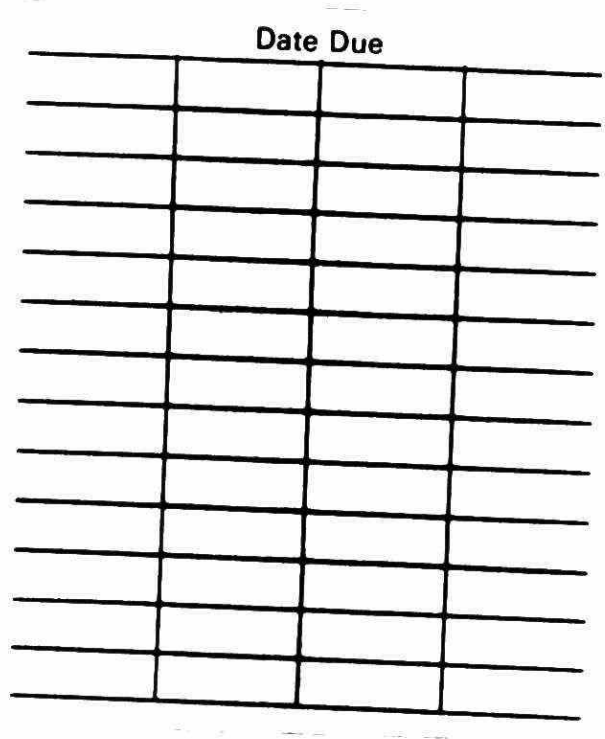
Sponsored By

POLICY & PLANNING BRANCH

MINISTRY OF THE ENVIRONMENT

TD
172.5
.057
1984
part 2
MOE

HAZARDOUS CONTAMINANTS
AND STANDARDS BRANCH
135 ST. CLAIR AVENUE WEST
TORONTO, ONTARIO M4V 1P5



TD
172.5
.057
1984
part 2

Proceedings : technology
transfer conference no. 5

76017

TD
172.5
052
1981
5/2

ISBN-0-7743-8797-1

PROCEEDINGS

TECHNOLOGY TRANSFER CONFERENCE NO. 5

November 27 and 28, 1984

Collated By: The Research Coordination Office

Organized By: The Research Advisory Committee

Sponsored By: The Policy and Planning Branch

POLICY AND PLANNING BRANCH

Ministry of the Environment

©1984 Her Majesty the Queen
in Right of Ontario as represented by
the Minister of the Environment

Copyright Provisions and Restrictions on Copying:

This Ontario Ministry of the Environment work is protected by Crown copyright (unless otherwise indicated), which is held by the Queen's Printer for Ontario. It may be reproduced for non-commercial purposes if credit is given and Crown copyright is acknowledged.

It may not be reproduced, in all or in part, part, for any commercial purpose except under a licence from the Queen's Printer for Ontario.

For information on reproducing Government of Ontario works, please contact Service Ontario Publications at copyright@ontario.ca

PREFACE

The proceedings provide the reader with a collection of the papers presented at Technology Transfer Conference No. 5 organized by the Ontario Ministry of the Environment.

Part 1 of the proceedings deals with general environmental research such as methodologies, cause-effect, fate, epidemiological studies relating to water, and liquid and solid waste research.

Part 2 presents papers relating to air pollution.

It is hoped that the proceedings would assist in technology transfer and in the utilization of research results obtained on Ministry-funded environmental research projects.

MINISTRY OF THE ENVIRONMENT

TECHNOLOGY TRANSFER CONFERENCE NO. 5

November 27 and 28, 1984

Sponsored By:	Policy and Planning Branch A. Castel, Director
Organized By:	Research Advisory Committee P. D. Foley, Chairman
Program Coordinator:	M. Moselhy
Program Committee:	J. Bishop D. Balsillie M. Moselhy
Organization:	D. Bartkiw D. Corr M. Moselhy J. Ralston G. Schmidt
Administration:	B. Malcolm

Mailing Address:

POLICY AND PLANNING BRANCH
Research Coordination Office
135 St. Clair Avenue West
Toronto, Ontario
M4V 1P5

Telephone: (416) 965-5788

ACKNOWLEDGEMENTS

The Ministry of the Environment's Research Advisory Committee would like to acknowledge the cooperation and efforts of the authors and Ministry staff who have contributed to the organization of its fifth Technology Transfer Conference.

The Committee would also like to thank the Policy and Planning Branch for sponsoring this year's conference.

The financial support of the Provincial Lottery to environmental and health-related research has been instrumental in the success of the Ministry Research Program and its technology transfer and is appreciated.

DISCLAIMER

The views and ideas expressed in this publication are those of the authors and do not necessarily reflect the views and policies of the Ontario Ministry of the Environment, nor does mention of trade names or commercial products constitute endorsement or recommendation for use.

COPYRIGHT

Anyone who wishes to republish any of the material in this volume or part thereof may obtain permission by writing to the Policy and Planning Branch, Ministry of the Environment.

CONTENTS

PART 1

Paper Number	Title	Page Number
-	Preface	
-	Conference Organization	
-	Acknowledgements	
-	Disclaimer	
1	Feature Paper: "Recent Trends in Drinking Water Treatment." V. L. Snoeyink, University of Illinois, U.S.A.	1
2	"Direct and Food Chain Uptake of Environmental Lead, Cadmium and Mercury in a Model Aquatic System." P. Stokes, University of Toronto, and P. Campbell, University of Quebec.	15
3	"Studies of the Nitrate Distribution and Nitrogen Transformation in a Shallow Sandy Aquifer near Alliston, Ontario." R. W. Gillham, R. C. Starr, F. F. Akindunni and S. F. O'Hannesin, University of Waterloo.	23
4	"Organic Contaminants in Groundwaters at Several Ontario Landfills." J. F. Baker, J. A. Cherry, D. A. Carey and J. P. Hewetson, University of Waterloo, and J. F. Pankow, Oregon Graduate Centre, Beaverton, Oregon, and M. Reinhard, Stanford University, California.	49
5	"Epidemiological Study of Disease Incidence and Recreational Water Quality at Selected Beaches in Southern Ontario." Nancy E. Brown and Patricia Seyfried, University of Toronto.	69
6	"Volatilization Rates of Organic Chemicals of Public Health Concern." T. P. Halappa Gowda and J. D. Lock, Gore & Storrie Ltd.	125
7	"Experimental and Environmental Modelling Studies of Hazardous Chemicals." D. Mackay, S. Paterson, B. Cheung and W. Y. Shiu, University of Toronto.	165

Paper Number	Title	Page Number
8	"Chemical Identification and Biological Assay of Environmental Mutagens, Promoters and Inhibitors." M. Katz, K. R. Sharma and A. S. Raj, York University.	191
9	"Collaborative Study on Short-Term Tests for Genotoxicity and Carcinogenicity: II. Carcinogen Assessment." D. M. Logan, York University and M. Salamone, MOE.	249
10	"The Development of a Freshwater Fish Test to Identify Aquatic Toxic Contaminants." I. R. Smith and V. E. Valli, University of Guelph.	271
11	"Field Measurement of Infiltration through Landfill Covers, Phase I." A. G. Hims and P. K. Lee, Gartner Lee Ltd. and R. W. Gillham, University of Waterloo.	303
12	"Development of Specific Protein Adsorbents for Selective Extraction of Trace Contaminants Significant to Human Health: Modelling of Fetal Cross-Placental Uptake Specificity." Carleton J. C. Hsia, University of Toronto.	329
13	"Effect on the Tissue of Young Fish and Rats of Exposure to Lead, Cadmium and Mercury." D. M. Nicholls, K. Kuliszeweska and M. J. Kuliszeweska, York University.	349
14	"Removal of Hazardous Contaminants in the Hamilton Water Pollution Control Plant." G. Zukovs, R. J. Rush and M. Gamble, Canviro Consultants Ltd.	385
15	"Assessing the Impact of Hazardous Immiscible Liquids in Soil." G. J. Farquhar and E. A. McBean, University of Waterloo.	421
16	"Effects of Metals from Mine Tailings on the Microflora of a Marsh Treatment System." R. M. Desjardins and P. L. Seyfried, University of Toronto.	449

Paper Number	Title	Page Number
17	"Revised Monitoring Scheme for Persistent and Toxic Organics in Great Lakes Sports Fish." J. A. Coburn and H. Huneault, Zenon Environmental Inc. and G. A. V. Rees and G. Crawford, MOE.	485
18	"Heavy Metal Mobilization and Biological Uptake: Cobalt Mine Tailings." E. Hanna, J. E. Hanna Associates Inc.	537
19	"Water Quality Analysis of Trout Farm Effluents." J. W. Hilton, G. Chapman and S. J. Slinger, University of Guelph.	561
20	"Design of Groundwater Monitoring Programs for Waste Landfill Sites." R. B. Schwartz and P. H. Byer, University of Toronto.	603

PART 2

Paper Number	Title	Page Number
	- Preface	
	- Conference organization	
	- Acknowledgements	
	- Disclaimer	
21	Feature Paper: "The Utility of Microsomal Monooxygenase Activity Assays in Health Risk Assessment of Exposure to Airborne Emissions of Chlorinated Dibenzodioxins and Dibenzofurans." David H. Cleverly, US-EPA, Research Triangle Park, North Carolina, U.S.A.	637
22	"Evaluation of Contaminated Water and Soil Sites as Sources of Airborne Hazardous Materials." D. Mackay, A. Hughes, J. Phyper and B. Cheung, University of Toronto.	643
23	"The Chemoreceptive Membrane as an Electrochemical Sensor for Trace Organic Species in the Atmosphere." M. Thompson, U. J. Krull, A. Arya, E. King and H. E. Wong, University of Toronto.	653
24	"Gas-phase Photochemistry of PCB's." N. J. Bunce, J. P. Landers and J. Langshaw, University of Guelph.	667
25	"The Hamilton Study: Refinement of SO_2 and Particulate Data for Exposure Estimation." L. D. Pengelly, C. H. Goldsmith, A. T. Kerigan, S. A. Toplack and H. McCage, McMaster University.	683
26	"The Dispersal of Airborne Particulates on a Short and Long-Term Scale." G. R. Palmer, J. D. MacArthur and P. P. Wilson, Queen's University.	691
27	"Monitoring Genotoxicity in the Atmosphere using Sister Chromatid Exchange in Mice." M. L. Petras and R. Piscitelli, University of Windsor.	717

Paper Number	Title	Page Number
28	"Quantification of Asbestos Air Pollution in Ontario." D. Verma, N. Clark and J. Julian, McMaster University.	741
29	"Sweet Corn, Cabbage, Cauliflower and Rutabaga Responses to Air Pollution in Southern Ontario." D. P. Ormrod, University of Guelph.	757
30	"The Impact of Ozone on Potato and Peanut in Ontario." G. Hofstra and J. Ensing, University of Guelph.	771
31	"Dioxins and Furans: Analytical Methodology, Leachates and Conditions for Condensation - Desorption on Stack Particulates." F. W. Karasek, G. M. Charbonneau, L. C. Dickson and T. Thompson, University of Waterloo.	777
32	"MOE's Volatile Organic Monitoring Development Program." E. Singer, M. Sage, R. Corkum, D. Corr, A. Szakolcai, Air Resources Branch, and W. Offenbacher, G. A. Rees and J. Osborne, Laboratory Services and Applied Research Branch, and G. Grosse, Southwestern Region, MOE.	813
33	"The Inhalable Particulate Program: Studies of Aerosol Deposition in the Lung and Pollution Source Characterization." J. F. Hicks, Air Resources Branch, MOE.	835
34	"Laser Induced Emission Spectroscopy of PAHs in Low Temperature Matrices." F. Morgan, G. Parnell, S. Filseth, and C. Sadowski, York University.	871
35	"Provision of PAHs and Aza-PAHs as Environmental Analytical Standards." V. Snieckus, University of Waterloo.	893
36	"Analysis of Polycyclic Aromatic Hydrocarbons and their Derivatives in Environmental Samples." M. Quilliam, J. Marr and R. Gergely, McMaster University.	903

Paper Number	Title	Page Number
37	"A Mass Spectrometric Study of Selected Air Pollutants." R. Marsh and R. Hughes, Trent University.	925
38	"Retrospective Correlation Spectroscopy and its Application to Atmospheric Monitoring." R. W. Nicholls, CRESS, York University.	945
39	"Development of a Tunable Diode Laser-Based Hydrogen Peroxide Monitor." F. Slemr, G. Harris, D. Hastie and H. Schiff, York University.	971
40	"Chemical Speciation of Airborne Particulates." D. Burgess and M. Browne, McMaster University.	993

The Utility of Microsomal Monooxygenase Assays in Health Risk Assessment of Exposure to Airborne Emissions of Chlorinated Dibenzo-p-dioxins and Dibenzofurans

by

David H. Cleverly

U. S. Environmental Protection Agency
Office of Air Quality Planning and Standards
Research Triangle Park, N. C. 27711

Prepared for presentation to the Ontario Ministry of the Environment, Research Advisory Committee, Technical Transfer Conference No. 5, Toronto, Canada, November 28, 1984.

The Utility of Microsomal Monooxygenase Activity Assays in Health Risk Assessment of Exposure to Airborne Emissions of Chlorinated Dibenzodioxins and Dibenzofurans

David H. Cleverly
U.S. Environmental Protection Agency
Research Triangle Park, North Carolina 27711

Halogenated dibenzodioxins and dibenzofurans have been quantified in stack gas emissions from a variety of stationary combustion sources. Quantitations have been reported in ng/m^3 and µg/m^3 levels. The most comprehensive data basis usually include tri through octachlorinated homologous groups instead of individual congeners. Speciating individual compounds is made difficult because of a world-wide deficiency in analytical standards. Thus, regulators are left with evaluating the health ramifications of human exposure based on a mixture of compounds as whole groups of compounds. A dilemma arises with regard to risk assessment because not every CDD or CDF isomer within each homologue is equal in toxicity, teratogenicity, or carcinogenicity, and the 2,3,7,8-TCDD congener remains the most extensively evaluated compound. Within the past decade significant advances have been made in observing the action of aryl hydrocarbons on a macromolecular level. A mechanism of eliciting the toxic response is postulated to occur by the CCD or CDF compound binding to a cytosolic receptor protein, then translocating to the cell nucleus and producing a coordinate induction of a number of enzymes including AHH and other microsomal monooxygenase activity. Receptor assays and AHH assays using various CDD/CDF congeners have shown a good correlation with enzyme induction and the pleotypical toxic response in rats and mice. Can this macromolecular mechanism be used in risk assessment to evaluate exposure to homologous groups of compounds? The utility of the microsomal monooxygenase activity assays in risk assessment will be discussed.

Summary

Quantitations of dibenzo-p-dioxins and dibenzofurans have been reported for tri through octachlorinated homologous groups in stack emissions of municipal and industrial waste incinerators. A delimma rises with respect to risk assessment as to how to evaluate these total chlorinated dioxin and furan emissions in terms of carcinogenicity when not every compound is equipotent, and 2,3,7,8-TCDD remains the most extensively evaluated compound. Within the past decade significant advances have been made in observing the action of halogenated aryl hydrocarbons on a macromolecular level. A mechanism of evoking a toxic response is postulated to occur by a halogenated dioxin and furan compound reversably and noncovalently binding to a cytosolic receptor protein, then translocating to the cell nucleus. The parent compound, not a metabolite, activates specific mRNA(s) that induce the synthesis of a number of enzymes including AHH and other microsomal monooxygenase activity. The avidity of the ligand-receptor bond is a function of the geometric configuration of the compounds. Thus, congeners with a chlorine substitution pattern at the four lateral positions of the dibenzo-p-dioxin molecule have the greatest affinity for the receptor and the maximum inducibility of AHH activity. Additional Cl substitution at positions 1,4,5 or 9 decreases AHH activity, and removal of one or more of the laterally attached Cl atoms diminishes activity even further. Receptor binding assays and AHH induction assays have been established as useful indicators of the potency of individual dioxin and furan congeners relative to 2,3,7,8-TCDD, as well as estimating the total PCDD/PCDF biological activity of a complex mixture of the compounds. The utility of the assays

is supported by the apparent correlation of AHH induction with toxicity. Several schemes have been devised to apply toxic equivalencies based on AHH induction or receptor binding assays in evaluating exposure from classes of chlorinated dioxin and furan emission at municipal waste incinerators. The Swiss Federal Office for Environmental Protection, for example, devised a potency weighting system based on AHH induction to convert total tetrachlorinated through octachlorinated dioxins and furans into 2,3,7,8-TCDD equivalents in the emissions of a municipal waste incinerator to facilitate risk assessment of exposure to all the reported chlorinated dioxin and furan homologues. Using this method the 2,3,7,8-TCDD equivalents of the mixture of chlorinated dioxins and furans was estimated to be 60 times the actual amount of 2,3,7,8-TCDD measured in the emissions. Another investigator devised a toxic equivalency method based on AHH induction to evaluate the magnitude of chlorinated dioxin and furan emissions from a municipal incinerator in The Netherlands. In that analysis the 2,3,7,8TCDD equivalents were estimated to be 80 times the actual amount of 2,3,7,9,8-TCDD measured. Bioanalysis of flyash collected from the ESP hopper to a MWC, as measured by the dose-dependent displacement of (^{3}H)2,3,7,8-TCDD bound to the protein receptor by the active congeners in the flyash extract, showed the mixture of PCDDs and PCDFs to be at least 45 times more active than the concentration of 2,3,7,8-TCDD present by analysis. Thus, various schemes of estimating 2,3,7,8-TCDD equivalancy by these examples have shown a range of 45 to 80 times the biological potency than the amount of 2,3,7,8-TCDD actually present.

The major shortcomings of utilizing the microsomal monooxygenase activity assays in risk assessment to airborne emissions of chlorinated

dioxins and dibenzofurans are: (1) enzyme induction has not been directly linked with carcinogenicity, or any other chronic toxicologic endpoint; (2) elucidation of specific intranuclear events leading to transcription of specific mRNAs, and translation of mRNAs into enzyme induction remains unknown; (3) the affinity and concentration of cytosol receptor are similar in the liver of mice, rats, rabbit, hamster and guinea pig, but the oral LD_{50} between the guinea pig and hamster differ by 5000 fold. Why? (4) the ultimate biochemical lesion of the proposed mechanism of toxicity is unknown; (5) the concentration of the Ah receptor in various human tissues has not been fully investigated, nor has a toxic response in humans been correlated with enzyme induction.

These gaps in fully elucidating the action of the drug metabolizing enzyme system in the presence of halogenated aromatic compounds should be resolved by extensive research. It is my opinion this model serves as the likely basis for understanding macromolecular pathways of carcinogenicity, teratogenicity and other chronic effects of exposure to PCDDs, PCDFs and related environmental pollutants. Lack of complete elucidation should not, however, preclude regulatory agencies from developing risk assessment methodologies based on AHH induction or receptor binding assays as a reasonable means of estimating the hazard of exposure to a complex mixture of PCDDs/PCDFs from emissions of stationary combustion sources. The responsibility of the regulator is to manage risk to the exposed population even before all the scientific information is available. Thus toxic equivalency schemes can be used as an interim basis of assessing risk to the exposed population residing near emitters of PCDDS and PCDFS.

Evaluation of Contaminated Water and Soil Sites as Sources of Airborne Hazardous Materials

D. Mackay
A. Hughes
J. Phyper
B. Cheung

Department of Chemical Engineering and Applied Chemistry
University of Toronto

ABSTRACT

Progress is reported on a project to develop two test procedures for estimating experimentally the emission rates into the atmosphere of chemical contaminants from soils and water. The work has involved the development of test equipment and specifications for operating conditions, the selection of "benchmark" chemicals and standard soils and water media. Two brief computer programs are being written to simulate the results from the test system and translate these results to the real environment.

INTRODUCTION

In this project our aim is to develop test protocols or procedures for assessing the likely emission rates of chemicals from non-point water and soil sources such as lagoons or contaminated soil sites. Details have been given in a previous report (Mackay et al 1983) and this is essentially an update on progress.

If it is suspected that a contaminant is being emitted from a water or soil source the apparently obvious approach is to collect an air sample over the site and analyse it for the contaminant. This approach is used in waste treatment landfills, and water impoundments with some success. (Thibodeaux et al 1984). Some disadvantages are:

1. the contaminant may be present in the background air at variable or unknown concentrations.
2. the air concentration measured will reflect the local micro-meteorology thus account of such dilution must be included.

3. concentrations may be so low that accurate determination is impossible. This is a particular problem with soils in which the measured air concentration may be influenced by the presence of wind-blown dust.

Another approach, which is regarded as complementary rather than competitive, is to simulate the non-point environmental conditions in the laboratory and measure the emission rate more accurately, possibly employing artificially elevated concentrations of the contaminant of interest but using the actual water or soil medium. A criticism of using elevated concentrations to achieve greater accuracy is that in certain situations it may be invalid to assume that the emission rate is proportional to concentration. But such situations can presumably be identified and if an extrapolation problem persists, lower concentrations can be used or the linearity assumption between emission rate and concentration can be explored experimentally.

We thus suggest a protocol in which a sample of the water or soil of interest is taken (with minimal disturbance), placed in a test vessel and subjected to an emission rate determination under controlled conditions of air-flow, turbulence and temperature. The emission rate can be measured by recovering the contaminant from the air effluent stream or by measuring the concentration reduction in the source (soil or water), or preferably both.

Our studies to date suggest that it is desirable to include one or more spiked "benchmark" contaminants (chemicals) in the determination, and repeat the test with a "standard" reproducible water or soil. The reason for these additions is that they can help to elucidate whether any anomalous results obtained are due to the unusual nature of the chemical of concern or the medium (soil or water), or both. The behaviour of the benchwork chemical

(of established properties) in the standard medium has presumably been well characterised in previous studies. Failure to reproduce that behaviour indicates a basic procedural error. If the benchmark chemical behaves as expected in the standard medium but unusually in the test medium, this indicates that the medium has some unusual property (eg. water containing a high organic or electrolyte content or soil containing a very high or low sorptive capacity). If the benchmark chemical behaves predictably in both the standard and test media it is likely that the test medium is fairly "normal" and that any unusual behaviour is attributable to the chemical. For example it may be subject to rapid degradation by photolysis or hydrolysis, or its reported vapour pressure may be erroneous.

The final stage is to examine the benchmark and test chemical data against a mathematical model of the emission process and confirm that the test results are in reasonable accord with expectations based on the known physical chemical properties of the chemical. If a mathematical model can be applied successfully to the test conditions, it can then be used with some measure of confidence to predict behaviour in the environment at various conditions of turbulence, concentration, temperature and even over a range of media composition or conditions.

The project has thus involved

(i) development of two test systems, one for water and one for soil

(ii) selection of benchmark chemicals

(iii) selection of "standard" water and soil media

(iv) testing the benchmark chemicals with the standard media at various test turbulence conditions with a view to determining conditions typical of the environment.

(v) assembly of two mathematical models in the form of easily usable programs suitable for use on microcomputers and transmittable as disks, and finally

(vi) testing the system on new chemicals, waters and soils

WATER SYSTEM

Equipment: The equipment is essentially that described in the previous report (Mackay 1983) but with minor modifications.

Air phase turbulence is induced using a blower connected to a rheostat and measured on a water manometer. The incoming air is cooled to the desined temperature by passing through a coil of copper tubing immersed in a water bath. The degree of interaction of the air flow with the air-water interface is determined by the position of the 90° elbow which directs air to impinge the wall of the glass vessel at different angles. In this work, the elbow is positioned at an angle of 45° with the straight copper tubing sections thus creating a counter clockwise swirling motion. Water turbulence is generated through the use of a propeller powered by a motor and measured on a revolution counter. The propeller is hung to a depth of 5 cm above the bottom of the vessel and rotates in clockwise direction i.e. opposite to the air flow. The glass vessel is innersed in a water-bath, the temperature of which is maintained at 25 °C, or at any other desined temperature.

Four benchmark solutes, toluene, p-xylene, naphthalene and phenanthrene have been tested in the standard medium of distilled water under 5 different combinations of air turbulence (i.e. blower rate) and water turbulence (i.e. stirring speed) conditions which are believed to be typical in the environment. The chemicals were chosen on the basis of the range of Henry's constants (H) they cover so that the values of K_G and K_L the gas and liquid phase mass transfer coefficients can be accurately determined.

The standard water is distilled water.

Results

The volatilization experiments were replicated and the results are generally reproducible within experimental error. The overall mass transfer coefficients (MTCs) were calculated from the slopes of the semi-logarithmic plots of concentration versus time. The individual values of K_G and K_L were determined from the relationship between MTC and H. We attempted to correlate these values of K_G and K_L with blower rate P, (expressed in terms of cm of water pressure drop) and stirrer speed S i (rpm) using equations of different forms. After many trials, the following form has been found to give the best fit.

$$K_L=(Sc_{LA}/Sc_L)^{0.5}\{C_1 + C_2[A(P/2)^M + B(S/105)^Q + (1-A-B)(P/2)(S/105)]\}$$

The correlation for K_G is identical except that the Schmidt number refers to that of the compound in the gas phase (air). The Schmidt number (Sc_L) correction factor is included to account for the difference between the individual solute liquid and gas phase mass transfer coefficients K_L and K_G and the average value (Sc_{LA}) as evaluated from the experiments.

C_1 is the value for K_L with no stirring or blowing and $(C_1 + C_2)$ corresponds to the value at a blower rate of 2 cm pressure drop and stirring speed of 105 rpm. Values of the constants A, B, M and Q for correlating K_L against P and S and the corresponding four values in the K_G correlation have been obtained. Further 'fine-tuning' of the correlations is desirable and necessary before applying them to new chemicals.

A mathematical model has been assembled for predicting the volatilization half-life of a chemical contaminant from water under known turbulent conditions. The model requires the input of the physical chemical properties of the compound of interest, namely aqueous solubility, vapour pressure or the Henry's constant and the environmental temperature. Using the two correlations for K_G and K_L as given previously, the model is capable of generating a set of K_G and K_L values from a range of P and S values. It further calculates the value of the MTC and ultimately the volatilization half-life from a knowledge of the ratio of the air-water exchange area to the volume of the water body or equivalently the average depth. The environmental K_G and K_L values can be estimated from the 10 metre wind speed using the correlations suggested by Mackay and Yeun (1983). From the functional plots of K_G and K_L on P and S, the laboratory conditions (i.e. P and S) to produce the respective environmental K_G and K_L values can be obtained. Thus the chemical of concern can be subjected to test under the desired turbulent conditions.

In summary, it is believed that the present water-test system is suitable for measuring solute emission from the water of concern at the desired temperature and turbulence conditions which are expected in the environment. It can be readily adapted for use at various temperatures, and various water qualities.

SOIL SYSTEM

The volatilization behavior of chemicals from soils is more complex than that from water bacause of the greater heterogeneity of the soil medium. The chemical may be present in several forms, pure chemical, sorbed on mineral or organic matter, dissolved in water and as vapour in air spaces. Transport

may be by diffusion or by bulk flow of air or water. In view of this complexity we have concentrated on (i) performing simple small-scale experiments involving volatilization from a soil column and (ii) assembling a computer model describing these processes.

The small scale apparatus was described in last year's report and has been operated using radio-labelled lindane as the benchmark chemical. Sorption isotherm experiments have also been conducted. As mass balance has been successfully obtained for the situation in which a known initial mass of chemical is present in the soil, then volatilization is allowed to occur and a reconciliation is made between that amount and those recovered in the soil at various depths and from the exit air stream.

A model, in the form of a numerical solution to the partial differential equation governing the partition and flux of the chemical has been developed and successfully fitted to the data. It is too complex for general use, thus a simplified version is being sought.

The final stage in this study will be the development of a larger scale system, possibly identical in dimensions to the water system in which actual soil samples will be tested for chemical volatilization loss and a protocol will be established similar in principle to the water case. This will require consideration of a standard soil and benchmark chemical(s).

During the course of this work it became apparent that we could compile a rather simple model describing the behavior of a chemical spill on soil (including volatilization). This aspect, which is a digression from the principal project, has proved to be quite successful and a paper on the subject

has been written for the Society for Environmental Toxicology and Chemistry (SETAC) meeting in November. A presentation will also be made at the Chemical Spills conference in Toronto in February sponsored by Environment Canada (EPS).

In general, the soil volalitization work is proceeding satisfactory but is slower than the water work because of the greater inherent complexity.

Mackay, D., Hughes, A., Phyper, J., "Evaluation of Contaminated Water and Soil Sites as Sources of Airborne Hazardous Materials Proc. Technology Transfer Conference No.4, p.702, Ontario Ministry of the Environment 1983.

Thibodeaux, L.J., Parker, D.G., and Heck, H.H., "Measurement of Volatile Chemical Emissions from Wastewater Basins. EPA report EPA 600/S2-095 August 1983, Cincinnatti OH.

Mackay, D., Yeun, A.T.K. "Mass Transfer Coefficient Correlations for Volatilization of Organic Solutes from Water "Environ. Sci. Technol. 17, 211 (1983).

The Chemoreceptive Membrane as an Electrochemical Sensor for Trace Organic Species in the Atmosphere

Langmuir-Blodgett Technology in the Development of Selective Chemical Sensors

M. Thompson, U.J. Krull, A. Arya, E. King and H.E. Wong

Department of Chemistry, University of Toronto,

80 St. George Street, Toronto, Ontario M5S 1A1

The thesis of the Chemical Sensors Group at the University of Toronto is that a selective chemical sensor configuration can be based on modulation of the transmembrane ion flux through thin lipid membranes by a stimulant (analyte)-chemoreceptor interaction at the membrane surface. In previous M. of E. Technology Transfer Conferences we have expounded theoretically and experimentally on this concept, and discussed examples of potential mechanisms for gas-sensing. In order to reach the ultimate goal of a discrete and integral sensor, it is clear that a robust system must be developed which involves supported thin film membranes on electronic devices such as chemically-sensitive transistors. In this regard, the Group has recently been examining the nature of molecular packing in lipid/cholesterol monolayers by analytical Langmuir-Blodgett experiments for correlation with Arrhenius-Eyring results on membrane ion conduction. Also, preliminary experiments have been performed on deposition of Langmuir films on hydrophilic substrates. The former work demonstrates clearly that internal membrane functions that are responsible for ion conduction can be controlled from the membrane surface. Secondly, some limited success has been achieved with respect to deposition of electrically functional films which respond to known electrochemical stimulants. Finally, the future possibilities with respect to device configurations, gas-sensitive chemistry, artificial intelligence and applications will be outlined.

Thesis Review

Cell membranes are relatively impermeable to ion flux, but interaction at a surface receptor site can stimulate a sudden transmembrane ion flux which propagates down the length of a neuron. The natural sense of smell, olfaction, is thought to involve this mechanism as is the operation of the synaptic nicotinic cholinergic receptor. In the former case recognition occurs through a process analogous to enzyme-substrate or antibody-antigen interaction where tertiary structure and electronic distribution govern the degree of stimulant binding to the receptor. Pattern recognition of stimulated areas across a two-dimensional network of receptors and spatial and temporal integration of stimuli then provides positive sample indentification and concentration data. In our work, the planar bilayer lipid membrane has been studied as a possible basic device structure for the detection of organic species. The basic premise for analytical signal generation is that a membrane-embedded complex can alter lipid matrix properties to influence transmembrane ion flux. The thesis behind this work is summarized in Fig. 1.

Langmuir-Blodgett (LB) Film Technology

The pioneering work of Langmuir and Blodgett in the 1920's was concerned with a simple method for preparing mono-and multi-layers of surfactant films. At that time it was discovered that insoluble surfactants could form organized assemblies at an air/water interface when external compression pressures are employed, and that these layers could be deposited intact onto various substates simply by forcing such supporting materials through the compresed film. This important technology is currently

undergoing a renaissance in thin film preparations for applications in molecular electronics, photoconducting polymers, drug encapsulation and electronic device fabrication. Also, the characteristics of pressure-area curves yield very valuable information concerning the spatial orientation and packing of components in monolayers. In our work, we have been using LB technology in both these areas, viz. as means of understanding molecular packing, and its importance in membrane ion conduction, in lipid films, and as a procedure for the production of stable supported membranes structures for device development. A summary of the preliminary results of these studies are the subject of this paper.

LB Film Characteristics and Phospolipid Membrane Ion Conduction

Two membrane parameters, dipolar potential and fluidity/packing, are largely responsible for the control of transmembrane ion conduction. In the former anisotropic membrane organization results in the formation of planes of dipolar charge, which act as electrostatic fields controlling membrane current. Alteration of the dipolar potential by a receptor-stimulant complex offers a possible mechanism for signal generation. The second important feature for control of ion current is related to the potential barrier associated with membrane fluidity/packing. Here, the diffusion of ions, in the absence of protein-based conduction mechanism, is intimately concerned with intermolecular interactions of lipid molecules. In order to probe this effect, cholesterol and its oxidized derivatives as dopants for membrane composition were used in both estimations of total Arrhenius-Eyring energy barrier (BLM experiments-see previous Ministry of Environment reports) and in average molecular area determination via the Langmuir-Blodgett trough. Typical pressure-area isotherms for phosphatidyl choline steroid-based films over water are

depicted in Fig. 2. These curves are used to determine the collapse pressure of the monolayer, which in turn can be employed to compute molecular area, i.e. the smallest average area that a molecule can occupy in the monolayer. Data was collected at 32 and 16 mN cm^{-1}. The standard deviation is molecular area determination in generally in the range 1-1.5 A^2. In Table 1 we summarize energy barrier data from bilayer work and Langmuir-Blodgett monolayer results from the PC/steroid film mixtures. Clearly, there is a highly significant variation in total potential energy barrier with approximately 1000 mV between extremes. Since the electrostatic dipolar field is expected to contribute up to 600 mV, it is obvious that fluidity/packing is a crucial additional parameter.

The collapse pressures of most of the PC/steroid mixtures were similar, thought that for the PC/3-one was much smaller. It is apparent the prevention of lipid carbonyl to 3-hydroxyl group hydrogen bonding in the case of the 3-one (pure and PC-mixed) has a major destabilizing effect. With respect to molecular packing, the sterols would be expected to exhibit facilitated alignment in the absence of puckered rings, or rings with many protruding functional groups. The data given in Table 1 is consistant with this concept, and indicates that the planar 5,7-diene and cholesterol have minimum areas, whereas molecules of greater substitution such as the diol and triol species result in maximum area. The influence of electrostatic effects and consequent hydrogen-bonding is clearly demonstrated by contrasting the average molecular areas of the steroids with the PC/ steroid mixtures. The order of size between the two series is inconsistent implying that chemical binding effects must overide simple packing considerations. At elevated compression, only the PC/3-one system has identical measured and calculated areas, as expected for a steroid incapable of extensive hydrogen bonding.

The important finding here is that correlation between BLM ion current and average molecular area shows that the intersticial spaces between lipid molecules is crucially important in transmembrane ion permeation. This result indicates that a transducer suitable for selective organic sensing can be based on receptor physics which controls local membrane intemolecular packing. If substantial local changes in dipolar potential folllow chemoreception and then align other dipolar species through dipole-dipole and dipole-induced interactions in the electrostatic field, a possible perturbation of packing could occur. This demonstrates that chemical amplification may be possible as a result of synergic dipolar potential and packing perturbation.

Stabilized Lipid Films by LB Technology

We have demonstrated that specialized lipid membranes exhibit significantly improved selectivity and sensitivity when compared with other electrochemical sensors. However, their practical employment is completely precluded by their extremely fragile structure. In the present work, we describe preliminary progress being made in the interfacing of ordered lipid films to polymer substrates by LB technology. This type of system is essential if the BLM transducer is to be combined with microelectronic technology.

A Langmuir-Blodgett film of phosphatidyl choline and cholesterol was compressed on the trough until a pressure of at least 30 $mN.m^{-1}$ was attained. A glass wafer coated with polyacrylamide gel on a Ag/AgCl substrate was then dipped through the compressed film, withdrawn and then dipped again. A small portion of the unprocessed clean silver initially deposited on the glass wafer was used as a connection to prepare an electrochemical circuit. A Ag/AgCl reference electrode, +25 mV DC power

supply and an electrometer completed the circuit for measurement of ion current through the deposited lipid layers (Fig. 3). Electrocemical probes (known to perturb BLM ion conduction) were introduced to the trough subphase in the vicinity to evaluate transducer operation. Cast films remained stable for many hours, but did not survive subphase withdrawal and re-immersion once the monolayer on the trough surface was removed.

Electrochemically successful BLM casting was readily observed as a 10,000 fold or greater reduction in ion current as shown in Fig. 4. Final current values in this case were in the range 10^{-9}-10^{-10} Acm^{-2}, and electrical shielding with a Faraday cage was necessary to reduce electrical interference. Only a fraction of all attempts to coat useful BLM structures onto gels were successful. The transient ion current increases observed in Fig. 4 an addition of a local concentrated volume of valinomycin, which rapidly dissipates into the large volume of the trough subphase, is consistent with the presence of a lipidmembrane of undefined structure. A second probe of interest is the dipolar species, phloretin. This small organic species (GMW 274) has a large 5.6 D dipole moment which can align against the inherent dipolar field of a BLM. This perturbation results in an increased current (Fig.4), only when monolayer or bilayer lipid structures are present.

Future Perspective

The work described above clearly demonstrates that lipid-film transducers have a future, both from the mechanistic point of view and with respect to stabilization. However, a great many research problems remain for solution:

1. The nature of potential chemoreceptor sites will have to be examined. These

may be synthetically produced (genetic engineering) or by extraction from natural media.

2. Methods for incorporation of receptor molecules into lipid films will have to be examined.
3. An important problem is the optimization of receptor location in lipid films to maximize the signals described above.
4. Much more work is needed on LB techniques for coating polymer films, particularly with respect to surface morphology and hydrophobicity (hydrophilicity).
5. Thin film polymer chemistry compatible with potential microelectronic structures is an obvious area for study.
6. Finally, the design and fabrication of device structures incorporating necessary electronic and chemometric components will be a crucial factor in the production of practical systems for gas sensing.

Acknowledgments

We are very grateful to the Ministry of the Environment, Province of Ontario for support of this work. Also we thank J. Janata of the Dept. of Bioengineering, University of Utah for much in the way of valuable discussion.

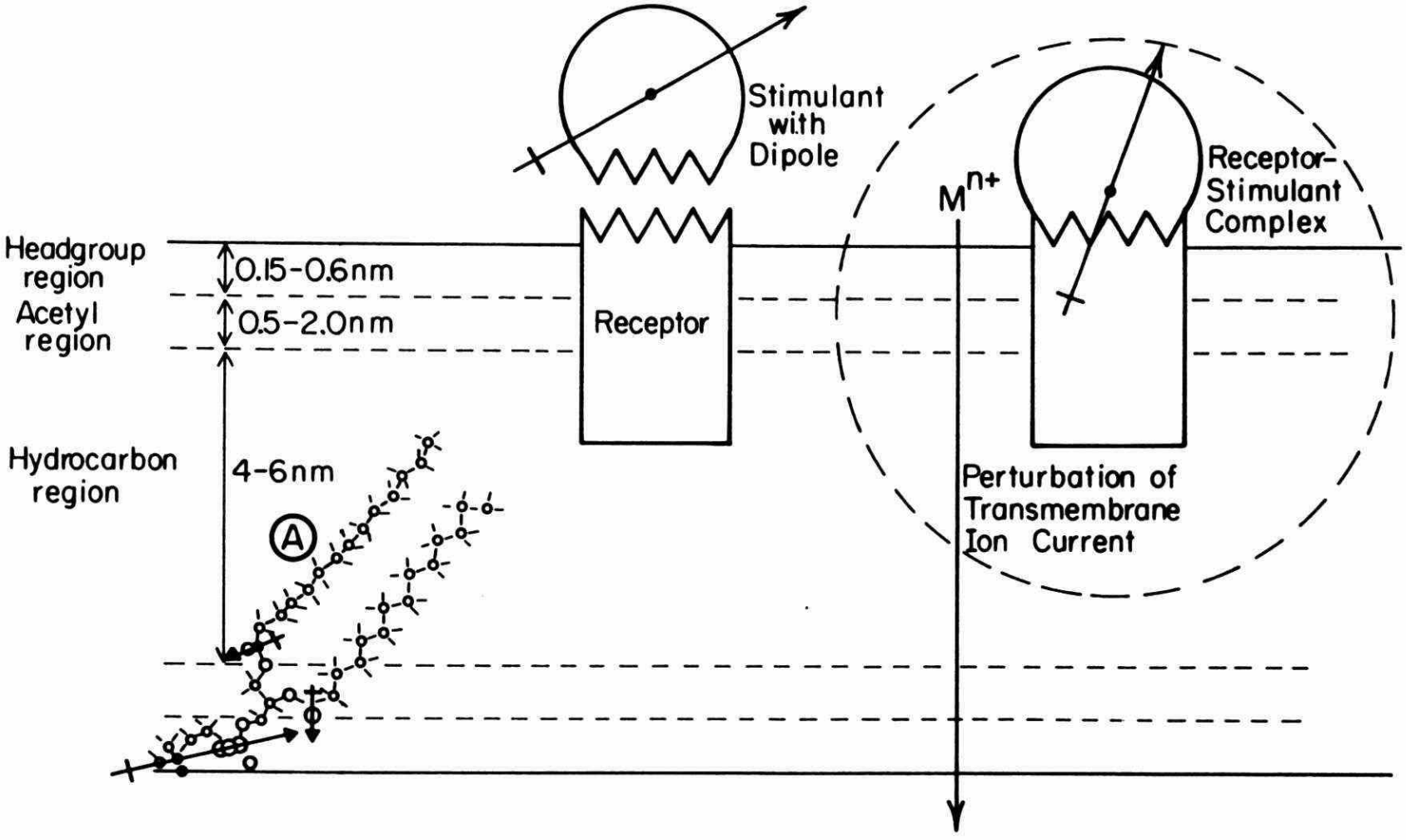
Figure Captions

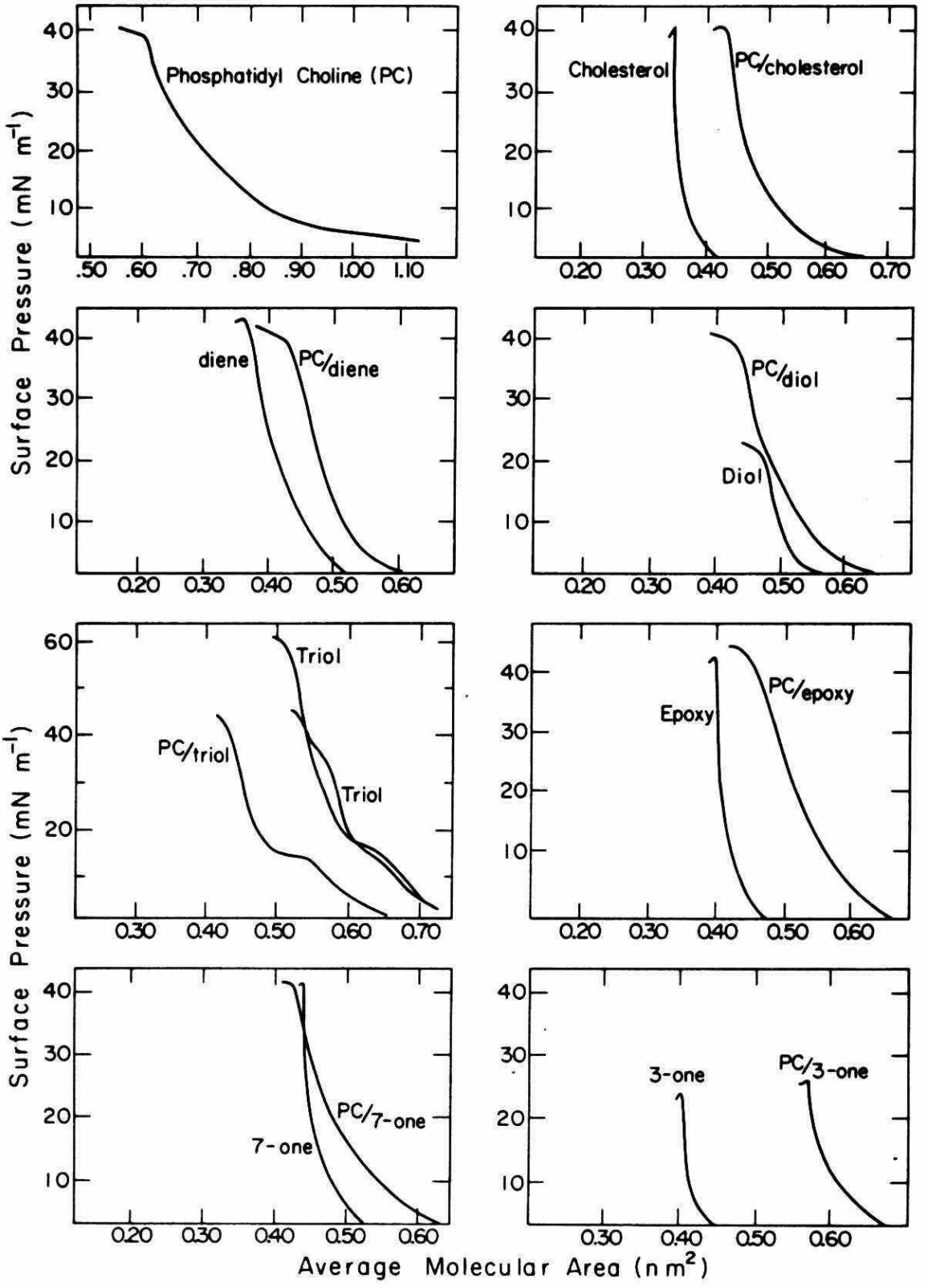
1. Receptor-stimulant modulation of lipid membrane ion permeability.
2. Pressure-area isotherms for steroid and PC/steroid mixtures over water at $21 \pm 1^{\circ}C$.
3. A schematic of simple system for measuring cation current through a BLM deposited onto polyacrylamide gel.
4. Electrochemical perturbation of deposited LB film by stimulants.

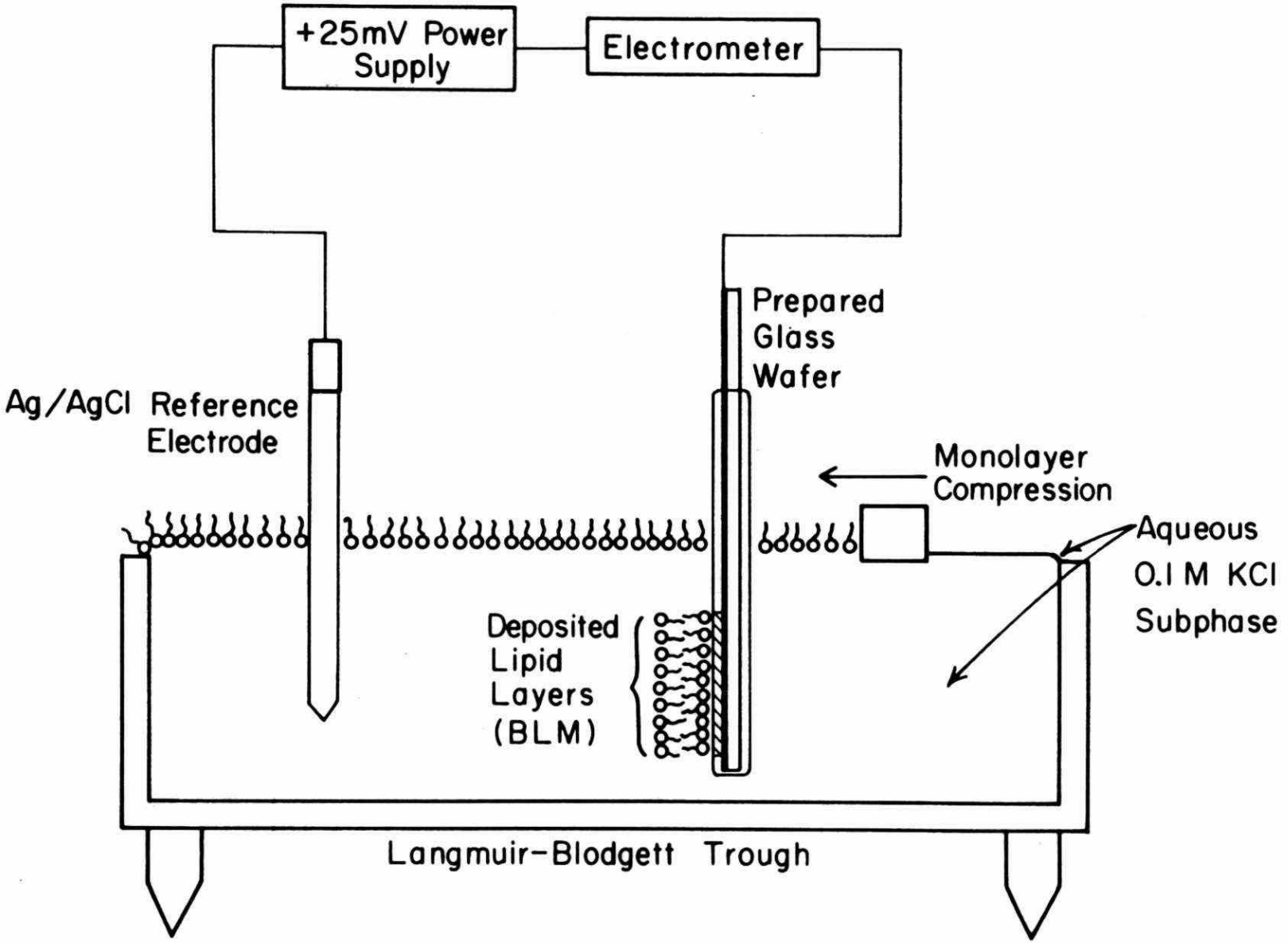
TABLE 1

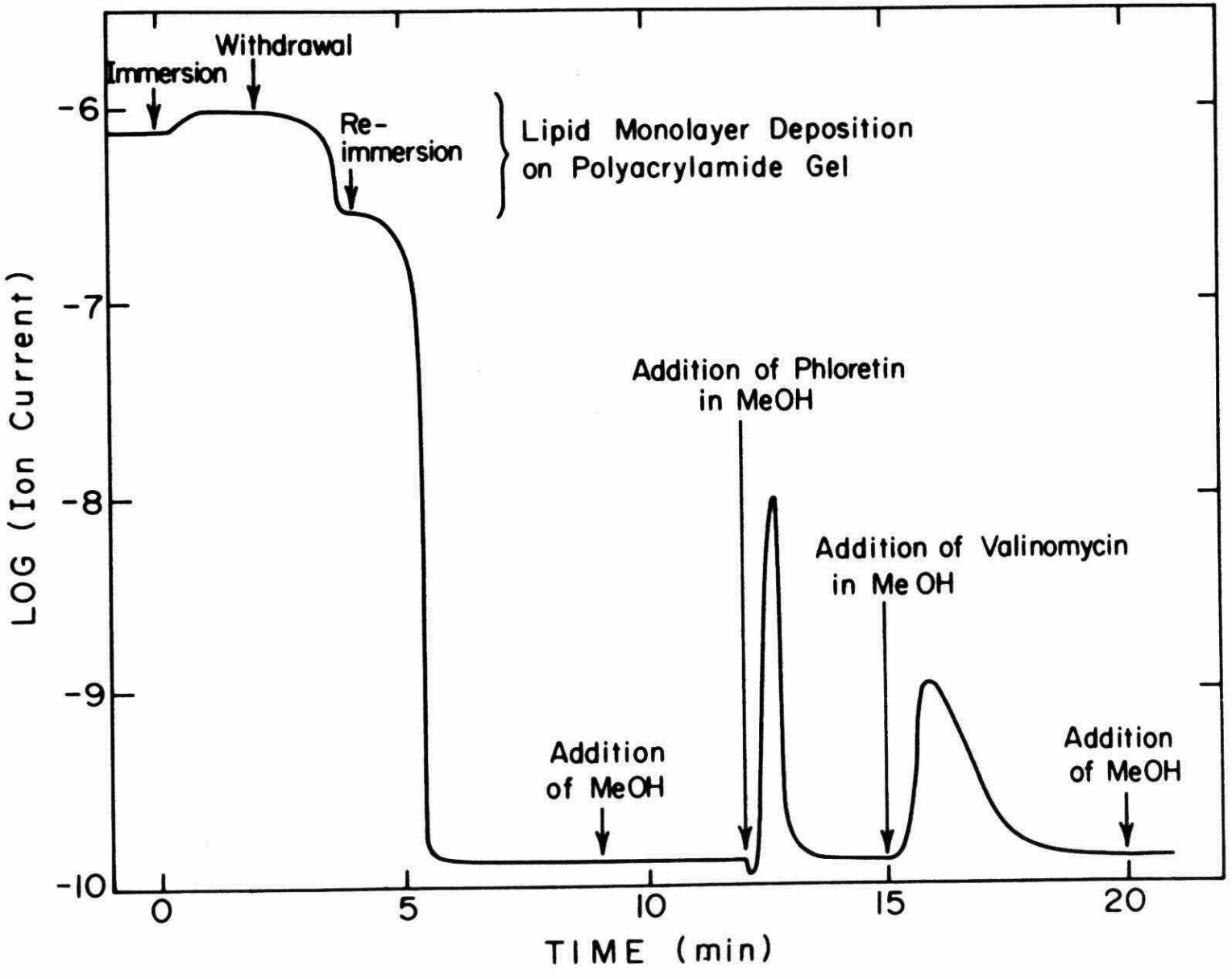
Arrhenius energy barriers (BLM) and LB monolayer data for steroids and PC/steroid mixtures.

Bilayer/ Monolayer Composition	BLM Energy Barrier (V)	Collapse pressure ($mN.m^{-1}$)	Areas at pressures (nm^2)		
			Collapse	$32mN.m^{-1}$	$16\ mN.m^{-1}$
5α-cholesten-3-ol		41.2	0.367	0.370	0.392
PC/cholesterol	1.18	43.0	0.368	0.466	0.483
5,7-cholestadien-3-ol		44.5	0.359	0.358	0.426
PC/diene	0.80	41.6	0.398	0.454	0.483
3β-hydroxycholesterol		20.1	0.484	-	0.492
PC/diol	-	43.0	0.432	0.444	0.505
Cholestan-3,5,6-triol		43.2	0.477	0.510	-
PC/triol	0.49	43.9	0.416	0.457	0.530
$5^{\alpha},6^{\alpha}$-epoxycholestan-3β-ol		46.1	0.389	0.390	0.408
PC/epoxy	0.35	44.1	0.445	0.463	0.528
3β-hydroxy-5-cholesten-7-one		43.2	0.427	0.439	0.466
PC/7-one	0.63	44.6	0.404	0.438	0.493
5α-cholestan-3-one		23.9	0.415	-	0.427
Pc/3-one	0.19	26.2	0.536	0.561	0.576
Phosphatidyl choline	-	43.1	0.611	0.702	0.863


Stimulant
with
Dipole
Receptor-
Stimulant
Complex
M^{n+}
Headgroup
region
0.15-0.6nm
Acetyl
region
0.5-2.0nm
Receptor
Hydrocarbon
region
4-6nm
A
Perturbation of
Transmembrane
Ion Current


Phosphatidyl Choline (PC)
Cholesterol
PC/cholesterol
diene
PC/diene
PC/diol
Diol
Triol
PC/triol
Triol
Epoxy
PC/epoxy
PC/7-one
7-one
3-one
PC/3-one
Surface Pressure (mN m⁻¹)
Surface Pressure (mN m⁻¹)
Average Molecular Area (n m²)


+25mV Power Supply
Electrometer
Prepared Glass Wafer
Ag/AgCl Reference Electrode
Monolayer Compression
Aqueous 0.1 M KCl Subphase
Deposited Lipid Layers (BLM)
Langmuir-Blodgett Trough


Immersion
Withdrawal
Re-
immersion
Lipid Monolayer Deposition
on Polyacrylamide Gel
Addition of Phloretin
in MeOH
Addition of Valinomycin
in Me OH
Addition
of MeOH
Addition
of MeOH
LOG (Ion Current)
-6
-7
-8
-9
-10
0
5
10
15
20
TIME (min)

Gas-phase Photochemistry of PCB's

Nigel J. Bunce, J.P. Landers, and J. Langshaw

Department of Chemistry and Biochemistry
University of Guelph, Guelph, Ontario, Canada N1G 2W1

ABSTRACT

We have been studying the gas-phase photochemical degradation of chlorinated aromatic compounds in static systems. Both chlorinated benzenes and chlorinated biphenyls behave similarly. Product studies reveal that the principal photochemical reactions of these substances parallel those observed in solution, with the products explicable for the most part in terms of a simple C-Cl homolysis

$$ArCl \xrightarrow{h\nu} Ar + Cl \rightarrow \rightarrow \text{products.}$$

A series of kinetic experiments showed that the disappearance of all the aryl chlorides studied follows a first order rate law. Procedures had to be developed to ensure that all of these rather involatile compounds were actually in the gas phase.

The present task at hand is to relate these rates of photodegradation to quantum yields. We have developed a simple procedure to allow this measurement to be made quickly, and hope to have some absolute quantum yields to present at the time of the conference.

Chlorinated aromatic hydrocarbons are widespread and persistent pollutants. The EPA priority pollutant list (1978) mentions chlorobenzene, the three dichlorobenzenes, 1,2,4-trichlorobenzenes, hexachlorobenzene, and the polychlorinated biphenyls (PCB's) as examples of priority pollutants. DDT is an example of a chlorobenzene derivative.

In addition to the many studies of the biological chemistry of these chlorinated hydrocarbons, there have also been numerous photochemical studies. The justification for these photochemical studies has been that because these chlorinated hydrocarbons absorb light in the region of the solar spectrum (although very inefficiently) there may be a chance that sunlight assisted degradation is one of the routes by which these substances disappear from the environment.

Pollutants such as the PCB's may be found in locations very remote from any industrial activity. They have, for example, been found in the snows of Antarctica[1]. It follows that they must have reached this location by transport through the atmosphere. This is reasonable, given the relatively high volatility of many of these compounds.

The research in which we are engaged is to understand the gas phase photochemistry of chlorinated aromatic compounds. We want to discover 1) the products of these reactions and 2) the detailed mechanisms by which the

reactions occur so that 3) we can try to estimate whether the photolysis of these compounds by sunlight plays a significant role in their chemistry while they are present in the atmosphere.

We must consider the concept of mechanism in a photochemical reaction. Besides the usual questions: "what intermediate species are formed en route to the final product?" and "how rapidly does each step in the pathway occur?", photochemical reactions pose two additional kinds of questions. These are: "which excited state of the starting material is involved?" and, "what is the 'quantum efficiency' of the reaction?" where the quantum efficiency is defined as the ratio below.

$$\text{Quantum efficiency, } \phi = \frac{\text{No. of molecules undergoing the process of interest}}{\text{Total no. of photons absorbed by the reactant}}$$

Excited states may be termed singlet or triplet; they differ in the relative alignments of the electron spins; for our purposes here we note only that triplet excited states tend to be quite a lot longer lived (microseconds) than singlet excited states (nanoseconds). The processes available to the excited states are:

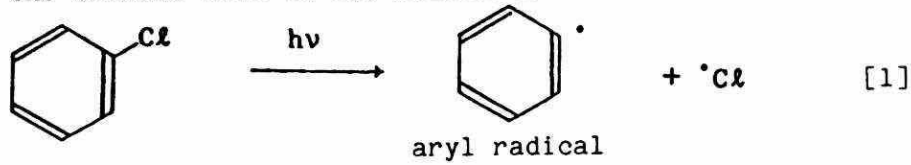
- return to the ground state with luminescence
- return to the ground state without luminescence
- singlet to triplet intersystem crossing (singlet only)
- chemical reaction.

Chemical reaction will proceed with more than negligible quantum yield only if the rates of the other competing processes are not too fast. Of course, in absolute terms, all chemical reactions of excited states must be very rapid, because of the speed of the competing processes which deactivate excited states. Consequently, photochemical reactions tend to occur only when they are energy releasing and have only small activation barriers.

A reasonably detailed background to our research was given in the Proceedings of the previous Technology Transfer Conference (1983)[2] and so we will simply summarize the major points briefly here. Absorption of light promotes atoms or molecules to "excited", that is, highly energized, states in which they may be more reactive than in their ground states. Aryl chlorides, with which we are concerned here, undergo C-Cℓ bond scission, at least in solution, following absorption of UV radiation. This reaction does not occur in the ground state, and hence, it represents a potential mechanism for degradation of these substances by light.

Liquid Phase Studies

Chlorinated aromatic compounds have been investigated photochemically for 15-20 years. Essentially all these studies have been made in the liquid phase (usually in solution) and there is very little background of gas phase photochemistry upon which to draw. The primary photochemical act in most cases appears to be cleavage of the carbon-to-chlorine chemical bond (eq. 1); this is the weakest bond in the molecule.

e.g. 

[1]

aryl radical

The products of this initial cleavage are free radicals, which are very reactive. In solution, the final products depend upon what other compounds are available to undergo reaction with these radicals. Removal of hydrogen giving eventual dechlorinative products, and addition to aromatic solvents, are typical fates of the free radicals.

The photochemical efficiency of the bond cleavage is strongly dependent on the energetics of eq. [1][3]. The excited state involved is usually a triplet; if the energy of the state above the ground state is comparable with, or greater than, the C-Cℓ bond energy, dissociation occurs efficiently

(high quantum yield). If the excited state energy is too low the reaction is very inefficient. Most estimates place the C-Cℓ bond energy in the region of 330 kJ mol^{-1}; Table 1 gives the triplet energies of some representative aryl chlorides.

Table 1. Triplet energies of aromatic systems

System		Triplet Energy, kJ mol^{-1}
Phenyl		350
Naphthyl		250
Biphenyl	not o-substituted	280
	o-substituted	330

Chlorinated benzenes and o-chlorinated biphenyls (Figure 1) tend to undergo dissociation with high efficiency ϕ 0.1-0.6. On the other hand, chlorinated napthalenes and non-o-chlorinated biphenyls are very resistant to photolysis, $\phi < 10^{-3}$. This is a steric effect. The ground state of biphenyl is best described as having a single bond between the two benzene rings (Figure 1a); a comparable description of the excited state has the rings coplanar (Figure 1b). Substitutents larger than hydrogen cause steric compression, which is relieved when the substituent (chlorine) departs. Additionally, the energy content of the o-excited state is higher, again because of steric compression (Table 1). This point is discussed in more detail in reference 4.

Vapour phase studies

Only one report of the gas phase photochemistry of chlorobenzene has appeared[5]. In that work, Ichimura and Mori photolysed chlorobenzene in an atmosphere of ethane. The products observed were benzene, HCℓ, and butane.

It is clear that under these conditions the reaction is exactly analogous to that observed in solution with, for example, cyclohexane. The products are explained by Scheme 1.

Scheme 1

$$PhCl^* \longrightarrow Ph^\cdot + Cl^\cdot$$

$$Ph^\cdot + C_2H_6 \longrightarrow PhH + C_2H_5^\cdot$$

$$Cl^\cdot + C_2H_6 \longrightarrow HCl + C_2H_5^\cdot$$

$$2C_2H_5^\cdot \longrightarrow C_4H_{10}$$

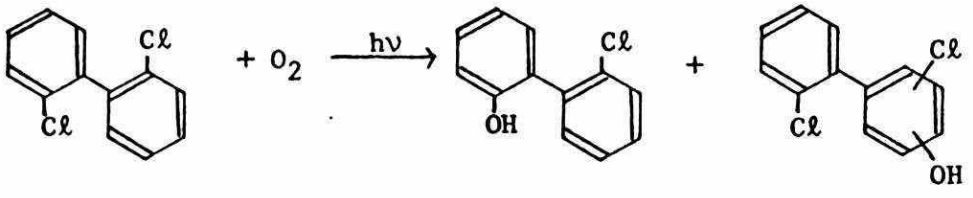
For the present purposes, what is significant is that the quantum yield of reaction (0.4) is very similar to that found in solution. In solution, there could be cage recombination (eq. 2) which would make the <u>observed</u> quantum yield of decomposition smaller than the <u>primary</u> quantum yield of decomposition.

$$(Cl^\cdot + Ph^\cdot) \longrightarrow PhCl \qquad [2]$$

The similarity of quantum yields suggests that this is not a problem in practice; more importantly, it suggests a primary $\phi_{decomp.}$ of ca 0.4 should be observed in any gas phase reaction of chlorobenzene. Therefore in ordinary air, we would expect that the first formed radicals in scheme 1 should disappear by reaction with oxygen, eq. 3.

e.g.  [3]

The expectation of eq. 3 appears to be fulfilled in the chlorobiphenyl series, where the only published gas phase study, that of Hustert and Korte[9], indeed gave a phenolic product eq. 4.

 [4]

In this study, 2,2'-dichlorobiphenyl underwent photodecomposition to afford two products. In one of them, hydroxyl replaced one of the chlorine substituents, presumably by some reaction analogous to eq. 3. The other product was incompletely identified, but contained a hydroxyl function additional to the two chlorines. We would expect, again by analogy with the solution phase studies, that PCB's containing ortho chlorines should be much more photolabile in the gas phase than those without.

Among chloro compounds which are not aromatic, a research group at Dow Chemical Co. has studied the simulated at atmospheric photodecomposition of simple aliphatic chlorides such as chlorinated ethenes and ethylenes[7]. These reactions were carried out with 10 ppm of the organic compound in the presence of ca. 5 ppm of NO to simulate a polluted atmosphere. Under conditions controlled to imitate bright sunlight, all the mono-, di-, and trichloroethylenes had half lives for decomposition $\tau_{1/2}$ of 5-12 h. Chlorobenzene is mentioned briefly in this paper, its $\tau_{1/2}$ was ca. 9 h. No products were identified.

The present work

Our preliminary experiments have not been designed to simulate natural sunlight. Instead we are using mercury arc lamps as the UV sources, and equipment constructed out of quartz or Pyrex glass. The rationale for this approach is that typical aryl chlorides have very poor spectral overlap between their absorption spectra and the solar spectrum at the Earth's surface. Environmentally only the tail of the aryl chloride absorption overlaps the shortest wavelength UV-B part of the solar spectrum. Since the same absorption band is excited by the quartz-filtered mercury arc, the chemistry should remain the same, but the reactions occur at a more conveniently rapid rate.

The first reaction chamber which we constructed consisted of a 12 litre flask equipped with three ground glass joints. The largest of these (60/50) accommodates an immersion well apparatus which projects inside the flask. The lamp, a 450 W "Hanovia" medium pressure mercury arc, rests in the centre of the immersion well and is cooled by a flow of water. We have available both quartz and Pyrex immersion wells; the former transmits all radiation λ >220 nm, the latter only λ >290 nm.

The remaining inlets to the flask are used to admit and remove gas. The chloroaromatic compound is placed in a reservoir, which may be heated if necessary. Gas (N_2 or O_2) is passed slowly through the reservoir, and entrains some of the vapour of the chlorocompound. After the gases leave the reaction chamber, they are condensed at -78^{o}C in a dry ice cold trap. After reaction the contents of the trap and the reaction flask are separately dissolved in a suitable solvent, and analysed by vapour phase chromotography and GC-mass spectrometry.

The photolysis times with the above mentioned equipment were inconveniently long, and a second apparatus was devised. This consisted of a 500 ml 3 necked flask. The central neck accommodated a 75W low pressure mercury lamp equipped with 24/40 standard taper (inner) ground glass joint. The other necks were used for purging the flask with gas and for introducing (and refluxing) the solvent which was used to remove the photoproducts from the flask.

Product Studies

Gc-ms analysis employed a VG Analytical model MM 12000 equipped with model 250 data system. It was interfaced to a Hewlett Packard 5790 gas chromatograph which was temperature programmed to allow elution of compounds of differing volatility. The chromatography column was a J&W DB-5 Fused Silica quartz capillary of length 50 m. The mass spectrometer was operated

in the E.I. mode with scans taken every 1.0 sec. Eluted compounds were compared with library spectra of authentic materials. We thank the operator, Dr. D. Fung, for help in identification especially for distinguishing among PCB isomers, where her experience of the retention times of authentic PCB compounds under these gas chromatographic conditions was particularly appreciated. In all cases, because of the extreme sensitivity of the gc-ms equipment, the starting materials were also analysed to confirm that the observed products were not merely impurities in the starting materials. The charts below summarise a number of photolysis runs, some in the large, and some in the small scale apparatus.

Chart 1. Qualitative experiments on ArCl photolysis analysed by gas chromatography (F.I.D.).

Experiment	Reactor	Result, Comments
1. o-Cl_2/N_2/10h/flow	L	PhCl, BP-Cl_3[a]
2. o-Cl_2/O_2/19h/static	L	PhCl, BP-Cl_3
3. o-Cl_2/CH_4/19h/static	L	PhCl, BP-Cl_3. Yield of PhCl not increased over expt.2.
4. o-Cl_2 + chlorophenol	L	chlorophenol disappears faster.
5. o-Cl_2/N_2/0.5h/static	S	Product concentration too low to detect by conventional glc
6. o-Cl_2/O_2/0.5h/static	S	
7. p-Cl_2/N_2/19hr/static	L	not analysed
8. p-Cl_2/O_2/19hr/static	L	" "
9. 1,3,5-Cl_3/N_2/0.5h	S	" "
10. 1,3,5-Cl_3/O_2/0.5h	S	" "

a BP-Cl_3 ≡ trichlorobiphenyl

Chart 2. Products from selected chlorinated benzenes upon gas phase photolysis at ca. 40°C

Expt. No.	Products	Scan #
1	Trichlorobenzenes (3)	50,60,73
	Biphenyl	127
	Monochlorobiphenyl (2)	224,227
	Dichlorobiphenyl (3)	248,286,333
	Trichlorobiphenyl (5)	347,356[a],370,396[a],446
2	Trichlorobenzenes (2)	50,73
	Dichlorophenols (2)	99,137
	Biphenyl	128
	Monochlorobiphenyls (2)	220,224
	Dichlorobiphenyls (4)	248,272,286,333
	Trichlorobiphenyls (5)	335,347,356[a],370,396[a]
	Tetrachlorobiphenyls (4)	416,441,454,483
3	Trichlorobenzenes (3)	50,60,73
	Dichlorophenol	137
	Biphenyl	128
	Monochlorobiphenyls (2)	220,224
	Dichlorobiphenyls (3)	272,286,333
	Trichlorobiphenyls (6)	335,347,356[a],370,396[a],446
	Tetrachlorobiphenyls (5)	416,424,441,454,483
4	Trichlorobenzenes (2)	50,60
	Biphenyl	128
	Monochlorobiphenyl	224
	Dichlorobiphenyls (3)	248,286,333
	Trichlorobiphenyls (5)	335,347,356[a],370,396[a]
5	Trichlorobenzene	71
	Dichlorophenol	68,78
6	Trichlorobenzene	60
	Dichlorophenol	68
7	Dichlorophenol	69
	Dichlorobiphenyl	333
	Trichlorobiphenyls (2)	383,395
8	Dichlorophenol	69
	Monochlorobiphenyl	232
	Dichlorobiphenyl	334
9	Dichlorobenzene	30,37
	Dichlorophenol	130,137
	Dichlorobiphenyl	231
	Trichlorobiphenyl	487
	Tetrachlorobenzene	123
10	Dichlorobenzene	25
	Dichlorophenol	134,142
	Monochlorobiphenyl	238
	Dichlorobiphenyl	341
	Trichlorobiphenyl	494
	Tetrachlorobenzene	126

a These two trichlorobiphenyls were trace impurities in the starting o-dichlorobenzene

Relative rate studies

The chloro compound 1.0µl was introduced into the 3-necked 500 ml flask by means of a microlitre syringe. Depending on the vapour pressure of the compound the flask could be immersed in a warm water bath to regulate the temperature inside the flask. After photolysis for a known period of time the products were removed by cooling the flask and then introducing a solvent (CH_2Cl_2) through one of the side arms by way of a reflux condenser. The solution was then heated to reflux in order to remove any condensed chloro compound from the vessel walls, and the solution was removed quantitatively prior to analysis by glc. The amount of reactant remaining after photolysis was quantitated and the data were treated by standard first order kinetics. Graphs 1-4 are appended and the results are summarised below.

Table: Observed first order rate constants for photolysis of 1.0µl of chlorinated aromatic hydrocarbons under identical conditions.

Compound	k_{obs}, min^{-1}	ϕ_r(solution)[a]
C_6H_5Cl	0.28	0.31
1,2-$C_6H_4Cl_2$	0.55	0.78
1,3-$C_6H_4Cl_2$	0.30	0.49
1,4-$C_6H_4Cl_2$	0.43	0.17
1,2,4-$C_6H_3Cl_3$	0.31	0.63
1,3,5-$C_6H_3Cl_3$	0.33	0.14
1,2-$C_6H_4Cl.C_6H_5$	0.29	0.35
1,3-$C_6H_4Cl.C_6H_5$	0.10	0.001
1,4-$C_6H_4Cl.C_6H_5$	0.09	0.0006

a Reference 8.

Actinometry

We have developed a new actinometry method that is based on a procedure which has been successfully employed for solution studies in our laboratory[9]. The chemistry involves the photorearrangement of the photoactiave compound azoxybenzene, eq. 5.

After the addition of alkali, the product is estimated spectrophotometrically as its anion at 458 nm. The procedure we have developed is based on the small photoreactor, except that an all-quartz flask is used.

(a) Irradiate the empty flask, which is surrounded by the actinometer solution. Measure the concentration of product (458 nm) and knowing ϕ=0.02, establish the photon dose transmitted through the flask.

(b) Irradiate the aryl chloride in the gas phase, again with the flask surrounded by the actinometer. Record the absorbance of the actinometer solution at 458 nm and the extent of ArCl decomposition.

(c) The difference between the light absorbed by the actinometer in (a) and (b) represents the light absorbed by ArCl. Then ϕ for ArCl is given by eq. 6.

$$\phi = \frac{\text{moles of photons absorbed by ArCl}}{\text{moles of ArCl recomposed}} \qquad [6]$$

Brief Discussion

The photolysis products can be rationalised by a conventinal free radical scheme.

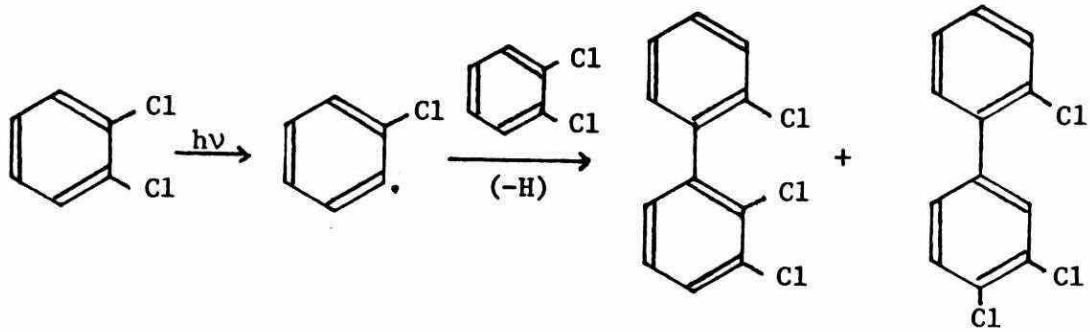
$$ArCl_n \xrightarrow{h\nu} ArCl_{n-1} + Cl$$

$$ArCl_{n-1} \begin{cases} \xrightarrow{O_2} \text{phenols} \\ \xrightarrow{[H]} \text{dehalogenation} \\ \xrightarrow{ArH} \text{biaryls} \end{cases}$$

$$\text{Biaryls (Cl)}_x \xrightarrow{h\nu} \text{Biaryls (Cl)}_{x-1} \text{ etc.}$$

Of these products, the phenolics are the hardest to detect. Experiment 4 shows why; the phenols are more photolabile than the initial reactants.

One notable feature of Chart 2 is the large number of isomers, especially trichlorobiphenyls, obtained. A conventional mechanism, as outlined below, would seem to predict only two trichlorobiphenyl isomers.



The large number of trichlorobiphenyls seems to point to photorearrangement of either the trichlorobiphenyls themselves, or the precursor dichlorobenzene. This point is under further investigation.

The relative rate experiments seem to indicate an overall reactivity that parallels the quantum yields in solution. This trend is in process of substantiation by means of quantum yield studies.

References

1. R.W. Risebrough, W. Walker, T.T. Schmidt, B.W. de Lappe, and C.W. Connors, Nature, 264, 738 (1976).
2. N.J. Bunce and J.P. Landers, Technology Transfer Conference No.4, Proceedings P. 863, November 1983.
3. N.J. Bunce, M.D. Bergsma, J.P. Bergsma, W. De Graaf, Y. Kumar, and L. Ravanal, J. Org. Chem., 45, 3708 (1980).
4. N.J. Bunce, Chemosphere, 11, 701 (1982).
5. T. Ichimura and Y. Mori, J. Chem. Phys., 58, 288 (1973).
6. K. Hustert and F. Korte, Chemosphere, 4, 153 (1974).
7. W.L.Dilling, C.J. Bredeweg, and N.B. Tefertiller, Env. Sci. Technol., 10, 351 (1976).
8. N.J. Bunce, J. Photochem., 15, 1 (1981); N.J. Bunce, P.J. Hayes, and M. Lemke, Can. J. Chem., 61, 1103 (1983).
9. N.J. Bunce, J. LaMarre, and S.P. Vaish, Photochem. Photobiol., 39, 531 (1984).

vap-ah2
njb/#5

THE HAMILTON STUDY: Refinement of SO2 and Particulate Data for Exposure Estimation

LD Pengelly, CH Goldsmith, AT Kerigan, SA Toplack, H McCague
Departments of Medicine, and Clinical Epidemiology and Biostatistics
McMaster University, Hamilton, Ontario, Canada

ABSTRACT

A study to investigate the effects of environmental factors on the respiratory health of 3500 children aged 7 to 10 years was conducated in Hamilton, Ontario from 1978 to 1982. Respiratory health was assessed by pulmonary function testing and by questionnaire, and environmental factors were determined from the questionnaire and by field measurement of air quality. Measurements were made of levels of sulphur dioxide (SO2) and suspended particulate matter. Two groups worked together on the project: one group carried out the epidemiological survey and the measurement of total suspended particulate (TSP) and particle size distribution (PSD); the other group carried out the field measurements of SO2 and the development of new instrumention (laser absorption spectrometer-LAS) for more sensitive measurement of SO2.

In order to estimate exposure of the children to ambient air pollution, we decided to input the data obtained at each site (for SO2, TSP, and PSD) into a quadratic response surface model for each pollutant, based on monthly average values for each site. From the response surfaces in pollutant concentration, and in easting and northing geographical co-ordinates, we could estimate exposures specific to each of the 49 schools in the study, and thereby calculate for each child a yearly exposure based on the time he or she was tested at that school. By examining the response surfaces visually, we determined that there were serious discrepancies in the data, especially for measurements of SO2; thus, we found it necessary to implement a data recovery programme which included rereading the original SO2 recorder charts. This experience has demonstrated the need for explicit manuals for the documentation and quality control of air pollution data, a process which we had already implemented for the particulate data. Relatively few problems have emerged in deriving particulate exposures.

(Supported by Ontario: Environment, and Health)
(Canada: National Health and Welfare)

INTRODUCTION

A study to investigate the effects of environmental factors on the respiratory health of 3500 children initially aged 7 to 10 years was conducted in Hamilton, Ontario from 1978 to 1982. Respiratory health was assessed by pulmonary function testing and by questionnaire, and environmental factors were determined from the questionnaire and by field measurement of air pollutants: SO2 and suspended particulate. Two groups worked together on the project: one group carried out the epidemiological survey and the measurement of total suspended particulate (TSP) and particle size distribution (PSD); the other group carried out the field measurements of SO2 and the development of new instrumentation (laser absorption spectrometer: LAS) for more sensitive measurement of SO2.

Field measurement of SO2 depended on Beckman 906A analyzers operated at one or the other of two sets of 8 sites on a 6-week rotation schedule. Operation of these analyzers (now obsolete) at the sensitivity levels required (Full Scale = 250 ppb) under these conditions (of frequent movement) proved to be very difficult, and made great demands on the manpower resources available for the SO2 network part of the project. As a result, the recorder charts which were the basic data source of the SO2 network information were accumulated over the years 1979 to 1981, relatively few of them being reduced to digital form for data entry to the computer. In the last few months of funding of the project, several different persons (who had not had field experience with the SO2 analyzers) read the charts. These readings were entered on data sheets which were subsequently used either to keypunch the data onto punch cards prior to loading them into the computer, or to enter them directly by terminal. In addition, it was determined that there were anomalies in some of the strip chart record time bases, such that the time elapsed indicated by the preprinted lines on the chart itself, did not agree with the time elapsed according to the time checks written on the chart by the technician. Usually it was possible to find an explanation for these discrepancies, and to make allowance for them at the time of chart reading. Records of analyzer zero and span checks were also available on some of the charts, and had to be entered in some form along with the rest of the data.

To deal with the problem of correcting the SO2 data for time, zero, and span variation, a computer program was written which made certain assumptions, producing an output of "polished" data in the form of a computer file. This file was then delivered to the epidemiology group for use in determining exposure estimates, which were subsequently to be used in examining the relationships of health outcomes to SO2 levels.

At this point the file was examined, and it was determined that many anomalies were still present (such as 37-day months, and measurements for a site when no instrument was present). It was decided to examine some samples of the original charts and to compare them with the "polished" file. This revealed further anomalies. At this point, an attempt was made to follow back an "audit trail" of the various processes which had been used to handle the data, so that we could determine the point at which the problems arose. Unfortunately, the audit trail had several gaps which were impossible to bridge. We reluctantly came to the conclusion that the most efficient process to use in recovering the SO2 data (providing that there was sufficient information on the charts) was first, to catalogue, and then to re-read, the charts according to strict written criteria.

We determined that 440 charts were available to us, covering the time period 1979-01 to 1981-12. When these charts were examined and catalogued, it was found that the estimated potential data recovery from them would likely be in excess of 50%, and for this reason we decided to carry out the process of re-reading the charts. This task is currently in progress, and we expect to have it completed in two to three months. We have instituted formal quality control procedures for both the cataloguing and the re-reading procedures. Given a written set of criteria for both processes, a random sample of 5% of all charts is being re-catalogued, and another such sample is being re-read. The necessity for quality control of the cataloguing process arises from the fact that the decision to accept or reject a chart for reading is made during the cataloguing process. Quality control of the reading process, together with a written protocol for reading, allows us to use more than one person for the chart reading task, with some confidence that there will be uniformity in the quality of the work.

PARTICULATE DATA

Refinement of the particulate data from this project was a much less demanding task, as a written protocol for data gathering and quality control was implemented from an early date in the project. Nevertheless, in order to have an easily comprehensible display of air quality data from the TSP and PSD networks, we developed some short computer programs which could be run on even the least sophisticated of current personal computers. These provided for the display of "contour maps" of TSP and PSD data, over the geographical area of the city. The inputs to the program were the response surface coefficients which had been determined on the basis of monthly means from all sites. The degree to which the response surfaces represented the data was known in all cases, and the signifigance of all coefficients was determined by statistical procedures. Once this was done, a "book" of maps was produced, which allowed for visual inspection of all of the particulate data. This provided an additional quality control procedure, which resulted in the exposure of a few residual anomalies in the data, which were subsequently corrected.

Exposure estimation has been carried out for the particulate data. From a study of the relationships of the locations of the homes of individual children, to the locations of the schools they attended, we found that over 95% lived within 1 km of their school. Accordingly, we decided to use the school location to determine the exposure level for all the children attending that school. Thus, knowing the geographical co-ordinates of a school, we could estimate the TSP concentration for a given month from the response surface for that month. We made the decision that, to calculate an exposure which would be meaningful in the context of a study of chronic (long-term) effects of the environment on respiratory health, we would require an estimate of particulate dose received based on exposure averaged over a year. We chose to create this dose average by taking the arithmetic mean of the monthly values determined from the response surfaces for the nine months previous to the month we studied a child, the month of study, and the two months following the study month. Thus, exposure estimates were made which were specific to each child.

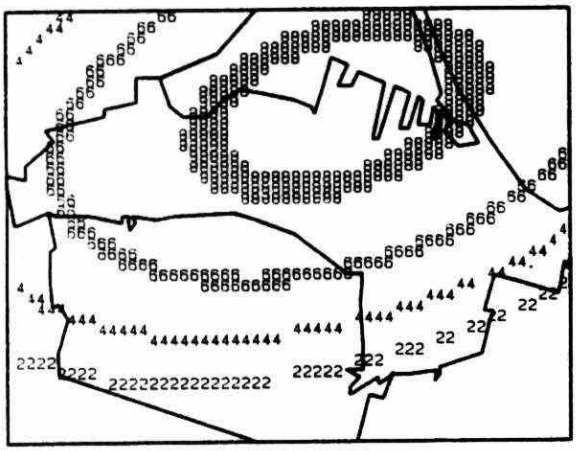
This procedure was carried out both for TSP measurements, and for derivatives of the PSD measurements, as well. The PSD measurements were summarized in two different ways: first, as mass median diameter (MMD), and secondly, as fine fraction (FF) and coarse fraction (CF). For a given month, MMD was calculated at a given site by taking the sum of the loadings of a given stage (or of the backup filter) of the cascade impactor for the (usually) 5 sample days of that month. A monthly MMD then was calculated (using the standard method) from the summed values for all four stages and for the backup filter. A response surface in MMD was then generated over the area of the city, and estimated exposure values for each school, and subsequently, for each child, were determined as before. We defined CF as that particulate matter trapped by the first 2 stages of the Andersen four-stage cascade impactor, and FF as that trapped by the next two, and the backup filter. This gave rise to a nominal differentiation in

particle size of >3.3 um (CF) and <3.3 um (FF). This differentiation is based on the pattern of deposition of particles in the lung, FF being preferentially distributed to small airways (<2 mm) where early chronic lung disease is thought to manifest itself. To calculate exposures based on the coarse fraction, we simply summed the first 2 stage loadings for all sample days in a given month, and then calculated a concentration based on that loading (in ug/m3). The FF concentration was calculated in a similar manner from the third and fourth stage and the backup filter loadings. Again, response surfaces in CF and FF concentrations were computed for each month, and corresponding exposure estimates were made in the manner already described.

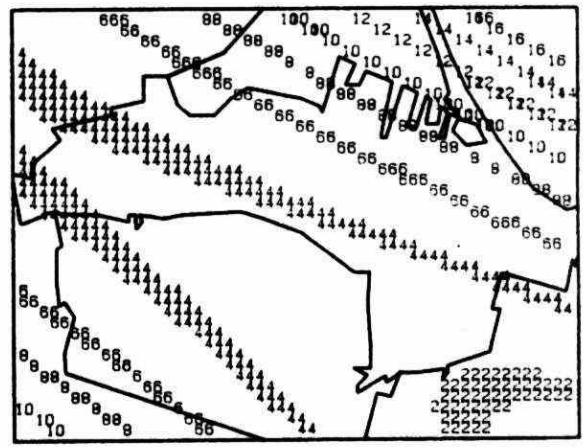
For each child, yearly estimates of exposure dose for TSP, MMD, CF, and FF were computed. In addition, the error inherent in each of these estimates were also estimated. Examples of response surfaces for TSP and MMD for May and December are shown in the Figures, The similarity in corresponding months of different years, and the differences between the months of the same year, should be noted.

This method of determining exposure levels of air pollutants has not previously been reported in conjunction with an epidemiological study of respiratory health. We have attempted to refine the exposure estimate relating to ambient air pollution to give as representative a value as possible for each subject in our study. However, from our studies of indoor air quality (previously reported here), we know that, in schools, particulate levels are not dependent on outdoor levels, while in homes, indoor particulate levels depend in part on the presence of smokers in the house. Thus, the exposure values we determine from outdoor data provide an estimate for the time the child is outdoors. However, only to the degree that particulate matter co-exists with other pollutants which penetrate indoors (such as NO2), do they provide a clue to the indoor exposure.

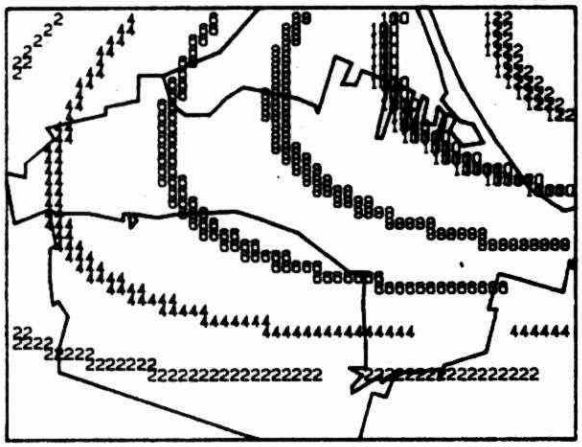
When the SO2 data are made available, we will be able to compute outdoor exposure in a similar manner to that described for the particulate data. We will also make use of the transfer functions which we obtained from the indoor study, to refine these estimates to take account of the exposure due to the penetrated SO2.



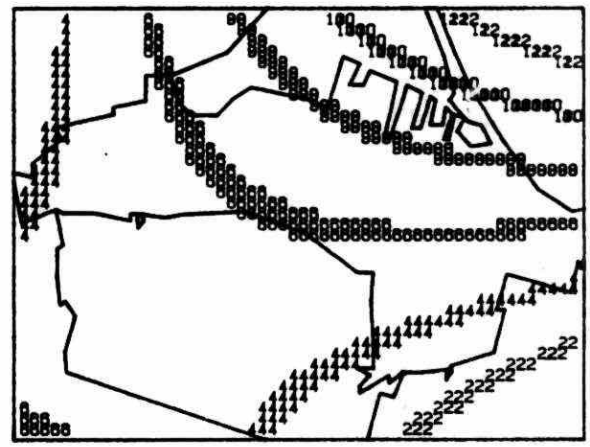
MAY 79



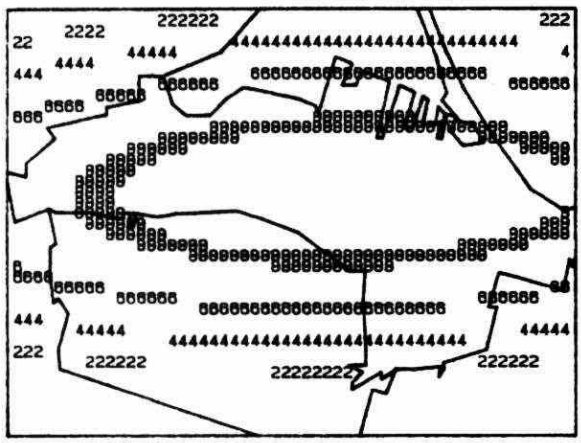
DEC 79



MAY 80



DEC 80



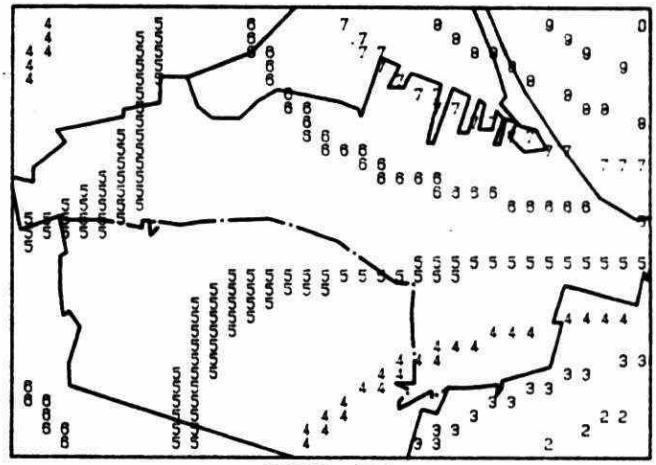
MAY 81



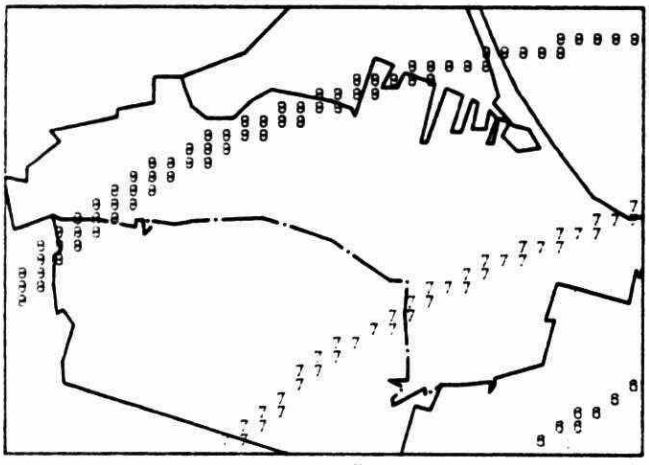
DEC 81



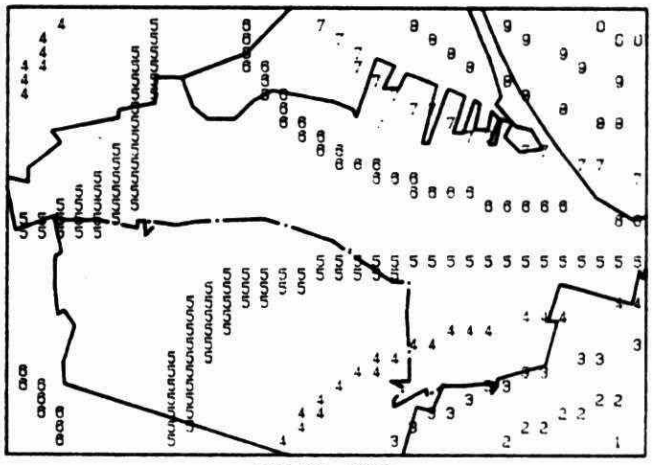
MAY 79



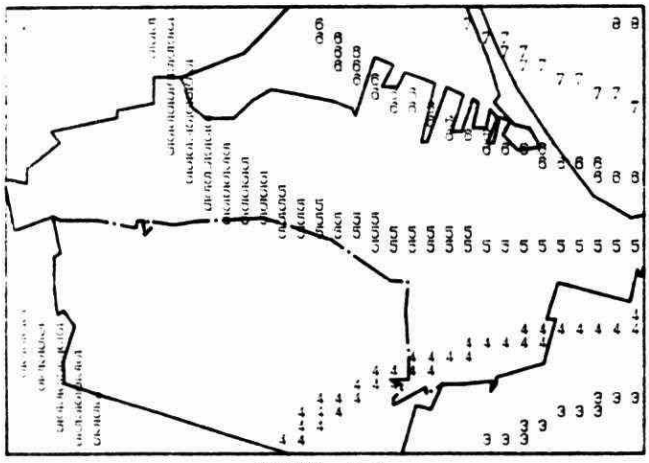
DEC 79



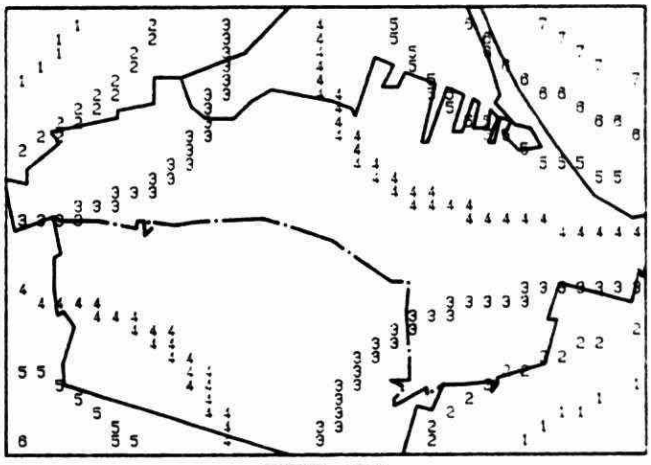
MAY 80



DEC 80



MAY 81



DEC 81

The Dispersal of Airbourne Particulates on a Short- and Long-term Scale

G.R. Palmer, J.D. MacArthur and P.P. Wilson

Department of Physics, Queen's University, Kingston, Ontario K7L 3N6

ABSTRACT

The local meteorological conditions, especially the wind velocity, are important when assessing the dispersal of air particulates from localized sources such as foundries and traffic intersections. To provide this information when measuring the element concentrations on an hourly basis with a streak filter, a microprocess-controlled meteorological station measuring components of the wind velocity, rain fall, temperature and light intensity has been constructed.

The system samples the parameters every seven seconds and stores a thirty-minute average of each parameter for later correlation with the element concentrations in the deposits. Besides monitoring the weather conditions, the microprocessor also records a thirty-minute average of the air flow through the sampler. The latter is found to vary significantly, possibly due to the relative humidity, and therefore needs to be known if accurate concentrations are to be determined. It is planned to install a transducer to measure this parameter.

The project to determine annual variations in pollution through the observation of element variations in tree rings has continued. Cores from several more trees from Sudbury have been examined with emphasis placed on measuring the lighter elements Si, Al and Mg. When PIXE analysis is done in air, the air path from the target to the Si(Li) detector strongly attenuates the X-rays from these elements. To reduce this problem, the detectors have been fitted with teflon cones extending to within a few millimetres of the target and hydrogen gas is bled into these cones to displace the air. Attenuation of the X-ray intensity is then only due to the detector's Be window. Interest in these elements arises from the conjecture that acid rain lowers the pH of the soil so that elements such as Al are freed from their minerals. These experiments are designed to test whether the concentrations of such elements increase in the rings with higher levels of acid rain.

Introduction

Many of man's activities to improve his material comfort produce waste byproducts which he discharges into the environment without due consideration of their effect on his "quality of life". These byproducts are often harmful to him, yet only recently has he begun to monitor these hazardous materials as they move through the environment. Using proton induced X-ray emission(PIXE) for determination of the elements present, we have investigated tree rings as a record of long term pollution. Also by collecting air particulates on a moving filter near a traffic intersection, we have studied short term pollution from a localized, time-dependent source.

Air Particulate Project

PIXE analysis of air particulates on streak filters have shown the necessity for simultaneous micro-meteorological data (Barfoot et al 1979, MacArthur and Palmer, 1983). Such local weather data, especially wind velocity, when correlated with time scans of element levels on the streak, are invaluable in source identification. In this report, the design and initial data collected by a microprocessor-based weather station are presented. This instrument has been constructed in combination with a streak filter apparatus to study the composition and dispersal of particulates from a busy traffic intersection in Kingston. Particular emphasis is being directed towards Pb and Br produced in gasoline combustion.

Streak Sampler and Weather Station

The streak sampler has been described in earlier reports (MacArthur et al. 1983a,b). The instrument pumps air upwards at a flow rate of approximately 0.1 l/min through Nuclepore filter with a pore size of 0.4 μm. The filter is

mounted in a 20 cm cartridge which is moved past a 2 mm x 4 mm pumping nozzle at 1 mm/hr. The instrument collects a 4 mm wide streak record of air particulates of approximately one week duration with a 2-hour time resolution. The sampler is believed to collect mainly the small particulates of the bimodal distribution of particle sizes typical of urban aerosols(MacArthur and Palmer, 1983).

In the past year, a microprocessor-based weather station has been added to the portable apparatus. Transducers interfaced to the microprocessor measure various meteorological parameters. Most sensors were commercially obtained; wind speed and direction - Sierra Misco Inc, Berkeley Ca., model 1036Hm; temperature - Yellow Springs Inst. Co., Yellow Springs, Ohio, model 44212 thermolinear composite; light - Clarex Electronics, Mount Vernon, N.Y., model CL5ms cadmium sulphide photoconductivity cell; rain - Edmund Scientific model 72165 digital rain gauge. It is planned to include a humidity sensor (Sierra Misco Inc, model 2040S) since fluctuations in flow are believed to arise from pore blockage in the Nucleopore during periods of high humidity (Air Resources Branch (MOE), 1978).

The flow meter (Fig. 1A) was constructed as a mass flow design (Sheingold, 1980). Two linearized thermistors (Yellow Springs Inst. Co. model 44202) are placed in the centre of a 1.3 cm metal tube, 7.6 cm on either side of a heater consisting of eight 1/8 W, 560 resistors. The resistors are in a grid pattern perpendicular to the air flow through the tube. The tube is insulated by ~5 cm of styrofoam. The two temperature sensors are on one side of a Wheatstone bridge (Fig. 1B). Thus the voltage measures the temperature difference between the sensors upstream and downstream from the heater. This temperature difference is determined by the mass flow of air which was calibrated at normal room temperature and pressure against volume flow using a rotameter.

A schematic of the computerized weather station is shown in Fig. 2. A microprocessor (Motorola M6809) samples the transducers interfaced to the various inputs (7 analog and one digital). In the current program all transducers are sampled every seven seconds, and for each input except rain and wind direction a running sum, is kept. After 256 samples of each parameter (i.e. 0.5 hr), an average is calculated for each sum. These 256-point averages are stored in an EPROM along with elapsed time. Pulses from the rain gauge on the digital input are totalled rather than averaged.

To circumvent the problem of the wind direction discontinuity at 360° and to obtain an indication of "wind distance", instantaneous N and E components of the wind velocity are calculated by the program after each 7 second sample. This is done using the sampled values of the wind speed and direction. First the A/D value of the wind speed is converted to km/hr using a look-up table based on the calibration of the anemometer. Second the A/D reading of the wind angle, θ, is used in a look-up table for either $\sin\theta$ (east component) or $\cos\theta$ (north component). These tables were obtained from the calibraton of the wind vane. Finally the north and east components are obtained by multiplication of the converted speed and $\cos\theta$ or $\sin\theta$ respectively. A running sum of these components is kept and at the end of 1/2 hour, total N and E components are stored on the EPROM. In addition an average wind speed is stored; however the sampled wind direction is not recorded. In later analysis, the total wind components are used to calculate a wind vector for each half-hour period from which the magnitude and direction can be obtained. This magnitude, compared to the average wind speed, provides an indication of wind variability (i.e. var=magnitude/speed) and wind distance (i.e. dis = magnitude x sample time) for each half-hour sample.

The weather station is designed for minimal operator control. However an LED display controlled through a keyboard enables the operator to verify

proper operation of the apparatus. With appropriate keyboard commands, instantaneous values of the sampled weather parameters may be displayed. Also an indication of any errors in writing to the EPROM may be detected.

The 4K EPROM used is sufficient for 8.5 days of data which is similiar in duration to that recorded on the streak filter. At the end of one week, both the EPROM and the filter are returned to the lab for analysis. The meteorological data are read into a PDP 11/60 computer where the A/D readings are decoded using the transducer calibrations. Fig. 5 shows scans of the weather parameters for a two week period.

PIXE Analysis of the Streak Filters

Element levels on the streak filter are measured by PIXE using an external proton beam from the Queen's Van de Graaff accelerator (MacArthur and Palmer, 1983). In this technique, characteristic X-rays are produced when protons hit the constituent atoms of the sample. The X-rays are detected in a Si(Li) detector and using pulse height analysis, a spectrum of the number of X-rays with a specific energy is produced. To enable detection of low energy X-rays from Na, Mg, Al, and Si, a teflon cone has been fitted to the snout of the detector. Hydrogen gas is bled into the cone to replace the air between the detector and sample and thereby eliminate the absorption of low energy X-rays by air. Fig. 3 shows a typical spectrum from a streak filter with and without H_2. A large increase in detection efficiency(Fig. 4) for the low energy X-rays is evident with the H_2 flowing.

Spectra are obtained at 1 mm intervals on a streak filter by moving the filter through the proton beam with microprocessor-controlled stepping motors. Thus spectra are obtained at one hour intervals on the one week streak filter. Each spectrum is fitted automatically by a non-linear least squares program (Bevington, 1969) to provide the identification and counts in each X-ray peak. Subsequently, another program collects all the fitted counts for a specific

element in the 180-odd spectra from each week. Typical scans of peak counts are shown in Fig. 6 for the major elements detected.

A final step in the analysis is to investigate possible correlations between various elements and the meteorological records. This is performed using a linear regression program. Fig. 7 shows a typical regression between two elements from a streak filter. A high correlation coefficient indicates the two elements likely have the same source. Such correlations are useful in tracing the source of pollution. A more sophisticated factor analysis (Roscoe et al., 1982; Heidam, 1982) is under development to further improve our source identification.

To calibrate the detection sensitivity of the various elements in a thin sample (i.e. a streak filter) for a particular experimental arrangement, an efficiency curve is obtained using several thin standards (Micromatter Corp., Eastsound Wa). These standards consist of known thicknesses,t, (typically 50 $\mu g/cm^2$), of one or two elements evaporated onto a 10 μm mylar film. X-ray spectra are collected from each standard with a total beam charge, q (μC) and subsequently peak counts, A_s, are obtained for each characteristic X-ray. Detector sensitivity, $\epsilon(E)$, (counts/μC-$\mu g/cm^2$), at each X-ray energy is then calculated from

$$\epsilon(E) = A_s/qt. \qquad (1)$$

A typical sensitivity curve is shown in Fig. 4. Very obvious is the considerable improvement in detection sensitivity at low energy provided by the use of H_2. Such efficiency curves are reproducible to 10% for a particular detector geometry and proton energy.

Element concentrations, C($\mu g/m^3$), in the sampled air may be obtained using the total air flow, Q = Tf(m^3), through the nozzle during a sample time, T(hr) at an air flow rate, f(m^3/hr). T is the time taken for the sample to move past the 2 mm nozzle (i.e. T = 2 hr for a filter movement of 1 mm/hr). Element

concentrations in the air can be calculated as

$$C = A_n A_p / q' \epsilon(E) Q \qquad (2)$$

where A_n = nozzle area($0.08 cm^2$)

A_p = peak counts for the characteristic X-ray

q' = accumulated charge (μC) on the streak sample during collection of the spectrum

$\epsilon(E)$ = detection efficiency (Counts/ μC-$\mu g/cm^2$) given by equation (1).

Air Particulate Results

The weather station and streak filter has been tested for a two week period (Aug 28 - Sep 14) in a residential area approximately 1 km SW of the intersection near which previous measurements were made(MacArthur and Palmer, 1983). Scans of the most relevant meteorological parameters recorded during this period are shown in Fig. 5. At present, the light sensor is adjusted to have maximum output in bright skylight; hence it provides an indication of cloud cover. The rainfall records should be valuable in investigating washout of air particulates as well as the quenching of natural dust. No correlation was obtained betweeen periods of rainfall and the air flow record (not shown). This suggests that the particulates were non-hygroscopic and did not cause pore blockage during periods of high humidity. Both the magnitude and direction of the wind velocity are useful in the present study of particulate dispersal from a point source. Considerable variation is evident in both the magnitude and direction of wind velocity. Several periods of up to 2-3 days with constant wind direction were detected. Also there were several periods during which the wind did not blow as indicated by the flat sections at the top of the direction graph.

PIXE analysis of the streaks collected concurrently with the above meteorological data has been made and the scans of several element levels are shown in Fig. 6. The very large increase in levels of Al, Si, Ca and Fe in

Fig. 6A on the morning of Aug 31 is suggestive of natural dust. The meteorological data shows that the wind, although weak during this time, was from the NW which may have carried dust from a construction site near the intersection under study. No other meteorological parameter appears correlated with this peak in the level of the 'natural' elements. Furthermore, Ca, likely derived from limestone of the region, shows several peaks in concentration which are absent in the scans for Al, Si and Fe.

No such increase in levels of S, Zn, Pb and Br, generally considered of anthropogenic origin, was observed on Aug 31 as is evident from Fig. 6B. High levels of S are correlated with winds from the South. Moreover S levels appear partially anticorrelated with rainfall which would indicate a washout phenomenon. The average levels of Br and Pb were in the ratio of 0.35 which is within the range observed for these elements in gasoline exhaust(Paciga et al. 1975). The level of these two elements are highly correlated, Fig. 7, with a correlation coefficient of 0.86. Partial correlation with rush hours is apparent during the period Sep 2,3 when strong winds blew consistently from the NE, a condition favourable for transporting automotive exhaust from the intersection to the sampling site.

Table 1 presents the average and maximum levels of the major elements detected in the streak filter during the period Aug 28 - Sep 14. The maximum levels for Al, Si, Ca and Fe are high due to the very large quantities of these elements observed on Aug 31. However the average concentrations appear consistent with our previous measurements in Kingston and with levels detected in other cities.

Tree Ring Project

In this investigation, the element concentrations in tree cores were determined with a spatial resolution less than the size of the rings in order to observe any trends which could be associated with anthropogenic activities nearby. Several such studies have been inconclusive in showing whether tree rings maintain a record of their environment(Baes III et al., 1981; Lepp, 1975). The problems are: element levels in trees are not known; elements may be transported radially within a tree; and uptake mechanisms are uncertain for most elements.

In this study, the elements in trees both near and distant from the nickel smelters in Sudbury have been measured with PIXE. Smelting at Sudbury has occurred since late in the nineteenth century with increasing concern about the effects of pollution until in 1972 a high stack was constructed by INCO in order to disperse the gaseous effluent. It was this change in dispersal which was sought from a record of element concentrations in the trees.

Experimental method

Cores of 1/4" diameter were taken from several trees. These cores were mounted in teflon blocks for rigidity. A flat surface was made with a fine file. Tests (MacArthur and Palmer, 1983) were performed to check that irregularities in the surface were less than a few micrometers and that these did not effect the results by preferentially absorbing low-energy X-rays.

The elements were measured by PIXE with an external beam from the Queen's microprobe. The proton beam of 3 MeV had a diameter of ~25 micrometers and an X-ray spectrum was accumulated while the beam moved ~100 micrometers over the flat surface of the core. Each spectrum obtained was automatically analyzed to identify the elements detected and to obtain the number of counts in each

peak. The system was calibrated with pressed samples of NBS(National Bureau of Standards, Wash., D.C.) pine needle, bovine liver and orchard leaf standards so that the number of counts for each element could be converted to a concentration. The calibrations from the major peaks, such as P, S, K, Ca were in agreement between standards to ~15%, while the calibrations for the weaker lines at concentrations of ~100ppm, such as Mn, Fe and Zn agreed within 50%. This inconsistency is likely due to pulse "pile-up" in the detector and to inhomogeneity in the standards.

Acid rain is believed to lower the pH of soil and release elements, principally Al, which are detrimental to vegetation. Therefore, air near the sample and in the path of the X-rays from the target to the detector was displaced by H_2 as described above in order to observe the lighter elements Si, Al, Mg and even Na.

Results

The most extensive results have been obtained for cores from two red pines, A growing at Azilda, 7.8 km NW of the high stack, which might be expected to be more contaminated than B from a tree growing at Penage, 32.5 km SW of the high stack. Core A came from a tree with a diameter of ~18 cm and on it the scan extended ~6.5 cm inward from the bark covering a period from the summer of 1981 to the summer of 1949. Core B came from a tree of similar diameter and on it the scan extended ~4.5 cm from the bark, covering a period from the summer of 1981 to the summer of 1924. The years were deduced from a count of the rings.

For observing trends, the data are best presented as scans. Fig. 8 shows such scans from core A for several of the elements. The graph labelled BREM depicts the integrated counts in the background under the peaks. These background X-rays arise when electrons "knocked on" by the protons are stopped in the material producing bremsstrahlung radiation. Its intensity is a measure

of the electron density in the material and hence for material of unchanging composition such as wood, the amount of material through which the beam passes. For a constant incident beam current, the bremsstahlung rate should be constant. The decrease in counts for spectra 320-380 is due to a change in the beam intensity which is difficult to monitor. The decreased counts in all other scans for these same spectra are due to less fluence rather than to a decrease in the element level.

Apparent from these scans are localized spots, the size of a few cells, where high concentrations are observed for nearly all elements. Trends are less distinct and, in particular, the summer-winter variation for Mn, reported previously is not apparent. This is possibly a result of the small size of the dark portion of the rings (~150 μm) compared to the step size(~100 μm); a situation causing the variation to be "washed out". However, the observed increase in the Mn level towards the center of the tree is similar to that observed previously and to that reported by Legge et al (1984) for pine trees in Alberta. Whether this is a general characteristic of the Mn level in trees is not yet clear. Mg may also show this same trend; as a quantitative estimate of this change, the average concentration of Mg for the years 1950-1960 is 460 ppm while that for the years 1963-1980 is 270 ppm. On the other hand, the concentration for Al increased from 150ppm to 250 ppm between these two periods. Several other elements, Si, K, and the heavy metals Cu and Zn, are uniformly distributed throughout the tree.

No dramatic changes in the sulphur level are observed. Before 1960 the average level of S was higher(330 ppm) than that after this date(200 ppm), especially if the levels in the last two years just inside the bark are not included. The surface and a region in the centre of the bark has a high sulphur content, perhaps evidence that the bark acts as a barrier to the uptake of S from the air.

PIXE readily provides a qualitative analysis of elements present in a sample. All the elements observed in both cores are shown in Table II with an indication of the number of spectra in which they were detected. Also shown is their average level assuming they were uniformly distributed in the wood (the levels in the bark are usually different). For those elements, observed in a large majority of the spectra, the accuracy of the average depends on the standard calibration. However, because the fitting program sets a lower limit for the detection of weak X-ray peaks, the average for elements found only a few times, is probably too low. A good example is Ni which was detected 18 times in 489 spectra obtained on core B. For these occurrences, the average concentration is 489/18 x 1 = 27ppm. The true level for Ni is between this value and that in the table.

The differences in element concentrations for trees near and distant from the smelters are similar to those observed previously, even though in the previous study the red pine analysed grew near Levesque St. in Sudbury; Mn and Cl have higher concentrations for the tree from Penage while S and the heavy metals, Fe, Ni, Cu and Zn, appear with lower concentrations in this core. The latter observation suggests that elements in the emission from the smelters do find their way into the trees. In this experiment, where the light elements have been detected for the first time, a very significant difference is observed in the levels of Al and Si between the trees from the two locations; in the tree farther from the smelters, Al and Si were rarely observed and then at only at very low concentrations.

Conclusions

The air particulate study has shown the PIXE-streak method to be extremely useful for detecting pollution events lasting a few hours. The multi-element capability of the PIXE method combined with the high temporal resolution of

the streak filter provides the facility for interelement correlation which is often decisive in source identification. Simultaneous meteorological data has been shown to further aid in the interpretation of pollution records and the understanding of short term pollution dispersion. Several questions have been raised by the data and further research will attempt to clarify the interpretations.

Element analysis of trees with PIXE provides a wealth of information about the concentrations of these elements and their distribution within the tree. The change in the dispersal of the effluent from the smelters at Sudbury has not produced a dramatic change in the S content of the red pines growing nearby. There are significant differences in the element levels, especially the mewtals Ti, Fe, Cu and Zn between pines growing near and far from the smelters. Some of these are probably due to different soils. Whether the very different levels in the light elements observed in the two red pines reglects their different environments brought about by the smelter emissions is a tantilizing question which is receiving further study.

Table I

Element Levels in Air at a Residential Site in Kingston

Element	Average Concentration ($\mu g/m^3$)	Maximum* Concentration ($\mu g/m^3$)
Mg	1.0	5.2
Al	1.5	15.2
Si	2.3	54.2
S	2.9	18.9
Ca	1.0	5.8
Cr	0.7	0.72
Mn	0.02	0.14
Fe	0.42	6.8
Cu	0.02	2.1
Zn	0.04	0.75
Br	0.04	0.26
Pb	0.11	1.1

*Maximum concentrations for Al, Si, Ca, and Fe are based on a very high incidence of these elements.

Table II

Concentrations of Elements in Red Pines

698 and 489 spectra were taken on cores from trees at Azilda near Sudbury and at Penage 32 km from Sudbury respectively. The number of spectra in which each element was detected is given.

	Azilda		Penage	
Element	#	ppm	#	ppm
Na	34	100	4	-
Mg	291	340	34	24
Al	206	170	22	<1
Si	567	505	5	<1
P	154	22	78	29
S	698	290	486	58
Cl	574	230	244	410
K	695	720	451	660
Ca	698	1960	470	810
Ti	242	11	109	<1
Mn	689	92	475	183
Fe	387	30	94	6
Ni	40	2.5	18	1
Cu	162	19	16	4
Zn	135	17	30	4

References

Air Resources Branch(MOE) (1978), "Performance Characteristics of the Nucleopore Air Sampling Filter", Internal Report No. ARB-TDA-46-78.

C.F. Baes, III and H.L. Ragsdale (1981), "Age-Specific Lead Distribution in Xylem Rings of Three Tree Genera in Atlanta, Georgia", Environ. Pollut., B2, pp. 21-35.

K.M. Barfoot, I.V. Mitchell, H.L. Eschbach, P.I. Mason and W.B. Gilboy (1979), "The Analysis of Air Particulte Deposits using 2 MeV Protons", J. Radioanalytical Chem., 53, pp. 255-271.

P.R. Bevington (1969), "Data Reduction and Error Analysis for the Physical Sciences", McGraw-Hill, New York

N.Z. Heidam (1982) "Atmospheric Aerosol Factor Models, Mass and Missing Data", Atmos. Envir, 16, pp.1923-1931.

A.H. Legge, H.C. Kaufmann and J.W. Winchester (1984), "Tree-Ring Analysis by PIXE for a Historical Record of Soil Chemistry Response to Acidic Air Pollution", Nucl. Instr. and Meth., B3, pp. 507-510.

N.W. Lepp (1975), "The Potential of Tree-Ring Analysis for monitoring Heavy Metal Pollution Patterns", Environ. Pollut., 9, pp. 49-61.

J.D. MacArthur, K.M. Barfoot and G.R. Palmer (1983a), "Long and Short Term Studies of Airborne Pollutants", Progress Report to Air Resources Branch, Ontario Ministry of Environment.

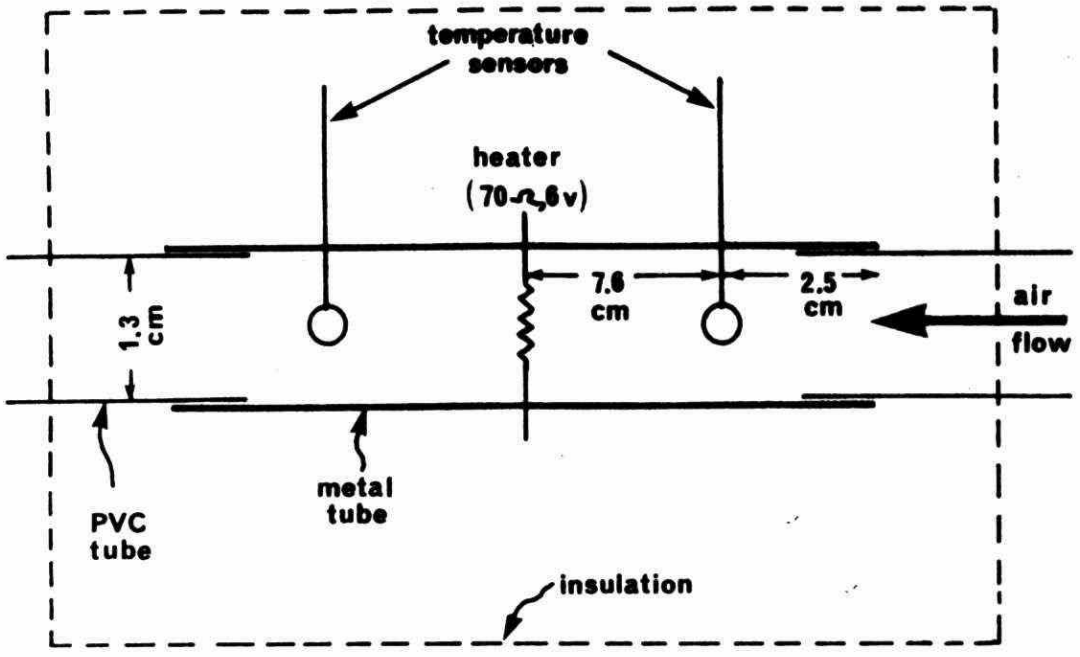
J.D. MacArthur and G.R. Palmer (1983b), "The Dispersal of Airbourne Particulates on a Short and Long Term Basis", Ontario Ministry of the Environment Technology Transfer Conference No. 4, Nov 1983, pp. 657-679.

J.J. Paciga, T.M. Roberts and R.E. Jervis (1975), "Particle Size Distributions of Lead, Bromine and Chlorine in Urban Industrial Aerosols", Envir. Sci. and Tech., 9, pp. 1141-1144.

B.A. Roscoe, P.K. Hopke, S.L. Dattner, J.M. Jenks (1982), "The Use of Principle Component Analysis to Interpret Particulate Compositional Data Sets", APCA Journal, 32, pp. 637-642.

D.H. Sheingold (1980), "Transducer Interfacing Handbook", Analog Devices Inc., Norwood, Mass.

A



B

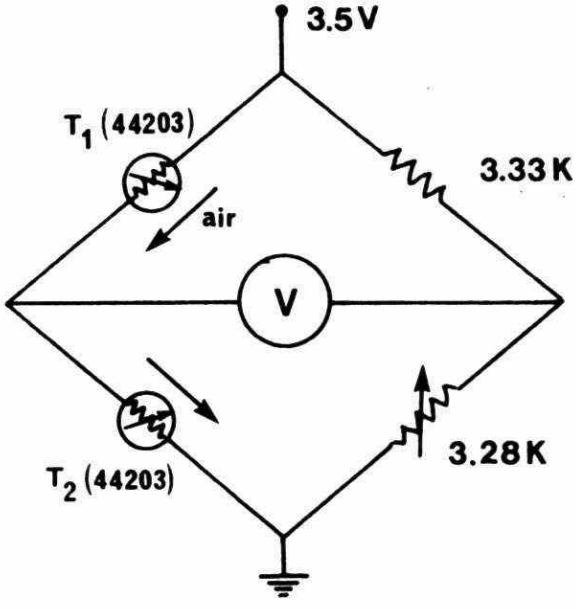


Fig. 1 Mass flow meter constructed to measure the air flow through nucleopore filter. Fig. 1A shows the heater, placed between two linearized thermistors inside a metal tube. Filtered air carries heat to the downstream sensor resulting in a temperature difference between the sensors which is proportional to the mass flow. Fig 1B shows the Wheatstone bridge used to convert the temperature difference into a voltage proportional to the flow.

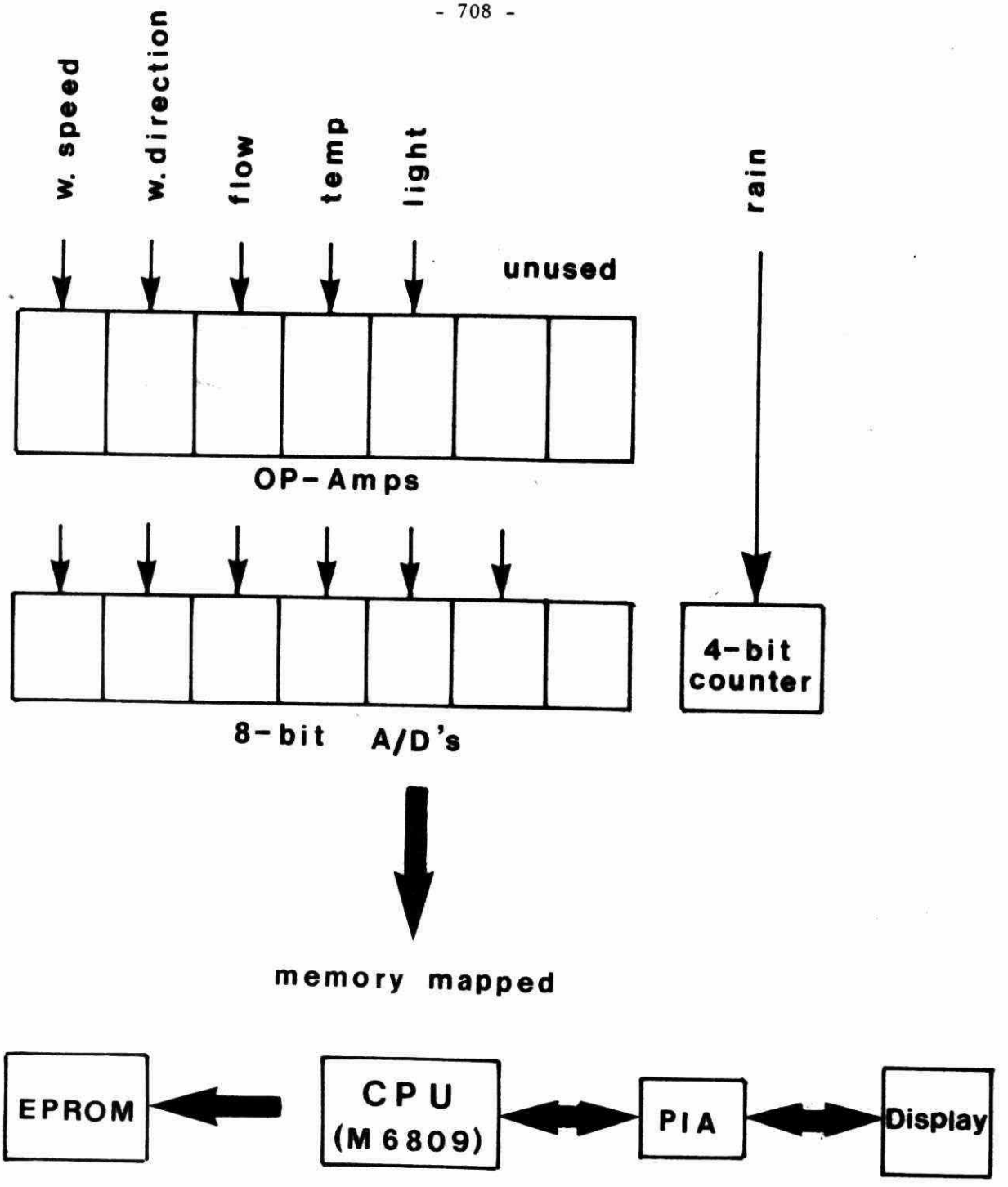


Fig. 2 Schematic of the microprocessor-controlled weather station. All inputs are sampled every 7 seconds by the CPU using memory mapping. Wind speed, flow, temperature and light readings are averaged and stored in a 4K EPROM after 256 samples (i.e. 0.5 hour). For the rainfall sensor a total count is stored. After each 7-second sample, the wind direction and speed are used to calculate North and East components of the instantaneous wind vector. These components are totalled and stored after 0.5 hr. Operation of the station may be monitored through the keyboard and display.

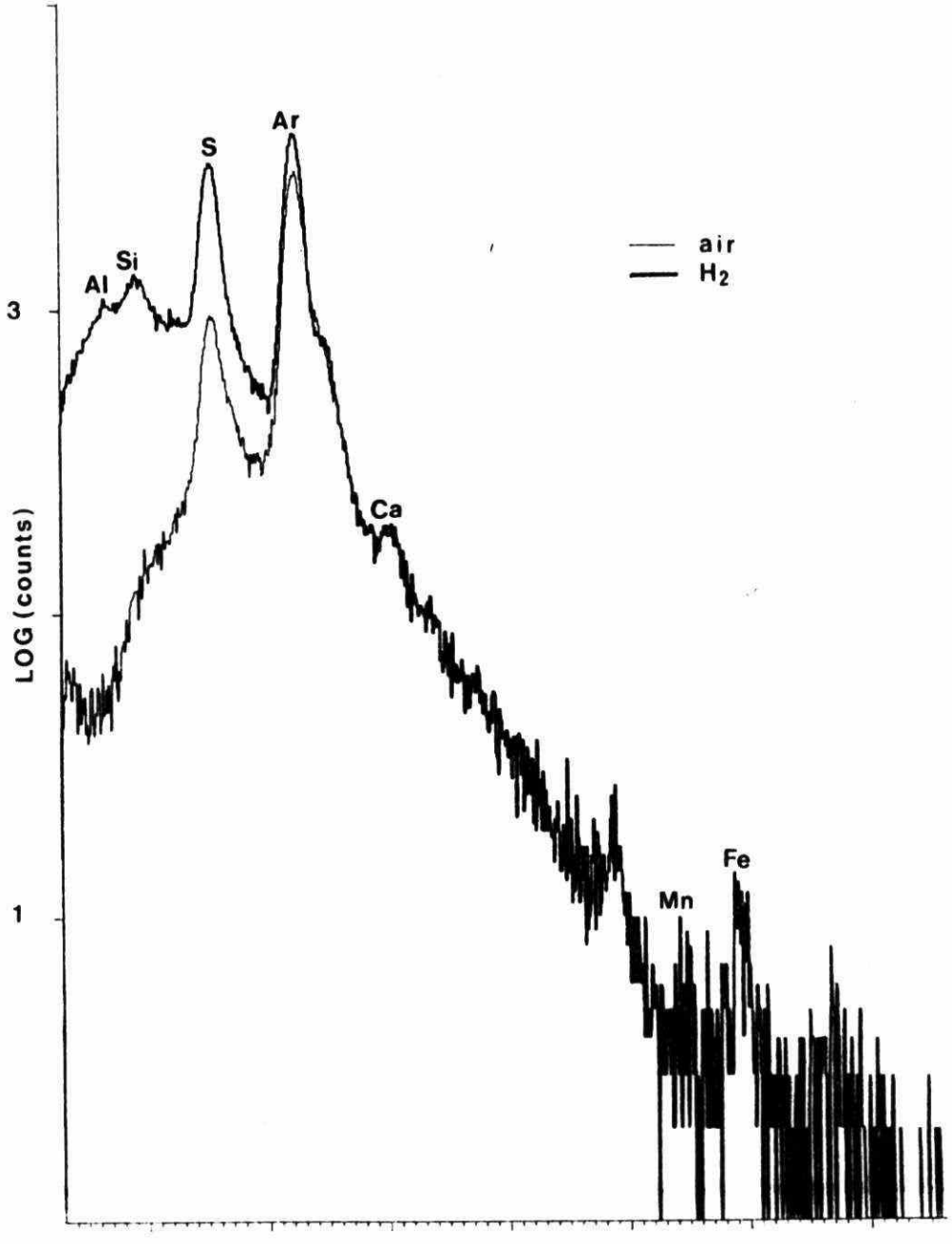


Fig. 3 Typical spectra from the streak filter without (light line) and with (dark line) H_2 displacing air in front and back of the filter as well as between filter and detector. The proton energy was 2.7 MeV while the fluence was 1.5 μC.

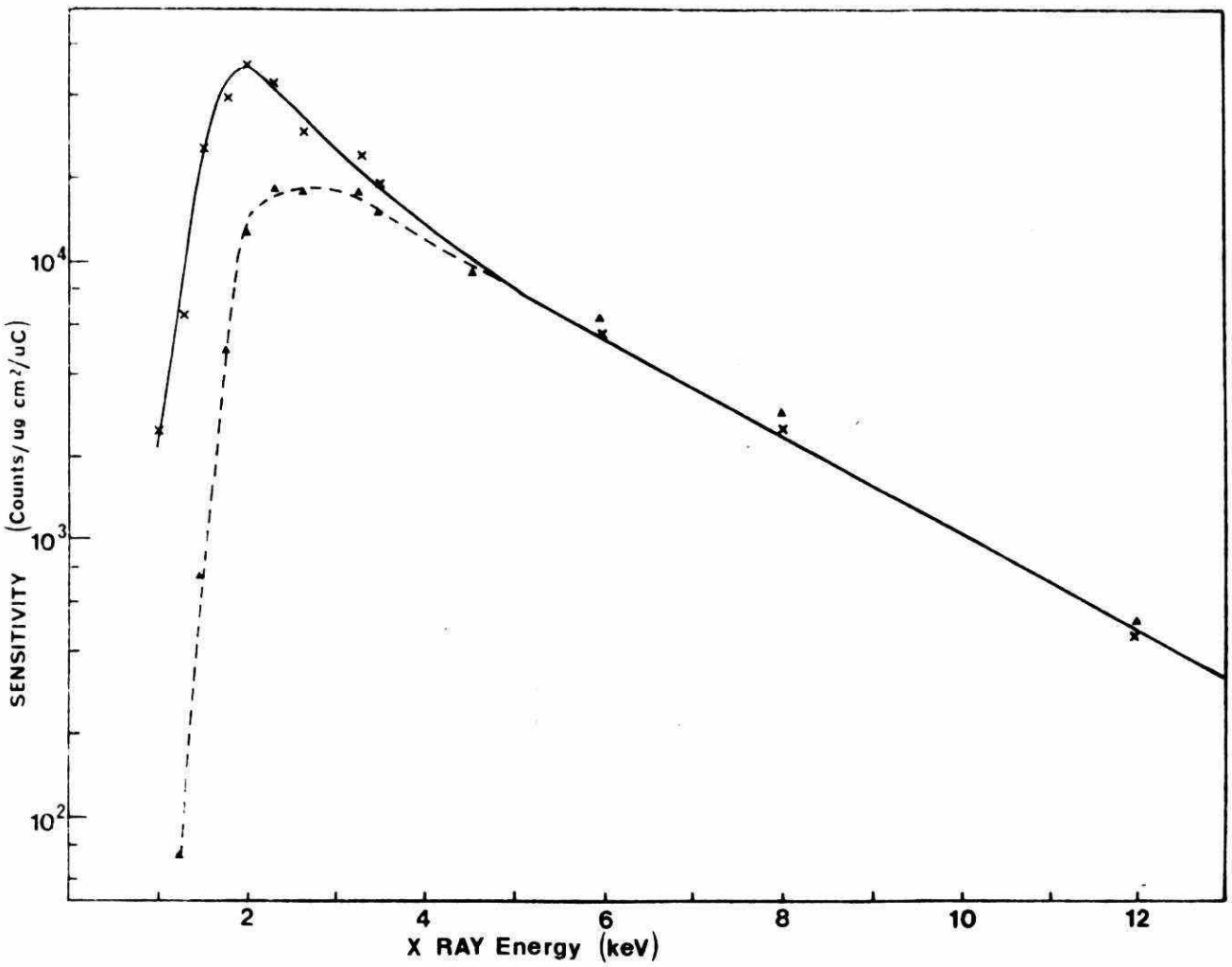


Fig. 4 The increase in sensitivity for the low energy X-rays with (solid line) and without (broken line) H_2 displacing the air between the target and detector. Thin standards from Micromatter Corp. were used for the calibrations.

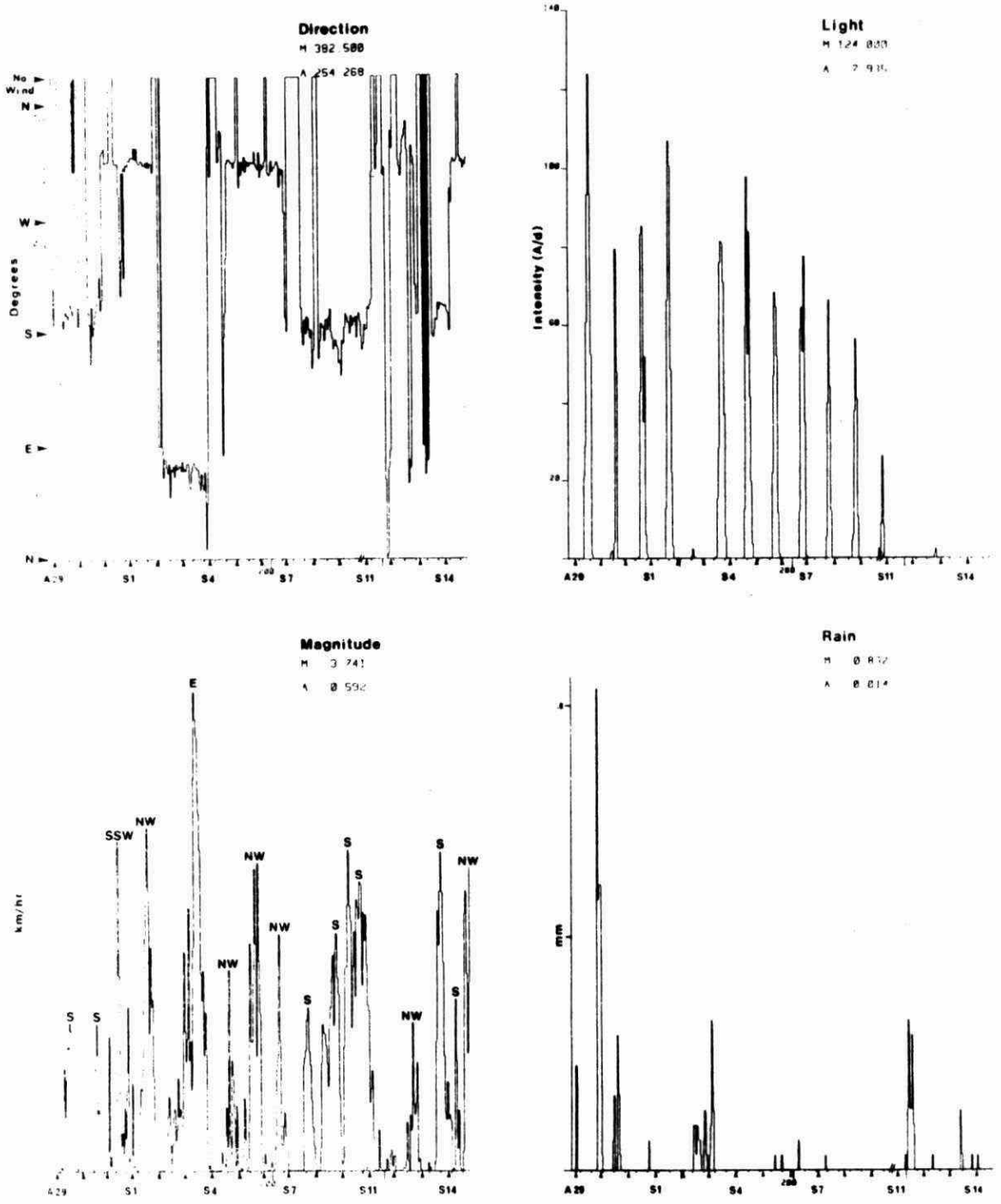


Fig. 5 Scans of meteorological parameters recorded at the sampling site during the study period Aug 28- Sep 14. The wind direction and magnitude were calculated using the total N,E components for each 0.5 hr period. The flat regions at the top of the wind direction graph represent periods of no wind.

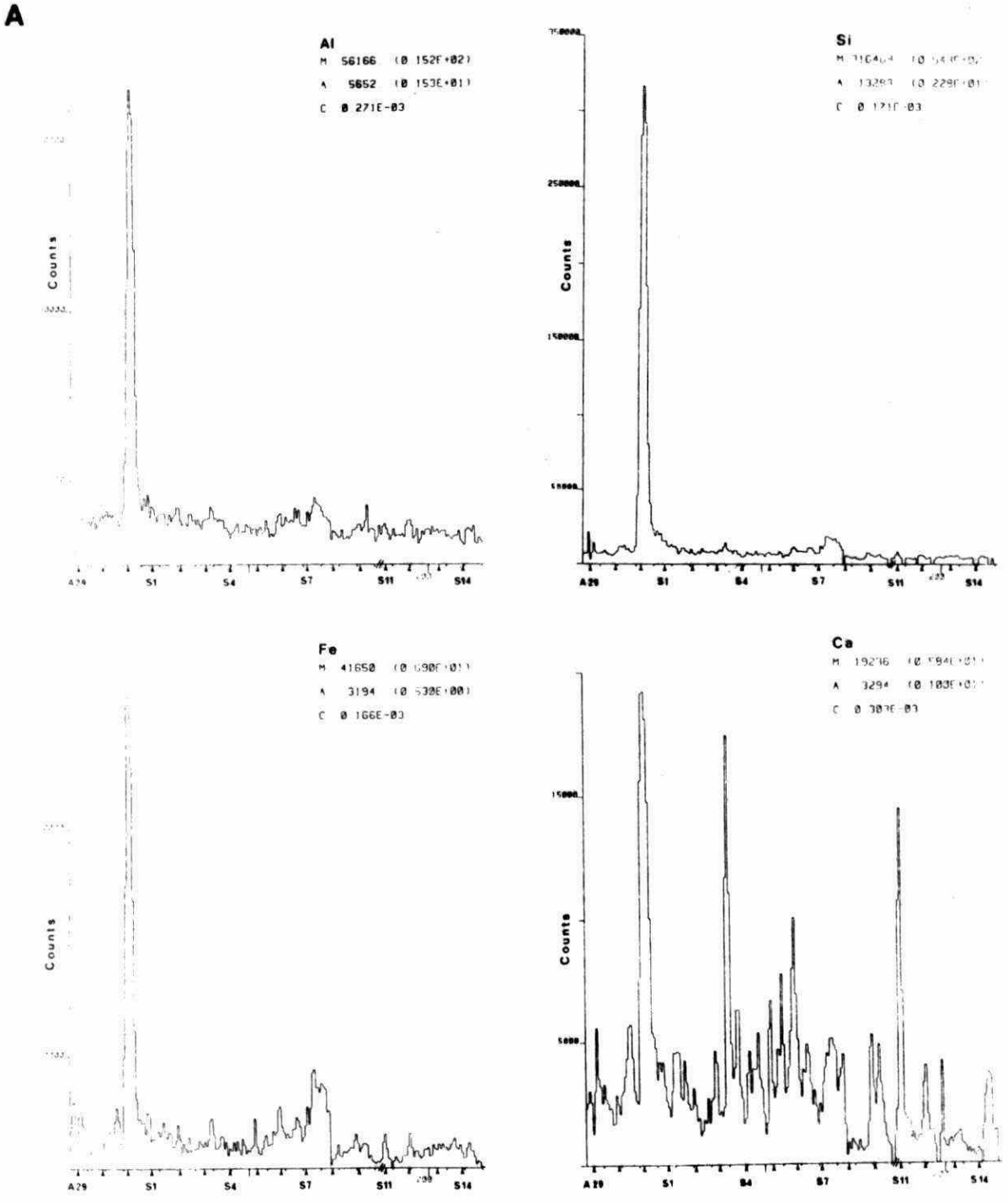


Fig. 6A Scans of the "natural" elements obtained by PIXE from the streak filter. Maximum, M, and average, A, values for the peak counts are shown for each scan with the values converted to air concentrations ($\mu g/m^3$) in brackets. The conversion constant, C, is calculated for a particular characteristic X-ray using equation (2).

B

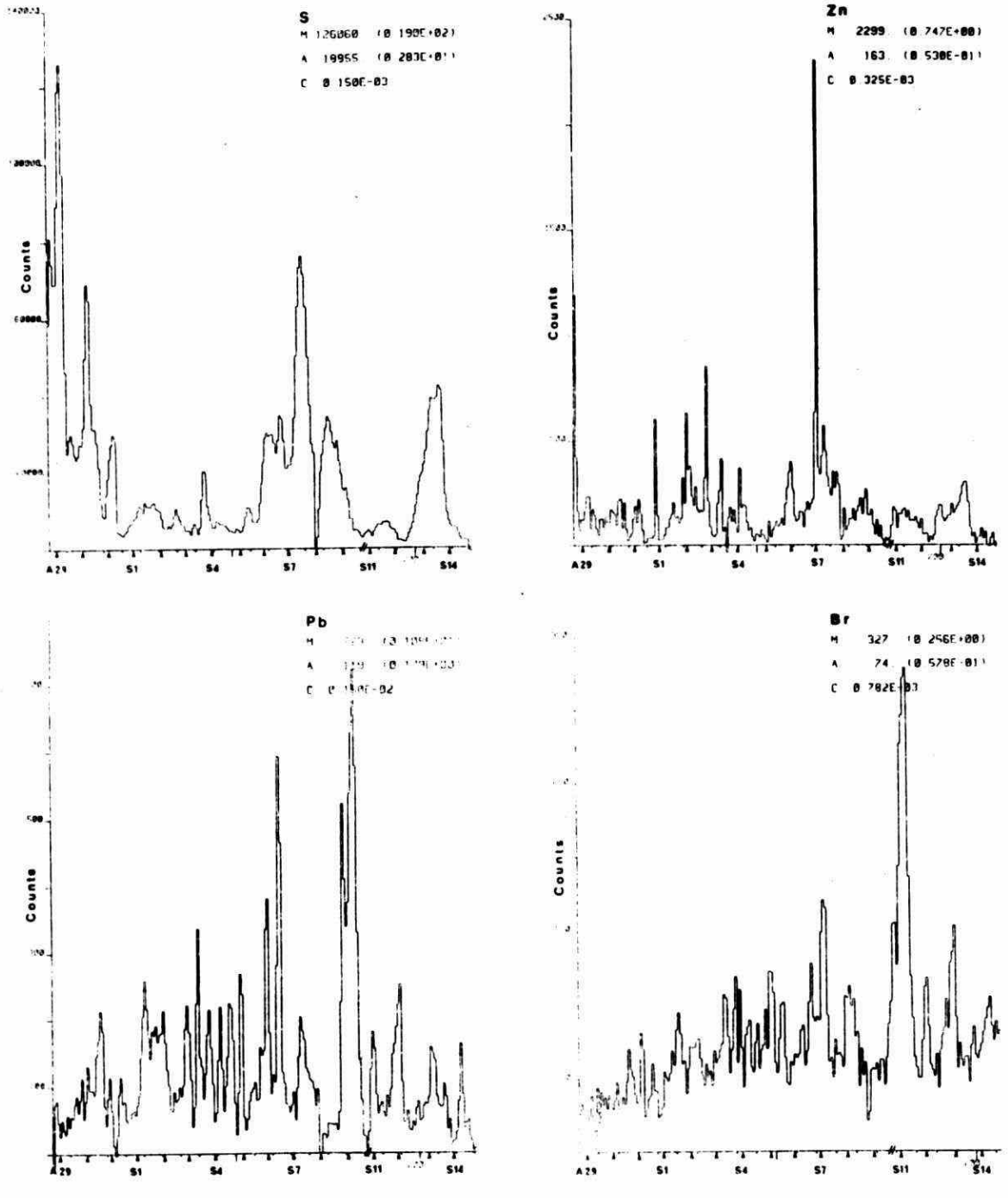


Fig. 6B Scans of the elements of anthropogenic origin.

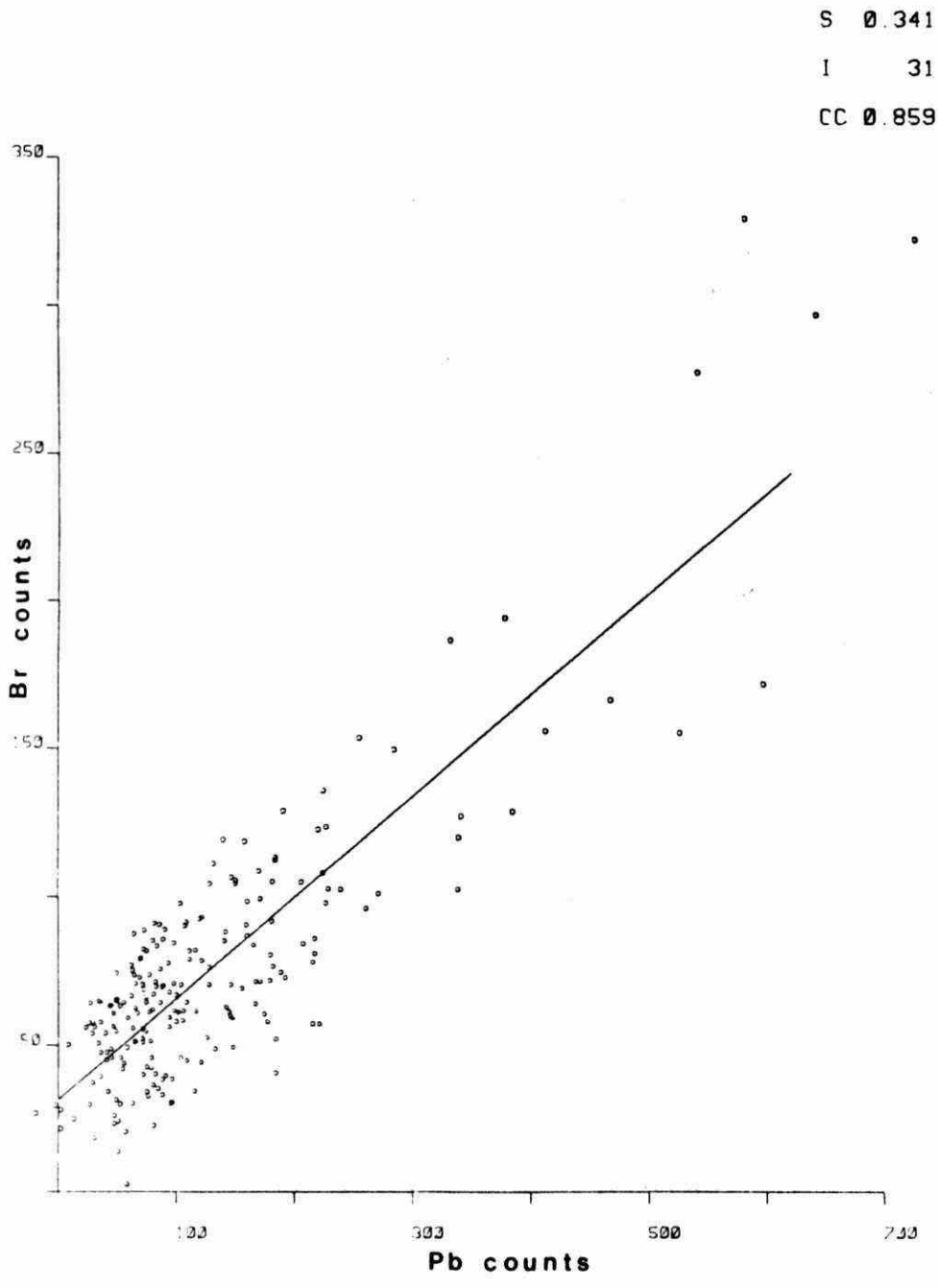


Fig. 7 Linear regression plot between the peak counts for the elements, Pb and Br. The correlation coefficient indicates the likelihood of a common source for the two elements while the slope indicates the X-ray ratio.

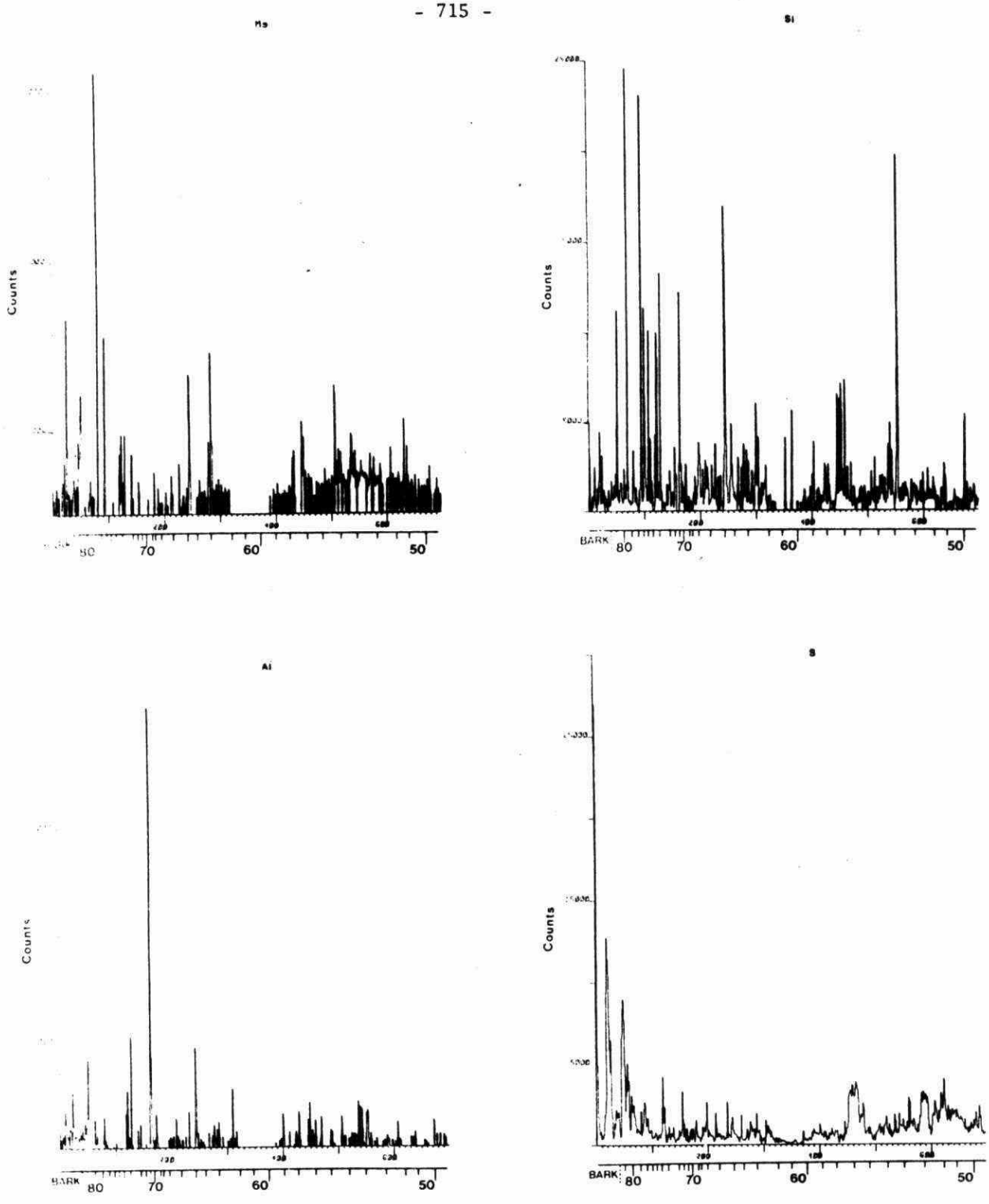


Fig. 8 Time scans for several elements observed in a core from a red pine from Azilda. The years extend from 1981 to 1950.

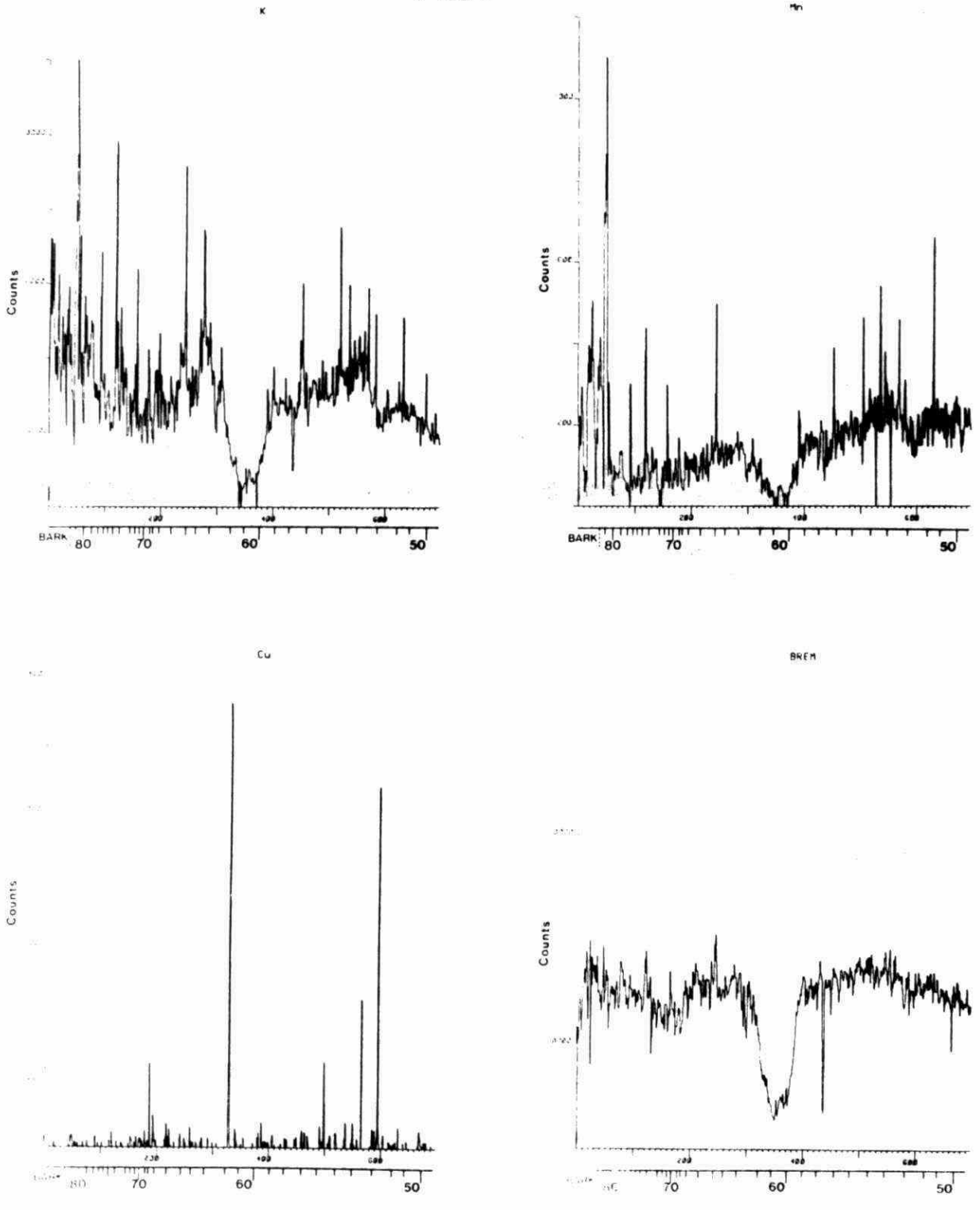


Fig. 8 Continued.

MONITORING GENOTOXICITY IN THE ENVIRONMENT USING SISTER CHROMATID EXCHANGES IN MICE

Authors: M. L. Petras and R. Piscitelli
Department of Biology
University of Windsor
Windsor, Ontario

To be presented at: Technology Transfer Conference No. 5
Ontario Ministry of the Environment
Airport Holiday Inn, Toronto

MONITORING GENOTOXICITY IN THE ENVIRONMENT USING SISTER CHROMATID EXCHANGES IN MICE.

M.L. Petras and R. Piscitelli, Department of Biology, University of Windsor, Windsor, Ontario.

ABSTRACT

Studies involving the exposure of tissue culture cells and of laboratory animals (via injection) to genotoxic agents have shown sister chromatid exchange (SCE) analysis to be a sensitive test for the detection of mutagenic and carcinogenic agents. Recently we suggested using the SCE test to monitor general genotoxicity levels in the environment by determining SCE levels of mice living in that environment. This report describes the procedure that has been developed, the results of the application of this procedure to mice inhabiting natural habitats and some of the limitations of this approach.

The SCE detection procedure which proved most suitable included the implanting of paraffin coated 5-bromo-2'-deoxyuridine tablets subcutaneously and staining slides with Fisher's Giemsa after they had been immersed in Hoechst 33258 and exposed to strong fluorescent lights for approximately 24 hours. These changes in the standard procedure allowed the routine processing of 20 samples per day. The limiting aspect is now the typing of slides since one person can routinely score no more than 6 per day.

C3H mice were used to standardize the procedure and as controls in all of the runs. C3H mice (61) gave a mean SCE value of 4.30 ± 0.516. Also 20 DBA/2J mice tested gave an overall SCE value of 5.23 ± 0.75. In either group there were no major deviations from the mean of the group.

Wild mice (285) from corn cribs gave a mean SCE value of 5.72 ± 1.08. There were, however, both geographic and temporal fluctuations. Mice collected in early spring, prior to crop spraying, gave SCE values of 5.93 ± 1.07 (17 mice) and 4.83 ± 1.25 (19 mice) from the Windsor and Ridgetown (96 km east of Windsor) areas, respectively. These results are consistent with those reported earlier. Temporal variations were most pronounced in the Ridgetown populations where the early May (prespraying) SCE values were 4.83 ± 1.25 (19 mice), the mid-May (spraying period) SCE counts were 6.77 ± 1.12 (16 mice), the mid-June (early post-spraying) values were 4.58 ± 1.20 (15 mice) and the late July values were $4.15 \pm .79$ (14 mice). The Windsor samples gave similar results.

To complement the work on wild mice, both C3H and DBA mice (90) were housed in twenty-gallon enclosures partially filled with corn. The results are consistent with those observed in wild mice.

Several experiments were also carried out in an attempt to elevate SCE values drastically. C3H mice were exposed to the herbicide bentazon (Basagran) for one hour and 8 hours while a field was being sprayed. Bentazon, a postemergent herbicide used on corn, was the most common spray used in the study area. The mean SCE values were 4.93 ± 0.52 (8 mice) and 5.45 ± 0.24 (8 mice), respectively. These results indicate that even a brief exposure to this herbicide will effect SCE values. Mice were also placed in an industrial setting where high concentrations of organic solvents were used. A three day exposure resulted in an increase of SCE levels in all six mice examined (mean = 5.22 ± 1.08).

Overall our results indicate that the SCE test will detect increases in genotoxic levels. These increases, some of which are due to widespread agents and others to localized factors, elevate SCE levels by from 25 to 50%. At least at present, such increases must be considered minor. Areas where high levels of genotoxic agents exist have not been satisfactorily identified. Results of such situations are essential before a conclusion on the value of the SCE approach is reached.

(This work is supported by a grant from the Ministry of the Environment, Ontario.)

INTRODUCTION

At the 1983 Technology Transfer Conference I proposed that there was a need for a nonspecific EARLY WARNING TEST TO DETECT CHANGES IN ENVIRONMENTAL GENOTOXIC LEVELS and that of the numerous tests available SISTER CHROMATID EXCHANGE ANALYSIS on wild mice had considerable potential [1]. The need for such a test is obvious since we are releasing into our environment tremendous quantities of genotoxic agents as byproducts of industrial processes, as pesticides in agriculture, as components of manufactured products, and even as derivatives of our lifestyle [2-18].

The sister chromatid exchange (SCE) test was selected because it has among others the following attributes: a) high sensitivity to most mutagenic agents [19], b) the possibility of testing large numbers of individuals, and c) applicability to organisms already present in the environment being monitored. The latter gives this test the potential to detect damage resulting from the synergistic interactions of genotoxins without first the time-consuming identification of these agents. House mice, Mus domesticus, were selected as the test organism because adequate samples of wild mice are readily obtainable [20], because they are easily housed in either the laboratory or population enclosures and because inbred laboratory strains are available for the establishment of SCE baselines and for controlled laboratory experiments.

The preliminary data reported last year supported the feasibility of this approach [1]. The present report includes: a description of the techniques developed to permit the examination of large sample sizes, further comparisons of mice collected during different seasons and at different sites, preliminary results on mice exposed to potentially high risk

conditions and results of experiments which indicate the sensitivity of the SCE test using natural routes of genotoxin intake.

METHODS

Animals Used:

Mice from two inbred strains,C3H/J and DBA/2J, were used to determine the baseline SCE level and C3H mice were used as controls in all runs. Both C3H and DBA mice were also used in the outdoor enclosures. The wild mice came from corn cribs at various locations in southwestern Ontario (see Fig. 1). Corn cribs were selected as the source of wild mice not only because adequate sample sizes could be obtained as the cribs were being emptied but also because mice coming from different cribs, of which there are hundreds in southwestern Ontario, are all exposed to the same diet and the same general environmental conditions. Heterogeneity in the environment stemming from agricultural practices and/or atmospheric fallout will of course exist.

All laboratory animals were kept under standard conditions with ample water and feed (Purina Laboratory Chow).

SCE Preparation:

The preparation of material for SCE examination involves the incorporation of 5-bromo-3'-deoxyuridine (BrdU) in newly formed chromatids. This was accomplished by embedding 50 mg tablets of BrdU, partly coated by melted paraffin, subcutaneously between the scapulae of anesthetized mice. A dose of 0.02 ml/g body weight of a 1.25% solution of avertin (4g tribromoethanol in 2.5ml amylene hydrate) put the mice into a deep sleep. Avertin does not effect SCE levels. Twenty-four hours later 4ug/g of

colchicine were injected intraperitoneally and three hours after that the mice were sacrificed by cervical dislocation. Femurs were removed and bone marrow cells were flushed into a warm (37C) hypotonic solution (0.075M) of KCl. The cells then were put through two stages of fixation in a cold glacial acetic acid/methanol mixture. On fixation, the cell suspension was applied dropwise to slides and air dried. After a 24 hour aging period, the slides were incubated in a fluorescent stain, Hoechst 33258 (10 ug/g of distilled water) for 15 minutes. The slides were then placed in a staining jar containing Sorensen's buffer (pH 8.0), covered with saran wrap and exposed to a bank of four fluorescent tubes at a distance of 15 cm for approximately 23 hours. At the end of this period a single slide was removed and stained with Fisher's Giemsa for 8 minutes. If no differential staining was seen the rest of the slides were exposed to the fluorescent lights for another ten minutes and another test slide was examined. This was repeated until satisfactory differential staining was observed and then all the remaining slides were stained.

This procedure eliminates serial injections of BrdU and handling of slides individually until the scoring is to be done. It also permits the staining of large numbers of slides at one time, since test slides insure that no run is lost because of poor differential staining of the chromatids. Now the limiting factor in processing a large number of animals in a short time frame is the scoring under a microscope. One person can score no more than four slides in an 8 hour day under optimum conditions.

Some of the early SCE results were obtained using 9 hourly injections of either 40 ug/g body weight or 80 ug/g body weight of BrdU. Further modifications occurred in staining. After slides were aged for 48 hour, they were heated to 87-89C for 15 minutes in a phosphate buffer and stained in 5%

Fisher's Giemsa (Kornberg and Freedlender technique [21].

Population Enclosures

There were two types of enclosures. Outdoors, 20 gallon galvanized garbage cans half filled with corn and covered with hardware cloth tops were used. For indoor situations or for attachment to mobile equipment, the enclosures were 5 gallon plastic pails partly filled with corn and again covered with hardware cloth tops. The corn provides the mice with sufficient water, nutrients and protection so that the enclosures once in place do not have to be disturbed for a considerable period. Even in the small containers there is sufficient corn to house six mice for four weeks undisturbed.

The large enclosures were placed near corn cribs on farms in Essex County. The smaller containers were either placed in industrial settings or attached to spraying rigs.

RESULTS

Table 1 presents a summary of pooled results from inbreds and wild mice maintained under either laboratory or natural conditions. Included are mice which were given BrdU in tablet form as well as results reported earlier in which the BrdU was injected interperitoneally in 9 hourly doses. These earlier results are included for the sake of comparison, since tentative conclusions were based on them.

Both laboratory-maintained C3H mice and laboratory-maintained wild mice which received BrdU in tablet form gave SCE values intermediate to the corresponding animals receiving high and low doses of BrdU via injections. This same pattern was not seen in the other groups. For instance, the pooled

values for the wild mice given tablets was only 5.70+0.11 as compared to 6.02+0.16 and 7.49+0.36 for the BrdU injection treated mice. The low value for the 1984 wild mice, especially relative to the SCE values in mice given 40 ug/g body weight, may be a reflection of the collecting period since most of the mice in the latter group were collected in late May and June, that is during the spraying season. There is also the possibility that the sensitivity of the test using BrdU tablets is reduced.

With the use of BrdU tablets the amount of BrdU absorbed by a mouse varies. The quantity absorbed ranged from 4 to 45 mg with the majority of mice falling in the 18 to 30 mg category. Since BrdU is itself an SCE inducer the results were examined for possible correlation between SCE levels and BrdU absorbed. For the entire range of BrdU absorbed in C3H mice the correlation was significant ($r = 0.3159$). If however the range between 18 and 30 mg was examined the correlation was not significant at the 5% level ($r = 0.1164$). For wild mice the correlation between the BrdU absorbed and SCEs was not significant at the 5% level ($r = 0.1869$) regardless of the amount of BrdU absorbed. Nevertheless, because of the C3H findings, only mice that absorbed between 18 and 30 mg are included in the analyses.

Since both males and females were collected from natural populations and typed for SCEs the first step in analyzing the data was to determine whether there was a significant difference between the two sexes. Among the wild mice, the males gave an SCE value of 5.59±0.17 and the females 5.81±0.16. This was not significant at the 5% level ($t = -0.8244$). For the C3H mice the males averaged 4.19±0.65 SCEs per cell and the females 4.47±0.45. Unfortunately only four of the C3H mice were females so the comparison is weak. From the data on wild mice where we had almost equal numbers of males and females we concluded that SCE levels were not significantly different in

the two sexes and so values for the two sexes were pooled.

Reports in the literature suggest that the SCE values in young and old mice differ [22-24]. Because the wild animals were classified into young and adult on the basis of size, a comparison was made. The SCE level was 6.28±0.21 and 5.49±0.13 in young and old mice, respectively. Twenty-three percent of the mice were young. Since this difference is not significant at the 5% level ($t = -1.1749$), data from the two age groups were pooled.

Corn Crib Data

Table 2 gives a breakdown of the data on the wild mice collected in 1984 and includes the 1983 mice for comparison. The samples are arranged by the time they were collected relative to herbicide spraying and by the general area from which they came. To the best of our information spraying in both Essex and Kent counties was begun about May 20. In Essex County, the Borrowman and Immison samples were collected prior to spraying. The remaining two samples were collected while spraying was being done or immediately after. The SCE values are not significantly different in these two groups ($t = 0.9507$; $p>0.05$). The most complete data were obtained in Kent County East where spraying began May 20 and continued into the middle of June. Based on the lifespan of the herbicides used, the effects of spraying should have diminished considerably by the end of June in this area. The pooled prespraying SCE value was significantly lower than the pooled spraying-period SCE value ($t = -3.2905$; $p<0.01$) in Kent County. Similarly the difference between the spraying period results and the postspraying SCE count was significantly different ($t = -5.1111$; $p<0.01$). However, the pre- and post-spraying SCE counts were very similar. Finally, in Elgin County Central populations were available for sampling only during the spraying

period and even during this period the population sizes and subsequently sample sizes were small.

The results from Kent County are consistent with the data obtained in 1983 when the prespraying season began somewhat later and extended into the first week of July because of a late and wet spring which delayed the planting of many crops. The results from Essex County suggest the same trend as that seen in Kent County and in 1983. Whether the lack of a significant difference between the samples collected before and during spraying in Essex County is the result of some early spraying of which we were unaware or the proximity of the sampling sites to industry cannot be determined from the information available.

In the 1983 report we indicated the suggestion of a geographic trend. The SCE values obtained during the spraying period in the three regions do not support the existence of a geographic gradient. In fact the SCE counts in all three areas are very similar and the differences are not statistically significant. However, a comparison of the SCE values of the samples collected before spraying from Essex and Kent shows a significantly lower value in the latter ($t = 3.5035$; $p<0.01$). As mentioned above the cause(s) of this difference, whether geographic or not, cannot be determined from present data.

One of the drawbacks of using mice inhabiting corn cribs for a systematic study such as the one described above is the timing of crib emptying. Frequently this timing is dependent on market fluctuations of corn prices and so cannot be predicted. As a result it was not possible to obtain post-spraying samples in Essex and Elgin Counties because no suitable cribs were being emptied at that time. In 1984 a second problem was encountered at some of the sites. Overall population densities were down to 40% of the

levels observed in the last ten years and as a result some of the samples were very small. This reduction in population densities may be due to the atypical temperature fluctuations which we had last spring. However in spite of this, obvious patterns are evident.

SCE Levels in Wild Mice Housed in the Laboratory

The effect on SCE levels of housing wild mice in the laboratory, under standard laboratory conditions, for six or more months is summarized in Table 1. For all three variations of the technique wild mice approached the baseline counts observed in laboratory maintained C3H animals. Table 3 documents a change that occurred in a sample from the Glendenning farm. The four mice originally typed from this area gave the highest SCE count of any of the 1983 samples. Some mice were saved for another purpose. Seven months after the capture, five males and five females housed in the laboratory were processed for SCE analysis. By this time the SCE level in these mice had dropped considerably although still above the baseline level for laboratory maintained C3H mice.

In 1984 the Glendenning farm was sampled in the post-spraying period. The SCE levels were low (Table 2).

Population Enclosures

To obtain further evidence regarding seasonal and/or geographic variations in SCE counts both C3H and DBA mice were placed in the larger enclosures at four sites in Essex County: Renaud, Laramie, Rocheleau and Trudell (see Fig. 1). With the exception of the November sample, mice were replaced monthly in the enclosures. The mice, therefore, had a four week exposure to the outdoor environment. No geographic pattern was observed.

Furthermore, as seen in Table 4, the SCE values were rather uniform throughout the sampling period except for the June 22 samples. Both C3H and DBA showed a considerable increase. These increases in SCE counts coincide with the spraying period.

In an effort to obtain more direct evidence on the effects of herbicide spraying in general and of exposure duration in particular, five-gallon enclosures filled with corn were attached to a sprayer for various time periods. The results summarized in Table 5 show a positive relationship between SCE levels and duration of exposure.

Preliminary attempts were made to place some of these five-gallon enclosures in industrial settings with high genotoxin potential. One run of four mice placed in a plastics moulding factory gave an average of 5.62 ± 0.51 SCEs/cell/animal.

Natural Routes For Introducing Mutagens

In the 1983 report I voiced concern about the way in which genotoxic agents were introduced in test animals. Normally this is done by injection. Two to three-fold increases were registered even with relatively low doses of mitomycin C (MMC) (2ug/g) and three- to four-fold increases with methyl methanesulfonate (MMS) (10 ug/g). Also the timing of the injections was found to be critical for maximum induction of SCEs for both compounds (see Table 6). To achieve SCE increases of similar magnitudes through MMS in drinking water, the animals had to be exposed to much greater levels of the mutagen ($\approx$72 mg/mouse or $\simeq$ 5mg/mouse/day for 14 days or $\approx$ 200 ug/g body wt/day for 14 days). Even under these conditions the SCE increase was less than three-fold.

The highest doses shown in Table 7 approach the maxima that may be given

mice because as the MMS concentrations increased in the drinking water the mice drank less and less. This resulted in dehydration and, if not taken off the MMS solution, the mouse would have died. It is because of this that the groups receiving the higher dose of MMS did not have six mice. The above results indicate that mutagens if absorbed naturally must occur in relatively high quantities (much higher than would be required for the injection procedure) to have a detectable effect on SCE levels.

These experiments also allowed a comparison between the tablet introduction of BrdU and serial BrdU-injection procedure. The evaluation was made by comparing ratios of [SCE at 90 mg]/[baseline SCE for the technique used]. For the injection procedure this ratio was 2.60 while for the tablets it was 2.14. Similar results were obtained for the 24 mg dose. These results suggest that although the baseline values show considerable variation in the two procedures, the sensitivities are not too different, with the BrdU-injection procedure being perhaps slightly more sensitive to increases in SCE induction.

DISCUSSION

The use of BrdU tablets and the new staining procedure not only made the preparation of material for the typing of sister chromatids less labour intensive but it also increased the probability of getting scorable slides. One bottleneck, the scoring of SCEs through a microscope, however still exists. The BrdU tablets resulted in lower baseline counts then those given by 80 ug/g injections but higher than 40 ug/g injections. The MMS data showed that in spite of this, the sensitivity of the procedure with BrdU tablets is not appreciably less than the injection procedure. This

reduction, if real, is more than offset by the reduction in handling time.

Because the amount of BrdU absorbed varied from mouse to mouse the correlation between BrdU absorbed and SCE levels was determined. Such a correlation was observed in the C3H mice when the entire range of BrdU absorbed was considered. If, however, only C3H mice which absorbed between 18 and 30 mg of BrdU were examined no significant correlation was found. So in subsequent analyses only mice which absorbed between 18 and 30 mg BrdU were used. Also because there was no significant difference between sexes and between age groups, the SCE values for males and females, and for young and mature mice were pooled.

Analyses of mice inhabiting corn cribs indicate that herbicides have an effect on SCE levels. This was also supported by the data from the outdoor enclosures and by mice in enclosures attached to spraying rigs. Whenever increases in SCE levels were observed the baseline was seldom more than doubled. There have been a few exceptions to this (e.g. Glendenning-1983) but these appear to be short lived. The specific causes for these high levels are not obvious from the present data. Ignoring the injecting of mutagens, and focussing on normal intake routes only high concentrations of MMS in drinking water have given high SCE values repeatedly.

The absence of highlevels of SCEs in situations which have been studied to date may reflect the absence of a crisis situation. What is needed at this point is a situation where the mutagen level is either known to be high or has the potential to be high and then to determine what effect this has on the SCE values. This is why we have begun to examine (1) industrial sites where solvents are being used in high concentrations and (2)drinking water where if necessary appropriate agents could be added.

The testing of an industrial site can be done easily by placing mice in

the small plastic enclosures filled with corn. Once in place these would not need to be checked for from 4 to 8 weeks and as a result no disruption of the work place need occur.

From time to time in those populations where large samples have been obtained the odd mouse has a high SCE level, three to four times the baseline level. There appears to be no obvious reason for this since the other mice in the sample have SCEs within the expected range. However, since SCEs appear to be associated with DNA repair mechanisms, one possibility is that these animals with the high SCE counts have a very efficient DNA repair system. Another possiblity might be that these mice do not detoxify certain compounds as rapidly as the other mice and that these compounds are responsible for the high SCE values. In any event an attempt should be made to determine whether there is a genetic basis for these high SCE values, especially since there is a genetic component to SCE induction in inbred strains of mice [25]. Should such a basis exist then a strain could be developed which would enhance the sensitivity of the SCE test.

CONCLUSION

The SISTER CHROMATID EXCHANGE TEST is still a viable candidate as a nonspecific EARLY WARNING TEST TO DETECT CHANGES IN ENVIRONMENTAL GENOTOXIC LEVELS. From the herbicide studies the SCE test appears sufficiently sensitive to detect changes in the environment but the increases have been relatively small. Its capabilities to detect crisis conditions have not as yet been evaluated. This should be done next.

REFERENCES

1. Petras, M.L., B. Nayak and R. Piscitelli. 1983. Monitoring genotoxicity in the environment using sister chromatid exchanges. Proc. Tech. Transfer Conference (Ontario) No.4: 795-817.

2. Fukino, H., S. Mimura, K. Inoue and Y. Yamane. 1982. Mutagenicity of airborne particles. Mutation Res. 102:237-247.

3. Mazaki, M., Takao Ishii and Masahiko Uyeta. 1982. Mutagenicity of hydrolysates of citrus fruit juices. Mutation Res. 283-291.

4. Husgafvell-Pursianen, K., J. Maki-Paakkanen, J. Norppa and M. Sorsa. 1980. Smoking and sister chromatid exchange. Hereditas 92:247-250.

5. Nicholas, A.H. and H. Van Den Berghe. 1982. Sister chromatid exchange and pesticides, with emphasis on organophosphates. Sandberg, A.A. (ed) "Sister Chromatid Exchange": 327-354. New York: Liss.

6. Lockard, J.M., J.W. Prater, C.J. Viau, H.G. Enoch and P.S. Sabharwal. 1982. Comparative study of the genotoxic properties of Eastern and Western U.S. shale oils, crude petroleum, and coal-derived oil. Mutation Res. 102:221-235.

7. Crossen, P.E., W.F. Morgan, J.J. Horan and J. Stewart. 1978. Cytogenetic studies of pesticide and herbicide sprayers. New Zealand Med. J. 88:192-195.

8. Behera, J. and S.P. Bhunya. 1980. In vivo effect of a commercial herbicide, Amiben, on bonemarrow and germ cells of mice. Caryologia 33:527-535.

9. Sobti, R.C., A. Krishan and C.D. Pfaffenberger. Cytokinetic and cytogenetic effects of some agricultural chemicals on human lymphoid cells in vitro: organophosphates. Mutation Res. 102:90-102.

10. Korte, C. and S.M. Jalal. 1982. 2,4-D induced clastogenicity and elevated rates of sister chromatid exchanges in cultured human lymphocytes. J. Heredity 73:224-226.

11. Moller, M. and I. Alfheim. 1983. Mutagenicity of air samples from various combustion sources. Mutation Res. 116:35-46.

12. Alink, G.M., H.A. Smit, J.J. van Houdt, J.R. Kolkman and J.S.M. Boleij. 1983. Mutagenic activity of airborne particles at non-industrial locations. Mutation Res. 116:21-34.

13. Nestmann, E.R., G.L. Lebel, D.T. Williams and D.J. Kowbel. 1979. Mutagenicity of organic extracts from Canadian drinking water in the Salmonella/Mammalian-Microsome assay. Environmental Mutagenesis 1:337-345.

14. Ohno, H., F. Hanaoka and M. Yamada. 1982. Inducibility of sister-chromatid exchanges by heavy-metal ions. Mutation Res. 104:141-145.

15. Stella, M., A. Montaldi, R. Rossi, G. Rossi and A.G. Levis. 1982. Clastogenic effects of chromium on human lymphocytes in vitro and in vivo. Mutation Res. 101:151-164.

16. Masaki-Paakknen, J., M. Sorsa and H. Vainio. 1981. Chromosome aberrations and sister chromatid exchanges in lead-exposed workers. Hereditas 94:269-275.

17. Shiraishi, Y. 1982. Effects of caffeine and chemical agents on SCE. Sandberg, A.A. (ed) "Sister Chromatid Exchange": 395-421. New York: Liss.

18. Raposa, T. 1982. SCE and chemotherapy of non-cancerous and cancerous conditions. Sandberg, A.A. (ed) "Sister Chromatid Exchange": 579-617. New York: Liss.

19. Abe, S. and M. Sasaki. 1982. SCE as an index of mutagenesis and/or carcinogenesis. Sandberg, A.V. (ed) "Sister Chromatid Exchange":461-514. New York: Liss.

20. Petras, M.L. and J.C. Topping. 1981. Studies of natural populations of Mus. VI. Sizes of populations inhabiting corn cribs in southwestern Ontario. J. Mamm. 62:146-153.

21. Kornberg, J.R. and E.F. Freedlender. 1974. Giemsa technique for the detection of sister chromatid exchanges. Chromosoma 48:355-362.

22. Reimer, D.L. and S.M. Singh. 1983. Cyclophosphamide induced in vivo sister chromatid exchanges (SCE). II. Effect of age and genotype on SCE, micronuclei and metaphase index. Mech. Ageing Dev. 21:59-68.

23. Schneider, E.L. and B. Gilman. 1979. Sister chromatid exchange and aging. III. The effect of donor age on mutagen-induced sister chromatid exchange in human diploid fibroblasts. Hum. Genet. 46:57-63.

24. Schneider, E.L., D. Kram, Y. Nakanishi, B. Monticone, R.R. Tice, B.A. Gilman and M.L. Neider. 1979. The effect of aging on sister chromatid exchange. Mech. Aging Dev. 9:303-311.

25. Reimer, D.L. and S.M. Singh. 1983. Cyclophosphamide-induced in vivo sister chromatid exchanges (SCE) in Mus musculus. III. Quantitative genetic analysis. Genetics 105:169-179.

ACKNOWLEDGEMENTS

We are grateful to the Ministry of the Environment of Ontario for providing support for this work. We would also like to thank Miss Janet Norsworthy and Mr. Bob Gowanlock for their technical assistance.

TABLE 1. Mean SCE values in inbred and wild mice maintained under several different conditions and given 5-bromo-3'-deoxyuridine (BrdU) through either subcutaneous implantation of 50 mg tablets or intraperitoneal serial injections.

MICE	MAINTENANCE CONDITIONS	SEX	BrdU TABLETS (50 mg)			SERIAL INJECTIONS 40 ug/g body wt			SERIAL INJECTIONS 80 ug/g body wt		
			No.	SCE	± SEM	No.	SCE	± SEM	No.	SCE	± SEM
C3H/J	Laboratory	m	79	4.18	0.06	32	3.39	0.07	18	5.63	0.14
		f	4	4.47	0.45						
DBA/2J	Laboratory	m	19	5.23	0.17	9	3.93	0.13			
Wild	Laboratory (minimum 6 months)	m	20	4.70	0.24	18	3.52	0.06	9	5.72	0.15
Wild	Corn cribs (within 24 hr)	m	73	5.59	0.17	49	6.02	0.16	22	7.49	0.36
		f	95	5.81	0.16						
C3H/J	Enclosures (Essex County)	m	52	4.40	0.11	14	5.62	0.14	12	10.27	0.34
DBA/2J	Enclosures (Essex County)	m	38	4.87	0.32						

SEM - Standard error of the mean calculated from SCE values of individual mice.

TABLE 2. SCE levels in wild mice collected from corn cribs in three regions of southwestern Ontario before, during and after the spraying of crops with herbicides. Even though the 1983 data were obtained using 80 ug/g body weight of BrdU instead of tablets, these data are included so that trends might be compared. The 80 ug/g body weight injections of BrdU give higher SCE values.

YEAR	LOCALITY	DATE	SCE COUNTS ± S.E.M.		
			PRESPRAYING PERIOD	SPRAYING PERIOD	POST-SPRAYING PERIOD
1984	ESSEX COUNTY WEST				
	Borrowman	5/05	5.72±0.25 (17)		
	Immison	5/15	5.61±0.32 (11)		
	Renaud	5/24		6.27±0.23 (18)	
	Laramie	5/28		6.37±0.27 (14)	
			5.70±0.19 (28)	6.35±0.17 (32)	
	KENT COUNTY EAST				
	Dhoudt	5/01	3.34±0.36 (4)		
	Selton	5/10	4.71±0.49 (8)		
	Dilliott	5/10	5.26±0.42 (7)		
	C. James	5/21		7.29±0.31 (16)	
	Clachan	5/21		5.73±0.83 (3)	
	McKinley	6/28		5.91±0.25 (12)	
	Alvinston	6/14		4.73±0.52 (7)	
	Glendenning	7/11			5.29±0.16 (7)
	Lachine	7/13			5.06±0.80 (2)
	McDougall	8/02			4.59 (1)
	Simpson	8/02			4.89±0.28 (21)
			4.65±0.43 (19)	6.66±0.24 (38)	4.89±0.18 (30)
	ELGIN COUNTY CENTRAL				
	Pels	6/25		6.23±0.67 (7)	
	Vandermaarl	6/25		6.09±0.34 (5)	
	Brown	7/04		7.23±0.99 (8)	
				6.62±0.46 (20)	
1983					
	Trudell	4/26	5.84±0.66 (4)		
	Laramie	5/11	5.74±0.30 (2)		
	Sinasac	5/11	6.47±0.33 (4)		
	Rocheleau	5/26	5.60±1.61 (2)		
	Houle	6/25		7.66±0.21 (6)	
	Glendenning	7/05		11.55±1.56 (4)	
			5.99±0.32 (12)	9.22±0.86 (10)	

TABLE 3. Comparison of mice tested immediately after being caught with mice from the same population after they had been maintained under laboratory conditions for seven months. The population is from the Glendenning farm sampled in 1983. This sample gave the highest SCE value of all the 1983 populations. BrdU was injected at 80 mg/g body weight/injection.

TIME OF TREATMENT	NO. AND SEX	SCE ± SEM
Within 24 hr of capture	4 males	11.64 ± 1.56
Seven months after being captured	5 males	5.40 ± 1.40
	5 females	5.25 ± 0.83

TABLE 4. SCE counts (± standard error of the mean) in inbred mice housed in outdoor enclosures on farms in Essex County.

DATE OF SAMPLE	C3H MICE		DBA/2J MICE	
	NO.	SCE COUNT	NO.	SCE COUNT
November 4	8	3.64 ± 0.13		
March 9	8	4.12 ± 0.33	6	4.68 ± 0.47
April 19	8	4.33 ± 0.25	6	5.34 ± 0.31
May 16	7	4.62 ± 0.23	6	4.79 ± 0.35
June 22	8	5.65 ± 0.17	6	5.82 ± 0.29
July 26	13	4.14 ± 0.20	14	3.86 ± 0.12

TABLE 5. Five-gallon plastic pails partially filled with corn were attached to a sprayer while a farmer was spraying young corn plants with a herbicide. C3H mice were placed in the pails.

DURATION OF EXPOSURE	NO. OF MICE	SCE COUNTS AND SEM*
2 hours	6	3.98. ± 0.32
8 hours	6	5.55 ± 0.15
3 days**	6	5.69 ± 0.42

* Standard error of the mean is based on SCE values in individuals.
** Mice were exposed for about ten hours per day.

TABLE 6. SCE values in C3H mice that received either 2 ug/g body weight of mitomycin C or 10 ug/g of methyl methanesulfonate at various times before and after the first injection of BrdU. Both compounds were dissolved in Dulbecco's phosphate buffered saline. Four mice were used for each chemical and each time period.

TIME (hours)	SISTER CHROMATID EXCHANGES	
	MITOMYCIN C	METHYL METHANESULFONATE
Control (no compound)	3.99	
-26*	5.88	7.67
-13	5.90	13.99
- 6.5		12.65
- 3.25		14.26
- 0.75	6.85	13.70
+ 2	7.75	
+ 6.5	8.61	
+13	11.88	14.16
+24	6.40	

* This refers to twenty-six hours before the initial BrdU treatment. All mice were injected with 40 ug/g body weight of BrdU.

TABLE 7. SCE values in C3H receiving methyl methanesulfonate (MMS) in drinking water over a short period of time (3 days) and a long period (14 days). BrdU was given both in tablet form (50 mg/tablet) and also injected (80 ug/g/injection and 9 serial injections). The results not only show the effects of MMS but also permit a comparison of the two BrdU procedures.

APPROXIMATE DOSE (mg) PER MOUSE FOR ENTIRE RUN	BrdU TABLETS		BrdU INJECTED
	THREE DAY RUN	FOURTEEN DAY RUN	(80 ug/g/INJECTION)
0	4.18 ± 0.06* (79)**	4.18 ± 0.06 (79)	4.72 ± 0.09 (8)
0.15	4.48 ± 0.22 (6)		5.32 ± 0.53 (6)
0.50	4.57 ± 0.49 (6)		6.99 ± 0.84 (6)
2	4.70 ± 0.18 (6)	3.95 ± 0.65 (6)	8.49 ± 2.67 (6)
7	5.30 ± 0.71 (6)	3.75 ± 0.08 (6)	7.27 ± 0.99 (6)
9		5.18 ± 0.37 (6)	7.23 ± 0.39 (6)
24	5.67 ± 0.41 (6)		7.46 ± 0.21 (5)
90		8.95 ± 2.40 (5)	12.25 ± 0.84 (3)

* Standard error of the mean based on SCE counts in individual mice.

** Number of mice examined.

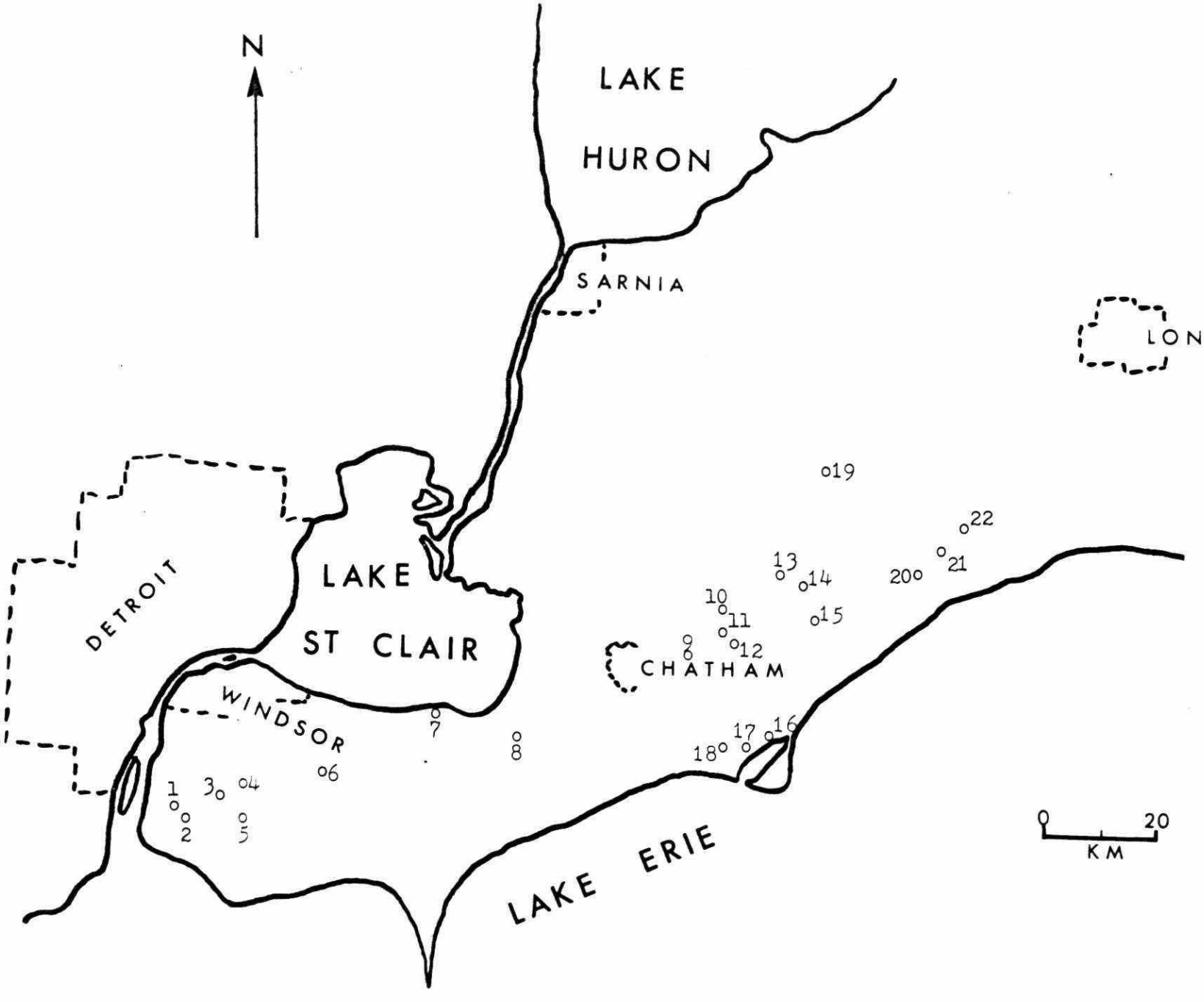


FIGURE 1

COLLECTING SITES

1. Renaud
2. Borrowman
3. Immeson
4. Laramie
5. Sinasac
6. Rocheleau
7. Houle
8. Trudell
9. Selton
10. Dhoudt
11. Lachine
12. Dilliott
13. C. James
14. Clachan
15. McKinley
16. Simpson
17. Glendenning
18. McDougall
19. Alvinston
20. Brown
21. Pels
22. Vandermaarl

QUANTIFICATION OF ASBESTOS AIR POLLUTION IN ONTARIO

BY: Dave K. Verma, Nancy E. Clark, and Jim A. Julian
Occupational Health Program
McMaster University
Hamilton, Ontario
Canada

QUANTIFICATION OF ASBESTOS AIR POLLUTION IN ONTARIO

Dave K. Verma, Nancy E. Clark, & Jim A. Julian
Occupational Health Program
McMaster University

ABSTRACT

Asbestos, a well known carcinogen, is estimated to account for almost half of all occupationally related cancers. The potential carcinogenic effect associated with even extremely low levels of asbestos is a major consideration in establishment of environmental asbestos standard for outdoor air.

In order to accurately assess the health risk associated with asbestos air pollution, the dose response curves based on optical microsopic (OM) fibre counts needs to be extrapolated downward in the size ranges of fibres only visible by Electron Microscopy (EM). Various factors that affects this relationship have to be considered. The presence of long thin fibres ($d < 1.5$ μm and $L > 8$ μm) that are considered most carcinogenic, in outside air is another critical factor.

Data on analysis of Environmental samples as well as occupational samples will be presented.

INTRODUCTION

It is well established that exposure to asbestos in occupational environments can cause lung fibrosis and various cancers among the workers.[1-5] The diseases associated with asbestos exposure include: asbestosis, lung cancer, mesothelioma and possibly cancers of other body sites. The evidence of asbestos related health effects has been amply demonstrated in numerous studies of groups of workers such as asbestos insulators, miners and millers, weavers and spinners, etc.[1-5]

In a study of U.S. cancer mortality, Doll and Peto[6] estimated that occupational cancers account for about 4% of all cancers in the United States. They also estimated the proportion of all U.S. cancer deaths currently due to asbestos to be around 1 to 2%.[6] This implies that asbestos may account for 25 to 50% of all present day occupational cancers in the United States.

The potential carcinogenic effects associated with even extremely low levels of asbestos is a major consideration in the establishment of an environmental asbestos standard for outdoor air. The recent Royal Commission on matters of health and safety arising from the use of asbestos in Ontario[1] has concluded that :

> "the individuals who have been afflicted with asbestos-specific disease have almost invariably been occupationally exposed to asbestos. However, there is incontrovertible evidence that mesothelioma has afflicted individuals who shared the domicile of an asbestos worker at the time this worker was exposed. There is weak evidence that individuals may have contracted

> disease from exposure to asbestos in the neighbourhood of asbestos plants. We have found no evidence that disease afflicts individuals who breathe asbestos in the outdoor air or inhale it as an occupant of asbestos containing buildings."

It is quite clear that exposure to even extremely low levels can cause asbestos related cancers (eg. mesothelioma). There can be only two explanations of the fact that the risk associated with low level asbestos contamination of outdoor air or asbestos containing buildings has not yet been fully demonstrated - i) that there is no measurable risk or ii) that there are many associated problems in the true assessment of such risk. Since there is no evidence to the contrary, it is as equally likely to be the latter as the former. There is no argument that the risk associated with low level asbestos contamination is very low compared to the risk of occupationally exposed groups.

There are many problems associated with proper assessment of the risk of low level asbestos exposure. One major problem is the extrapolation of the dose-response relationship for such exposures.[7] In order to accurately assess the health risk associated with asbestos air pollution, the dose-response based on optical microscope (OM) fibre counts needs to be extrapolated downward to the size ranges of fibres only visible by Electron Microscopy (EM).

A research method[7] has been proposed for such extrapolation of the dose-response curve based on optical microscope (OM) fibre counts to EM counts so that the health risk associated with measured concentrations of asbestos air pollution can be estimated.

The objective of the approach is to establish the relationship: $C_{OM} = f\ (C_{EM}$, Operation, Process, fibre types, etc.).

An important factor in the risk assessment of low level exposure is the presence of long thin fibres. Long thin fibres, considered to be the most carcinogenic for mesothelioma, lung and other cancers, are those longer than 8 μm and thinner than 1.5 μm or perhaps 0.25 μm.[8,9]

In this paper we describe research work relating to i) establishment of relationship between C_{OM} (optical microscopic fibre counts) and C_{EM} (electron microscopic fibre counts) of occupational samples and ii) asbestos enumeration of environmental samples. Earlier work in our on-going research was aimed at establishing and examining various electron microscopic methods and related issues.[7,10,11] An interim sampling and counting strategy has been developed.[7]

METHODS

Experimental work examined occupational and environmental samples using both OM and EM methods.

Occupational Samples

Occupational exposure samples have been obtained from different processes of several operations (mining, manufacturing) involving chrysotile asbestos. The samples are taken on a 37 mm diameter mixed cellulose ester filter paper using a personal sampling pump at the flow

rate of 2 litres/minute. The exposed filter is divided into 8 equal pie shaped wedges: 2 to be used for phase contrast optical microscopy (PCOM) analysis, 4 wedges for direct EM analysis and 2 for use with an indirect EM technique - all are assigned randomly.

Environmental Samples

Environmental samples have been collected from four areas - rural, urban, near an asbestos using company, and from within an asbestos contaminated building. The samples are taken on a 8" X 10" mixed cellulose ester filter using a Hi-Vol Sampling pump. A portion of the filter paper (generally 50% of the filter) is ashed and used for indirect EM analysis. A portion of the remaining filter is used for direct EM and the rest is used for optical count using phase contrast microscopy (PCOM/OM).

The sample collection proecedure is summarized in Figure 1.

Counting and Sizing

The counting and sizing for all samples involved utilizing both optical and electron microscopes.

Standard NIOSH phase contrast microscopic techniques[2] have been used to evaluate fibre concentrations by optical microscopy. Transmission Electron Microscopy has been employed for EM measurement. We have utilized our interim fibre counting strategy[7] where 20 grid openings are evaluated. The evaluation is carried out by photographing the entire grid

opening at 709X and then examining the negative on a microfiche reader at 27X magnification. This approach cuts down the amount of EM time and reduces the operator fatigue while maintaining excellent resolution. We have also developed software on an Apple II+ microcomputer interfaced with a sonic digitizer to measure fibres directly off the microfiche screen or micrographs. The salient points regarding counting and sizing are shown in Figure 2.

RESULTS

The results showing the relationship between C_{OM} and C_{EM} in occupational samples given in Table 1 were recently presented at the XXI International Congress on Occupational Health in Dublin, Ireland.[12] The EM results were obtained using the direct method. The results of the environmental samples are summarized in Table 2. Only measurements from the indirect method have been reported here since the Ontario Ministry of Environment uses the indirect method to assess compliance with their interim standard (0.04 fpcc, ≥ 5 µm in length). Also, in some cases, the direct method did not give measurable concentrations.

DISCUSSION

The results in Table 1 shows that the relationship between C_{OM} and C_{EM} in occupational samples varies with various operations and processes. The concentrations measured by EM (C_{EM}) are much higher than C_{OM}. The

ratios range from 13:1 to 33:1. When only those EM fibres that fall into the size range visible by OM, referred to here as electron microscopic count optical equivalent $C_{EM}(OE)$, are compared to the C_{OM}, the ratios still range from 2:1 to 5:1.

It was also noted that in occupational samples long thin fibres ($d < 1.5$ μm and $L > 8$ μm) are found in increasing proportion of total EM fibre counts as asbestos processing moves from mining to manufacturing.[12]

Air concentrations of asbestos fibres > 5 μm in length increases in the following order:rural air, urban air, ambient air of an asbestos-using-company (AUC).

$$\text{rural} < \text{urban} < \text{AUC}$$

There is little difference between rural and urban air for the percentage of asbestos fibres >5 μm in length and the percentage of long, thin fibres ($L > 8$ μm, $d > 1.5$ μm) to total EM fibres. They are, however, significantly higher for AUC ambient air.

The long, thin fibres that are considered most carcinogenic were found in all environmental samples. Ambiguous results were obtained for indoor air samples of an asbestos contaminated building. Table 2 shows low asbestos concentrations along with an absence of long, thin fibres. Further samples of indoor air need to be analyzed to verify this result.

The results show that all air samples, whether rural, urban, AUC or indoor, are several orders of magnitude lower than the present Ministry of Ontario guidelines for ambient air. Optical microscopy counts, as

expected, were all below the practical detection limit, thus confirming our beliefs that optical microscopy should not be used in assessing environmental asbestos exposure.

The Ontario Royal Commission on Asbestos[1] has reviewed the standard setting process used by the Ontario Ministry of Environment in arriving at the ambient air guideline of 0.04 fibres $\geq$ 5 μm in length by the EM method. They neither fully endorse or reject the Ontario's existing guideline because of the continuing lack of agreement in the scientific community on how environmental measurement should be taken. The commission, however, believes that Ontario's interim standard of 0.04 fibres/cc provides more than adequate protection to the public.

Further research on the levels of environmental asbestos exposure are clearly needed.

ACKNOWLEDGEMENTS

The authors would like to thank Drs. D. Corr and P. Roberts of the Ontario Ministry of Environment for their valuable advise and help. We also thank Mrs. Sharon Piedimonte and Mr. Andy Sebestyen for their help in the preparation of the manuscript.

We are grateful to the Ontario Ministry of Environment for their financial support.

REFERENCES

1. Report of the Royal Commission on Matters of Health and Safety arising from the use of asbestos in Ontario, Vols. 1 to 3, 1984

2. NIOSH (1972), Criteria for a Recommended Standard ... Occupational Exposure to Asbestos, U.S. DHEW Publications, Cincinnati, Ohio

3. The Final Report of the United Kingdom Advisory Committee on Asbestos 1979

4. ONTARIO MINISTRY OF THE ENVIRONMENT, (1975) Asbestos as a Hazardous Contaminant, Report No. ARB TDA 01-75

5. WALTON, W.H., (1982), The Nature, Hazards and Assessment of Occupational Exposure to Airborne Asbestos Dust: A Review, Ann.Occ.Hyg., 25, 117-247

6. DOLL, R., and PETO, R., (1981), The Causes of Cancer, (Oxford Medical Publications), Oxford University Press

7. VERMA, D.K., CLARK, N.E., and JULIAN, J.A., (1983), Methods for Sampling and Analysis of Asbestos Air Pollution in Ontario", In Proceedings of Technology Transfer Conference No. 4, Part 2 of the Ontario Ministry of Environment, Nov 29/30, 1983, pp 544-568

8. STANTON, M.F., and WRENCH C., (1972) Mechanism of Mesothelioma Induction with Asbestos and Fibrous glass. J.Natl.Can.Inst., 48:797-821

9. STANTON, M.F., and LAYARD, M., (1978) The Carcinogenicity of Fibrous Minerals, In: Gravett, G.D., LaFleur, P.D., and Heinrich, K.F.J. (Eds.) Workshop on Asbestos: Definition and Measurement Methods (National Bureau of Standards Special Publication #506)

10. VERMA, D.K., (1982) Asbestos Analysis Methods and Air Pollution in the Outdoor Air in Ontario, Presented at Ontario Ministry of Environment Air Resources Branch Research Grant Program Annual Seminar, Toronto, Ontario (Jan. 19/20, 1982)

11. VERMA, D.K., (1983) Methods for Sampling and Analysis of Asbestos Air Pollution in Ontario, Presented at Ontario Ministry of the Environment Resources Branch Research Grant Program Annual Seminar, Toronto, Ontario (Jan 18/19, 1983)

12. VERMA, D.K., JULIAN, J.A., and CLARK, N.E., (1984) Quantification of Asbestos fibres for assessing low dose effects. Presented at the XXI International Congress in Occupational Health, Dublin, Ireland Sept 9-14, 1984. Published in the Book of Abstracts, pp 398

TABLE 1

OCCUPATIONAL SAMPLES: COM VS CEM (FB/CC)
CHRYSOTILE ASBESTOS

OPERATION	PROCESS	NUMBER OF SAMPLES	ALL FIBRES CEM:COM	CEM(OE) : COM
MINING	Mining	2	25:1	5:1
	Crusher	5	33:1	2:1
	Milling	8	33:1	2:1
MANUFACTURING	Dumping and Loading	8	17:1	2:1
	Brake Industry	13	13:1	3:1

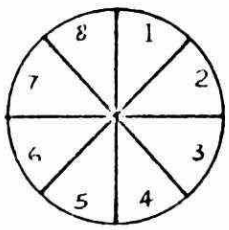
TABLE 2 - ENVIRONMENTAL SAMPLES

Location	No. of Samples	EM				PCOM
		No. of all Fibres Observed	Asbestos(Chrysotile) fibres as % of all fibres		Fb/cc	Fb/cc
			L > 5 µm	L > 8 µm d > 1.5 µm	L > 5 µm	L > 5 µm
OUTDOOR - Rural	3	151 (22-339)	6 (4-9)	2 (ND-3)	.0002 (.000035-.00051)	.0002 (ND-.00056)
- Urban	2	44 (32-55)	5 (4-6)	3 (2-3)	.0004 (.0003-.0007)	.0003 (.0002-.0004)
- Manufacturing	1	88	40	18	.003	.0006
INDOOR - Asbestos Contaminanted Building	1	113	1	ND	.00001	.0004
					MOE INTERIM AMBIENT AIR GUIDELINE 0.04	

FIGURE 1

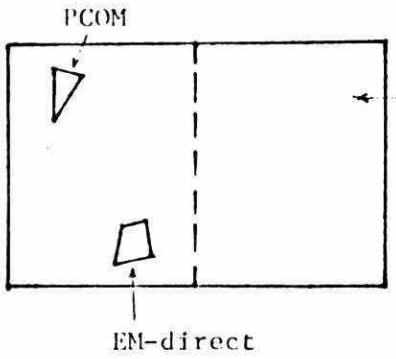
RESEARCH PROTOCOL: (a) SAMPLE COLLECTION

1) Occupational Samples - sample on millipore filters
- cut into 8 sections
- select randomly:
  - 2 PCOM
  - 4 EM-direct
  - 2 EM-indirect (ashed)



~ 37 mm ~

2) Environmental Samples - sample onto 8" X 10" millipore filter



- transfer to 37 mm filter as above

FIGURE 2

RESEARCH PROTOCOL: (b) COUNTING/SIZING

1) PCOM

- examine at least 20 random fields of view (maximum 100)
- follows Ontario Regulations
- count all visible fibres: > 5μ length
  < 3μ diameter
  ≥ 3:1 aspect ratio

2) TEM

- select 20 openings at random on grid
- photograph entire opening on plate film at 720X
- examine negative on microfiche reader at 32X (Effective Magnification ≈ 23000X)
- count/size all fibres with aspect ratio ≥ 3:1
- identify all fibres by morphology (chrysotile or unknown)
- record bundles

Sweet Corn, Cabbage, Cauliflower and Rutabaga Responses to Air Pollution in Southern Ontario

D.P. Ormrod

Department of Horticultural Science

University of Guelph

Sweet Corn, Cabbage, Cauliflower and Rutabaga Responses to Air Pollution in Southern Ontario

D.P. Ormrod
Department of Horticultural Science
University of Guelph

Abstract

Replicated field experiments were conducted in 1984 at the University of Guelph - Ontario Ministry of Agriculture and Food Research Station at Cambridge, Ontario; at the Ontario Ministry of Agriculture and Food Horticultural Experiment Station at Simcoe; and at the Canada Department of Agriculture Research Station at Harrow. Randomized block split-plot experiments were conducted with control (water), benomyl and mancozeb chemical protectant sprays applied to the plants weekly throughout the growing season. The use of these chemical protectant sprays was based on laboratory studies with a wide range of chemicals and on literature references. There were six cultivars of corn and two each of the other three species at each location with one planting date for sweet corn and two planting dates for cabbage, cauliflower and rutabaga. Cabbage and cauliflower plants were set up with transplants while seeds were used for sweet corn and rutabaga. Tobacco indicator plants of the cultivar 'Bel W-3' were placed in each plot. The extent of leaf injury on the tobacco plants was evaluated weekly. Injury on the tobacco leaves correlated well with ozone monitoring data. Harvests of these plots are continuing. Yield data analyses and interpetation are not yet complete and will be reported later.

Sweet Corn, Cabbage, Cauliflower and Rutabaga Responses to Air Pollution in Southern Ontario

D.P. Ormrod

Department of Horticultural Science

University of Guelph

Introduction

Southern Ontario crop production areas are subjected to recurring ozone (O_3) episodes during the growing season. While the responses of many crops to O_3 in the field in southern Ontario have had considerable study in the past, those of sweet corn have had little attention and cabbage, cauliflower and rutabaga have not been studied. The production of these crops for the fresh market or for freezing (sweet corn, cauliflower) or canning (sweet corn) is important in commercial horticulture. In addition, all four species are widely grown in home gardens. Studies elsewhere have indicated that at least some cultivars of these species or related species are sensitive to O_3. Experiments in the field in southern Ontario are necessary to permit evaluation of cultivars of each species under the weather and pollution conditions characteristic of this area. An understanding of species and cultivar sensitivities, location effects, weather interactions, amelioration techniques and various other air quality relationships is essential for an understanding of pollution limitations on productivity of these crops.

A study was undertaken in 1984 to evaluate sweet corn, cabbage, cauliflower and rutabaga responses to O_3 pollution in southern Ontario

by means of detailed observations of the nature and extent of injury during the 1984 growing season, and by undertaking chemical protectant treatment experiments in the field. The objectives of the study were to determine yield and quality effects, to correlate observed injury with O_3 monitoring data taken at several locations, to evaluate cultivar sensitivity, and to determine the nature of leaf injury and growth retardation.

These objectives were approached by conducting field experiments at the Simcoe Horticultural Experiment Station, Harrow Research Station, and Cambridge Research Station with evaluation of six cultivars of sweet corn with one planting date and two cultivars each of cabbage, cauliflower and rutabaga with two planting dates. Plants were given weekly sprays of the O_3 protectants benomyl (Benlate) or maneb (Dithane). Data on yields and other response variables allowed some assessment of species, cultivar, planting date, chemical protectant and location interactions.

Commercial Importance of Sweet Corn, Cabbage, Cauliflower and Rutabaga

The commercial production of sweet corn, cabbage, cauliflower and rutabaga is an important horticultural activity with about $21 million, $8 million, $9 million, and $5.5 million farm cash value in Ontario, respectively, each year. In addition, all these species are important home garden vegetables. Approximately 17,000 hectares of sweet corn are grown in southern Ontario. Sweet corn is well-adapted to southern Ontario and is an important contributor to farm income, as well as to the prosperity of the food processing industry.

Field Experiments

Replicated field experiments were conducted at the Ontario Ministry of Agriculture and Food Horticultural Experiment Station at Simcoe; at the Canada Department of Agriculture Research Station at Harrow; and the University of Guelph - Ontario Ministry of Agriculture and Food Research Station at Cambridge. At each location, randomized complete block split-plot experiments were conducted with weekly chemical protectant treatments, six cultivars of corn with one planting date, two cultivars each of cabbage, cauliflower and rutabaga with two planting dates, and six blocks in each experiment. The protectant treatments were sprays of water, 1000 ppm benomyl (Benlate), or 3600 to 14,300 ppm maneb (Dithane M-22) on all species. The sprays were applied weekly to all foliage on each plot. The cultivars were selected from the recommendation lists of the crop committees of the Ontario Ministry of Agriculture and Food.

The experimental design was a split-plot with cultivars as whole units and the sprays as sub-units. For the corn, there were six 5.4 meter long rows in each whole unit with alternate rows untreated and the three different spray treatments applied to the other rows. Row spacing was 75 cm with 20 cm spacing between the 26 plants within rows.

There were three 3.3 meter rows for the rutabagas and six 4.95 meter rows for the cabbage and cauliflower. Untreated rows separated each block. Row spacing was 80 cm with 18 cm between the 18 rutabaga plants and 45 cm between the 10 cabbage and cauliflower plants in each row.

After harvest, adjustments for actual plant numbers were made.

Nine tobacco indicator plants, cultivar 'Bel W-3', were placed randomly throughout each plot.

Results

Sweet Corn

Simcoe - Highest yields were obtained from 'Golden Jubilee' and 'Stylepak' plots and lowest yields from 'Northlite' and 'Comanche' (Table 1). Weekly applications of maneb significantly increased yield of all cultivars while benomyl sprays had no significant effect on yield. The overall average yield increase with maneb was 9.4% and the lack of statistical significance of the interaction of cultivar and spray indicated that all cultivars were behaving essentially the same.

Harrow - Highest yields were obtained from 'Golden Jubilee' plots and lowest from 'Northlite' (Table 2). Weekly applications of maneb increased yield of all cultivars with an overall average yield increase of 12.9%. All cultivars responded similarly to the maneb sprays.

Cambridge - Highest yields were obtained from 'Golden Jubilee' and 'Seneca Horizon' plots and lowest from 'Comanche' plots (Table 3). Maneb sprays increased yield in all but one cultivar with the overall average yield increase 12.8%. Decreased yield in 'Seneca Horizon' with maneb sprays was reflected by a significant interaction of cultivar and spray.

General - 'Golden Jubilee' was the highest-yielding cultivar at all three locations while the relative positions of other cultivars varied among locations indicating that cultivar yield is dependent on the relationship of local weather and soil factors and genetic

yielding potential. Benomyl sprays were ineffective at all locations indicating that this fungicide does not have a measurable impact on sweet corn productivity in ozone-prone regions. Maneb sprays significantly increased yield at all three locations with similar overall per cent increases at each location and, with one exception, consistent effects on all cultivars. Maneb has been shown to be an ozone-protectant on plants. If the yield increases with maneb can be assumed to be a reflection of ozone-induced decreases in yield then the overall decrease at all locations would be 11.7%, a value near that estimated by the Ontario Ministry of Environment (1984).

Rutabaga

Simcoe - Rutabaga yield was similar regardless of cultivar, planting date or protectant spray (Table 4).

Harrow - The two cultivars had similar yields in the first planting but 'Laurentian' outyielded 'Altasweet' in the second planting (Table 5). There were no significant spray effects.

Cambridge - 'Laurentian' had higher yields than 'Altasweet' in both plantings but there was no significant effect of protectant sprays (Table 6).

General - There were either no cultivar differences in yield or 'Laurentian' yielded more than 'Altasweet'. While the two planting dates resulted in similar yields at Simcoe, the second planting was higher yielding at both Harrow and Cambridge. Either benomyl and maneb are ineffective at the concentrations used in protecting this species from ozone or the species itself is ozone insensitive under field conditions.

Cauliflower

Simcoe - The only statistically significant effect was the higher yield of 'Snow Crown' than of 'Imperial' in the second planting (Table 7).

Harrow - The yield of 'Snow Crown' was higher than that of 'Imperial' in the both plantings (Table 8). No other effects were significant.

Cambridge - 'Snow Crown' markedly outyielded 'Imperial' at both planting dates but there was no significant effect of protectant sprays (Table 9).

General - As for rutabagas these studies indicated either better performance of the cultivar 'Snow Crown' or no difference between the cultivars. Planting date effects on cultivar response were noted but there were no significant effects of either chemical protectant spray on yield at any location.

Cabbage

Harvesting of the cabbage plots had not been completed in time for inclusion of the yield data in this report. The cabbage data are to be reported at a later date.

General Discussion

Weekly sprays of maneb had a consistent beneficial effect on yield of sweet corn at all three locations and with all but one cultivar, but this chemical was not effective on rutabagas or cauliflowers. Laboratory studies have indicated that these species are sensitive to ozone so further research with maneb sprays on rutabagas and cauliflowers appears to be necessary. Attention should be given to other application rates and frequencies. Such research

should be done first in laboratory facilities in which ozone dose can be controlled to ensure injury when needed.

Benomyl sprays were ineffective on all species suggesting that it has low efficacy for control of ozone effects in these species. Benomyl is effective as an antiozonant on some species but not others at the concentration used. A different concentration may be required for each species or this chemical may be ineffective at any concentration in some species.

Reference

Linzon, S.N., R.G. Pearson, J.A. Donnan and E.N. Durham. 1984. Ozone effects on crops in Ontario and related monetary values. ARB-13-P4-Phyto. Ontario Ministry of the Environment.

Acknowledgements:

Support from the Ontario Ministry of the Environment, Air Resources Branch, Research Grants Program is gratefully acknowledged. The cooperation and assistance of the following are much appreciated: Mr. Arthur Loughton, Director, Horticultural Experiment Station, Simcoe, Ontario, for providing field space and occasional technical assistance; Dr. Albert Liptay, Research Scientist, Agriculture Canada, Research Station, Harrow, Ontario, for providing field space; and R. Barnet and R. Gates for technical assistance.

Table 1. Effect of weekly chemical sprays on husked wt of sweet corn at the Simcoe Horticultural Experimental Station (g plot^{-1})

Cultivar	Spray Treatment			
	Water	Benomyl	Maneb	All
1. Seneca Horizon	4510	4650	5310	4820
2. Northlite	3730	3730	4040	3830
3. Stylepak	5980	6450	6200	6210
4. Golden Jubilee	6520	6520	7250	6760
5. Comanche	4000	3840	4400	4080
6. Silver Queen	5380	5000	5720	5370
All	5020	5030	5490	5180

Statistical significance: Cultivar**
Spray**
Cultivar X Spray ns
Yield increase with maneb sprays: 9.4%
In all tables:
** - highly significant differences (P<0.01)
* - significant differences (P<0.05)
ns - not significant at P<0.05

Table 2. Effect of weekly chemical sprays on husked wt of sweet corn at the Harrow Research Station (g plot^{-1})

Cultivar	Spray Treatment			
	Water	Benomyl	Maneb	All
1. Seneca Horizon	5050	5040	5360	5150
2. Northlite	3840	3320	4090	3750
3. Stylepak	5300	5450	5990	5580
4. Golden Jubilee	6430	6610	7730	6920
5. Comanche	4070	4520	4960	4520
6. Silver Queen	4110	4530	4410	4350
All	4800	4910	5420	5040

Statistical significance: Cultivar**
Spray**
Cultivar X Spray ns
Yield increase with maneb sprays: 12.9%

Table 3. Effect of weekly chemical sprays on husked wt of sweet corn at the Cambridge Research Station (g plot^{-1})

Cultivar	Spray Treatment			
	Water	Benomyl	Maneb	All
1. Seneca Horizon	5100	4610	4290	4670
2. Northlite	3310	3060	3500	3290
3. Stylepak	2880	3270	3900	3350
4. Golden Jubilee	4850	4500	5430	4930
5. Comanche	2580	2660	3460	2900
6. Silver Queen	3710	4220	4760	4230
All	3740	3720	4220	3890

Statistical significance: Cultivar**
Spray**
Cultivar X Spray*
Yield increase with maneb sprays: 12.8%

Table 4. Effect of weekly chemical sprays on yield of rutabagas at Simcoe Horticultural Experiment Station (g plot^{-1})

Planting	Cultivar	Spray Treatment			
		Water	Benomyl	Maneb	All
1	1. Altasweet	8800	8160	8760	8570
	2. Laurentian	9050	8490	9200	8910
2	1. Altasweet	8160	9510	8840	8840
	2. Laurentian	10720	8860	8950	9510
	All	9180	8760	8940	8960

Statistical significance: Cultivar ns
Spray ns
Cultivar X Spray ns

Table 5. Effect of weekly chemical sprays on yield of rutabagas at Harrow Research Station (g plot^{-1})

Planting	Cultivar	Spray Treatment			
		Water	Benomyl	Maneb	All
1	1. Altasweet	6680	6880	6480	8570
	2. Laurentian	6020	7300	6390	6570
2	1. Altasweet	8040	8730	9140	8640
	2. Laurentian	10650	9980	9360	10000
	All	7850	8220	7700	7920

Statistical significance: Cultivar Planting 1 ns, Planting 2*
Spray ns
Cultivar X Spray ns

Table 6. Effect of weekly chemical sprays on yield of rutabagas at Cambridge Research Station (g plot^{-1})

Planting	Cultivar	Spray Treatment			
		Water	Benomyl	Maneb	All
1	1. Altasweet	7500	7550	7080	7380
	2. Laurentian	10270	9500	9690	9820
2	1. Altasweet	8750	8540	8140	8480
	2. Laurentian	10260	10900	9450	10200
	All	9200	9120	8590	8970

Statistical significance: Cultivar Planting 1**, Planting 2*
Spray ns
Cultivar X Spray ns

Table 7. Effect of weekly chemical sprays on yield of cauliflowers at Simcoe Horticultural Experiment Station (g plot^{-1})

Planting	Cultivar	Spray Treatment			
		Water	Benomyl	Maneb	All
1	1. Snow Crown	6190	5280	4950	5470
	2. Imperial	5160	4540	4630	4780
2	1. Snow Crown	4010	4310	4090	4140
	2. Imperial	2900	13330	3430	3220
	All	4560	4360	4280	4400

Statistical significance: Cultivar Planting 1 ns, Planting 2*
Spray ns
Cultivar X Spray ns

Table 8. Effect of weekly chemical sprays on yield of cauliflowers at Harrow Research Station (g plot^{-1})

Planting	Cultivar	Spray Treatment			
		Water	Benomyl	Maneb	All
1	1. Snow Crown	7920	7610	7910	7810
	2. Imperial	6980	5840	5340	6050
2	1. Snow Crown	5060	6040	6400	5830
	2. Imperial	4270	15320	3570	4390
	All	6060	6200	5800	6020

Statistical significance: Cultivar Planting 1**, Planting 2*
Spray ns
Cultivar X Spray ns

Table 9. Effect of weekly chemical sprays on yield of cauliflowers at Cambridge Research Station (g plot^{-1})

Planting	Cultivar	Spray Treatment			
		Water	Benomyl	Maneb	All
1	1. Snow Crown	4290	3860	4280	4140
	2. Imperial	1990	2460	2510	2320
2	1. Snow Crown	4070	5390	4590	4680
	2. Imperial	1970	12130	1870	1990
	All	2080	3460	3310	3280

Statistical significance: Cultivar Planting 1**, Planting 2*
Spray ns
Cultivar X Spray ns

The impact of ozone on potato and peanut in Ontario

G. Hofstra and J. Ensing. Dept. of Environmental Biology, Univ. of Guelph.

ABSTRACT

In an attempt to establish dose-response functions for O_3 impact on various crops a number of approaches have been used. The approach used most widely in the U.S. is open-top chamber method. This method is costly and therefore other approaches have been evaluated.

The antioxidant, EDU, which was very effective in reducing bronzing in white bean, has been used on potato and peanut for several years. Control of oxidant injury on potato with EDU is only partial, and does not appear to provide a very accurate estimate of yield losses in O_3-sensitive cultivars. EDU gave effective control of oxidant injury in peanut with significant yield responses in sensitive cultivars.

EDU treatments were used to estimate what yields would be without significant oxidant injury and to compare the yields to those of insensitive cultivars. Yield differences between sensitive and insensitive cultivars, attributable to O_3, were used to develop a dose-response function using cumulative O_3 dose for July and August.

Developing the dose-response function for potato presented some major difficulties because of large gaps in the O_3 data base for past years and for gaps in cultivar yield data at Simcoe for sensitive cultivars.

The yield data for peanut were more complete, but spanned fewer years. Using differences in yield between sensitive and insensitive cultivars in cultivar trials offers another approach to establishing dose-response functions, but is dependent on consistent monitoring data.

Introduction

Economic loss assessment from air pollutants is still a rather inexact science. On the other hand visible injury symptoms from the phytotoxic air pollutants are generally well recognized on most species. The most phytotoxic air pollutant in North America, O_3, produces a variety of symptoms from bronzing to chlorotic stipple to black spot. The proportion of the foliage injured can be quite accurately estimated using various assessment techniques. On crops where the foliage is marketed as in green bunching onions, lettuce, spinach or gladiolus, the degree of foliar injury can be translated into economic losses. A small amount of injury in these cases can result in large economic losses.

In crops where parts other than the foliage are harvested the assessment of economic losses has proved much more difficult. The relationship between foliar injury and yield loss is complex and influenced by many factors. The relationship not only varies with species but can vary greatly with cultivar. The relationship between plant leaf area and yield is not constant. Some cultivars can have a considerable proportion of the leaf area removed without a significant effect on growth or yield. Other factors such as stage of maturity, frequency and intensity of air pollutant episodes, moisture status are some of the main factors influencing sensitivity.

Various methods have been used over the years to assess losses. The simplest and least costly has been visual assessments in the field. For some crops these assessments can be fairly accurate. For example the white bean crop is sensitive only after peak flowering. At flowering an experienced grower can estimate what the yield will be if no significant stress occurrs. Growers have estimated yield losses of up to 50% in white bean from O_3. Studies with the antioxidant EDU, which gave up to 75% control of foliar injury, showed losses of close to 40%. If foliar injury had been completely suppressed the value would have been closer to 50%. For other crops this method does not seem to be as effective, particularly if the losser are much less dramatic than for white bean. Several other methods have been used in Ontario on various crops.

Open-Top Chambers

Enclosures in the field have gained tremendously in popularity, particularly in the U.S. The ANCLAN program utilizes many open-top chambers on a wide variety of crops. These chambers have the main advantage of allowing the crop to be grown under close to ambient conditions. Particularly sunlight, a very important environmental factor in pollutant response is close to ambient. Temperature conditions are also generally within 1 or 2 degress of ambient. However, wind conditions are more or less constant in the chambers, influencing the pollutant flux to the leaves. Rainfall is uneven because of the walls and no dew forms in the chambers. The chambers are more useful for crops where individual plants are small and the population is relatively uniform. As plant size and variability increases so does the number of chambers required.

Chambers have not had wide use in Ontario. Their use on onion in the Bradford Marsh suggested that unfiltered air reduced yields as much as 39% in 1975 (Wukasch and Hofstra, 1977). However, the plants in the chambers,

although treated in every way as plants outside, differed considerably in appearance. The effects of the altered morphology on O_3 sensitivity is not known.

Antioxidants

A wide variety of chemicals offer plants some protection against oxidant injury. A number of widely used fungicides have antioxidant properties. Few chemicals have been produced for use on plants for the sole purpose of protecting against air pollution. The one exception was the compound ethylene diurea (EDU). For a time it was made available as an experimental chemical, but has since been withdrawn because of limited commercial potential.

EDU did offer the potential of doing impact assessments on a much larger scale and on crops difficult to grow in open-top chambers. In Ontario EDU was used extensively on a variety of crops over the past 9 years. On some crops such as white bean and peanut it has been very effective, reducing foliar injury, while on crops like potato it has been marginally effective and on corn totally ineffective.

Yield losses in white bean were felt to be substantial at times and EDU confirmed that (Table 1). In onion losses from O_3 were undocumented and treatments with EDU showed that yield reductions did occur in some years on susceptible cultivars (Table 1). Results were similar to those obtained with open-top chambers. Peanut, a relatively new crop in Ontario, has cultivars which are also very sensitive to O_3. Field trials with EDU have shown yield losses of 32% (Table 1). Although yield losses in potato cultivars like Norland and Norchop are assumd to be substantial in high ozone years, EDU has been ineffective as a tool to provide objective assessments. Control of foliar injury is generally less than 50% and only sporadically has reduced injury been reflected in increased yield (Table 1).

On the other hand EDU has proved to be a useful tool in sorting out interactions between O_3 injury and parasitic diseases. In onion, blast caused by Botrytis is a major disease. It was shown that by reducing O_3 injury with EDU the incidence of disease decreased. Similarly in potato EDU by reducing O_3 injury reduced the severity of early blight. In both cases a fungicide treatment in combination with EDU gave better disease control and increased yields (Table 2).

Because EDU enhanced early blight control, over the past 2 seasons attempts have been made to enhance disease control through the use of fungicides with antioxidant properties. Although there has been substantial O_3 injury and heavy early blight infestations in both years the effects of chemical treatment were small and not statistically significant (Table 3). It appears that an antioxidant reduces the rate of development during the early stages, but by mid-August the disease has overwhelmed the sensitive cultivars. The disease epidemic is very rapid in mid-August and antioxidants have only a small effect in delaying it.

Because O_3 injury is substantial on some cultivars of potato and antioxidants had given poor control of the injury an attempt was made to compare yields of sensitive and unsensitive cultivars over years with varying O_3 levels.

Dose-response Models

Various attempts have been made to develop models of economic losses in crops and the O_3 dose to which the crop is exposed. This approach should work best on those crops where the effects of environmental variables are small on O_3 sensitivity as in peanut, or on those crops where the major factors such as moisture, are controlled as in potato. To reduce the effects of various environmental factors such as temperature, the approach used was to compare the response of sensitive and insensitive cultivars grown side by side.

The cultivar trials conducted for various crops on an annual basis were used for the cultivar comparisons. For potato this proved to be more problematic than anticipated. The results of the potato trials at various locations are compiled each year, but there is no depository for the data. Secondly, within potato one can only meaningfully compare yield among cultivars within a similar maturity range. For potato almost all the early maturing cultivars are sensitive to O_3. Thirdly, the cultivars used in the trials from year to year and place to place are not consistent. Thus there are many gaps for various cultivars. Fourthly, there is a low level of confidence in any single years data. Seed stock from year to year may or may not be virus free. For yield comparisons data over several to many years are used. Because of the many large gaps in O_3 data over the last ten years as well, the approach to compare O_3 dose and relative yield in potato was abandonned.

The approach appears to offer more promise in peanut. Although the cultivars used in a trial in any one year are not always consistent, O_3 sensitivity in peanut appears to be present in certain types. Cultivars within a certain type all tend either to be sensitive or insensitive although these are differences among cultivars within types. Peanut data span relatively few years at present and dose-response models are preliminary.

Conclusions

Not any one approach to yield loss assessment appears to be suitable for all species. Some species are more suited to open-top chambers, others respond well to the use of antioxidants. Dose-response models have the advantage of being able to predict losses from monitoring data and seem the more desirable approach. This approach does require the accumulation of many years data on various cultivars. Several locations with differing O_3 doses would considerably augment the data base. Crops such as peanut, bean, soybean and perhaps others seems to best suited for this approach.

Publications cited on studies supported by OME.

Wukasch, R.T. and G. Hofstra. 1977. Ozone and Botrytis spp. interaction in onion-leaf dieback. Field studies. J. Am. Soc. Hort. Sci. 102:543-546.

Wukasch, R.T. and G. Hofstra. 1977. Ozone and Botrytis spp. interactions in onion-leaf dieback. Open-top chamber studies. Phytopathol. 67:1080-1084.

Toivonen, P.M.A., G. Hofstra and R.T. Wukasch. 1982. Assessment of yield losses in white bean due to ozone using the antioxidant EDU. Can. J. Plant Pathol. 4:381-386.

Holley, J.D., G. Hofstra and R. Hall. 1984. Effect of reducing oxidant injury and early blight on fresh weight and density of potato tubers. Phytopathol. (accepted).

Ensing, J., G. Hofstra and R.C. Roy. 1985. The impact of ozone on peanut exposed in the laboratory and field. Phytopathol. (In press).

Hofstra, G., R.T. Wukasch and D.M. Drexler. 1983. Ozone injury on potato foliage as influenced by the antioxidant EDU and sulphur dioxide. Can. J. Plant. Pathol. 5:115-119.

Table 1. Increases in yield in various crops obtained with the use of the antioxidant EDU.

Crop	Max. yield increase	Reference
Onion	38	Wukasch & Hofstra, 1977
Peanut	32	Ensing et al. 1985
White Bean	36	Toivonen et al. 1982
Potato	25	Hofstra et al. 1983

Table 2. The effect of adding an antioxidant (EDU) to the fungicide treatments for disease control.

Crop	Relative Yield			
	Control	Fungicide	Fungicide + EDU	Reference
Onion	31.8	46.1	43.2	Wukasch & Hofstra, 1977
Potato	17.20	19.10	20.80	Holley et al. 1984

Table 3: The effect of adding a fungicide with antioxidant properties to the control program of early blight Norchip potato.

	1983	1984	1983	1984
	kg/row		Specific	Gravity
Control	7.8	7.1	1.072	1.074
Fungicide	9.7	7.5	1.078	1.079
Combination treatment	9.3	7.3	1.076	1.079

DIOXINS AND FURANS: ANALYTICAL METHODOLOGY, LEACHATES AND CONDITIONS FOR CONDENSATION-DESORPTION ON STACK PARTICULATES

F.W. Karasek, G.M. Charbonneau,
L.C. Dickson, and T. Thompson

Chemistry Department,
University of Waterloo,
Waterloo, Ontario, Canada. N2L 3G1

DIOXINS AND FURANS: ANALYTICAL METHODOLOGY, LEACHATES AND CONDITIONS FOR CONDENSATION-DESORPTION ON STACK PARTICULATES

F.W. Karasek, G.M. Charbonneau, L.C. Dickson, and T. Thompson, Chemistry Department, University of Waterloo, Waterloo, Ontario, Canada. N2L 3G1

ABSTRACT

It is now known that dioxins and furans enter the environment from combustion processes and commercial chemicals. Although there are established methods used for their analysis in water, sediment, biological tissue and particulate matter, methodology improvement and study is necessary to fill in gaps in our detection ability. Several of these related studies are currently being conducted. All these methods depend upon GC/MS techniques.

Methodology for the analysis of dioxins at ultra-trace levels (parts-per-quadrillion) employing AMBERLITE XAD-2 resin is presented. Apparatus for on-field sampling has been designed comprising of a magnetically coupled gear pump, stainless steel tubing, glass fiber filter, a stainless steel column containing the resin, and two flow meters. In the first phase of the project, the testing of the resin, adsorptive losses to glass and teflon precluded the complete characterization of the resin. The second phase of the project is currently underway where actual sampling of the influent and effluent from an Ontario water treatment plant will be sampled.

The absorption and desorption rates of dioxins and furans on flyash are being studied. Flyash from the Commissioner Street incinerator was heated in a pyrex tube under a flow of nitrogen. Organic material desorbed from the first sample was collected on exhaustively extracted flyash downstream. Three temperatures and three nitrogen total volumes were investigated. The desorption losses of dioxins were determined for the heated flyash sample using tetra-, penta-, hexa-, and hepta-chlorodibenzodioxins as external standards.

Procedures for the analysis of organic contaminants in water treatment chemicals are being developed. The water treatment chemicals examined are inorganic materials in the form of solids or aqueous solution. Solid samples are Soxhlet extracted and subsequently analyzed by gas chromatography/mass spectrometer (GC/MS). For liquid samples, the organics are extracted from the aqueous medium into an organic solvent using liquid-liquid extraction techniques. Compounds tentatively identified by GC/MS analysis include branched alkanes and alkenes, long chain alcohols and fatty acids, various substituted cyclic and aromatic compounds, phthalates and their derivatives, ketones, nitrogen-containing compounds, sulfur-containing compounds, and some halogenated hydrocarbons. The total organic content in these samples are found to range from several hundred parts-per-billion (ppb) to approximately twenty parts-per-million (ppm).

INTRODUCTION

Environmental pollution by trace organic compounds originates from various processes of industry, automobiles, combustion, and waste disposal. Many of these compounds, such as polychlorinated dibenzodioxins (PCDD) and polychlorinated dibenzofurans (PCDF), are highly mutagenic and toxic. A number of investigations have been done in the studies of the chemical characterization of these organic compounds. However, the increasing concern about the effects of these environmental pollutants on human health dictate such studies to be carried on in much more detail.

In the past few years more emphasis has been given to the analytical chemistry of water. This interest has arisen mainly from a concern about the potential health problems caused by trace constituents in water and in particular drinking water. It is quickly becoming evident that for a great many suspected species there are no methods with the sensitivity necessary for analysis at the levels at which they are thought to exist. Such is the case with PCDDs.

The investigation of very low concentrations of these compounds is a complex problem which can only be presently solved using a concentration step prior to instrumental analysis. Preconcentration using sorbent trapping techniques are methods of choice in many cases. Amberlite XAD-2 and XAD-4 resins have been used extensively to sorb a variety of compounds from water. Junk et al. developed a reliable technique where water containing organic compounds is passed through a column packed resin and the adsorbed organics are subsequently desorbed using diethyl ether (1). The method was effective for pesticides at concentrations of 20 parts-per-trillion (ppt). The method was later used for the recovery of 2,3,7,8 tetrachlorodibenzo-p-dioxin (2378-TCDD) at the ppt level (2).

Musty et al. used XAD resins for the recovery of chlorinated insecticides and polychlorinated biphenyls (PCB)(4). Rees et al. evaluated XAD resins in the ppt range for a variety of compounds (4). Coburn developed a method for the analysis of PCBs and organochlorine pesticides (5).

The major analytical advantages associated with the sorbent trapping technique compared with solvent extraction are simple chemistry, no need for transportation of large volumes of water, and sampling can be carried out by relatively unskilled personnel. Presently the Ontario Ministry of the Environment (MOE) transports large volumes of water to the Toronto Laboratory for subsequent solvent extraction. The present method is laborious and expensive, whereas sorbent trapping techniques are more amenable to a large scale water monitoring program for the dioxins.

The analysis of gas-phase PCDD and PCDF in stack emissions is complicated by the desorption and condensation of these compounds in the EPA Method-5 sampling train (6). In particular, PCDD and PCDF on the particulates on the filter can desorb and bias the results high. Conversely, gas-phase PCDD and PCDF can be absorbed by the particulate giving a low bias. The purpose of this study is to investigate the condensation and desorption behaviour of these compounds. This report presents the results of a preliminary investigation into the desorption rate of PCDD from flyash.

The preparation of potable water requires the use of a variety of water treatment chemicals. These chemicals are typically inorganic compounds added in the parts-per-million (ppm) range or lower. Even though these compounds are considered to be quite pure there is nonetheless the possibility that they contain trace impurities. Such impurities would then be introduced into the water system during the application of the water treatment chemicals.

There is a great deal of concern today with respect to the effect of the various organic compounds which man comes into contact with during a typical day. Thus it is desirable to minimize the chances of exposure to hazardous chemicals used in daily applications. Such quality assurance requires the development of analytical methodology for the detection and identification of any trace organic contaminants which may exist in water treatment chemicals.

EXPERIMENTAL

Study of Dioxins in Water

In order to study the adsorption of PCDD using the resin an experimental set up, illustrated in figure 1, was conceived. The apparatus consists of 20 liter glass bottles, teflon tubing, a magnetically coupled gear pump, stainless steel column containing the resin, and a valve used to control the flow. Deionized water, previously purified by passing through a column containing XAD-2, XAD-4, and XE-340, was pumped from the 20 liter bottle through a SWAGELOK T joint equipped with a rubber septum. A solution containing 1234-TCDD, 12347-P_5CDD, 123478-H_6CDD, 1234678-H_7CDD was then introduced to the flowing water using the rubber septum. The solution containing the dioxins was then pumped through the resin packed column. Diethyl ether is introduced at the top of the column and allowed to percolate through the resin. The sorbed dioxins are then desorbed. The effluent, collected in a thick walled test tube, contains both water and ether which are separated by freezing out the heavier water in liquid nitrogen and decanting the ether. Benzene is then added to the ether and the volume reduced to several mL by rotary evaporation under reduced pressure. Final

concentration to 100 µL is achieved by blowing the sample down with a gentle steam of high purity nitrogen. The sample is then analyzed by GC/MS.

Initial work showed XAD-2 gave better recoveries for 1234-TCDD than XAD-4. Therefore, XAD-2 resin was used for all experiments. The recoveries for an aqueous solution of dioxin having a concentration of 5 ppt were determined at 50, 150, 300, 450, and 600 mL/min column flow. In order to study the losses during the experiment a comprehensive step by step study was undertaken. The losses where evaluated by rinsing the equipment with methylene chloride followed by volume reduction using a method similar to that already described. In an effort to reduce losses to the glass bottle acid pretreatment using chromic acid was undertaken. The glass bottle was carefully washed with chromic acid, washed with copious amounts of water and the recovery study performed in the regular manner.

Injecting into the water flow stream was thought to affect the losses to the bottle. Therefore, spiking was modified such that the dioxin solution was introduced by injecting directly into a quarter-filled bottle being mixed using a stirring bar. The bottle was subsequently filled with additional water while still maintaining stirring action. The recovery study was then performed in the usual manner.

The erratic overall recoveries led to a study of the separation procedure for the water and diethyl ether. The recovery of the freezing out technique using liquid nitorgen was evaluated by spiking ether containing water. The resulting mixture was separated using the conventional method.

Study of Desorption of Dioxins on Flyash

Flyash from the Commissioner Street incinerator was used as supplied by the MOE without further mixing or size fractionation. Approximately 18

g of flyash was heated in a Pyrex tube 45 cm X 2 cm ID under a 100 mL/min. flow of nitrogen. Three temperatures, 100, 150 and 200°C and three nitrogen totals, 94, 188, and 282 L, corresponding to heating times of 16, 32, and 48 h were investigated. The apparatus is shown schematically in figure 2.

The flyash was transferred to a thimble with a medium porosity glass frit and extracted with 400 mL benzene in a Soxhlet extractor for 16 hours. The extract was concentrated by the procedure described above. The final extract was brought to 300 µL. In the event that particulate matter was suspended in the extract, after the initial concentration step the extract was transferred to a centrifuge tube and centrifuged to drive the particulates to the bottom. The extract was then transferred with rinsing to the pear-shaped flask.

Study of Organic Impurities in Water Treatment Chemicals

Water treatment chemicals examined were in the form of inorganic solids and aqueous solutions of inorganic materials. Solid samples were Soxhlet extracted for a period of 24 hours using dichloromethane (300 mL) as the extraction solvent. Following the extraction period, the organic extract is concentrated down to 100 µL. The extract is then analyzed by GC/MS.

Aqueous solutions undergo a sample preparation which includes conventional liquid-liquid extraction techniques. The samples were extracted with a one litre separatory funnel using three 100 mL aliquots of dichloromethane. Each aliquot is passed through a sintered glass funnel containing a layer of sodium sulphate purified by being Soxhlet-extracted with 300 mL of methanol and dichloromethane for successive 24 hour periods. The organic extracts are then concentrated according to the same procedure used for the solid samples and subsequently analyzed by GC/MS.

Gas Chromatographic and Gas Chromatographic/Mass Spectrometric Analysis

A Hewlett-Packard 5880A gas chromatograph with a flame ionization detector (FID) and cool on-column injector was used for the GC analyses. Chromatographic separations were obtained using a 25 m x 0.31 mm I.D. SE-54 fused silica capillary column (cross-linked, Hewlett-Packard, Avondale, PA. U.S.A.) with helium as the carrier gas.

The GC/MS analyses were carried out on a Hewlett-Packard 5987A gas chromatograph/mass spectrometer with an HP 1000 data system and cool on-column injector. Two fused silica columns, 25 x 0.31 mm I.D. SE-54 (cross-linked, Hewlett-Packard) and 30 m x 0.32 mm I.D. DB-5 (J & W Scientific, Rancho Cardova, CA., U.S.A.), and two GC/MS interfaces (direct inlet and open-split) were used for different studies. The HP5987 GC/MS/DS has a mass spectra search system, Probability Based Matching (PBM) and Self-Training Interpretive Retrieval Systems (STIRS) based on over 70,000 reference spectra. Electron impact (EI) mass spectra (70 eV) and chemical ionization (CI) mass spectra with methane as the reagent gas were obtained for the different studies. For the EI linear scan mode, scanning ranged from 50 to 500 amu at 630 amu/s. The linear scanning for CI experiments was from 60 to 500 amu at 630 amu/s. The selected ions of $[M]^+$ and $[M+2]^+$ of each dioxin congeners were used in the selected ion monitoring (SIM) mode and their integrated areas were employed for quantitation with the external standards.

All solvents used were "distilled in glass", UV grade (Caledon Laboratories Ltd., Toronto, Ont. Canada). The standards of dioxin congeners used were purchased from Ultra Scientific Inc. (Hope, Rhode Island, U.S.A.) and Cambridge Isotopes (Woburn, MA. U.S.A.).

RESULTS, DISCUSSION AND FUTURE STUDIES

Study of Dioxins in Water

Using the apparatus shown in Figure 1 percent recoveries found for the dioxins using an aqueous solution of 5 ppt are given in TABLE I. Flow optimization was impossible with the initial experimental apparatus. The erratic recoveries showed no dependency with flow rate through the resin. Recoveries did vary with degree of chlorination and the higher chlorinated species had the lowest overall recovery. The losses to the apparatus for a column flow of 150 ml/min are given in TABLE II. The majority of the losses are due to adsorption on the glass bottle used to contain the spiked dioxin solution. The losses and column recovery using pretreatment with chromic acid are given in TABLE III. The losses and column recovery for the varied spiking techniques are given in TABLE IV. Acid washing as well as changing the spiking technique did not significantly increase overall recoveries.

Percent recoveries from multiple experiments for the study of the separation technique for the water and ether are given in TABLE V. Junk et al. (1,2) found the freezing out technique reliable for the recovery of many organic compounds including TCDD but our data suggests differently, especially for the higher chlorinated species.

Future work will centre on improving overall recoveries, using sodium sulphate as a drying agent and perhaps using a different experimental set-up.

Study of Desorption of Dioxins on Flyash

The precision of the extraction step was estimated by extracting flyash samples in triplicate and determining the total organic carbon (TOC)

in each extract. 1 μL aliquotes of each extract was injected twice into GC with FID, and the TOC determined by multiplying the total area by an average response factor.

The TOC analyses of the three flyash extrcts are presented in Table VI. Bartlett's Test for homogeniety of variances was used to ensure the variances of the three extracts were not significantly different from each other (7). The precision of the extract step, as estimated by the pooled standard deviation, was three percent.

The amount of each PCDD congener, expressed in ng PCDD/g flyash, lost due to heating is presented in Table VII and presented graphically in Figure 3. The data was tested for temperature and time effects by a 2-way Model I analysis of variance (ANOVA) without replication (7). Within each group of PCDD congeners there was no significant effect due to temperature or heating time at the five percent confidence level. The precision of the quantitation procedure was estimated from the ANOVA to be eight percent. The percentage lost for each congener is presented in Table VIII and graphically in Figure 4. The lack of a dependence upon temperature and heating time is readily seen.

Considering the high percentage of material desorbed and the lack of correlation with temperature or heating time, it is possible that the majority of the PCDD were lost in the first few hours. Since all the PCDD were not desorbed even after heating for 48 hours at 200°C it is possible that some organic material is more tightly bound (chemi-sorbed) to the surface of the flyash and would not desorb under the experimental conditions, while the majority is just adsorbed through van der Waals forces (physio-sorbed). The apparent rate of desorption would then reach a plateau as the heating time increased. This is illustrated in Figure 5.

The presence of two different types of adsorption is supported by the data of Rordorf (8). He measured the vapor pressure of 2,3,7,8-TCDD to be 3.9-15.9 x 10^{-2} Pascal at 100°C and found its decomposition temperature in nitrogen to be between 850 and 1100°C.

There were few qualitative changes in the organic content of the flyash due to heating, as shown in Figure 5. The major peak at 28.2 minutes in the unheated sample was missing in the heated sample. This compound, identified by spectra library matching as molecular sulphur (S_8), likely to be decomposed during heating. Some of the major components detected in the undesorbed flyash were detected in the trap flyash chromatogram. The large peak at 45 min. was identified as a phthalate ester. This likely originated by desorption with nitrogen from the Tygon tubing used to connect the gas supply to the flow meter.

The levels of dioxins found in the trap flyash are shown in Table IX. The data indicates that some dioxins were desorbed and reached the trap flyash without decomposing. The low levels detected would indicate that most of the dioxins were deposited on the glass tube and connections upstream of the trap, or, less likely, passed through the cooled trap without being absorbed.

Since the MOE has changed its sampling time from 24 to 4 hours and changes could be expected to occur at shorter times, it would be sensible to bracket this time in the next set of experiments. In addition, changes should be made to reduce the variability in the analyses. The flyash should be sieved and a fraction of particles with small diameter and narrow size distribution used to improve homogeneity and approximate the size distribution of the flyash trapped on the filter in the sampling system.

Study of Organic Impurities in Water Treatment Chemicals

Tables X to XVI list the compounds which have been tentatively identified based on the work done up to this stage in the project. These identifications were made based on GC/MS analysis with the PBM and STIRS Library search. Since many compounds may give similar mass spectra other methods of compound identification must be employed. Some work has been done using chemical ionization mass spectrometry to aid in this task. Many organic compounds do not give significant molecular ion peaks under normal electron impact conditions. As a molecular ion peak is very useful in establishing the molecular weight and chemical formula of a compound it is desirable to utilize an ionization technique which will yield information regarding the molecular ion of the unknown compound. This is accomplished using methane gas chemical ionization which is a soft ionization technique (with respect to normal electron impact techniques). Most compounds classes give characteristic molecular ion peaks (9), which usually are $[M+1]^+$ or $[M-1]^+$, and therefore it is possible to see if the compound identification based on the library search of the EI mass spectrum is in agreement with the corresponding CI mass spectrum. An excellent example of this was demonstrated in several samples in which the library search listed the most probable identity of one particular compounds in the organic extract as being 3-nitro-1,2-benzene dicarboxylic acid. The molecuar weight of this compound is 211 yet the CI mass spectrum showed a significant peak at 391 amu which appeared to be the molecular ion peak. The second most probable match was that corresponding to the bis(2-ethylhexyl) ester of 1,2-benzenedicarboxylic acid which has a molecular weight of 390 and would be expected to give a major $[M+1]^+$ peak. The difference in the probabilities of the two matches was usually only a few percent which implies that

they have very similar EI mass spectra. Although they may also be distinguishable on the basis of retention times the information obtained from the CI mass spectrum is another form of confirmation of identification which may be particularly useful in cases where standards or retention time information cannot be obtained. Chemical ionization mass spectra may also be useful in cases where two components coelute thereby giving an EI mass spectrum which will not yield a valid identification based on the library search. In such cases the appearance of two significant peaks in the upper amu range canindicate to the fact that the mass spectrum does not correspond to a single component.

The total organic content of each chemical tested is listed in Table XVII. It was determined by GC/FID analysis already described.

Future work in the development of analytical methodology for the analysis of trace organic contaminants in water treatment chemicals will include more extensive use of chemical ionization mass spectrometry as well as the use of retention indicies for compound identification. Also a different column, a Supelcowax 10 bonded phase capillary column, which is more suited to the analysis of polar compounds than the general purpose DB-5 column will be used to obtain more efficient chromatographic separation. Once the qualitative aspect of the methodology has been developed, quantitation of the various compounds found in the water treatment chemicals will follow.

REFERENCES

1. G.A. Junk, J.J. Richard, M.D. Grieser, D. Witiak, J.L. Witiak, M.D. Arguello, R. Vick, H.J. Svec, J.S. Fritz, G.V. Calder, J. Chromatogr. 1974, 99, 745.

2. G.A. Junk, J.J. Richard, H.J. Svec, J.S. Fritz, J. Amer. Water Works Assoc. 1976, 68,218.

3. P.R. Musty, G. Nickless, J. Chromatogr. 1976, 120,369.

4. G.A.V. Rees, L. Au, Bull. Environ. Contam. Toxicol. 1979, 22,561.

5. J.A. Coburn, I.A. Valdmanis, A.S.Y. Chau, J. Assoc. Official Anal. Chemists, 1977, 60,244 .

6. Ministry of the Environment Report # ARB-TDA-66-80, "Source Testing Code Version #2", November 1980.

7. Zar, J.H., "Biostatistical Analysis," Prentice-Hall, New York, 1974.

8. Rordorf, B.F. "Thermodynamic and Thermal Properties of Polychlorinated Compounds: The Vapor Pressures and Flow Tube Kinetics of Ten Dibenzo-p-Dioxins", Abstracts of 4th International Symposium on Chlorinated Dioxins and Related Compounds, Ottawa, Ontario, Canada, October, 1984.

9. Harrison, A.G., "Chemical Ionization Mass Spectrometry," CRC Press, Florida, 1983, pp. 87-114.

FIGURE CAPTIONS

Figure 1: Diagram of apparatus for recovery study of PCDD from water.

Figure 2: Schematic of apparatus for desorption of PCDD from flyash experiments.

Figure 3: Amount of dioxins lost due to desorption, expressed in ng/g flyash. Flyash was heated at 100°C, 150°C and 200°C for 16 hours, 32 hours and 48 hours with a flow of 100 mL/min dry nitrogen.

Figure 4: Amount of dioxins lost due to desorption, expressed as a percentage of the amount originally present on the flyash.

Figure 5: Illustration of the proposed function of amount of dioxin desorbed per arbitrary unit of time when adsorbed via the two mechanisms of physio-sorption and chemi-sorption. If most of the dioxins were desorbed in the first few hours (physio-sorbed), then during the sampling interval used, 16 to 48 hours, there would be little difference seen in the total amount of the more strongly chemi-sorbed dioxins desorbed between the conditions used.

Figure 6: Total Ion Chromatograms (TIC) of extracts of the original, desorbed and trap flyash. The desorbed flyash was heated for 48 hours with a nitrogen flow of 100 mL/min. at 200°C. Analysis conditions were: 25m X 0.32 mm ID SE-54 cross-linked fused silica capillary column; He carrier flow 39 cm/s; on-column injection port at 80°C; column temperature 90°C for 1 min. then programmed to 300°C at 3°/min.; quadrupole mass spectrometer scanned from 50 to 500 amu at 630 amu/s.; direct capillary interface between GC and MS.

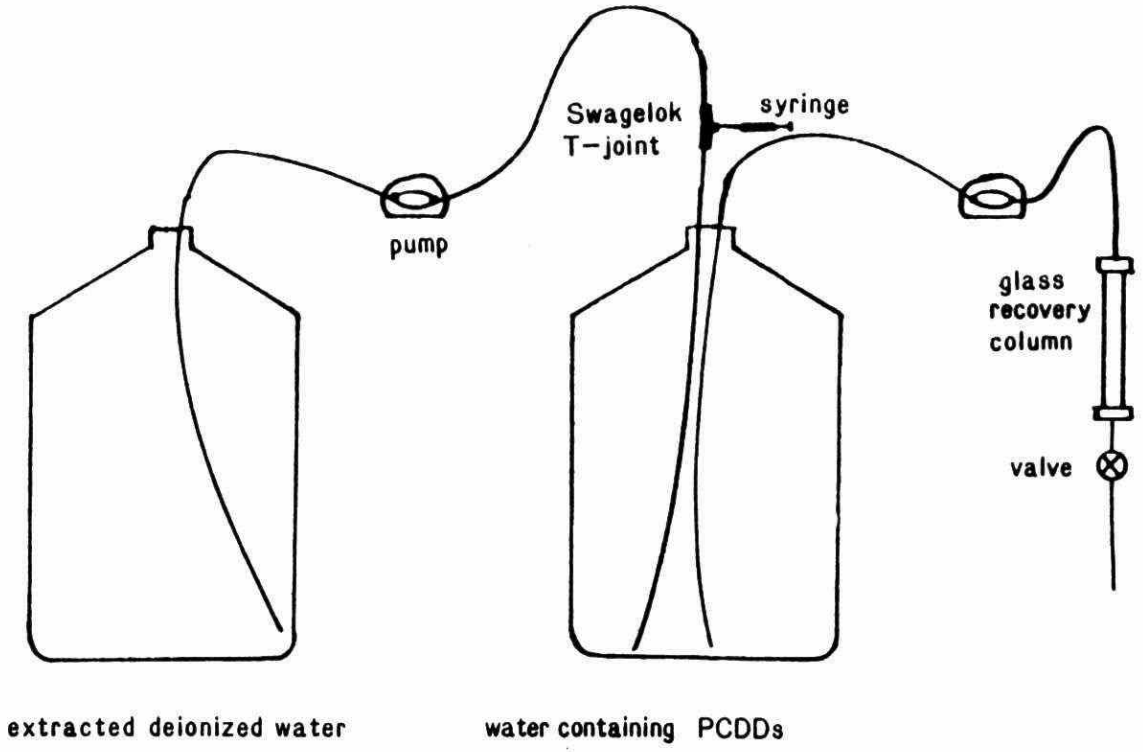


Figure 1 : Apparatus for recovery studies of PCDDs

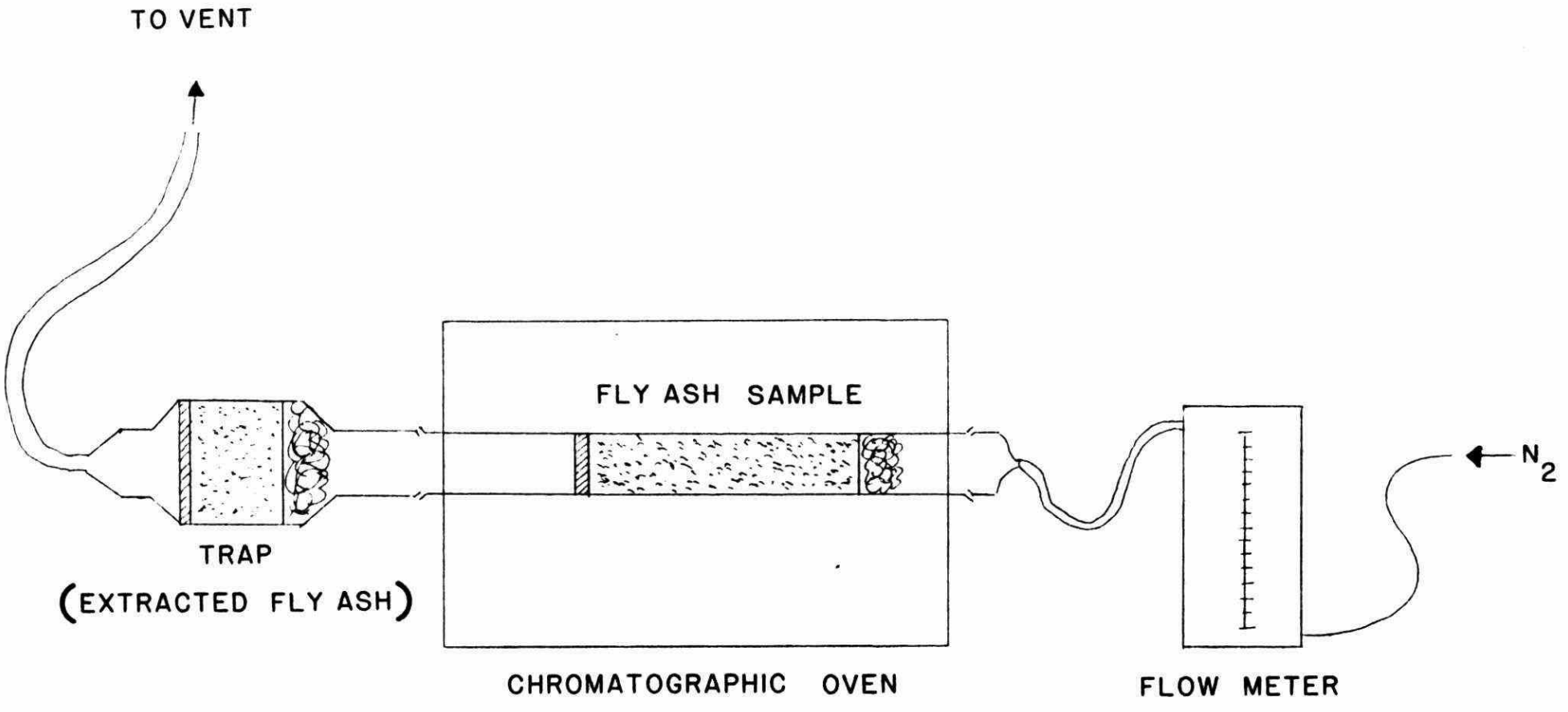


FIGURE 2 SCHEMATIC OF APPARATUS FOR DESORPTION OF PCDD FROM FLY ASH EXPERIMENTS

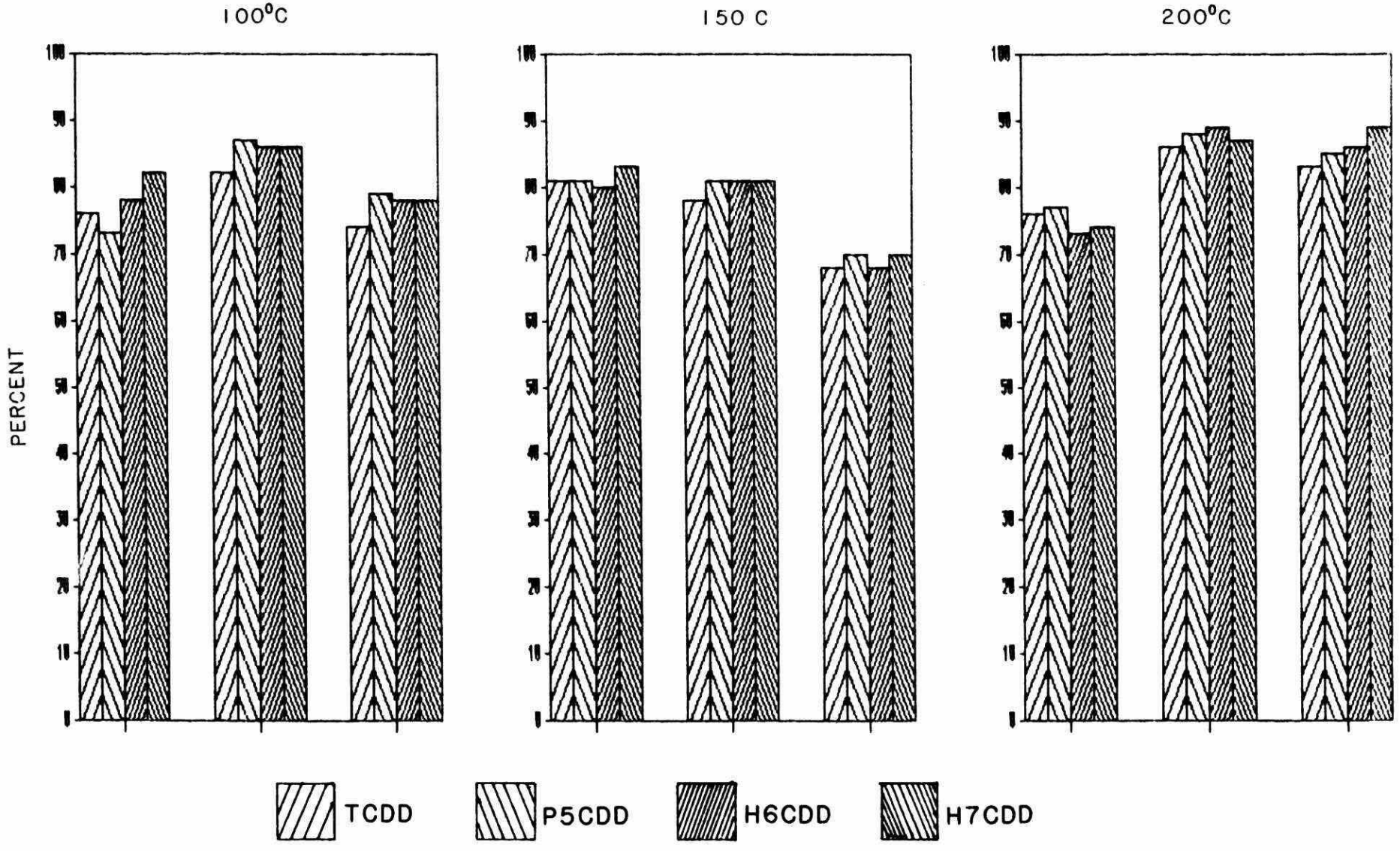


Figure 3 PERCENT DIOXINS LOST BY DESORPTION

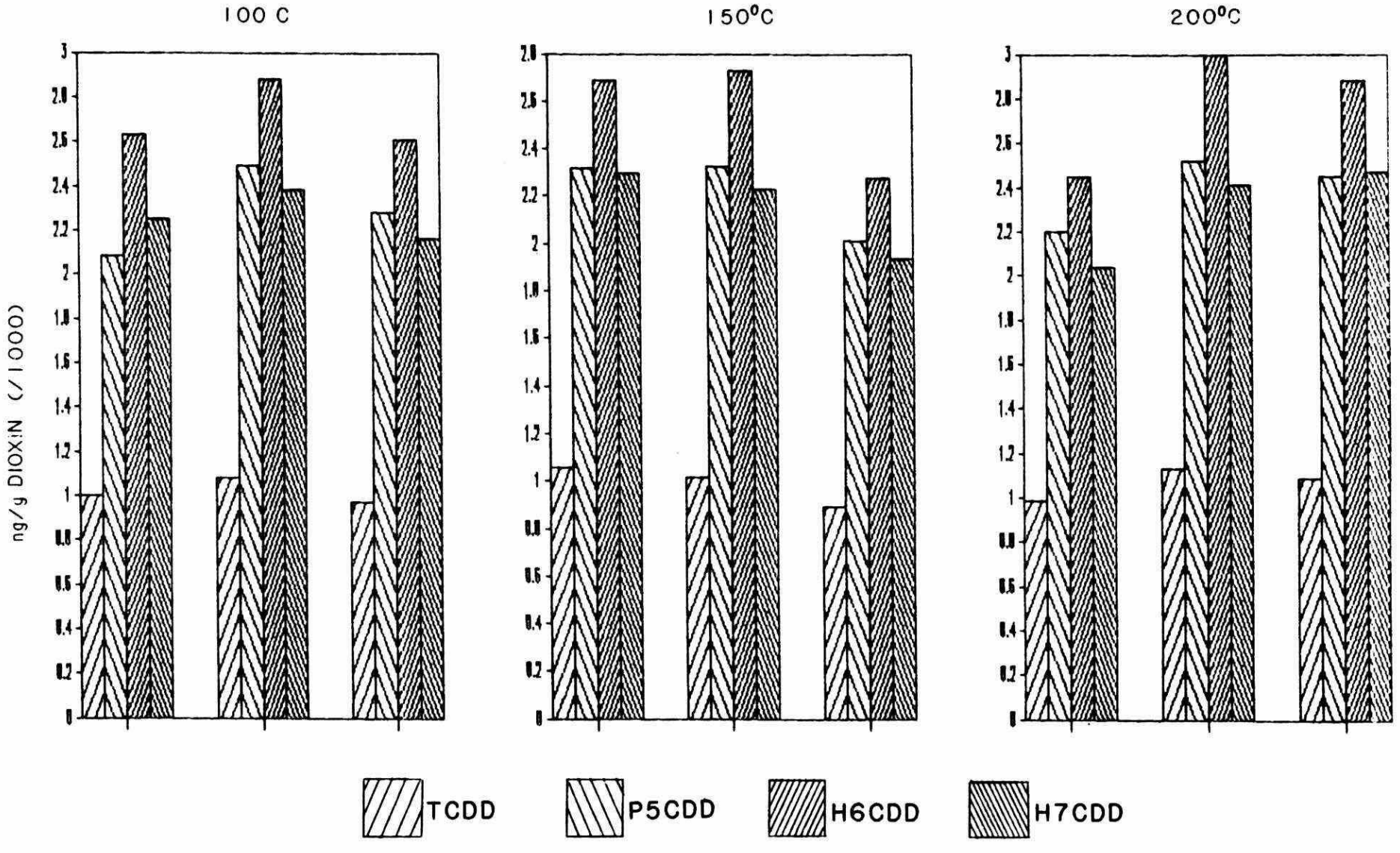


Figure 4 AMOUNT OF DIOXINS LOST BY DESORPTION

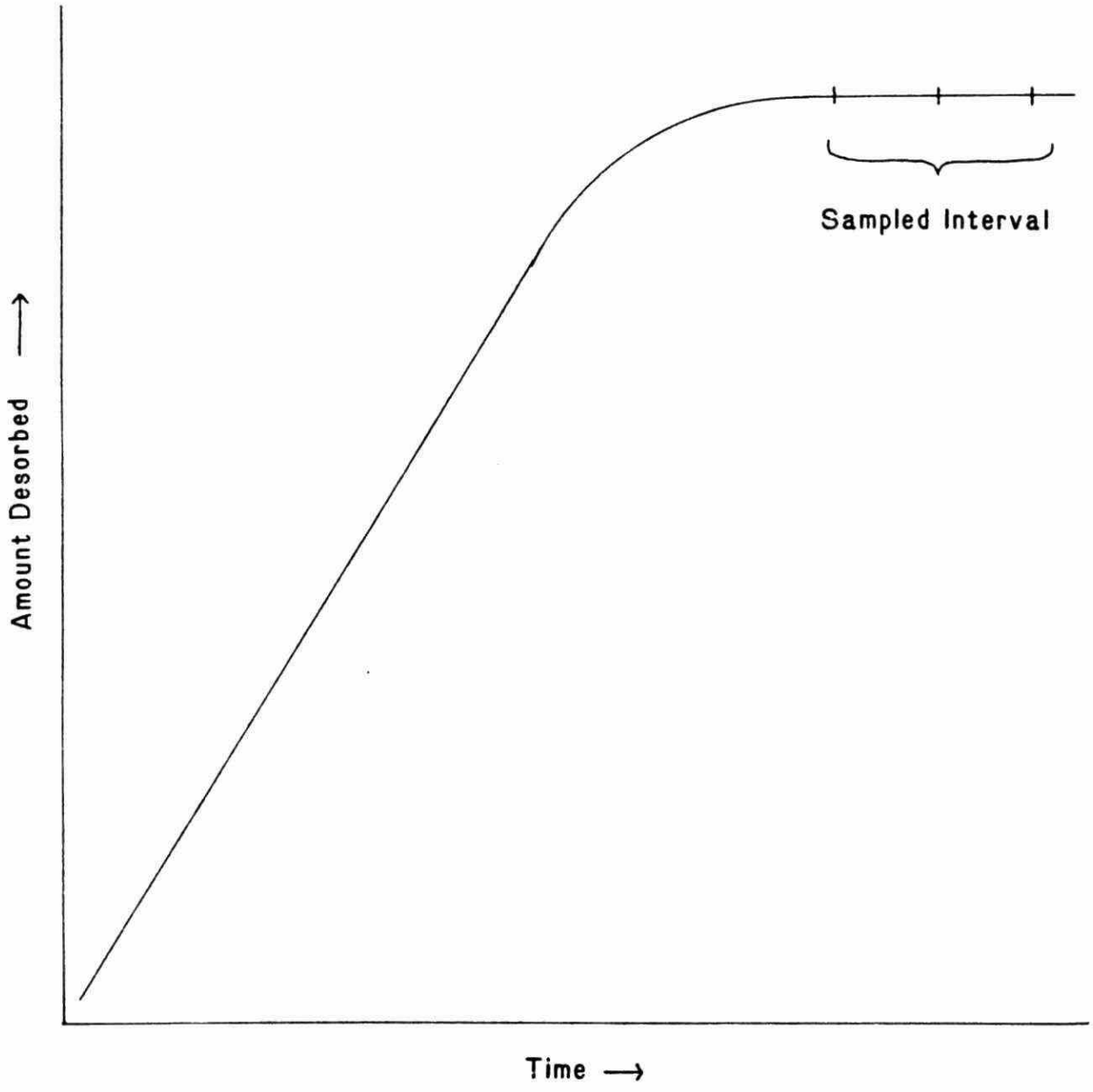


Figure 5 Change of Desorption Rate with Time

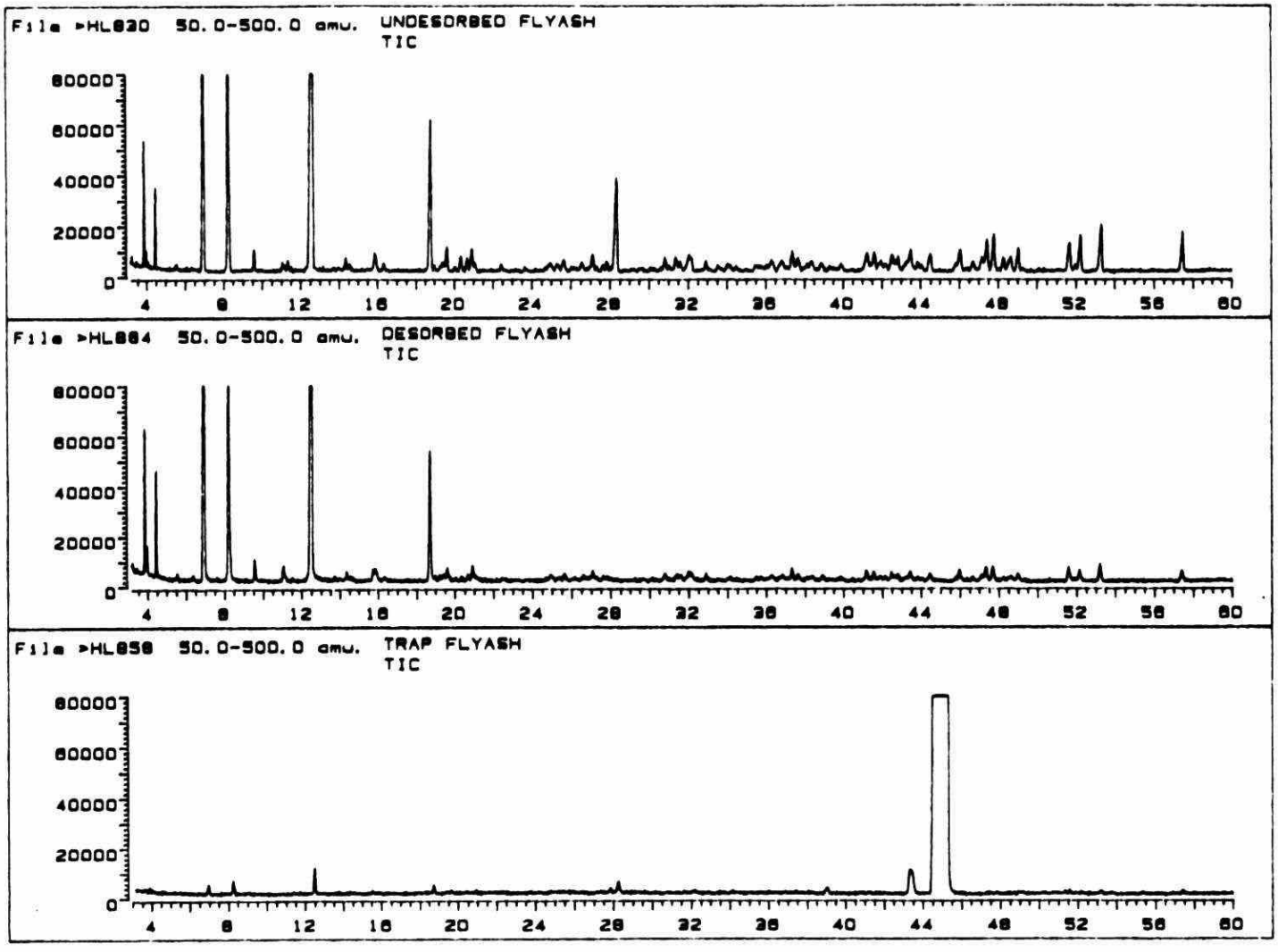


Figure 6 LINEAR SCAN ANALYSES OF FLYASH

TABLE I : Percent recovery of dioxins from water at various flow rates

Sample Flow Rate (ml/min)	% Recovery of Chlorinated Dioxins tetra	penta	hexa	hepta
50	60	22	18	15
150	33	23	24	16
300	73	42	21	10
450	68	20	32	19
600	67	43	22	8

TABLE II : Losses and recovery reported as percent recovery at 150 ml/min

	% Recovery of Chlorinated Dioxins tetra	penta	hexa	hepta
resin	65	49	25	15
bottle	6	15	31	43
tubing	18	10	15	22
total	89	74	71	80

TABLE III : Losses and recovery reported as percent recovery for acid treatment of bottle at 150 ml/min

	% Recovery of Chlorinated Dioxins tetra	penta	hexa	hepta
resin	59	41	46	71
bottle	3	9	25	29
tubing	4	11	31	37
total	66	61	102	137

TABLE IV : Losses and resin recovery reported as percent recovery for modified spiking technique at 150 ml/min

	% Recovery of Chlorinated Dioxins			
	tetra	penta	hexa	hepta
resin	60	49	31	30
bottle	6	14	23	30
tubing	4	6	9	11
total	70	69	64	71

TABLE V : Recovery study of freezing out technique reported as percent recovery

	% Recovery of Chlorinated Dioxins			
	tetra	penta	hexa	hepta
recovery 1	44	43	44	46
recovery 2	50	51	52	52
recovery 3	60	57	51	58
recovery 4	59	61	63	59
recovery 5	73	63	59	61

TABLE VI TOTAL ORGANIC CARBON IN FLYASH EXTRACTS

EXTRACT		MOE I	MOE II	MOE III
INJECTION	1	10340[a]	9780	9670
	2	10540	10310	8840

Average TOC is 9912 micrograms/gram; pooled standard deviation (S.D.) is 296 micrograms/gram; relative standard deviation (R.S.D.) is 0.029.

[a] micrograms organic carbon/gram flyash

TABLE VII AMOUNT OF DIOXINS LOST DUE TO DESORPTION

	TEMPERATURE								
	100 C			150 C			200 C		
TIME	16 h	32 h	48 h	16 h	32 h	48 h	16 h	32 h	48 h
DIOXIN									
TCDD	1000[a,b]	1080	970	1060	1020	890	990	1130	1090
P5CDD	2080[c]	2490	2280	2320	2330	2010	2200	2520	2450
H6CDD	2630[d]	2880	2610	2690	2730	2280	2450	3000	2880
H7CDD	2250[e]	2380	2160	2300	2230	1940	2040	2410	2470

[a] ng dioxin congener/g flyash
[b] S.D. 74 ng/g; R.S.D. 0.07
[c] S.D. 176 ng/g; R.S.D. 0.08
[d] S.D. 225 ng/g; R.S.D. 0.08
[e] S.D. 176 ng/g; R.S.D. 0.08

TABLE VIII PERCENT OF DIOXINS LOST DUE TO DESORPTION

	TEMPERATURE								
	100 C			150 C			200 C		
TIME	16 h	32 h	48 h	16 h	32 h	48 h	16 h	32 h	48 h
DIOXIN									
TCDD	76	82	74	81	78	68	76	86	83
P5CDD	73	87	79	81	81	70	77	88	85
H6CDD	78	86	78	80	81	68	73	89	86
H7CDD	82	86	78	83	81	70	74	87	89

TABLE IX

AMOUNT OF DIOXINS ABSORBED ON ORGANIC-FREE[a] FLYASH

	TIME			
	16 h		48 h	
	100 C	150 C	150 C	200 C
DIOXIN				
TCDD	4.4[b]	3.4	22	37
P_5CDD	0.1	5.1	48	49
H_6CDD	10.4	8.5	69	73
H_7CDD	16.7	7.0	83	67

[a] Soxhlet extracted for 48 hr with benzene
[b] ng dioxin/g flyash

TABLE X

SODIUM BICARBONATE

COMPOUND	CHEMICAL FORMULA	MOL. WT.
2-butoxyethanol	C6H14O2	118
2-ethylhexanol	C8H18O	130
2,3,3-trimethyl-1-butene	C7H14	98
1,2-benzenedicarboxylic acid, bis(2-ethylhexyl) ester	C24H38O4	390*

TABLE XI

SOLID ALUM (EAR FALLS)

COMPOUND	CHEMICAL FORMULA	MOL. WT.
2-octanone	C8H16O	128
3-nonanone	C9H18O	142
butylurea	C5H12N2O	116
2-butenoic acid (Z)	C4H6O2	86
dihydro-5-propyl-2(3H)-furanone	C7H12O2	128
sulphur (molecular)	S8	256
1,2-benzenedicarboxylic acid, bis(2-ethylhexyl) ester	C24H38O4	390*

* confirmed by CI mass spectrum

TABLE XII

SODIUM SILICOFLUORIDE

COMPOUND	CHEMICAL FORMULA	MOL. WT.
2,3-dimethyl-2-pentanol	C7H16O	116
cyclohexanol	C6H12O	100
methylcyclohexane	C7H14	98
1-(methylpropyl)cyclohexane	C10H20	140
2-methyl-4-heptanone	C8H16O	128
4(8)-p-menthen-3-one	C10H16O	152
2,6-bis(1,1-dimethylethyl)-2,5-cyclohexadiene-1,4-dione	C14H20O2	220*
2,5-dibutylthiophene	C12H20S	196
phosphoric acid, tributyl ester	C12H27O4P	266
1-dodecanol	C12H26O	186
1-tetradecanol	C14H30O	214
ionol 2	C16H26O	234
sulphur (molecular)	S8	256*
1,2-benzenedicarboxylic acid, bis(2-ethylhexyl) ester	C24H38O4	390*

TABLE XIII

SOLID ALUM (SMITH FALLS)

COMPOUND	CHEMICAL FORMULA	MOL. WT.
hexanoic acid	C6H12O2	116
3,4-dimethyl-1-hexene	C8H16	112
1,1-diethylhydrazine	C4H12N2	88
nonanoic acid	C9H18O2	158
decanoic acid	C10H20O2	172
2,6-bis(1,1-dimethylethyl)-2,5-cyclohexadiene-1,4-dione	C14H20O2	220*
1-dodecanol	C12H26O	186
tetradecanoic acid	C14H28O2	228
cyclododecane	C12H24	168
tetradecanol	C14H30O	214
pentadecanol	C15H32O	228
hexadecanoic acid	C16H32O2	256
octadecanoic acid	C18H36O2	284
1,2-benzenedicarboxylic acid, bis(1,1-dimethylethyl) ester	C24H38O4	390*

TABLE XIV

FERRIC CHLORIDE SOLUTION

COMPOUND	CHEMICAL FORMULA	MOL. WT.
chloromethylbenzene	C7H7Cl	126
cyclohexanone	C6H10O	98
1,1-dichloro-1-propene	C3H4Cl2	110
1,2-dichloroethene (E)	C2H2Cl2	96
sulfinylbismethane	C2H6OS	78
1,2-benzenedicarboxylic acid, dibutyl ester	C16H22O4	278
sulphur (molecular)	S8	256
heneicosane	C21H44	296
1,2-benzenedicarboxylic acid, butyl phenylmethyl ester	C19H20O4	312
1,2-benzenedicarboxylic acid, bis(2-ethylhexyl) ester	C24H38O4	390

TABLE XV

SODA ASH

COMPOUND	CHEMICAL FORMULA	MOL. WT.
2-methylcyclopentanone	C6H10O	98
2-methyl-2,4-pentanediol	C6H14O2	118*
2-ethylhexanol	C8H18O	130
methylcyclohexane	C7H14	98
2,6-bis(1,1-dimethylethyl)-2,5-cyclohexadiene-1,4-dione	C14H20O2	220*
1-dodecanol	C12H26O	186
1-tetradecanol	C14H30O	214
1-dodecene	C12H24	168
eicosanol	C20H42O	298
1,2-benzenedicarboxylic acid, bis(2-ethylhexyl) ester	C24H38O4	390*

TABLE XVI

CALCIUM OXIDE (LIME)

COMPOUND	CHEMICAL FORMULA	MOL. WT.
methylbenzene	C7H8	92
2,3-dichloro-2-methylbutane	C5H10Cl2	140
4-hydroxy-4-methyl-2-pentanone	C6H12O2	116
cyclohexanol	C6H12O	100
2-methylcyclopentanone	C6H10O	98
1-chloro-2-methylbenzene	C7H7Cl	126
2,4-dimethylhexane	C8H18	114
3,3-dimethylhexane	C8H8	114
6-ethyl-2-methyloctane	C11H24	156*
3-methyl-2-cyclohexen-1-one	C7H10O	110
3-methylundecane	C12H26	170*
2,2,5-trimethyldecane	C13H28	184*
3,3,5-trimethyldecane	C13H28	184*
2,2,3,4,6,6-hexamethylheptane	C13H28	184*
1,1'-biphenyl	C12H10	154*
1-hexadecene	C16H32	224*
1-dodecanol	C12H26O	186*
1-methyldecylbenzene	C17H28	232
1-ethylnonylbenzene	C17H28	232
octylcyclohexane	C14H28	196
1-methylundecylbenzene	C18H30	246
1-octadecene	C18H36	252*

3-eicosene	C20H40	280*
9-docosene	C22H44	308*
9-tricosene	C23H46	322
ethylcyclodocosane	C24H28	336*

TABLE XVII

SAMPLE	APPROXIMATE TOTAL ORGANIC CONTENT (ppm)
Sodium Bicarbonate	0.03
Solid Alum (Ear Falls)	65
Sodium Silicofluoride	0.2
Solid Alum (Smith Falls)	150
Ferric Chloride Solution	1.1
Soda Ash	0.2
Calcium Oxide (lime)	100

MOE'S VOLATILE ORGANIC MONITORING DEVELOPMENT PROGRAM

E. Singer, D. Toner, M. Sage, R. Corkum - Air Resources Branch, MOE
D. Corr, A. Szakolcai - Air Resources Branch, MOE
W. Offenbacher, G. Rees, J. Osborne - Lab Serv & Applied Research Br. MOE
G. Grosse - Southwestern Region, MOE

ABSTRACT

Although MOE possesses sophisticated mobile monitoring capability for organic vapours, these units cannot perform all of the large number of required surveys. Therefore a Volatile Organic Monitoring Development Program was established jointly by the Air Resources Branch, Laboratory Services and Applied Research Branch and the Regions of MOE. The objective of the program was to develop simple on-site sampling, off-site analytical methods for organic vapours.

Major milestones in the program included:

1. Cartridge development - Adsorbents;
2. Pump evaluation and sequential sampler development;
3. Standards generation;
4. Volatile organic preconcentrator development;
5. Analytical methodology development - Dual column chromatography with retention index identification/confirmation.
6. Determination of sample integrity - Effects of storage time and temperature;
7. Field testing.

The above developments and results are described. Further needs of the program are also highlighted.

A poster session manned by several of the collaborators will follow the presentation.

INTRODUCTION

This volatile organic compounds (VOC) monitoring development program represents the cooperative effort of the Air Resources Branch, Laboratory Services Branch and the Regions of the Ministry of the Environment.

In particular, the objective of the program is to develop simple on-site sampling, off-site analytical methods for VOC's. As a background to the program, the answers to the questions: Why measure? What to measure? How to measure? will be explored briefly.

WHY?

In general, measuring VOC's in air could have several different objectives. Firstly, a general hazard assessment of the ambient air in cities would involve assessing the distribution of a wide variety of gaseous organic mutagens and suspect carcinogens and comparing this distribution to rural back-ground levels. Secondly, the assessment may be site-specific, targeting specific toxic compounds near chemical production facilities, waste sites, incinerators, mobile sources etc. The objective may be hazard assessment or to determine if the facility is in compliance with established standards or guidelines. Thirdly, the assessment may be site-specific, with the objective being odour assessment, or determining if the facility is in compliance with odour based standards or guidelines.

WHAT ORGANIC VAPOURS?

Several recent or ongoing VOC programs have been reported. A very comprehensive monitoring effort for airborne toxic substances is being carried out in New Jersey (R. Harkov, 1982; R. Harkov, 1983). Characterization of ambient atmospheres in seven U.S. cities has been carried out recently (H. B. Singh, 1982).

In connection with mobile sources, VOC's in city air during peak traffic periods have been measured (E. Hasanen, 1981). Also, VOC's associated with heavy-duty diesel and light-duty gasoline-powered vehicles have been characterised (C.V. Hampton, 1983). Selected volatile organic compounds in three urban areas of Canada have been determined (D. K. W. Wang, 1984).

Considering these programs together with some MOE surveys near industrial facilities, one can observe that, predominantly, the following classes of VOC's are being found and measured:

- Aliphatic Hydrocarbons (e.g. n-octane to n-heptadecane, etc)
- Chlorinated Aliphatic Hydrocarbons (e.g. Trichloroethylene, Perchloroethylene, Methylene chloride, etc).
- Aromatic Hydrocarbons (e.g. Benzene, Toluene, Xylene, Styrene, etc).
- Chlorinated Aromatic Hydrocarbons (e.g. Chlorobenzene, Trichlorobenzenes, etc).
- Aldehydes/Ketones (Methyl Ethyl ketone, Formaldehyde, Acetaldehyde, etc).
- Esters (e.g. Ethyl acrylate)
- Phenols (e.g. para-Cresol)

HOW?

Sampling methods for VOC's divide into two broad areas: Total sample and selective sample collection methods (W. Thain, 1980).

With the total sample collection methods, an evacuated glass or stainless steel vessel is allowed to fill with an air sample or a pump is used to fill a gas sampling bag (e.g. Tedlar).

With the selective methods, only part of the sample is collected. These methods divide into active (S.I. Lamb, 1980) and passive (L.A. Wallace, 1982) sampling methods. In the active methods the sample is drawn by a pump through a solvent or target compound specific reagent in an impinger or through a sorbent or combination of sorbents in a glass or stainless steel cartridge. Trapping occurs by

selective solubility in a solvent, by reaction with a specific reagent forming a non-volatile derivative or by adsorption on sorbents, respectively. In the passive methods, the sample diffuses to the sorbent or combination of sorbents or diffuses to a reagent and is trapped by the same processes noted above.

Off-site analytical methods for the above samples include GC, HPLC, and thermal or solvent desorption in combination with GC, GC/MS or HPLC.

VOLATILE ORGANIC MONITORING DEVELOPMENT PROGRAM

Giving due consideration to the above trends and developments, the MOE has adopted a generalized sampling method which involves active (pumped) sampling through adsorber cartridges (Figure 1). Various analytical techniques are later applied to the cartridges. The most generally applicable broad spectrum method is the thermal desorption method as illustrated in Figure 1.

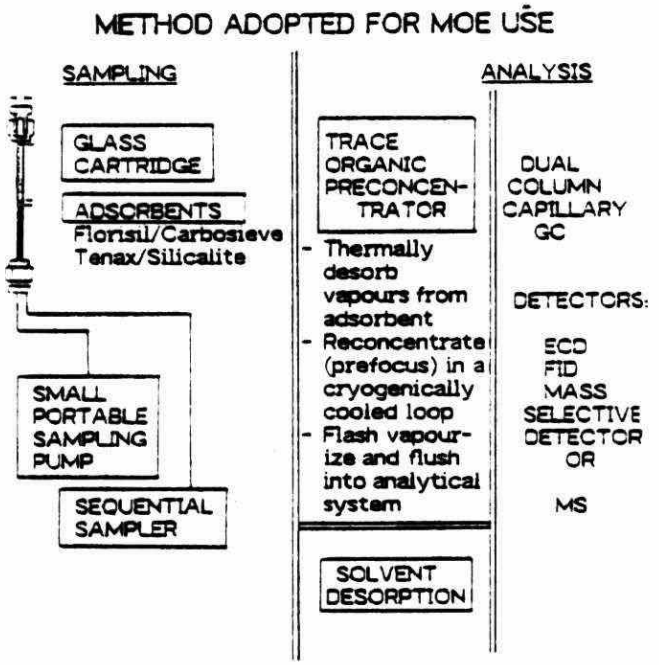


Figure 1. Adopted Method

Central to the method adopted is the thermal desorption of the vapours from the cartridge adsorbents. This was chosen because of the inherent advantages. It is faster than solvent desorption, because no sample preparation is required. Sensitivity is enhanced since the entire sample is analysed. There is no solvent peak to interfere with early eluting compounds. Finally, the entire desorption process, via a carousel mechanism, shows promise of becoming automated. An inherent disadvantage is that the sample can be analysed only once. Major milestones in the program to develop the above monitoring methodology are detailed below.

1. Cartridge development; Adsorbents; Cartridge cleaner

Various porous polymeric and inorganic sorbents have been used for the collection of organic vapours. Two major factors dictated our selection.

On the one hand, the thermal desorption process, the adsorbent cleaning process and desired sorbent stability under reasonable storage conditions, required, that the adsorbent be inert and thermally stable at high temperatures. The latter requirement especially, tends to favour inorganic sorbents.

On the other hand, it was required that the adsorbents have good retention capacity for a wide range of organic vapours. Table 1 below, shows the types of compounds expected to be monitored, opposite the adsorbents which would be most suitable for that purpose.

The four adsorbents shown in Table 1 were selected and combined into two combination cartridges: Tenax TA/Silicalite and Florisil/Carbosieve S. Further advantages were gained this way. The Tenax TA/Silicalite combination yielded a hydrophobic cartridge which may be useful in sampling during wet atmospheric conditions, as well as, in minimizing freeze up of the cryocooled loop during the prefocusing step. Secondly, the Florisil/Carbosieve S combination yielded a cartridge of very high thermal stability, which is therefore easily cleaned giving

negligible background and is therefore useful for determination of trace quantities of trapped organics. Thirdly, both combinations combine a weaker and a stronger adsorbent which may be an advantage in trapping ability during sampling, when flow is from the weaker to the stronger adsorbent. It is also an advantage during desorption where the flow is reversed.

Table 1. Types of Compounds, Adsorbents and their Properties

Types of Compounds to be Monitored	Adsorbent	Adsorbent Properties
Volatile, Non-Polar Aromatic and Chlorinated Aromatic/Aliphatic Hydrocarbons b.p. range: 80 - 200°C	Tenax TA	Hydrophobic Weaker adsorbent
Volatile Organics (molecular size<6Å)	Silicalite	Highly Hydrophobic Stronger adsorbent
Organochlorine Pesticides, PCB's, PAH's	Florisil	Very clean, low background Weaker adsorbent
Highly Volatile Non-Polar Organics b.p. (-15 to 100°C)	Carbosieve S	Very clean, low background Stronger Adsorbent

Glass was chosen over stainless steel as the material for the cartridges, based on previous experience with stainless steel (i.e. ghost peaks) and cost considerations. The cartridges are 120 mm in length and 10 mm in diameter (i.e. OD) and are packed with equal amounts (30-35 mm) of each adsorbent pair.

Several ways of sealing the cartridges were considered. These included heat crimped fluorinated polypropylene (FEP), Ultra-Torr fittings and Swagelock caps with Teflon or graphite ferrules. Finally a Teflon plug and ferrule in combination with a nylon nut was chosen. This way only virgin Teflon is in contact with the inner atmosphere of the cartridge. The plug is easily hand tightened and the smooth surface of the nylon nut discourages over tightening by the use of wrenches.

Before a cartridge can be used for sampling, it must be cleaned of any adsorbed impurities. This can be done by desorbing them with heat and flushing them with an inert carrier gas until such time that their analysis shows an acceptable background.

A thermal cartridge cleaner was designed and built for our applications, to clean a large number of cartridges in a short period of time. The cartridge cleaner consists of a heated aluminum block with 24 cavities drilled into it. At the bottom of each cavity is a high temperature Viton O-ring which seals against the outside of the cartridge and a small orifice to allow for the flow of desorption gas. Ultra pure inert gas (N_2 or He) enters the cleaner via a port located below the orifice plate and flows upward through the cartridges desorbing the impurities. The temperature of the heating block can be set with the push-button potentiometer of the controller which also displays the temperature by an LED.

With this system, cartridges can be cleaned by heating to 350°C under a flow of 20 ml/min of nitrogen for two hours, followed by cooling under a nitrogen flow, and subsequent capping.

2. Pump evaluation and sequential sampler development

The choice of sampling systems was dictated by MOE's regional sampling needs. A need was expressed for two types of samplers:

(a) An inexpensive, portable sampling system for quick investigations.

(b) A more sophisticated sequential sampler for more accurate and detailed surveys.

For quick investigations several portable pumps on the market had to be evaluated. Selection citeria were cost, portability, durability, performance, ease of manual operation and ease of calibration. Performance characteristics tested for were flow stability over time with varying temperatures, flow compensation with varying pressure drop and battery life.

Test results showed that two pumps were best suited for the present purpose. One, however was of a modular design, available as a totally manual pump with the option of upgrading it to a programmable mode. Based on this versatility and lower cost, the Gillian HFS 113U was selected. It has a flow range from 1-5000 cc/min, shows a flow decrease of less than 10% after running for two hours at 3°C, can compensate the flow through cartridges with dissimilar pressure drops to less than a 5% deviation and has a battery life of eight hours with continuous use.

For more detailed surveys, a more sophisticated sequential sampler was designed and built. It can sample twelve cartridges sequentially and may be programmed for start-up, shut-off and sampling duration. The flow rate is accurately controlled by a mass flow controller and there is a total volume indicator for each of the twelve sampling lines. The latter feature ensures that even in the case of an extended power failure, the total volume sampled on each cartridge is known. The internal battery, when fully charged, will operate the sampler through twelve hours of continuous use in the event of a power shortage. Similarly, the sampler can be used in remote locations where power is unavailable. A stainless steel hood protects the cartridges from wind and rain. Individual cartridges, while in the sampler, are sealed at both ends by a gravity seal (i.e. a Teflon ball inside a stainless steel fitting).

3. Standards generation

An ability to generate a standard or mixtures of standards dynamically was needed both for instrument calibration as well as for charging cartridges and challenging passive samplers with conditions resembling the real environment. The

dynamic method involves producing standards continuously in a stream of air, at a known concentration, at ambient levels if required, at a known temperature and at atmospheric pressure. Using the dynamic method, losses associated with wall effects are minimized once equilibrium is established between the chemical vapour passing through the system and the vapour which is retained on the walls of the system by condensation, adsorption, etc.

With the above in mind a vapour standard generator, shown schematically in Figure 2, was designed and built.

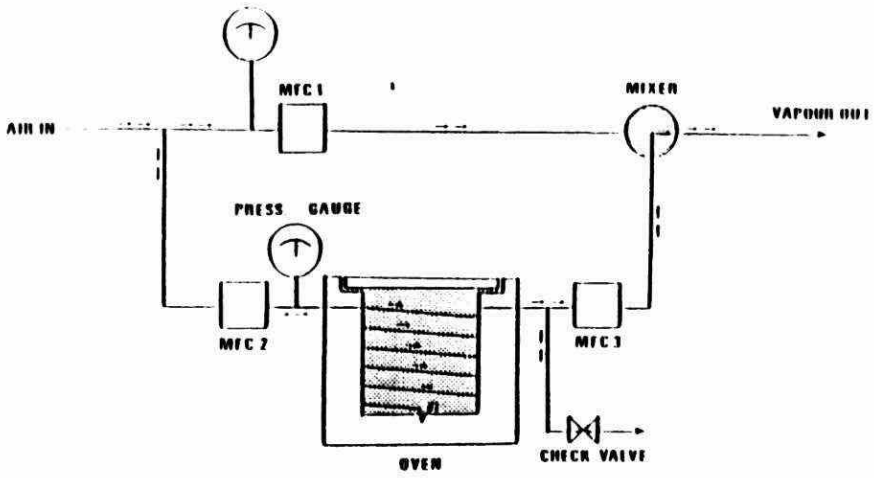


Figure 2. Vapour Standard Generator

The generator features the use of precision bore diffusion tubes and consists of a thermostatically controlled stainless steel oven containing the tubes, mass flow controllers and an auger type mixer. Initial vapour generation takes place continuously in the oven. The oven can contain up to seven tubes at once, allowing for multi-compound charging of cartridges. Diffusion rate of vapours from the diffusion tubes is a function of oven temperature, air pressure in the oven, length and bore diameter of the tube and the compound's diffusivity and

vapour pressure. Flow of pure dry air into the oven is mass-flow controlled. Both the vapour containing air flow from the oven to the mixer and the diluent air flow into the mixer are mass flow controlled. The diluent flow of air is adjustable from one to ten litres per minute. Thus by various combinations of oven temperature, diffusion tube length and bore diameter and amount of diluent flow various concentrations of vapours can be generated in a stream of air. Diffusion tubes can be calibrated gravimetrically.

The outflow from the mixer of the vapour generator enters a water jacketed glass manifold which has six glass sampling ports for loading cartridges, a septum sampling port for syringe samples and an exhaust port. The manifold was needed since, to duplicate environmental conditions, one wants to pull, rather than push, the sample from the flowing air stream, through the cartridges by a sampling pump.

One particular use for this vapour generator-manifold combination (as will be described in section 6) is to load cartridges, over a period of time with a certain concentration of vapours in air. In this particular configuration each glass sampling port on the manifold is equipped with a Teflon stopcock-fitting combination. This permits cartridges to be attached without premature exposure to the manifold vapours. The upstream components of the sampling train consist of Teflon fittings, limiting orifices, a multiport Valco valve and one or two sampling pumps. Limiting orifices compensate for pressure drop differences between cartridges giving a deviation, in flow rate for any two ports, of less than 10%. The Valco valve is such that it allows all cartridges to continue sampling while with a second sampling pump, one cartridge flow can be selected for some particular experiment (e.g. a breakthrough study).

As an interim measure, for gc calibration and quality assurance purposes, a simpler, static standard generator method is also being utilized. This consists of a two litre glass bulb equipped with septum, stopcock, internal

magnetically stirred pillar with one vane and external heating mantle. Standards in this arrangement are good for about three days and therefore are freshly prepared once or twice per week to minimize wall losses over longer periods of time.

4. Volatile organic preconcentrator development

As noted previously, the central feature of the monitoring method adopted is the thermal desorption of the vapours from the cartridge adsorbents. However, direct desorption of the relatively bulky adsorbents into a capillary column system of a gas chromatograph was an incompatible situation both on the basis of flow rates and time scales (i.e. See 'Flows' and 'Time' in Figure 3). In order to bridge this incompatibility an organic preconcentrator was designed and built. The essential parts of the system is an external cartridge desorber, coupled to a cryogenic capillary prefocusing loop which in turn is coupled to a gas chromatograph. An electronic programmer controls programmable valves, heating elements and mass flow controllers, which in turn control gas flows, coolant (e.g. liquid N_2) flows, the timing of heating and cooling cycles and temperatures. Its overall purpose is to desorb the VOC's from the cartridge and to introduce the desorbed vapours to the head of a g.c. column in a narrow slug. This is done in three stages as shown schematically in Figure 3.

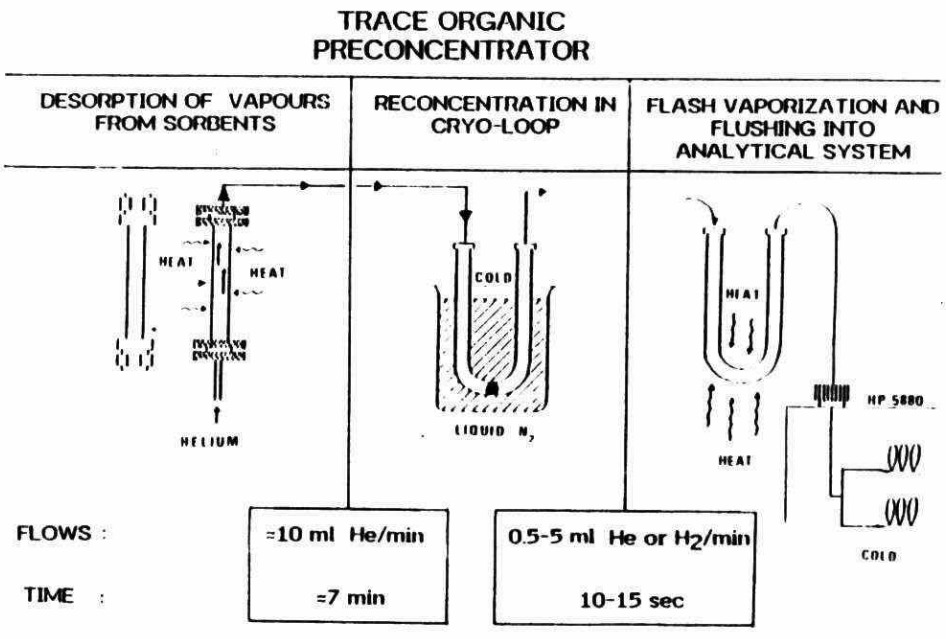


Figure 3. Operations of Trace Organic Preconcentrator

In the first step, the cartridge to be analysed is inserted in the external cartridge holder which has been programmed to a certain temperature. A preselected flow of inert desorption gas for a specified period of time desorbs the vapours from the adsorbents (e.g. typical flows and time for this step is shown in Figure 3).

In the second step, the desorbed vapours are swept through narrow heated lines to a section of nickel capillary tubing (i.e. prefocusing loop) kept cold by an envelope of liquid nitrogen. In this cryocooled loop the organics recondense into a narrow liquid slug (i.e. prefocus).

In the third and final step the prefocused organics are flash vapourized by rapid resistance heating (i.e to $> 300^{o}C$ in 10-15 seconds) of the nickel capillary and are swept into the gas chromatoghraph using capillary column compatible flow rates (i.e. 0.5-5 ml/min). Carrier gas at this stage can be helium or hydrogen.

For gc calibration, an external septum or valve controlled sampling loop is used, through which direct injection onto an internal cartridge or the cryocooled loop can be made.

This volatile organic preconcentrator was initially developed for ARB's sophisticated Mobile Air Monitoring Units. Thus it has some added features. In addition to the external cartridge desorber mentioned above, it contains two permanent internal cartridges packed with sorbents and mounted in an aluminum block. They can be cooled to below ambient temperature (with CO_2 cooling) for trapping highly volatile organics. Furthermore in an on-site sampling, on-site analysis situation one can sample onto one cartridge while the other cartridge is desorbing a previously acquired sample. As noted before, the preconcentrator is fully automated and all these cycles, temperatures and flows can be programmed

according to the needs of the analysis.

5, Analytical methodology development - Dual column capillary chromatography with retention index identification/confirmation

As implied in the preconcentrator development section, dual column capillary gas chromatography, with FID or ECD detectors, is the current analytical finish to the monitoring methodology for repeated, routine applications. Mass, spectrometry or mass selective detector (MSD) based detection methods are envisioned for special applications.

Development of the analytical methodology began as soon as the first prototype of the trace organic preconcentrator was built. It was recognized that in the ng/m^3 concentration range, air can easily contain organic components numbering in the thousands and upwards range. Thus specialized techniques are required.

In particular, the HP-5880 gas chromatograph, with multiple detector and recorder capabilities, is used. As shown in Figure 3, the prefocused organics from the preconcentrator are split on to two capillary columns of different polarity (e.g OV-1 and SE-54) and analysed simultaneously with temperature programming. Cryogenic cooling of the oven can be used to keep the initial sample plug to minimum size.

After analysis, as shown in the upper left of Figure 4, all data from both simultaneous analyses (e.g. retention times (RT), area counts, relative response factors, etc) are transferred automatically from the HP-5880 to an HP-86 computer. This frees the g.c. immediately for the next analysis.

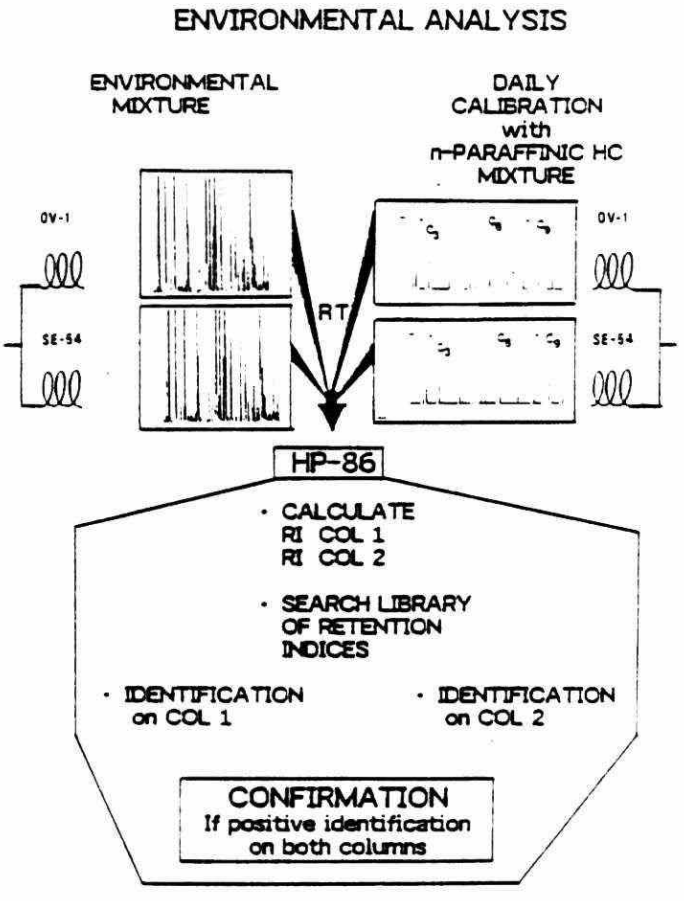


Figure 4. Schematic of dual column capillary g.c. with retention index identification/confirmation methodology

The computer program calculates retention indices (RI) of all identified peaks in the environmental mixture, co-utilizing data obtained daily from a calibration run with an n-paraffinic hydrocarbon mixture (i.e. shown on upper right of Figure 4). Already residing in the HP-86 computer is a library of retention indices for environmentally relevant compounds, set up previously on the same

analytical system. The computer program then compares the RI's of the environmental mixture with the library of RI's of known organics. A tentative identification report is printed out for each column. In the final confirmation report only compounds with positive identification on both columns are printed (i.e bottom of Figure 4).

6. Determination of sample integrity - effect of storage time and temperature

With several areas of the volatile organic monitoring methodology developed, there remains an important consideration before a relatively simple on-site sampling, off-site analysis system can be established. It can be safely anticipated that cartridges, after sampling, will be subject to a variety of adverse conditions (e.g. high temperature in trunk of a car in summer; rattling on transport to lab; various storage time periods between sampling and analysis depending on laboratory workload; etc). Therefore, the criteria, which will best preserve the integrity of the sample until analysis need to be established.

Critical factors which may affect sample integrity are the seal of the cartridge, the temperature of storage and transportation, the elapsed time between sampling and analysis and the type and concentration of organics collected.

As noted in section 1, a good Teflon cartridge seal has been developed. In order to investigate the effect of the other critical factors and to determine the optimum conditions for preserving sample integrity, a contract is currently underway with the Ontario Research Foundation (ORF). Six target compounds, representing four chemical classes, were chosen for this study:

Hexane (Aliphatic Hydrocarbons)

Toluene, o-Xylene (Aromatic Hydrocarbons)

Carbon Tetrachloride, Trichloroethylene (Chlorinated Aliphatic Hydrocarbons)

O-Dichlorobenzene (Chlorinated Aromatic Hydrocarbons)

These compounds are important environmentally and they also represent the physical and chemical properties of their respective classes. The ORF study is subjecting both adsorbent combinations (i.e Florisil/Carbosieve S and Tenax TA/-Silicalite), loaded at three concentration levels with the six target compounds to:

- three temperature storage regimes (4°C, 20°C, 35°C)
- five storage time intervals (immediately, 2-3 days, 1 week, 1 month, 4 months).

The optimal storage and transfer routine, having the least effect on sample integrity, will then be recommended.

7. Preliminary results, field testing and future needs

Preliminary experiments give an estimate of the precision of the combined loading and analytical technique. This involves the dynamic loading of the six target compounds noted in Section 6, at high, medium and low ambient concentrations over a 30 minute period, on both types of cartridges. Cartridges are desorbed and analysed within a few hours. The average standard deviation for five of the six compounds (i.e. one of the adsorbent combinations does not appear to efficiently retain carbon tetrachloride) and cartridges is about 40%.

Preliminary results from field testing the monitoring methodology is shown in Figure 5 and Figure 6. Side-by-side sampling was performed with Florisil/-Carbosieve S cartridges using both sequential samplers (SS) and personal pumps (G), next to the Mobile Air Monitoring Unit's (i.e. MAMU) internal cartridge sampler (MMI) as well as the MAMU's external cartridge/sequential sampler (F/MS/SC/S) combination (Figure 5). Similarly, the sampling was performed using Tenax TA/-Silicalite cartridges (Figure 6). It is noteworthy that the MAMU's adsorbent combinations are different and that the cartridges mounted in the preconcentrator in the MAMU are cooled below ambient temperature (i.e. $\approx 0°C$).

Date: 25/9/84 Time: 14:51 p.m. SAMPLE**	MAJOR PEAKS (ug/m^3)						MINOR PEAKS (ug/m^3)					
	iso-butane	2-methyl butane	pentane	benzene	toluene	m-xylene	3-methyl pentane	hexane	1,1,1,-trichloro ethane	ethyl benzene	1,3,5,-trimethyl benzene	decane
MMI	421	123	28	10	2	9	11	9	7	3	2	4
F/MS/SC/S	392	111	26	27	18	8	8	14	ND	2	2	3
F/C/S	300	92	21	6	10	2	7	6	2	1	ND	2
F/C/S	200	50	11	3	11	6	4	6	ND	2	1	2
F/C/G	437	56	11	4	12	10	8	8	ND	2	2	5
F/C/G	223	49	10	3	11	5	5	6	ND	2	1	1

Figure 5. Side-by-side sampling with Florisil/Carbosieve S Cartridges.

Sampling Time: ½ hour
Sampling Rate: 100 ml/min

** SAMPLE DESCRIPTIONS:

MMI - Mobile Air Monitoring Unit internal cartridge (cooled to 0°C)

F/MS/SC/S - Mobile Air Monitoring Unit external cartridge and Sequential Sampler (at ambient temperature)

F/C/S - Florisil/Carbosieve S + Sequential Sampler (at ambient temp.)

F/C/G - Florisil/Carbosieve S + Gillian Portable Pump (at ambient temp.)

T/S/S - Tenax TA/Silicalite + Sequential Sampler (at ambient temp.)

T/S/G - Tenax TA/Silicalite + Gillian Portable Pump (at ambient temp.)

Date: 1/10/84 Time: 13:05 p.m. SAMPLE**	MAJOR PEAKS (ug/m^3)						MINOR PEAKS (ug/m^3)					
	iso-butane	2-methyl butane	pentane	benzene	toluene	m-xylene	3-methyl pentane	hexane	1,1,1,-trichloro ethane	ethyl benzene	1,3,5,-trimethyl benzene	decane
MMI	150	57	14	13	45	20	8	9	297	6	3	8
F/MS/SC/S	120	57	14	12	46	20	8	11	119	6	3	8
T/S/S	126	59	15	36*	45	19	9	12	130	6	3	7
T/S/S	121	52	13	43*	45	16	9	10	107	5	3	5
T/S/G	ND	17	5	62*	25	7	4	6	6	2	1	2
T/S/G	ND	10	3	62*	25	4	3	3	4	1	ND	ND

Figure 6. Side-by-side sampling with Tenax TA/Silicalite Cartridges.

* - Benzene is a suspected impurity on Tenax TA.

Sampling Time: ½ hour

Sampling Rate: 100 ml/min.

** SAMPLE DESCRIPTIONS:

MMI	-	Mobile Air Monitoring Unit internal cartridge (cooled to 0°C)
F/MS/SC/S	-	Mobile Air Monitoring Unit external cartridge and Sequential Sampler (at ambient temperature)
F/C/S	-	Florisil/Carbosieve S + Sequential Sampler (at ambient temp.)
F/C/G	-	Florisil/Carbosieve S + Gillian Portable Pump (at ambient temp.)
T/S/S	-	Tenax TA/Silicalite + Sequential Sampler (at ambient temp.)
T/S/G	-	Tenax TA/Silicalite + Gillian Portable Pump (at ambient temp.)

As can be seen, despite the different samplers, different sample handling, different adsorbents and different times of analyses, reasonably similar concentrations in air were determined - a very encouraging result.

The uniformly lower results obtained with Tenax TA/Silicalite and the portable pump (Figure 6) is thought to be due to a sampling flow rate problem, (i.e. to the excessively fine mesh size of the Silicalite, which seemed to have formed through use and handling of the cartridges). This created too large a pressure drop, which the portable pump could not compensate for. More work and improved quality control in meshing the Silicalite is required.

FUTURE NEEDS

With simple air monitoring methodology suitable for use by relatively inexperienced field personnel now imminent for at least four classes of compounds (i.e. Aliphatic and Aromatic Hydrocarbons; Chlorinated Ali-phatic and Aromatic Hydrocarbons), several important tasks remain:

- automation of the desorption step
- determination of any other chemical classes which lend themselves to this monitoring methodology
- determination of effects of humidity on adsorption and storage
- development of monitoring methodology for several odorous chemical classes:
    - (a) Mercaptans
    - (b) Aliphatic Amines
    - (c) Aldehydes and Ketones
    - (d) Carboxylic Acids (C_1 -C_5).

    Adoption, with modification, of recent methods (V.B. Stein, 1982; K. Kuwata, 1983; V. Hoshika, 1982) is a possibility presently being investigated.

REFERENCES

- R. Harkov and R. Fischer. 1982. Development and Initiation of an Integrated Monitoring Program for Toxic Air Pollutants. 75th APCA Meeting, New Orleans, June 1982.

- R. Harkov, B. Kebbekus, J. W. Bozzelli, P. J. Lioy, 1983. Measurement of Selected Volatile Organic Compounds at Three Locations in New Jersey during the Summer Season. JAPCA 33, 1177

- H. B. Singh, L. J. Sakas, R. E. Stiles, 1982. Distribution of Selected Gaseous Organic Mutagens and Suspect Carcinogens in Ambient Air. Environ. Sci. Technology. 16, 872.

- E. Hasanen, V. Karlsson, E. Leppamak, M. Juhala, 1981. Atmospheric Environment, 15, 1755.

- W. Thain, 1980. Monitoring Toxic Gases in the Atmosphere for Hygiene and Pollution Control. Pergaman Press, 1980.

- C. V. Hampton, W. R. Pierson, D. Schuetzle, T. M. Harvey, 1983. Hydrocarbon Gases Emitted from Vehicles on the Road. 2. Determination of Emission Rates from Diesel and Spark-Ignition Vehicles. Environ. Sci. Technology 17, 699.

- S. I. Lamb, C. Petrowski, I. R. Kaplan, B. R. T. Simoneit, 1980. Organic Compounds in Urban Atmospheres: A Review of Distribution, Collection and Analysis. JAPCA, 30, 1098.

- L. A. Wallace, W. R. Ott, 1982. Personal Monitors: A State-of-the-Art Survey. JAPCA, 32, 601.

- V. B. Stein, R. S. Narang, 1982. Determination of Mercaptans in Air by Gas Chromatography with Photoionization Detection. Anal. Chem. 54, 991.

- K. Kuwata, E. Akiyama, Y. Yamazaki, H. Yamazaki, Y. Kuge, Y. Kiso, 1983. Trace Determination of Low Molecular Weight Aliphatic Amines in Air by Gas Chromatography. Anal. Chem, 55, 2199.

- K. Kuwata, M. Uebori, H. Yamasaki, Y. Kuge, Y. Kiso, 1983. Determination of Aliphatic Aldehydes in Air by Liquid Chromatography. Anal. Chem., 55, 2013.

- Y. Hoshika, 1982. Gas Chromatographic Determination of Lower Fatty Acids in Air at Part-per-Trillion Levels. Anal. Chem., 54, 2433.

- D. K. W. Wang, T. F. Dann, J. Mar, 1984. Analysis of Selected Volatile Organic Compounds in Three Urban Areas of Canada. Preliminary Data Report. Pollution Measurement Division, Environmental Protection Programs Directorate, Environment Canada.

THE INHALABLE PARTICULATE PROGRAM: STUDIES OF AEROSOL DEPOSITION IN THE LUNG AND POLLUTION SOURCE CHARACTERIZATION

John F. Hicks
Air Resources Branch

Abstract

This presentation outlines the activities of the inhalable particulate program over the past two years. A brief synopsis of the dichotomous sampler - energy dispersive x-ray particulate analysis system used for a network of 11 Ontario sites introduces the presentation. Studies in particulate deposition and uptake in the body, and the source-receptor modelling of atmospheric aerosols constitute the main body of the talk. Finally, the dichotomous sampler - x-ray analysis system with source-receptor modelling is shown to have excellent possibilities of not only determining the degree of particulate pollution, but also which sources contribute the greatest amount and present the greatest risk to human health.

THE ONTARIO INHALABLE PARTICULATE PROGRAM

John Hicks

Air Resources Branch

The dichotomous sampler - X-ray analysis system is presently operating at eleven sites in Ontario. The samplers are located primarily in urban centers although two are operating in rural settings. Data generated from this network will be used to:

1. provide information for setting an inhalable particulate standard;
2. provide accurate particulate mass elemental concentration data at these local sites.
3. determine the feasibility fo the 10 um particle inlet head;
4. generate data for source-receptor modelling applications.

The Dichotomous Sampler

The dichotomous sampler is modelled after inertial virtual impactors which fractionate particles according to their aerodynamic characteristics, simulating the behaviour of the particle in the lung. Developed from the cascade centripeter, it is designed to sample those particles less than 10 um. in aerodynamic diameter and to separate them into the coarse (2.5 to 10 um.) or the fine fraction (less than 2.5 um). The size-segregated aerosol is filtered by a chemically inert teflon membrane filter. The aerosol on the filter can be analyzed later in the laboratory. The dichotomous sampler has a much lower sampling rate than the Hi-Vol, sampling 24 m^3 in each 24-hour period.

Inlet Head

The inlet head was designed to allow particles smaller than 10 um. into the sampler. Particles greater than this are too prone to gravitational settling to

enter the inlet tube. The head is cylindrically symmetric to provide uniform sensitivity to particulates, independent of the wind direction. The inlet only allows particles which are capable of entering the respiratory system into the sampler.

Virtual Impactor

From the inlet head, the sampled particles pass down through a vertical tube to the virtual impactor, which separates the particles into their respective coarse and fine modes. In this regard it simulates a conventional impactor but instead of an impactor plate, it creates a void relative to the inertial flow. Larger particles are carried into this void because of their greater inertial momentum. Once the aerosol is aerodynamically fractionated into two air streams it is collected on teflon filters.

Automation

The degree of automation varies with the make of the sampler. All have programmable timing mechanisms and feedback control loops to maintain a steady pressure drop across the impactor and filters. This feedback system is essential for the maintenance of the correct size fractionation as weather conditions change or the filter resistance increases with particulate load. some models can change samples automatically either at a pre-specified time or when the flow resistance of the sample is too great to maintain established fractionating cutpoints.

Weighing and Handling the Filters

Dichotomous sample filters are weighed prior to and after exposure at the Laboratory Services Branch. A number of experiments have been implemented to determine optimum weighing and sample handling proctices. Some operational errors can be minimized with proper equipment and control, but other errors such

as occasional leakage of particulates through the snap ring seals must be considered as inherrent errors until the technology is improved. This was apparent with all dichotomous samplers tested.

Analysis of Samples

Loaded teflon filters are analyzed by an energy dispersive XRF unit (ORTEC TEFA III) operated by Laboratory Services Branch. This instrument is capable of rapidly and non-destructively analyzing the filters for 34 elements.

The analyte detection limits of the instrument are dependent upon the mass loading of the filter. The appropriate detection limits for an average sample are:

ug/filter		ug/m^3 air	ug/filter		ug/m^3 air	ug/filter		ug/m^3 air	ug/filter		ug/m^3 air
Mg	0.1	0.004	Ti	0.24	0.01	Ga	0.01	0.0004	Zr	0.6	0.03
Al	0.24	0.01	V	0.06	0.003	Hg	0.02	0.0008	Pd	0.03	0.001
Si	0.30	0.01	Cr	.036	0.02	As	0.18	0.008	Ag	0.06	0.003
P	0.12	0.005	Mn	.004	0.0002	Se	0.06	0.003	Cd	0.6	0.03
S	1.1	0.046	Fe	0.12	0.005	Br	0.12	0.005	In	0.1	0.004
Cl	0.3	0.01	Ni	.06	0.003	Pb	0.3	0.01	Sn	0.1	0.004
K	0.18	0.008	Cu	.06	0.003	Rb	0.06	0.003	Sb	0.2	0.008
Ca	0.24	0.01	Zn	0.12	0.005	Sr	0.06	0.003	Ba	3.0	0.13
Y	0.02	0.0008	La	0.7	0.03						

The detection limits are given as ug/filter, i.e. the minimum amount of analyte necessaary to be on the filter to induce a signal, as well as the equivalent airborne concentration.

Source-Receptor Modelling

The inhalable particulate program is presently implementing chemical-mass balance methods of medelling source contributions to local airsheds. The model, programmed for an IBM PC, weighs the influence of various sources to the ambient air sample. Elemental source profiles are statistically "fitted" to the ambient profile. By determining the most probable set of sources contributing to the sample, the relative influence of the source on the airshed can be assessed. This method of modelling has been found to be ideally suited to the dichotomous - Xray analysis system. Although, this modelling method has been used with sucess in the assessment of local winshed situations, it's application to long range pollution appears limited.

Inhalable Particulates and Health

The dichotomous sampler - Xray analysis system is presently being used to determine the relationships between inhaled particulates and health. These studies include the Triministry Blood Lead Level Study, the Gage Research Institute Asthmatic Study, and a Woodsmoke Assessment survey.

If the health effects of inhaled particulated can be inferred from ambient sampler measurements and source-receptor modelling applied to the sample, then the effects of a single pollutant source on public health can be inferred. The dichotomous sampler - Xray analysis system with source receptor modelling shows excellent promise of providing this type of information.

Studies in Aerosol Deposition in the Lung

Inhalable particulate has been shown to deposit in the respiratory system in varying quantities depending on the initial aerosol concentration, the region of impact and the aerodynamic behaviour of the particualte. A number of experimental and theoretical models have found the human respiratory system can be reduced to three regions of different deposition characteristics, clearance ability, and susceptibility to damage. Laboratory tests within insoluble man-made aerosols have produced a deposition model whereby the behaviour of aerosol size fractions in each region can be estimated and predicted. Generally, particulates capable of being inhaled, are divided into fine and coarse size fractions which deposit in the lower and upper respiratory regions respectively. The technology used to measure and control atmospheric particulate matter, as well as the proposed standards of regulation are all based upon the distinct aerosol size ranges defined by this deposition model.

The deposition model is based upon measurements using insoluble tests aerosols which are not altered or absorbed in the warm moist conditions of the respiratory tract (Table 1). Air which is respired is quickly saturated with humidity and water may condense upon inhaled aerosols while in flight. Insoluble aerosols will not be affected but soluble particles will absorb the condensed water and continue to grow until exhaled, absorbed by the lung walls upon deposition, or a droplet results. The acquision of water while in flight will give the particle/droplet different aerodynamic properties which may change the site of deposition. For this reason the model may not accurately predict particulate deposition.

The experiment was to measure atmospheric particulate with two identical dichotomous samplers. The samples fractionate the aerosol into the two aerodynamic size fractions which the model defines as fine and coarse particulate or those size fractions which correspond to lower and upper inhalable dusts respectively. The only difference between the samplers was that one was heated and humidified to simulate conditions the aerosol encounters upon inhalation in the respiratory system. The other sampler was operated under standard field conditions. If the humidified conditions have little or no effect upon the aerosol the two pairs of measurements should be identical within experimental error. If there is a significant shift in aerosol measurements between the two samplers, the data can be analyzed to determine the degree of condensational growth of the particulate. This data can then be applied to the deposition model of respiratory deposition.

Table 1

LIST OF TEST AEROSOLS USED IN DEPOSITION STUDIES

Test Aerosol	Researcher	Solubility in Water
Ferric Oxide	Lippmann (1977)	insoluble
Triphenyl Phosphate	Altshuler et al. (1967)	insoluble
Carnauba Wax	Giacomelli-Maltoni (1972)	insoluble
Polystyrene Latex	Martens and Jocobi (1973)	insoluble
di(2-ethylhexyl) sebacate	Heyder et al. (1973)	insoluble
di(2-ethylhexyl) sebacate	Rudolf et al. (1974)	insoluble
china clay	Brown (1950)	insoluble
polystyrene	Foord et al. (1980)	insoluble

EXPERIMENTAL PROCEDURE

The dichotomous sampler fractionates find (d 2.5 um) and coarse d = 2.5 um) particulates at the arbitrary 50% cut-point of 2.5 um in aerodynamic diameter. This cutpoint should not be construed as being the definitive point between all particles which deposit in the upper and lower respiratory regions. Rather it is the point which defines which region the majority of the deposited particulates will settle or impact. Since the dichotomous sampler measures inhalable particulate fractions on this simplified deposition model, and the dichotomous sampler will become the instrument of use by most pollution monitoring agencies, it is fitting to use the same simplified deposition cutpoint as defined by the sampler in this experiment.

Humidifer Column

The modified inlet tube or humidifer column was designed to use the same attachment configuration as the replaced tube to the virtual impactor assembly and the 15 um inlet head.

Adsorbent artifical chamois was wrapped around a wire mesh cylinder of 1 cm. I.D. by 1 meter long dimensions. The mesh provided structual support to the chamois roll. The chamois material has great water retainment ability and is easily shaped to form. The chamois wire mesh roll is then covered in a plastic wrap to prevent water leakage to the exterior and any air leakage through the column. The column was then inserted into a 3 cm inside diameter x 90 cms long stainless steel conduit tubing to give structural strength and weather resistance. The open ends of the columns were fitted with the required fittings to allow attachment to the dichotomous sampler between the virtual impactor assembly

and the inlet head. A small hole 3 mm diameter was drilled through the outer shell to the chamois and the top of the column and a bulkhead fitting is inserted to allow water to be added to saturate the chamois. Heating tape was wrapped around the humidifer tube just below the bulkhead fitting to provide vapourization of the water as it entered the tube and to warm the ambient air to 37°C. The wattage through the heating tape was controlled externally by a variable transformer since the amount of heat required varied with the temperature of the incoming ambient air.

The inner bore of the column was modified to be conducive to laminar streamlines and prevent unnecesary air turbulence which might cause settling or impaction of particulates on the column walls. Ragged edges at the top of the wire-chamois wrap were covered over by a funnel bottom to reduce aerosol impaction in this area. Similarly the wire mesh-chamois wrap fitted around the virtual impactor attachment tube to enable excess water droplets to escape external to the virtual impactor and not fall into the impactor jet. An additional precaution to prevent internal water leakage was taken by maintaining the jet surface at a higher temperature, thereby evaporating any stray water droplets before they entered the virtual impactor assembly. In this experiment the columns were made in duplicate with only one requiring the heating tape. Each sampler was fitted with one column to duplicate any wall losses on one to the other. Still, it is thought that wall losses were minimal due to the vertical positioning of the column and the streamlined flow through the tube.

Virtual Impactor - Filtration Assembly

Once again air is warmed and humidified as it is maintained for a short period of time for the condensational process to occur. This was attained by lengthening the tube and maintaining the particulates in the required atmosphere

for the designated time. The resulting coarse and fine particulates were then fractionated by the virtual impactor into their respective flowstreams and filtered. To prevent condensation on the coarse and fine filters and tubing the humidified atmosphere was dried. This was achieved by raising the temperature of the fractionated airstreams and thereby lowering the relative humidity. Another length of heating tape, controlled by a separate variable transformer was used for this purpose. The flexible heating tape was wrapped around the filter inlet tubes, but also around the filter holders and the impactor housing. It must be noted that if too much heat was applied to the impactor it would conduct up into the humidifier column walls and cause irregularities in the humidification stage. Similarly excessive heating of the teflon filter holders would cause the filter rings to leak and uneven particulate deposition or leakage will occur on the filters.

Accessory Materials

Water flow to the chamois must be continuous and well controlled to avoid excessive build-up and leakage into the impactor. This was accomplished with a syringe injection drive unit designed for gas chromatograph samples. A 50 ml. syringe was used to inject water for approximately two hours depending on the humidity of the ambient air. The syringe had to be refilled regularly throughout the sampling run. The syringe was connected to the bulkhead by tygon tubing.

The dichotomous sampler, complete with humidifier column was mounted in a metal cabinet where the variable transformer, syringe drive unit and external heating tape could be protected from inclement weather. The sampling inlet was allowed to protrude from through a hole in the top of the cabinet. A space heater was also placed within the cabinet to maintain the syringe temperature above freezing if sub-zero weather was encountered.

Consequences of Sampler Modifications

There was a possibility that these design modifications might affect the performance of the sampler. However, calculations showed the change in inlet air volume due to heat expansion and vapour addition to be minimal and of little consequence. The change in volume due to vapour addition would vary depending upon the initial humidity of the inlet air, but should never exceed 0.3%. However, the expansion of the inlet air due to heat, as it was brought to 37°C. in the humidifier column, was noticeable. Although the expansion due to heat does not affect the volumetric flow rate at the pump (the air is cooled to ambient temperature between the filters and the pump) it will affect the flow through the impactor jet and hence, the cutpoint itself. The cutpoint is dependent upon the Stokes number of the jet according to:

$$\text{Stk \#} = \frac{p_p C V_o D_p^2 / 18u}{W/_2}$$

The change in the stokes number due to expansion and the change in cutpoint can be found from Marple's graphs of impactor operating characteristics. The volumetric change of the air passing through the jet was calculated to lower the cutpoint from 2.5 um. as specified for the sample to 2.42 um. aerodynamic diameter for an average sampling day. Although the change in cutpoint was significant and should be noted it was expected that the net effect on coarse-fine filter deposition would be small.

Once the flow is fractionated the air is again heated to reduce the humidity and "dry" the air to prevent condensation on the filter. The drying of particulates at this point is inconsequential since size fractionation has already

been accomplished. In fact, the drier the aerosol, the better it will deposit and not form a solution upon the filter matrix. The hydrophobicity of the telfon filters retards any unwanted solution leakage through the filter pores. The addition of heat to the filtration flow lowers the humidity of the air from 95% to 50% R.H. This is dry enough to prevent any condensation on the filters. The air is cooled after filtration to ambient temperature and the condensed water is collected in catch jars at this point.

Differences in sampling efficiency of the two columns appeared to be minimal. Results from samplers modified with humidifier columns agreed well when no humidity is added.

Heat and Temperature Gradient In The Column

The humidity and temperature profiles depicted in Figures 1 - 3 show the change in the conditions of the sample air as it flows through the 1 metre long column. Sample air takes 1.0 second from the time of entrance of the column to the entrance to the impactor jet by which the sample is properly fractionated. The column is divided into 10 cm sections each of which corresponds to 0.1 seconds of air flow.

By using a value of 1.0 seconds in this experiment the residence time of particles in this column would approximately correspond to the time it takes particles to proceed from the nose to the the terminal bronchioles. The column effectively simulates the passage of particle laden air upon inhalation through the naspharyngeal and tracheobronchial regions.

Operation

Although both samplers were fitted with humidifer tubes only one was actually operated to inject water vapour and heat to the sample flow. The samplers were placed in the same area where similar samples could be compared but at a great enough distance away from each other to diminish any mutually interfering effects. The samplers were visually checked every 2 hours to maintain identical operation. (e.g. Flow rates can vary as ambient temperature increases). Parameters such as outdoor temperature and humidity, and sampler column temperature and humidity (95% R.H. @ 37^{o}C.) were checked at this time. The syringe system on the humidified column was refilled with distilled water every two hours. Syringe flow rate and variac wattage to the heating elements was adjusted to account for any change in ambient temperature or

humidity. Although the sampler requires regular adjustment it maintains stable operating parameters within prescribed limits (95% $\pm$ 3% R.H. and $37^{o} \pm 4^{o}$C.). From theoretical considerations as described previously, variations of the parameters with these limits should not produce any noticeable variation from the desired conditions.

Through experience it was found that adequate samples could be acquired after 28 hours of operation. During heavy pollution episodes this could be shortened to as low as 4 hours depending upon the Air Pollution Index as given hourly by the Ontario Ministry of Environment. Samples of adequate quality were taken during periods of light to abnormally heavy pollution levels.

Every sample consisted of four filters, a fine and coarse filter deposit from both the humidified (wet) and unhumidified (dry) sampler. Each filter was designated a code according to its placement. They are - DF - dry-fine or the fine deposit of the unhumidified, unheated sampler, DC - dry -coarse or the coarse deposit of the unhumidified, unheated sampler. And WF - wet-fine or the fine deposit of the humidified, heated sampler and WC - wet-coarse or the coarse filter of the humidified heater sampler.

Location

The two samplers were placed upon the roof of a downtown Toronto office building. The location is subject to pollution of vehicular, industrial, and natural origin. The samplers were well ventilated and were subjected to identical weather conditions. As noted earlier the humidifier tube, heating tape, syringe mechanism, virtual impactor and filter holders of the "wet" sampler were contained in a weather proof cabinet to protect the electrical apparatus from weather damage.

Fig. 1 AIR HUMIDIFICATION PROFILE AS IT PASSES THROUGH COLUMN

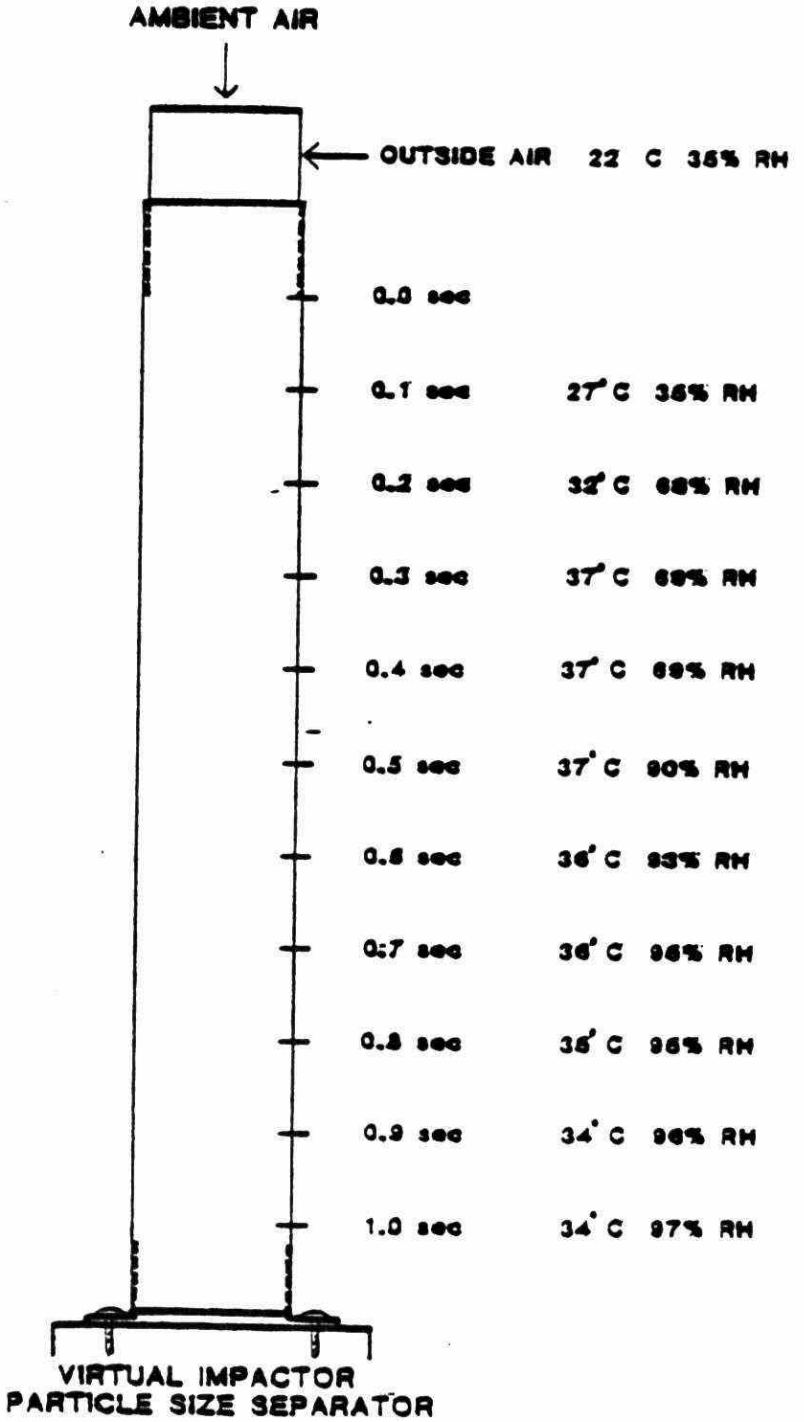


Fig. 2 TIME VS. TEMPERATURE
(COLUMN ENTRANCE TO IMPACTOR JET)

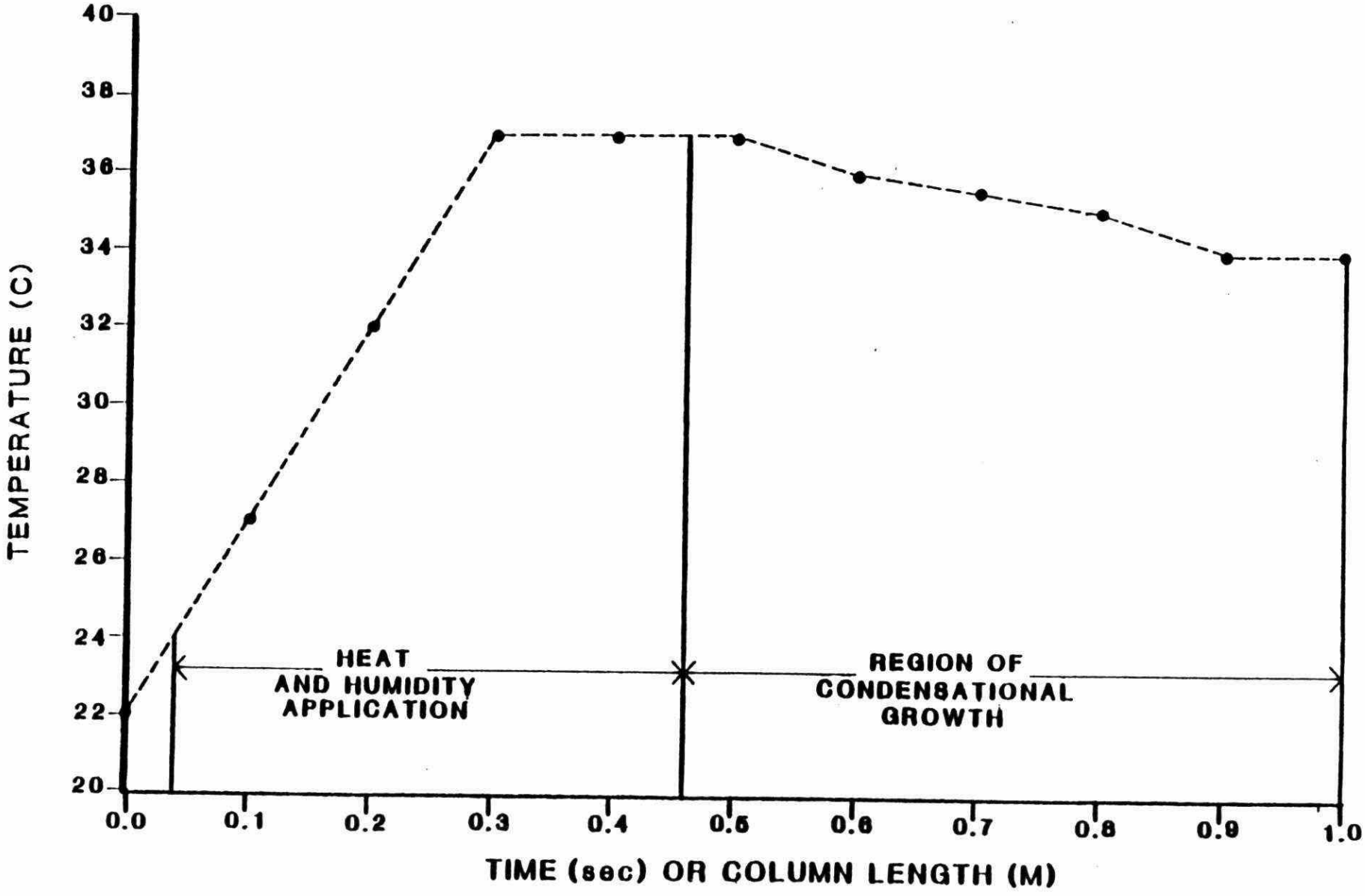
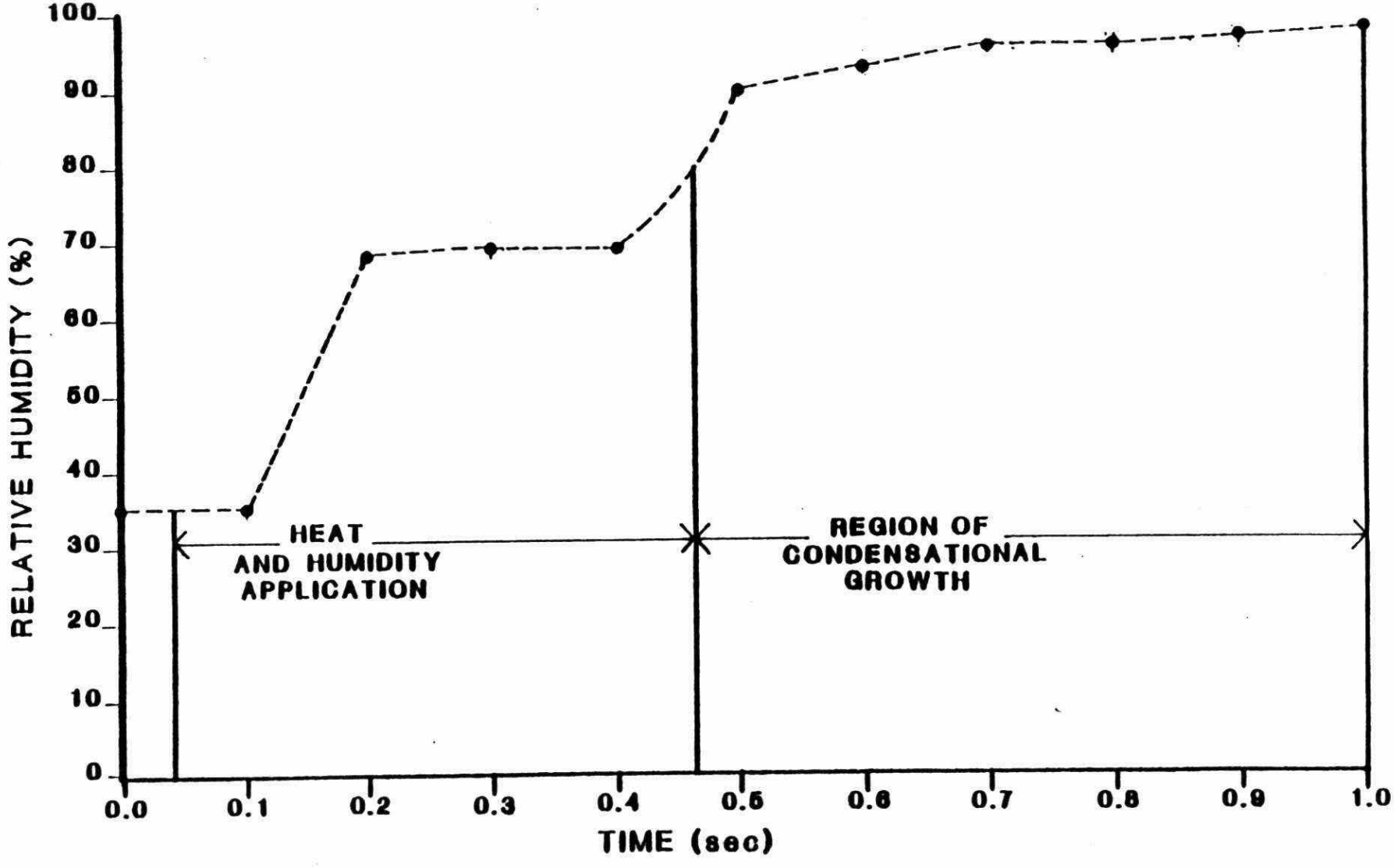


Fig. 3 PER CENT RELATIVE HUMIDITY VS TIME
(COLUMN ENTRANCE TO IMPACTOR JET)



(Each 0.1 sec is equal to flow

Gravimetric Analysis

Filters were weighed before sampling and after exposure. The difference between the two weights was the particulate load on the filter. Each of the four filters was weighed before and after sampling in constant atmospheric of 25°C. and 42 ± 2% R.H. Changes in these standard conditions may result in inaccurate weights mainly due to the adsorption of water from the air by the particulate. The particulate laden filters may be subject to static charge buildup. Therefore, all filters are irradiated with a weak polonium source prior to weighing. This effectively negated any static charges on the matrix and the particulate. The balance used was an electromicrobalance (CAHN 50) which weighs consistently to ± 2 ug. Sample loading was usually 100 ug greater. Therefore adequate precision could be obtained with this gravimetric method to discover any significant particle displacement from fine to coarse size ranges. Filters were maintained in an upright position to prevent weight loss due to drop-off. Particle drop might have been significant due to the inert nature of the teflon filters. The filters were kept in closed petri dishes for futher protection from air current and displacement.

If condensation growth of the heated and humidified particulates occurred the following results would be expected upon weighing of the simultaneously operated sampler filters:

1) The unhumidified - unheated fine deposit (DF) would be greater in weight than the humidified - heated fine deposit. This would be because humidified fine particles, which grow greater than 2.5 um due to the warm humidified air, enter the coarse flow and depositing upon the humidified coarse filter. If these same particles were left unheated and unhumidified, as with the "dry" sampler, they would deposit upon the fine filter and not the coarse.

2) A similar increase in particulate weight would be found upon the coarse humidified filter but would not be found upon the unhumidified coarse filter.

Precursor Experiments

Expt. 1: Determination of Solubility of Fine and Coarse Environmental Particulate

The solubility of fine and coarse particulate in water was determined. The solubility of each aerosol fraction would indicate the percentage of particulate subject to condensation growth. As described previously only soluble particles will grow. Insoluble particles will only acquire an insignificant thin film of water and will not dissolve.

Experiment

Five fine and five coarse loaded filters were weighed. Each filter was placed upright in a Buchner funnel and attached to a vacuum flask. Once the vacuum was turned on the filter was centered to prevent the suction of air or water around the edge of the filter, and maintain a flow through the teflon pores. Three millilitres (3 ml) of deionized, distilled water at 22°C were added in one milliliter (1 ml) aliquots to the loaded surface of the filter by a syringe. The aliquot was added in such a way as to cover completely the loaded surface. The water was sucked through the filter pores by vacuum filtration. The filters were dried and weighed again. The procedure was repeated for each filter. The difference between the two weighings would measure the degree of solubility of the loaded particulate.

Table 2

Solubility of Fine and Coarse Particulates - Gravimetric Data

Filter #	Initial Load (ug.)	% Loss
Coarse Fractions		
1681C	464	51
1689C	503	45
1691C	392	36
1695C	566	34
1697C	655	50
Fine Fractions		
1690F	633	72
1694F	206	60
1696F	538	73
1698F	691	71
1704F	280	73

Average Loss

Coarse Particulate - 43%
Fine Particulate - 70%

Range of Values

Coarse Particulate - 34-52%
Fine Particulate - 60-73%

Table 1

Average % Solubility of Fine Particulate

Element	Avg. Soluble Fraction (%)
AL	55
SI	21
P	77
S	93
CL	76
K	90
CA	66

Table 1 (Cont'd)

Element	Avg. Soluble Fraction (%)
TI	8
V	55
CR	24
MN	65
FE	14
CU	48
ZN	59
AS	56
SE	72
BR	73
ZR	12
CD	83
BA	55
PB	69
Total Mass	70

Conclusions

From the data it can be concluded that approximaely 70% of the fine particle weight and 43% of the coarse particle weight is soluble. Although the results of the fine solubility were very consistent, the percentage solubility of the coarse fraction appeared to vary daily. The upper limit of coarse solubility is approximately 50% of the total load. The fine particulate appears to be much more soluble than the coarse and this may be due to the difference in chemical composition between the two. Although some insoluble fine particles could be washed down the 2.0 um pores with the soluble effluent and thereby overestimating the soluble fraction, it appears from visual inspection that there was little migration of insoluble particles towards the flask vacuum holes. Loss of fine insoluble particles by this route is probably not significant. Coarse particles (greater than 2.5 um aerodynamic diameter) would not be able to pass through the 2.0 um pores in this way. Elemental analysis of the particulate shows many of the hazardous species to be largely soluble.

Results of Main Experiment

Sampling of Environmental Particulates

Results were gathered in October to December 1982. Some results were obtained during the pollution inversion October 26 to 29 when the Toronto Air Pollution Index exceeded 53 (32 is considered a warning level and at 52 major sources of pollution may be ordered to periodically shutdown). Sampling was undertaken under many different weather conditions and times of day. Each sample set consisted of four filters (2 pairs of coarse and fine filters, one pair being from the humifidied sampler and the other from the standard sampler).

Seven sets of samples were gathered to determine the similarity between the standard sampler and the test sampler without its humidification unit operating. However the heat was still applied to the unit. Standard graphs were produced for these samples to determine their sampling similarity.

As can be seen from Table 3 the coarse filter mass loadings from this test were fairly close to a one to one relationship. The equation $y = 1.04 x - 7.7$ (where y is the unhumidified test sampler coarse mass loading in ug/filter and x is the standard sampler coarse mass loading in the unit) was determined from the measurements. Similarly the fine mass loadings of the two samplers to follow the equation $y = 1.02 x - 4.8$ (where X is the standard column fine mass loading in ug/filter and y is the unhumidified test column fine mass loading in the same units).

The test sampler was then run with the humidity unit operating when the incoming particles were heated and humidified in the test sampler but not in the standard sampler. Fifteen acceptable sets of samples were gathered for the final statistical analysis. They are listed in Table 4.

All showed the humidified fine mass to be lower (after the sample was redried) in weight than the standard sampler fine mass. Also all humidified coarse loadings (after drying) were found to be greater in weight than the standard sampler coarse loading. The total loading of each sampler was always within $\pm$ 10% of the other, as defined by the quality control test stated previously.

These results are graphed in Figures 4 - 6. The standard curves from Table 3 are also plotted for comparison. These graphs show a significant shift in the following parameters.

1) Fine mass which is prehumidified is less than that of the standard test ($y = 0.872\ x + 4.0$)

2) Coarse mass which is prehumidified is greater than that of the standard test ($y = 1.14\ x - 1.1$).

3) The total mass relation is similar to that found in the standard test.

From these results it appears that some fine particles grow to coarse sizes when humidified in a lung inhalation environment. Approximately 10 to 15% of the fine particles grew to coarse sizes in the test sampler.

Table 3
Comparison of Dry Column and
Humidifier Column
(Heated but Unhumidified)
Mass Loadings (ug.)

Dry Column			Wet Column (Unhumidified)		
Coarse	Fine	Total	Coarse	Fine	Total
427	533	980	439	562	1000
255	332	587	256	324	580
264	389	653	261	393	664
186	210	296	188	214	402
211	283	494	206	279	485
255	306	561	261	311	572
85	124	210	83	124	207

Table 4
Comparison of Dry Column and
Humidified Columns
Mass Loadings (ug.)

Dry Column			Wet Column (Unhumidified)		
Coarse(DC)	Fine	Total	Coarse	Fine	Total
351	347	698	406	306	712
141	108	249	159	97	256
80	123	203	98	105	203
158	187	345	185	160	345
148	193	341	158	180	338
110	173	283	117	164	281
95	163	258	119	145	264
102	63	165	106	60	166
75	108	183	84	98	182
154	85	239	166	76	242
143	220	363	172	196	368
112	260	372	133	227	360
128	146	274	143	126	269
208	138	346	227	133	360
124	221	345	143	198	341

Fig. 4 COMPARISON OF COARSE MASS LOADINGS FROM DRY AND HUMIDIFIED COLUMNS

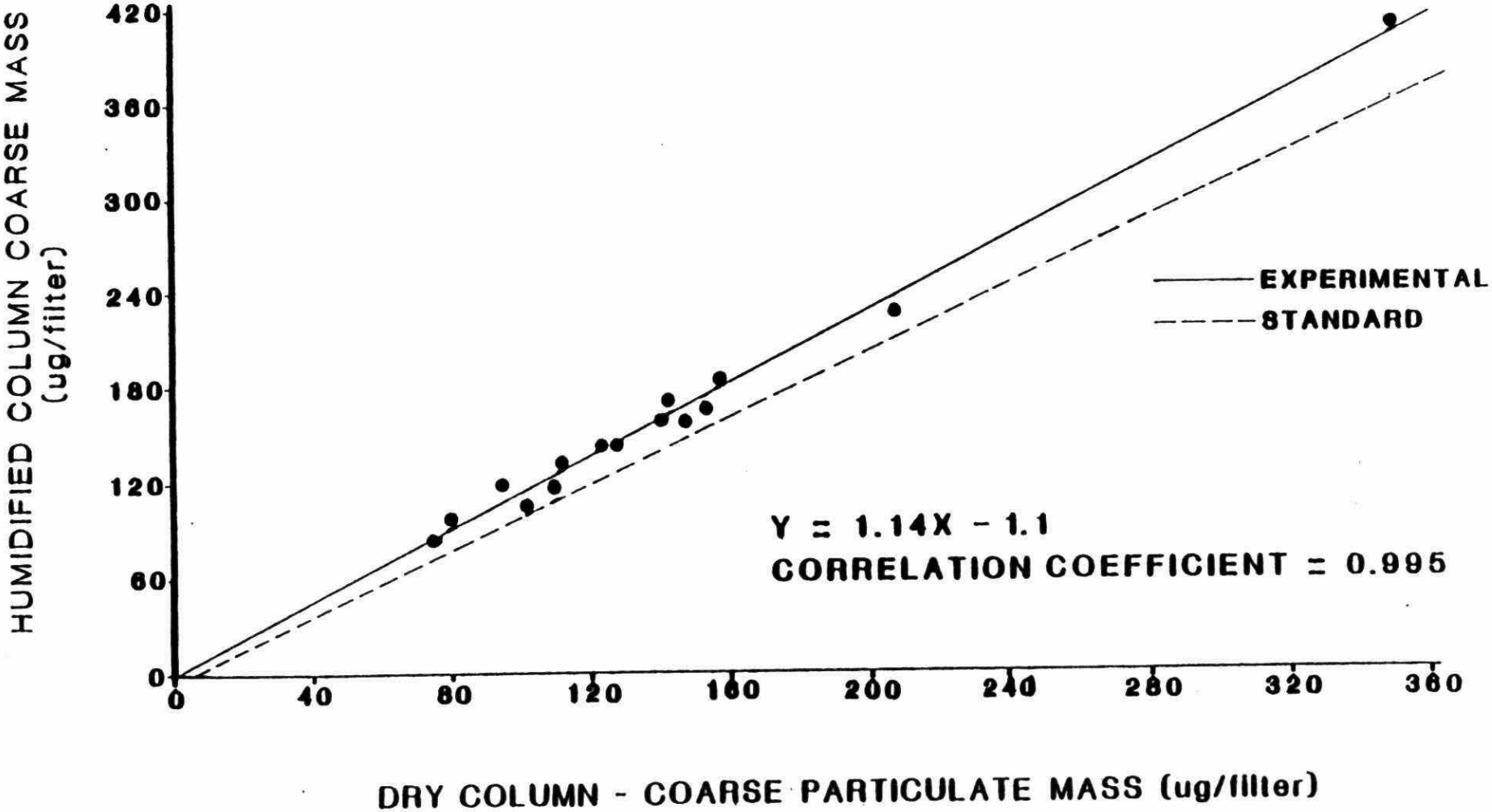


Fig. 5 COMPARISON OF FINE MASS LOADINGS FROM DRY AND HUMIDIFIED COLUMNS

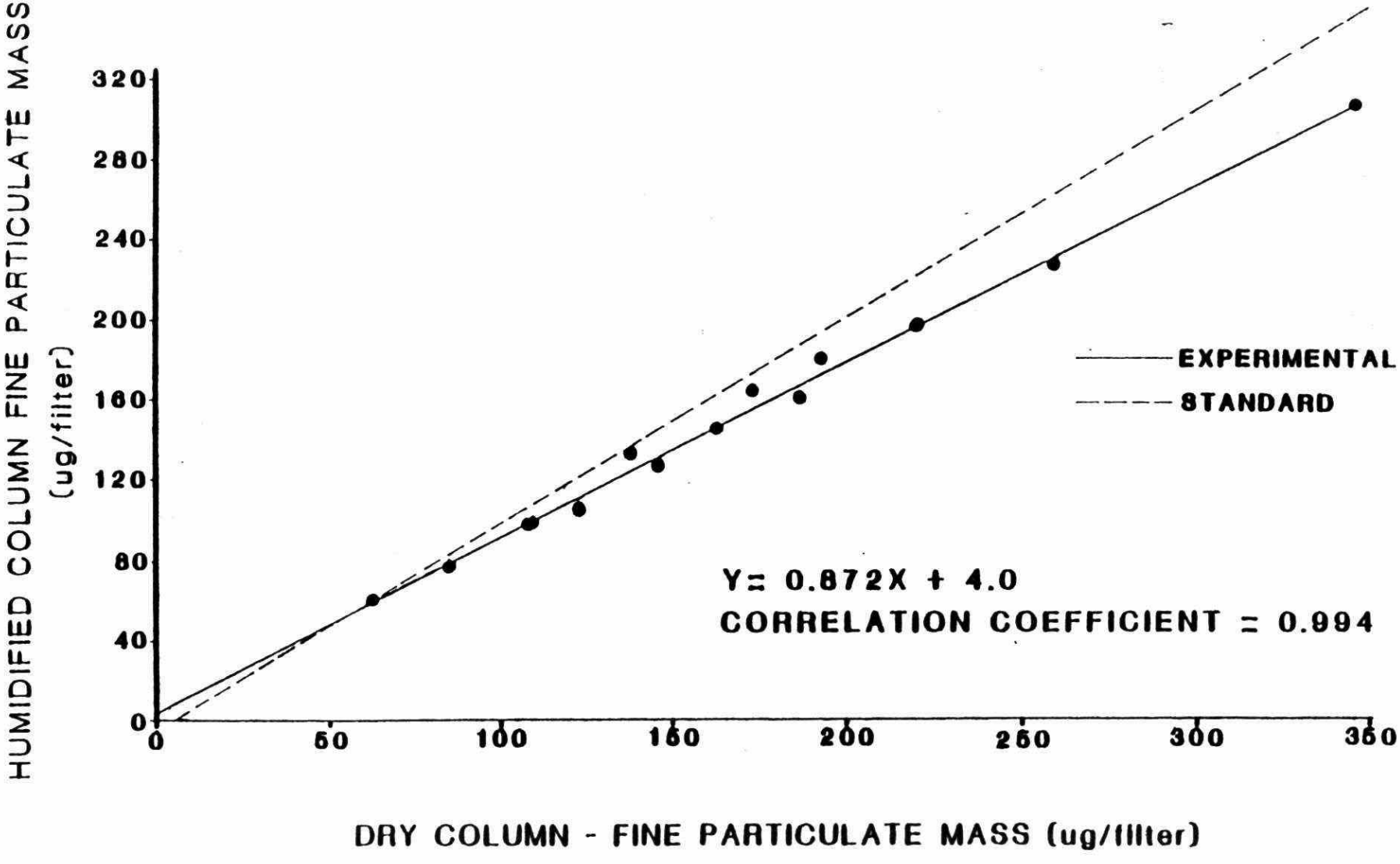
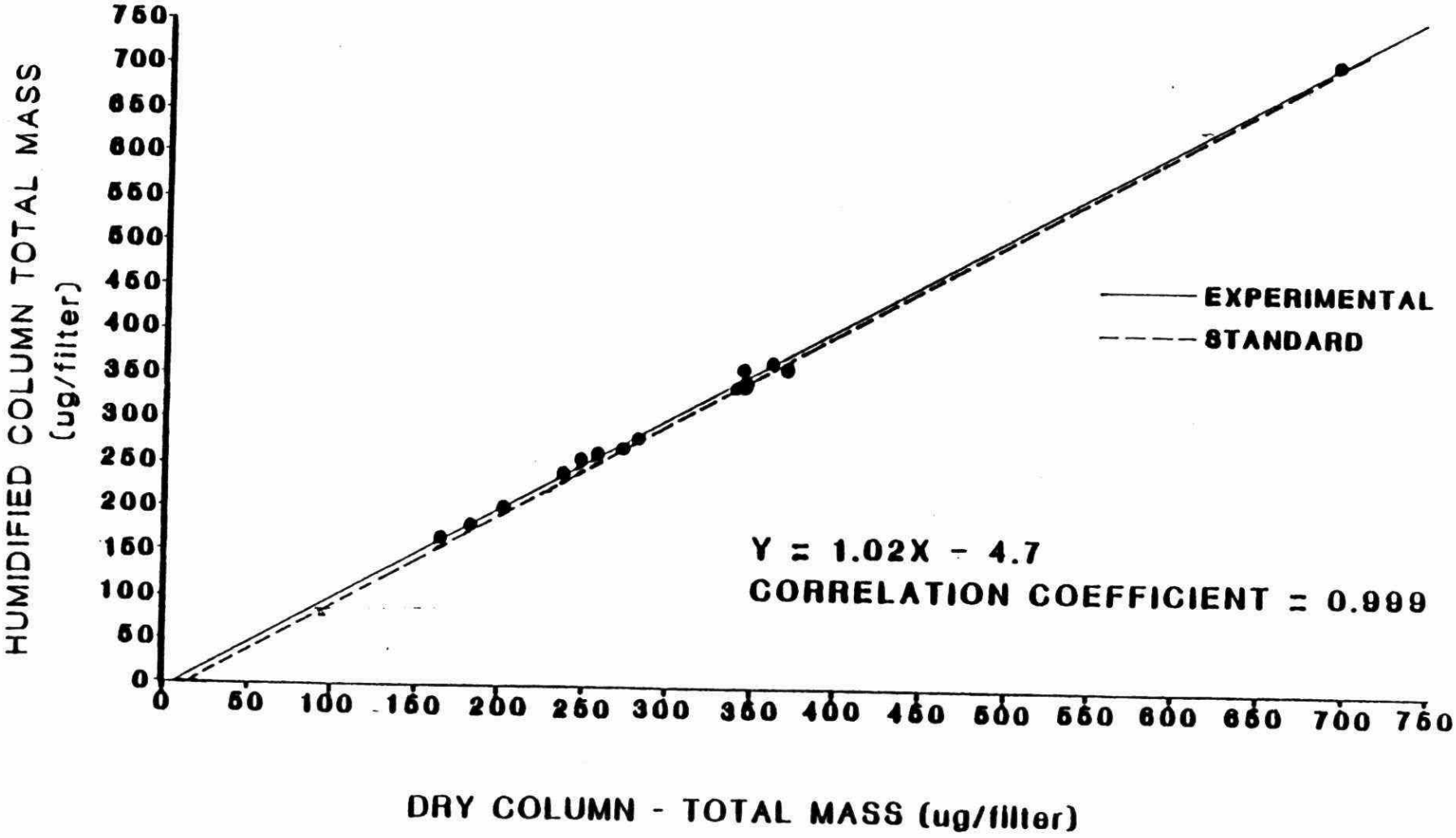


Fig. 6 COMPARISON OF TOTAL MASS LOADINGS FROM DRY AND HUMIDIFIED COLUMNS



DISCUSSION

An investigation of the processes of condensation growth of particles is necessary in any comprehensive study of particulate deposition in the lung. In the past, most deposition studies used insoluble aerosols which do not change size when exposed to atmospheres of high humidity such as that within the lung. Other studies of soluble particles exposed to humidified atmospheres indicated a rapid growth of the particles into droplets three to fives times their original dry size. It was following these discoveries this study was begun. Environmental particulates were exposed to lung humidities (95% R.H.) for an exposure time of 1.0 second and the growth measured. The areas of measurement were the difference between the fine (less than 2.5 um mmad) and coarse particulate (between 2.5 and 15 um mmad) or the percentage mass of particles which grew from fine to coarse sizes. Because fine particulate deposits with most frequency in the alveolar region of the lung and coarse particulate within the tracheobronchial region, any size growth across the 2.5 um cutpoint would also represent a change in the site of most probable deposition.

Three experimental phases were completed. The first was to determine the mass percentage of soluble particulates in environmental aerosols. In downtown Toronto (the site of experimentation) approximately 70% of the fine particulate and 43% of coarse particulate was found to be soluble. In the second phase of experimentation, microscopic examination of soluble NaCl particles showed the particles became droplets upon humidification. The droplets were

dried upon the application of heat to the system (thereby lowering the relative humidity of the system). This was necessary to the efficient filtration of the experimental aerosols. This second phase of experimentation also tested the apparatus used to determine the growth of aerosols. This was a humidification tube which simulates conditions found in the human respiratory tract. The third phase of experimentation was performed outdoors using environmental particulate. The third phase was the most difficult to control and produced the most relevant results. Data indicated a growth of approximately 10% of the fine particulate to coarse sizes upon humidification. Therefore a small amount of fine particles which would normaly deposit in the alveolar region in the lung would more probably deposit in the tracheobronchial region during inhalation an exhalation.

Particles subject to growth would be more likely to deposit (due to their greater mass) as they grew throughout the breathing cycle. A 1.0 um particle may be as much as 4 or 5 um in diameter by the time it is expired. Therefore the probability of deposition of all particles inhaled is increased.

The rapid solution of particles into droplets in the lung is impressive. The results of these experiments lead one to question what happens to the droplets once they are deposited. Most clearance mechanisms noted in the literature are based upon the fact that the deposited particle is insoluble. However soluble particles will become droplets while airborne or when deposited within the lung. It is not known whether major clearance mechanisms are applicable to droplets and whether the droplets are able to permeate the lung tissues. Adverse health effects due to deposition of particulates which are soluble may be underestimated.

REFERENCES

Altshuler, B., E.D. Palmes, and N. Nelson, Regional aerosol deposition in the human respiratory tract, In C.N. Davies, Ed., Inhaled Particles and Vapours II. Proceedings of an International Symposium organized by the British Occupational Hygiene Society, Cambridge, 28 September-1 October 1965, Oxford: Pergammon Press, pp. 323-335, 1967.

Brown, J.H., Cook, K.M. Ney, F.G. and Hatch, T., Influence of particle size upon the retention of particulate matter in the human lung, Amer. J. Public Health, 40, pp. 450-458, 1950.

Foord, N., Black, A. and Walsh, M., Regional deposition of 2.5 - 7.5 um. diameter inhaled particles in healthy male non-smokers, J. Aerosol Sci., 9, pp. 343-357, 1978.

Giacomelli-Maltoni, G. Meladri, D. Prodi, V. and Tarroni, G., Deposition efficiency of monodisperse particles in human respiratory tract, Am. Ind. Hyg. Assoc. J., pp. 603-610, Sept. 1972.

Heyder, J., Gebhart, G., Physical factors determining particle deposition in the human respiratory tract, J. Aerosol Sci., 11, pp. 505-515, 1980.

Lippmann, M., Regional deposition of particles in the human respiratory tract, pp. 213-232, In D.H.K. Lee, H.L. Falk, and S.D. Murphy, Eds., Handook of Physiology, Section 9: Reactions to Environmental Agents, Bethesda, MD, The American Physiological Society, 1977.

Marple, V.A., A Fundamental Study of Inertial Impactors, Ph.D. Thesis, University of Minnesota, Publ. No. 144, 1970.

Rudolf, G., and J. Heyder, Deposition of aerosol particles in the human nose, In V. Bohlau Ed, Aerosole in Naturwissenschaft, Medizin and Technik, Proceedings of a conference held in Bad Soden, October 16-19, 1974, Bad Soden, West Germany, Gesellschaft fur Aerosolforschung, 1984.

LASER INDUCED EMISSION SPECTROSCOPY OF PAHs IN LOW TEMPERATURE MATRICES

F. Morgan and G. Parnell, Physics Dept.

S. Filseth and C. Sadowski, Chemistry Dept.

York University
Downsview, Ontario M3J 1P3

Abstract

Polynuclear Aromatic Hydrocarbons (PAH) are numerous, and sometimes nasty, constituents of our environment. Present analysis techniques are hard pressed to deal with the demands for identification and quantification. Emission spectroscopy in suitable normal alcane matrices at low temperatures can offer a complementary technique. A reference library of spectra, coupled with a "standards free" digital processing technique has been considered. Some of the pain involved in making the necessary transfer of technology is examined as well as the expected joys.

Introduction

Polynuclear Aromatic Hydrocarbons (PAH) can be innocuous, as for example benzo (e) pyrene; or they can be mutagenic; or they can be carcinogenic (e.g. benzo (a) pyrene) or they can be both (1). Innocuous ones are not a problem, but any others are. The severity of the problem which they present will depend on their abundance in the environment and the degree to which they can cause mutation or cancer. Clearly a strong carcinogen that is present in substantial quantity is a great concern, whereas an equally strong carcinogen which is virtually non-existent is not a concern. The carcinogenic and mutagenic concerns are best addressed by biologically based studies. Abundance in the environment is a two stage process - sampling and then analysis. Analysis for PAH is something of a many headed hydra, that mythological monster who grew additional heads as rapidly as they were cut off.

PAH molecules are numerous. Their ubiquity can be traced to their formation in most combustion processes, and their presence in fossil fuels. Moreover, in addition to the hundreds of known PAH's there are likely a host of unknown ones as well. Worse yet, there are derivatives of PAH compounds, in particular the nitrated PAHs, which seem to be even nastier than the original PAH molecules. Faced with this huge collection, one feels daunted by the task of analysis. Currently, the favoured technology is high pressure liquid chromatography, a process that is coping but its practioners are feeling the strain. In addition, doubts linger about its completeness. Are there compounds 'twixt or 'tween the spectral peaks which are observed? In short, there is room for other approaches, most likely as complements rather than as alternatives.

Another Approach

One such approach is spectroscopy, i.e. the emission or absorption of radiation. Generally, it has been poorly suited to the analysis of PAH compounds because the spectra of individual compounds have not been well differentiated, especially at room temperature. However, one spectroscopic technique, equally suited to absorption and emission, has been able to produce sharp, line-like features. This technique, Shpol'skii spectroscopy (2,3), is now close to 25 years old. It relies on two important aspects to produce these "quasi-line" spectra. Firstly a low temperature is used, i.e. the PAH molecules are frozen in some solvent. The freezing eliminates rotation which causes the usual broad spectral features at room temperature. Secondly, the solvent is chosen to "fit" the structural form of the PAH molecule. Normal alcanes do this, e.g. octane. As a result of the "fit", there are only a few possible orientations for the PAH molecule relative to the solvent matrix. This ensures but a few interaction energies which in turn produces but a few shifted spectra which then combine to form the resultant spectrum. The resultant spectrum thus contains distinct lines. Such a distinct spectrum can be used to characterize the presence of a particular P.A.H. molecule.

One additional aspect of the emission spectra of these molecules is important for analytical purposes, viz. Kasha's rule applies (4). Kasha pointed out that the lifetime of a molecule in an upper level of the first electronic state is negligibly small, so that within a few picoseconds of an excitation the molecule has "relaxed" to the lowest level of the first electronic state. Hence, all emission spectra have a common upper level and so the resultant spectral features will not depend on the excitation wavelength. The importance of this will become evident subsequently.

Strategy for Spectroscopic Analysis

Emission (or absorption) spectroscopy requires narrow, well defined, features that are unique for each molecule in order to use the features as conclusive proof of the presence of the molecule. Shpol'skii spectroscopy provides this; and the spectral pattern of these features will be independent of the excitation wavelength. So the strategy seems plain. Dissolve the sample in a suitable alcane, e.g. octane, then freeze this solution quickly, to reduce the temperature of the frozen sample below 20° Kelvin.

A light source is needed to produce emission or absorption spectra. Although the same spectral features will arise from any wavelength of excitation which is at least as energetic as the difference between the lower ground state of the PAH molecule and the ground state of the first electronic level, the intensity of the pattern does vary with wavelength. Hence the source should be wavelength tunable. Additionally, the more intense is the source, the more easily observed is the emission or absorption spectrum. Dye lasers can supply the necessary intense, absorption narrow band, tunable radiation.

Identification of PAH molecules by spectral features requires a collection of spectra obtained by excitation at known wavelengths. Basically, that implies the accumulation of spectra to form a "reference library". Fortunately, there are several groups, as well as ourselves, who are interested in Shpol'skii spectra of PAH compounds (6,7,8). That is the good news. Unfortunately, there is no agreed standard for solvent, or temperature, or excitation wavelength. The latter, when it is spectrally narrow, may select one of the PAH molecules orientations rather than exciting all of them (6). Warmer temperatures (above 20°K) may produce larger linewidths in the observed spectral features, which reduces peak intensity (9) and may cause some features to coalesce. A change in solvent will shift spectral features. Thus, in the absence of agreed standards, the contributions of other workers are not as useful as they should be. That is the bad news. In practice, then, individual laboratories require their own spectral reference library. Given the plethora of compounds, a judicious selection is important. To date, our work has concentrated on benzo (a) pyrene, benzo (k) fluoranthene, benzo (ghi) perylene, perylene, pyrene, benzo (e) pyrene, and benzo (b) floranthene.

Apparatus

A closed cycle He refrigerator is used to reduce the sample temperature to about 15°k. Temperatures are measured by a calibrated silicon diode whose resistance is a function of temperature. Thus the voltage produced when a constant current is driven through the diode indicates the temperature. Rapid freezing is ensured by plunging the sample,contained in its holder, into liquid nitrogen; followed by insertion into the refrigerator's cold housing whose temperature is close to that of liquid nitrogen. The refrigerator continues to cool the frozen sample to the desired temperature. Good thermal contact is necessary, but attaining it can be problematical.

Excitation of the sample is provided by a narrow spectral band, (few hundredths of a nanometre line width) tunable dye laser (tunable over a few hundred nanometers) which is pumped by a pulsed gas laser. The pulse repetition rate is several Hertz, while the pulse duration is several nanoseconds. Time resolved spectra of the PAH molecules can be obtained; and it has been done by others (7). Use of a tunable dye laser enables excitation spectra (i.e. an

absorption spectrum) or fluorescence spectra (i.e. an emission spectrum) of the sample to be obtained. Changes in tuning range may require changes in the type of dye solution. Extraneous emissions from the dye laser can be a troublesome source of scattered light.

A monochromator is used to resolve the resultant fluorescence into its component spectral features, which are detected by a photomultiplier tube. Scattered light from the relatively intense laser source can provoke problems such as sharp line "grating ghosts" or a momentary saturation of the photomultiplier tube. Electrical current pulses from the photomultiplier tube can be processed by an electrometer, using simple R-C averaging followed by recording on a strip-chart recorder. An alternative, and inherently superior technique, is the use of a gated integrator used as a "box-car" averaging device. This device only "opens" its electronic gate for a specified duration, and the electrical signal which passes through this gate is averaged over several successive pulses. A voltage signal, proportional to the average value of the fluorescence signal detected by the photomultiplier tube, can be routed to a strip chart recorder or sent to an analog-to-digital converter for digitization and subsequent storage by a microcomputer. Either recording technique can be used to provide digitized spectral data, but only the "box-car" technique can be used for time resolved spectra.

Results

Along with the promise of a useful contribution to the difficult problem of analysis of an environmental sample for PAH compounds, technological transfer also brings the pair to implementation. This past year has certainly brought a fair share of such pains, as will be noted in the subsequent discussion.

Cooling proved to be a vexatious problem. Temperatures below $20^{o}k$ are needed to obtain a narrow line width for the PAH fluorescence (9). The helium refrigerator certainly produces such temperatures at the cold finger, but good thermal contact with the sample inserted into the cold finger has been elusive. Originally, we used a sealed pyrex ampoule into which a degassed sample had been introduced. As a sample handling procedure it was marvellous; but it produced poor thermal contact, giving temperature differences between sample and cold finger of close to $60^{o}k$. This difficulty forced a change in our sample handling procedure. Now we use a copper cylinder which slides into a corresponding hole in the cold finger. The sample holder and the cold finger are "keyed" to preserve the correct orientation of the sample to the incoming laser excitation radiation. This radiation strikes the frozen sample after passing through a quartz window which is cemented in place with a low temperature epory (10). Thermal contact is much better but it is not yet optimal. Occasionally, there are substantial differences between the sample temperature and that of the cold finger.

Examination of a variety of compounds requires use of different excitation energies. In particular benzo (e) pyrene benzo (b) fluoranthene, and pyrene require excitation at wavelengths below 380 nanometers. Operation of the dye laser at such wavelengths revealed an unsuspected problem, a moderate amount of broad band radiation. This unwanted radiation does not present a problem in the excitation of the sample; but it is a serious problem in the detection of fluorescence from the sample since it is scattered from the surface of the sample, thus masking the desired sample fluorescence. Elimination of this unwanted broad-band radition is still a pressing concern. Its cause is clear,

viz. amplified spontaneous emission from the amplifier section of the dye laser, but its cure is not complete.

On a cheerier note, we completed the acquisition of spectra from several PAH compounds; benzo a) pyrene, benzo (ghi) perylene, benzo (k) fluoranthene, and perylene. Thus spectra from laboratory samples will form part of the reference library needed for the analysis of environmental samples. Additionally, we have examined the effect of solvent choice on the spectrum of benzo (ghi) perylene (11). On the basis of that study we have decided to use n-octane as a standard solvent. This represents a change from our original choice of n-keptane. Fewer lines from individual molecules, and a better structural "fit" with more PAH compounds are the benefits from this change. Both benefits aid analysis.

The total number of PAH compounds and their derivatives is staggering. Just as staggering is the problem of analysis for so many compounds. Often, such analysis requires the use of reference standards to calibrate the apparatus. Such standards are needed from time-to-time to ensure that the apparatus is functioning reliably, e.g. HPLC columns have to be calibrated with standards. This is a further staggering number of reference compounds. Shpol'skii spectroscopy should not need such calibration standards, provided:

(a) the same solvent is used for both sample and reference spectra
(b) both reference and sample spectra have been corrected for variations in laser intensity
(c) both reference and sample spectra have been corrected for variation in monochromator and photomultiplier response

We have taken one step towards examining such a "calibration free" approach. We have developed an analog to digital conversion system which takes the "box-car" averaged output, digitizes it, and stores it in the memory of a microcomputer from where it can be transferred to a floppy disc or to a mainframe computer. Additionally, provision has been made to correct for variations in laser intensity which cause fluctuations in fluorescence intensity. Testing the latter will be the next step.

Analysis of environmental samples is the goal. Thus far, we have concentrated on the production of a "reference library" of spectra from laboratory samples. However, we have spectra from a few environmental samples which were given to us by Concord Scientific (12). Comparison of these spectra with our laboratory reference spectra shows clear evidence that benzo (a) pyrene is present. There is little indication that other PAH compounds are present, although HPLC analysis indicated otherwise (12). The cause of this discrepancy is not clear, though it may lie in storage and handling procedures since there was an extended delay between the two analyses.

Conclusion

Bitter experience in freezing PAH samples to low temperatures has led to modified procedures and apparatus which now give reliable low temperature Shpol'skii matrices. The tunable dye alser provides a satisfactory light source although scattered light from amplified spontaneous emission arising from its amplifier section complicates the acquisition of reference spectra for some PAH molecules. Useful reference spectra for benzo (k) fluoranthene, benzo (ghi) perylene, benzo (a) pyrene, and perylene have been obtained. A

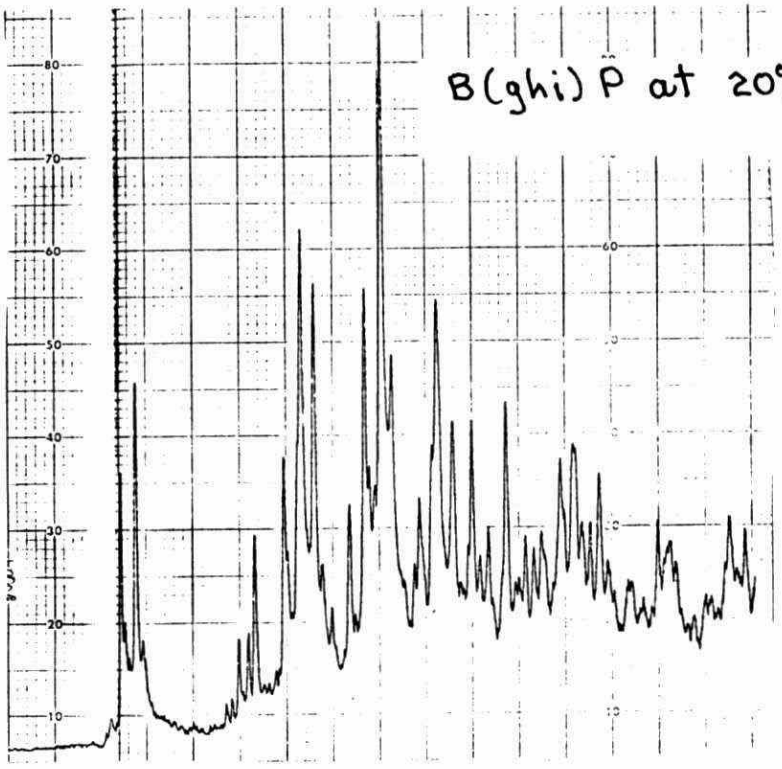
comparison of spectra from an environmental sample with reference spectra indicates benzo (a) pyrene is present. Normal octane appears to be the best single solvent for Shpol'skii spectroscopy of environmental PAH compounds. A satisfactory technique to obtain "normalized" reference spectra and store them in digital form for computer based searches is underway. The first stage in the realisation of the technique has been completed.

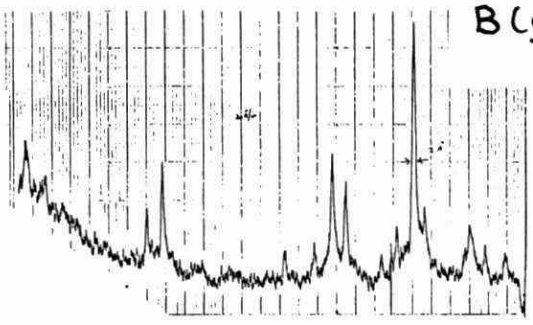
Acknowledgments

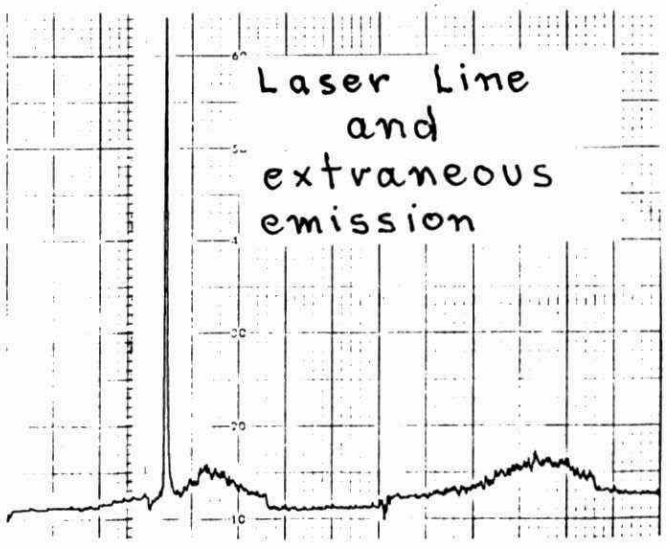
We thank Mr. Robert Eng for his assistance with the computer based reference spectra. We are also grateful to York University, the Ontario Ministry of the Environment, and the Canadian Natural Sciences and Engineering Research Council for their assistance.

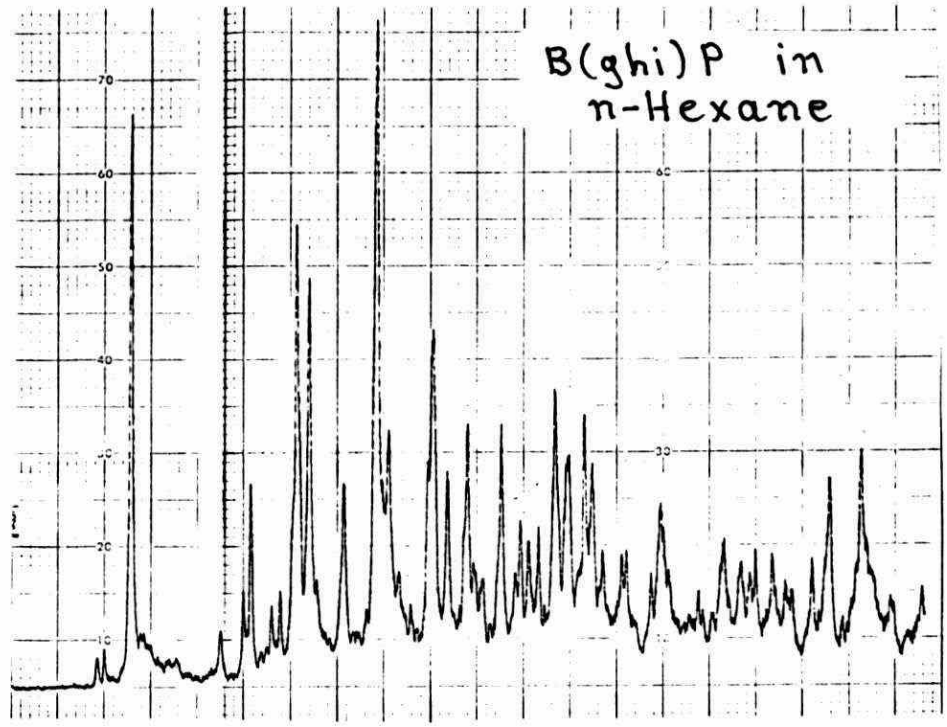
References

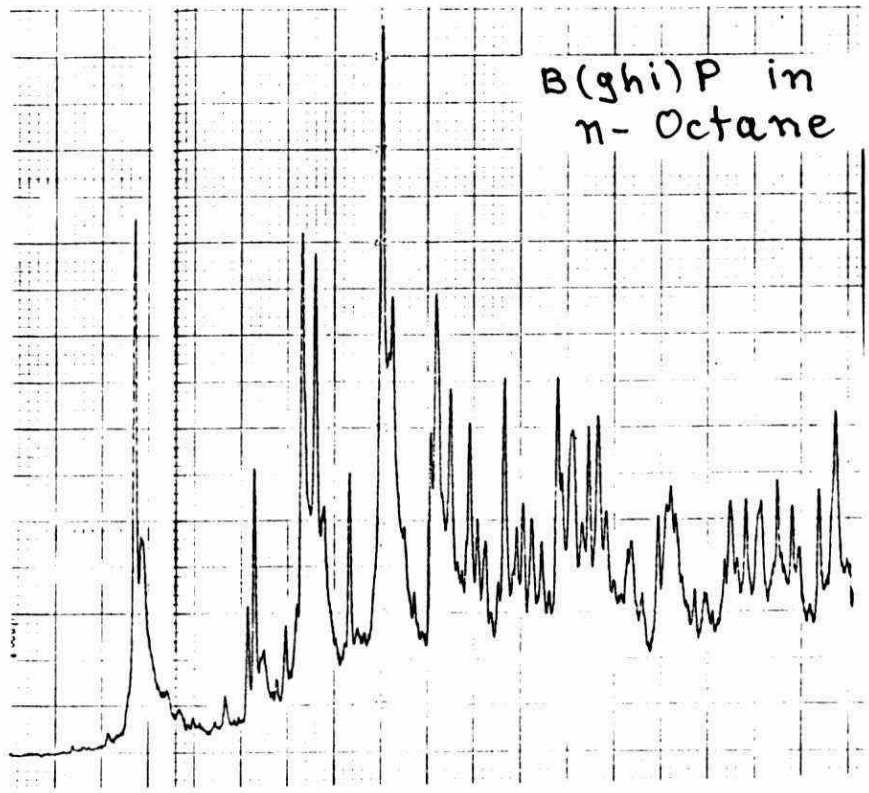
1. Handbook of Polycyclic Aromatic Hydrocarbons (1983), ed. A. Bjørseth publ. M. Dekker Inc. (N.Y.)
2. Shpol'skii, E.V. (1959) Soviet Physics Uspekhi 2 378-392.
3. Colmsjö, A. (1981) The Practice and Utility of the Shpol'skii Effect in Chemical Analysis, publ. Univ. of Stockholm.
4. Wayne, R.P. (1970) Photochemistry, pbl. Butterworths (London)
5. Nakhimovsky, L. (1983), Proc. of 8th Int'l. Symp. on PAH, ed. A. Dennis and M. Cooke.
6. Atlas of Shpol'skii Spectra (1981) A. Colmsjö and C. Östman publ. Univ. of Stockholm (Stockholm) ISBN 91-7260-590-1
7. Lamotte, M. (1983), Proc. of 8th Int'l. Symp. on PAH, ed. A. Dennis and M. Cooke.
8. Yang, Y. et al. (1981), Proc. of S.P.I.E. - Int. Soc. Opt. Eng. 286, 126-130.
9. Yang, Y. (1981), Ph.D. Thesis, Iowa State Univ. "Laser Excited Shpol'skii Spectroscopy for the Sensitive Excitation and Determination of Polynuclear Aromatic Hydrocarbons" Available from Univ. Microfilms Int'l Ann Arbor, Mich.
10. Delta Bond 155, manufactured by E.G. & G. Wakefield
11. Richards, J.L., and Rice, S.A. (1971), J. Chem. Phys. 54, 2014-2023.
12. Caton et al. (1983), Proc. Tech. Transfer Conf. #4, 716-743, ISBN-0-7743-8797-1

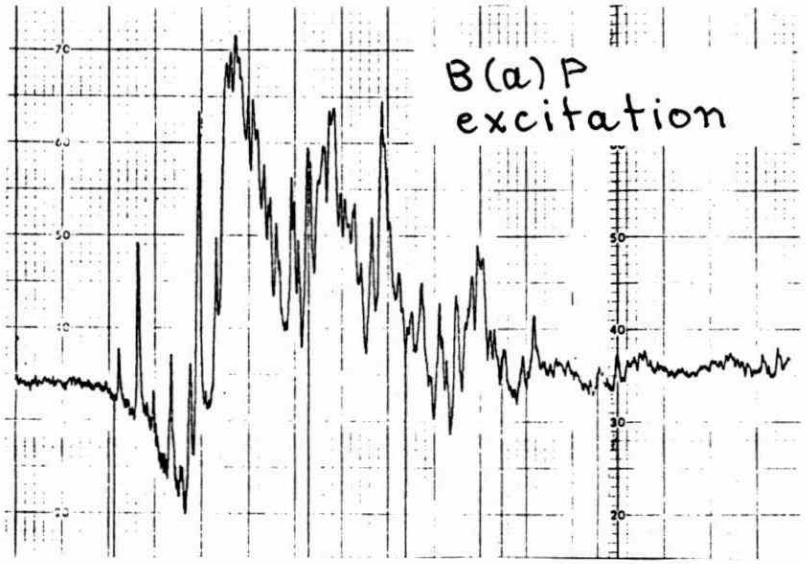

B(ghi) P at 20°k

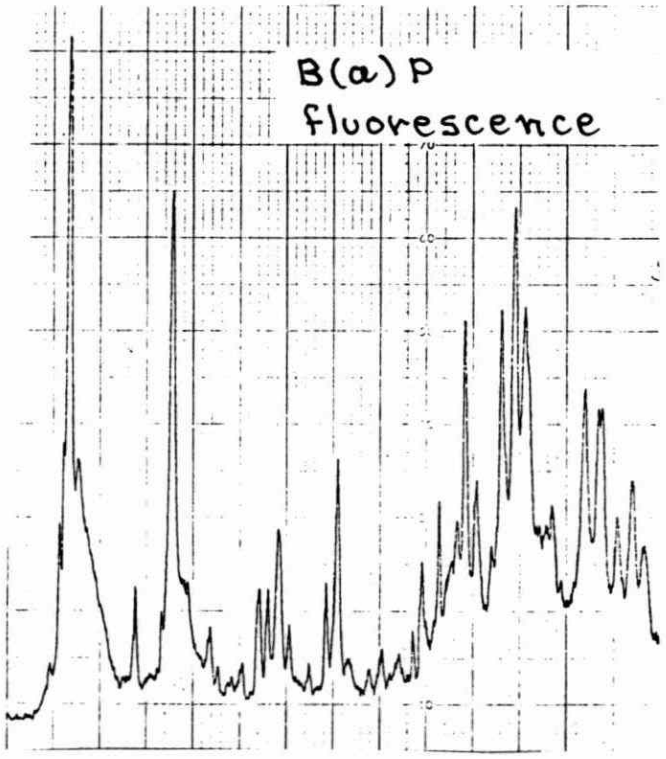

B(ghi)P at 50°k

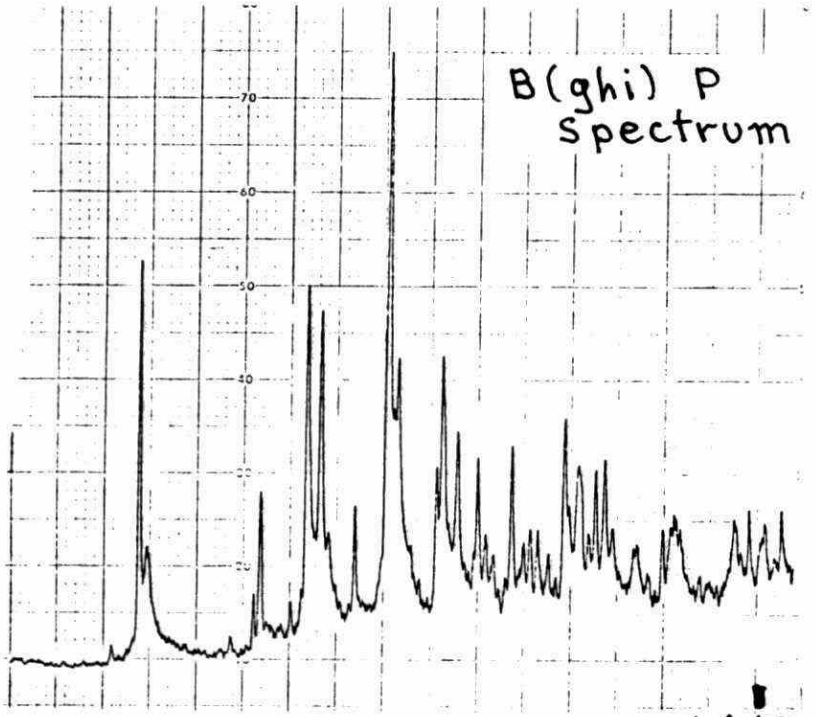

Laser Line
and
extraneous
emission


B(ghi)P in
n-Hexane

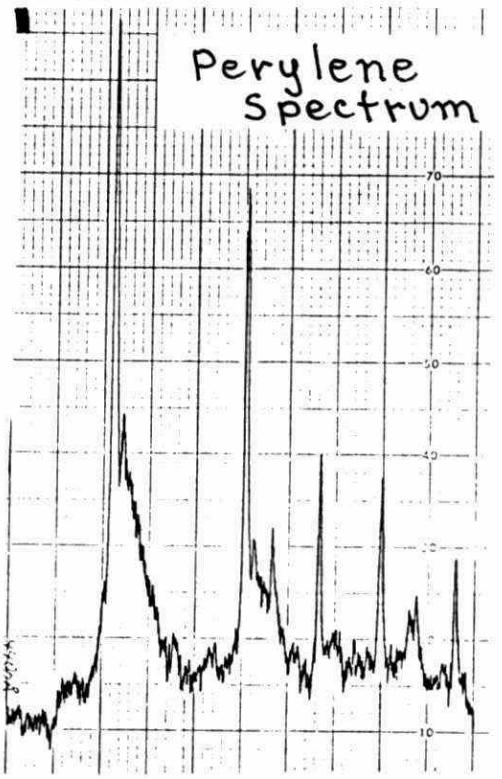

B(ghi)P in
n- Octane

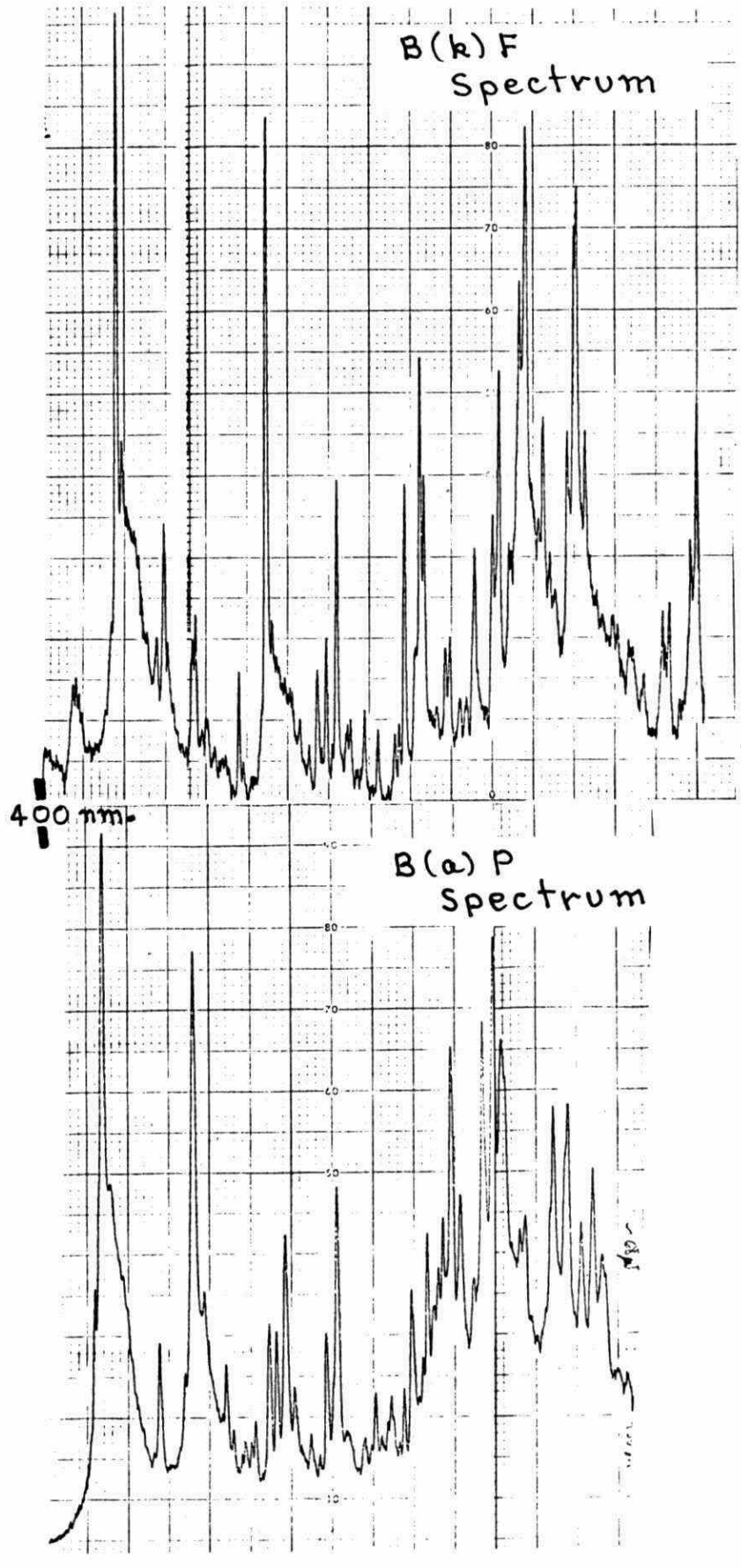

B(a)P
excitation


B(a)P
fluorescence

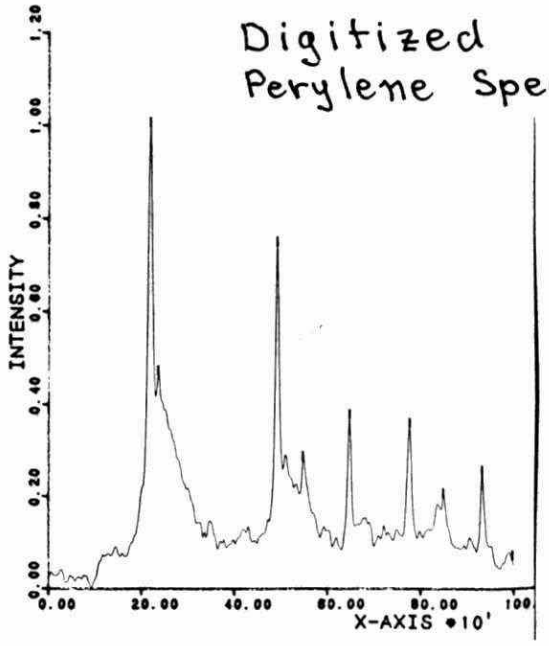

B(ghi) P
Spectrum
70
60
50
40
30
20

440 nm.

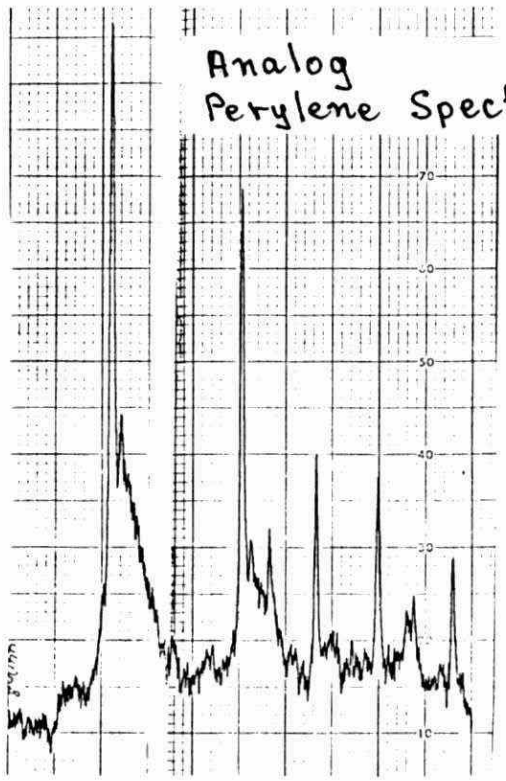

Perylene
Spectrum
70
60
50
40
10


B(k) F
Spectrum
400 nm
B(a) P
Spectrum

Digitized
Perylene Spectrum



Analog
Perylene Spectrum



Provision of PAHs and Aza-PAHs as environmental analytical standards

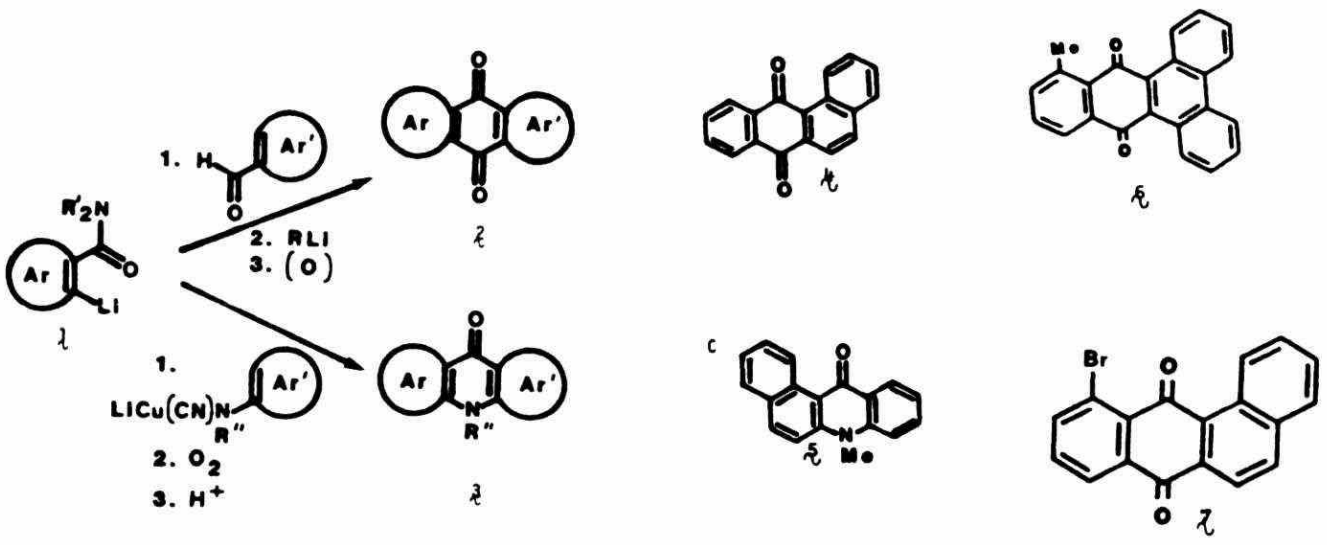
V. Snieckus

Guelph-Waterloo Centre for Graduate Work in Chemistry
Department of Chemistry
University of Waterloo
Waterloo, Canada N2L 3G1

ABSTRACT

The discovery of a tandem directed ortho metalation strategy (**1** → **2**) for the preparation of condensed aromatic substances in 1981 initiated a program in our laboratories aimed at providing a variety of PAHs and aza-PAHs of environmental interest. Using the directed metalation tactic, a variety of PAH-quinones (e.g. **4**) and their corresponding PAHs were prepared by routes which were efficient, short, and involved minimum handling of toxic intermediates. By a new modification (**1** → **3**) the method was expanded to the preparation of aza-PAHs (e.g. the condensed acridine **5**). The finding that silicon substitution may be used to protect reactive aromatic methyl groups allowed the regiospecific and general synthesis of methyl-substituted PAHs (e.g. **6**). Conceptually similar methodology was derived from silicon protection of aromatic C-H sites which led to the synthesis of halo-substituted PAHs (e.g. **7**).

All synthetic PAHs were purified by HPLC, characterized by high resolution NMR, and standardized by GC-MS methods. Over 20 compounds have been provided to the Ministry of the Environment for use in environmental research.



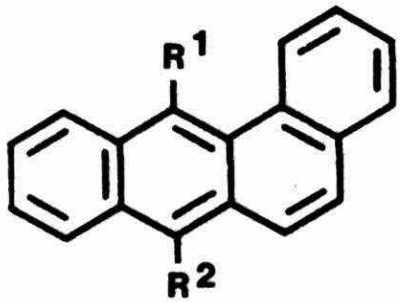
INTRODUCTION

The correlation of structure with carcinogenic activity of polycyclic aromatic hydrocarbons (PAHs) is paramount to an understanding of the role PAHs play in the mechanism of carcinogeniesis[1]. In particular, methylbenz[a]anthracenes (MBAs), which are recognized environmental contaminants[2,3] have received much attention in studies concerned with structure-carcinogenic activity relationships.[4] Mono bromobenz[a]-anthracenes are of interest in studies concerned with the varying carcinogenic activites of 7-methylbenz[a]anthracene (7-MBA, **1**), 12-methyl-benz[a]anthracene (12-MBA, **2**), and 7,12-dimethylbenz[a]anthracene (DMBA, **3**). [5] The bromo analogues may be readily converted into the corresponding tritio derivatives which are then used to measure the rate of

electrophilic aromatic substitution at the tritiated site in attempts to correlate structure with carcinogenicity.[6]

The elaboration of the directed ortho metalation strategy by employing the concept of silicon protection of the more reactive metalation sites[7] has recently been used in the syntheses of peri-methyl substituted PAH precursors.[6] Herein we describe further utility of silicon in the directed ortho metalation strategy of tertiary benzamides for the regiospecific syntheses of brominated PAH precursors.

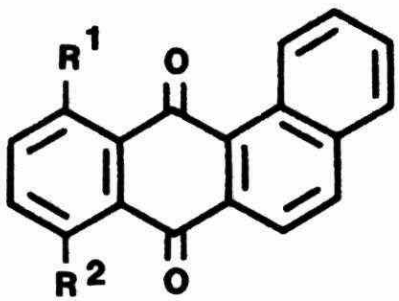
Our efforts in this area have initially been directed towards the syntheses of 8-bromo-7,12-benz[a]anthraquinone **15** and 11-bromo-7,12-benz [a]anthraquinone **16** which can then be converted to the corresponding DMBA derivatives **17** and **18** according to established procedures.[5]

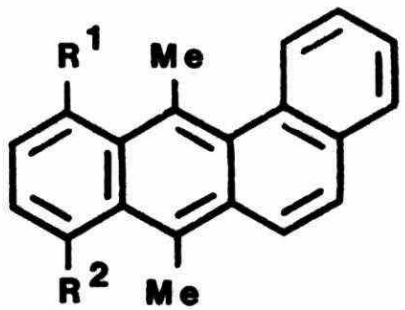


1, $R^1 = H$, $R^2 = Me$

2. $R^1 = Me$, $R^2 = H$

3. $R^1 = R^2 = Me$





15. $R^1 = H$, $R^2 = Br$

16. $R^1 = Br$, $R^2 = H$

17. $R^1 = H$, $R^2 = Br$

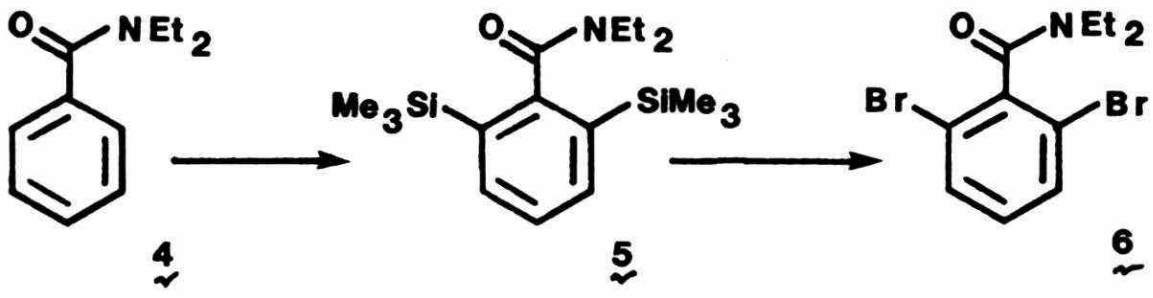
18. $R^1 = Br$, $R^2 = H$

RESULTS AND DISCUSSION

The strategy for the regiospecific preparation of polysubstituted benzene derivatives by the directed ortho metalation[9] of aromatic tertiary amides and 2-oxazolines has been applied to the construction of a variety of polycyclic aromatic hydrocarbons allowing their preparation in quantities sufficient for use in biological and metabolic studies.[10]

As an extension of our studies concerning the utility of silicon in the directed ortho metalation reaction of tertiary benzamides, the dibromo derivative **6** was required. It was envisaged that mono metal-halogen exchange on **6** followed by condensation with aryl aldehydes would allow access to mono-bromo PAH quinones via previously delineated methodology.[7,8] Treatment of N,N-diethylbenzamide **5** with an excess (2.2 eq) of s-BuLi/TMEDA at -78°C for 1 hour in THF followed by quenching with an excess of chlorotrimethylsilane furnished in good yield the 2,6-bis-silylated benzamide **5** (Scheme 1). Treatment of **5** with an excess of Br_2 in CCl_4 afforded cleanly the desired dibromo derivative **6** via a double ipso bromo desilylation.[11]

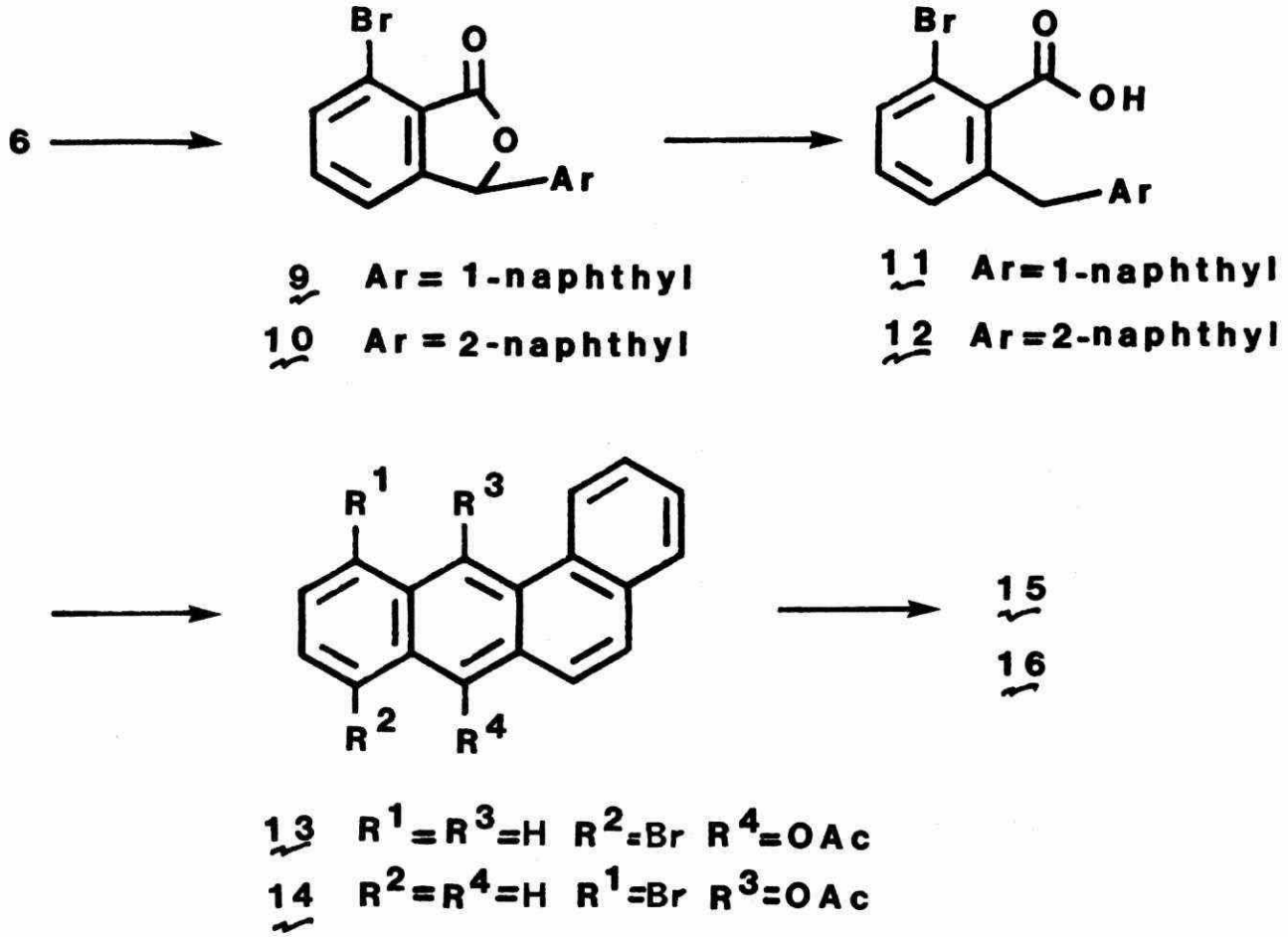
SCHEME 1



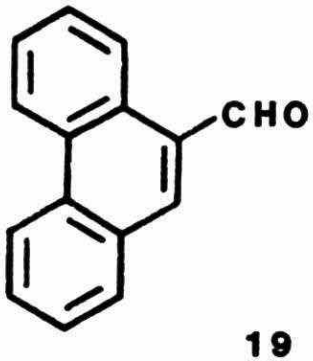
4 5 6

When **6** was treated with 2 equivalents of t-BuLi at -78°C[12] in THF for 30 min. followed by quenching with either 1-naphthaldehyde **7** or 2-naphthaldehyde **8**, smooth mono metal-halogen exchange occurred as evidenced by isolation of the bromo phthalides **9** and **10** after treatment with a catalytic amount of p-toluene sulfonic acid in refluxing toluene (**Scheme 2**).

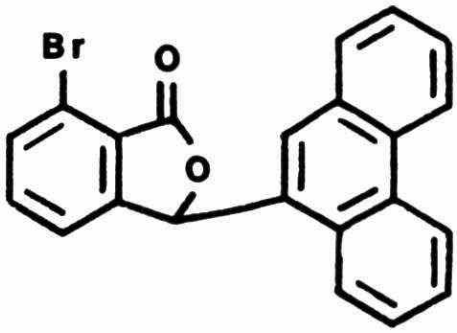
SCHEME 2



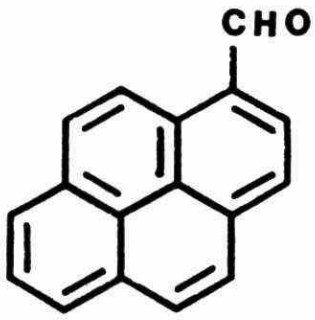
To avoid loss of the bromo functionality under the hydrogenolysis conditions used previously,[7,8] the phthalides **9** and **10** were treated with anhydrous hydriodic-hypophosphorous acid in glacial acetic acid[5,13] to



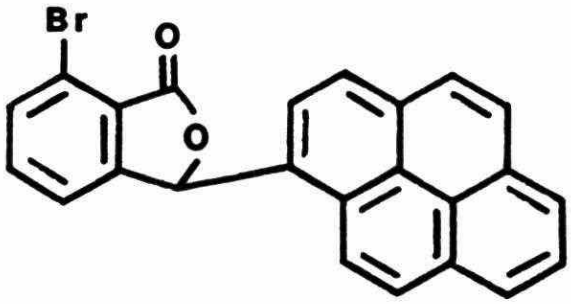
19



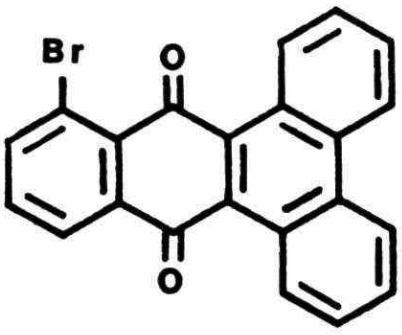
20



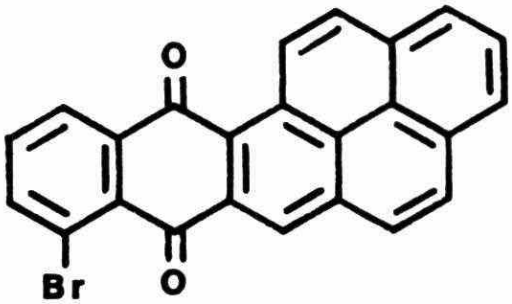
22



23



21



24

give the desired bromo(naphthylmethyl)benzoic acids **11** and **12**. Cyclization of **11** and **12** to the desired acetoxy derivatives **13** and **17** was effected with $ZnCl_2$ in acetic anhydride-acetic acid and subsequent oxidation ($Na_2Cr_2O_7$)[11] led to the desired bromo benz[a]anthraquinones **15** and **16**. The conversion of **15** and **16** to the DMBA derivatives- **17** and **18** using either MeMgBr or MeLi followed by treatment with $SnCl_2$-HCl has been previously reported.[5]

More highly condensed bromo-PAH quinones such as **21** and **24** were prepared in a similar manner by quenching the mono lithio derivative derived from **6** with either 9-phenanthrene carboxyaldehyde **19** or 1-pyrene carboxaldehyde **22**. Subsequent acid treatment afforded the desired bromo phthalide intermediates **20** and **23** respectively.

The use of silicon in the directed ortho metalation of tertiary benzamides thus allows convenient access to brominated PAH precursors in quantities suitable for environmental[5] and metabolic[4] studies.

ACKNOWLEDGEMENTS

We thank the Ontario Ministry of the Environment (Air Resources Branch) for financial support of our synthetic programs.

References and Footnotes

1. Watube, T.; Ishizuka, T.; Isobe, M.; Ozawa, N. Science, **1982**, 215, 403.
2. Hoffman, D.; Schmeltz, I.; Hecht, S.S.; Wynder, E.L. In: Polycyclic Hydrocarbons and Cancer. ed. H.V. Gelboin and P.O.P. Ts'o, Academic Press, New York, **1978**, Vol. 1, pp. 85-117.

3. Thomas, R.S.; Lao, R.C.; Wang, D.T.; Robinson, D.; Sakuma, T. Determination of polycyclic aromatic hydrocarbons in atmospheric particulate matter by gas chromatography-mass spectrometry and high- pressure liquid chromatography. In: Carcinogenesis, ed. R.I. Freudenthal and P.W. Jones, Raven Press, New York, **1976**, Vol. 3, pp. 9-19.
4. Newman, M.S. Carcinogenic Activity of Benz[a]anthracenes. In: Carcinogenesis, ed. R.I. Freudenthal and P.W. Jones, Raven Press, New York, **1976**, Vol. 1, pp. 203-207.
5. Newman, M.S.; Hussain, N.S., J. Org. Chem. **1982**, 47, 2837. Newman, M.S.; Prabhu, V.S.; Veeraraghavan, S. Ibid., **1983**, 48, 2926.
6. Newman, M.S.; Lilje, K.C., J. Org. Chem., **1979**, 44, 4944. Ansell, H.V.; Taylor, R. Ibid., **1979**, 44, 4946.
7. Mills, R.J.; Snieckus, V., J. Org. Chem., **1983**, 48, 1565.
8. Mills, R.J.; Snieckus, V., Tetrahedron Lett., **1984**, 479.
9. Gschwend, H.W.; Rodriquez, H.R., Org. React. (N.Y.), **1979**, 26,1.
10. For cases involving $CONEt_2$ see Jacobs, S.A.; Harvey, R.G., Tetrahedron Lett., **1981**, 1093. Doadt, E.G.; Iwao, M.; Reed, J.N.; Snieckus, V., Polynuclear Aromatic Hydrocarbons, ed. Cooke, M., and Dennis, A.J. Battelle Press, Columbus, Ohio, **1982**; p. 413. See also Ref. 8. For cases involving 2-oxazolines see Newman, M.S.; Kannan, R., J. Org. Chem., **1979**, 44, 3388. See also Ref. 5.
11. Mills, R.J.; Snieckus, V., Tetrahedron Lett., **1984**, 483.
12. The requirement of 2 equiv. of RLi for each metal-halogen exchange step was first recognized by Seebach: Seebach, D.; Neumann, H., Chem. Ber., **1974**, 107, 847. See also Saulnier, M.G.; Gribble, G.W., J. Org. Chem., **1982**, 47, 757 and references cited therein.
13. Platt, K.L.; Oesch, F., J. Org. Chem., **1981**, 46, 2601.

ANALYSIS OF POLYCYCLIC AROMATIC HYDROCARBONS AND THEIR DERIVATIVES IN ENVIRONMENTAL SAMPLES

M.A.Quilliam, J. Marr, and R.J. Gergely

Department of Chemistry, McMaster University, Hamilton

ABSTRACT

In recent years it has become clear from work with microbial mutagenesis assays and chemical fractionation techniques that there are many hazardous substances present in environmental samples that are still largely uncharacterized. Studies have shown that much of the mutagenic activity in urban airborne particulate extracts is associated with compound classes other than the PAHs and that much of the activity is of the "direct-acting" type. Several studies have shown that nitrated and oxygenated polycyclic aromatic hydrocarbons (nitro-PAHs and oxy-PAHs) are probably the principle direct-acting mutagens in automobile exhaust and urban air particulate samples. The environmental significance of these mutagens is not yet fully established, however, due in part to the lack of analytical methods for their determination and in part to the fact that many of these compounds may be formed as artifacts during the sampling step. Studies have shown that some PAHs can react readily with filter media, nitrogen oxides, sulfur oxides, ozone, and gas-phase photochemical smog to form a variety of derivatives. This paper will present some of the chromatographic and mass spectral methods that we have been developing for the analysis of PAHs and PAH derivatives and the results of our joint investigation with Concorde Scientific into new artifact-free methods of sampling.

INTRODUCTION

The chemical composition of environmental samples such as urban air particulate matter is very complex, consisting of hundreds of organic and inorganic components. Over the last decade, many efforts have been directed to the determination of the levels of known carcinogenic compounds, particularly polycyclic aromatic hydrocarbons (PAHs) such as benzo[a]pyrene, in the organic solvent extractable fraction. However, in recent years it has become clear from work with microbial mutagenesis assays and chemical fractionation techniques that there are many hazardous substances present that are still largely uncharacterized. For example, studies have shown that much of the mutagenic activity in urban airborne particulate extracts is associated with compound classes other than the PAHs and that much of the activity is of the "direct-acting" type (1). The term "direct-acting" applies to those substances that cause reversion of Salmonella test strains in the Ames microbiological reversion assay (2) in the absence of the microsomal fraction of rat liver. The latter provides the oxidative "activation" of many chemicals to the reactive intermediates that act as the ultimate mutagens or carcinogens.

Several studies have shown that nitrated and oxygenated polycyclic aromatic hydrocarbons (nitro-PAHs and oxy-PAHs) are probably the principle direct-acting mutagens in automobile exhaust and urban air particulate samples (3,4). The environmental significance of these mutagens is not yet fully established, however, due in part to the lack of analytical methods for their determination and in part to the fact that many of these compounds may be formed as artifacts during the sampling step. Recent studies have shown that some PAHs can react readily with filter media, nitrogen oxides, sulfur oxides, ozone, and gas-phase photochemical smog to form a variety of derivatives (5).

This paper will present some of the chromatographic and mass spectral methods that we have been developing for the analysis of PAHs and PAH derivatives, and the results of our joint investigation with Concorde Scientific into new artifact-free methods of sampling.

METHODS

Methylene chloride, acetone and methanol were "distilled in glass" quality purchased from Caledon Laboratories Ltd. (Georgetown, Ontario). Hexane and isopropanol were "HPLC grade" purchased from BDH (Toronto, Ontario).

Samples were extracted with methylene chloride overnight in a Soxhlet extractor. Following concentration to about 10 mL in a rotary evaporator, the organic extract was filtered to remove particulates (0.5 um Teflon filter, Millipore Corp., Bedford, MA) and evaporated to dryness under a stream of nitrogen. The weight of the dried residue was then determined.

The extracted organics dissolved in 1 mL of CH_2Cl_2 were injected into a silica Sep-Pak (Waters Associates Inc., Milford, MA) that had been previously washed with 5 mL CH_2Cl_2. With CH_2Cl_2 used as the eluent, the first 10 mL was collected and evaporated to 200-300 ul under a stream of nitrogen. This solution was injected directly onto a 30 x 1 cm Sephadex LH-20 column (Pharmacia Fine Chemicals, Dorval, Quebec) previously equilibrated in and eluted with methanol/methylene chloride (3:1). The eluent was monitored at 254 nm. The aromatic fraction, typically in the 15-25 mL range (defined by naphthalene and picene standards), was collected and evaporated to dryness.

In the final clean-up step a normal phase semi-preparative HPLC with a 250 X 9.4 mm M9 PAC column (Whatman Inc., Clifton, NJ) with a hexane/isopropanol

mobile phase was used. The sample was dissolved in methylene chloride/hexane (1:5) prior to injection. Excessive amounts of methylene chloride could not be used since separation efficiency and retention times are altered. The sample was eluted from the M9 PAC column using a mobile phase of 0.5% isopropanol/hexane isocratic followed by a gradient from 0.5% to 30% isopropanol/hexane from 10 min to 35 min. The collection points for the various fractions were determined by previously injecting standard compounds (naphthalene/picene, nitroanthracene/nitropicene, etc.). Fractions were evaporated to dryness and dissolved in a known volume of acetone for the final GC analysis or in acetonitrile for HPLC analysis.

A Varian 3700 gas chromatograph equipped with an on-column injector (J&W Scientific Inc., Orangevale, CA). and flame ionization (FID) and nitrogen-phosphorus (NPD) detectors was used for GC analyses. An effluent splitter provided simultaneous FID and NPD detection. Fused silica capillary columns were used: 30 m X 0.32 mm I.D., 0.1 um DB-5 (J&W Scientific Inc.). All analyses were performed with a temperature program of 100^{o} to 320^{o} at 5^{o}/min. An Apple II+ microcomputer (Apple Computer Inc., Cupertino, CA) equipped with a 12-bit analog-to-digital converter, multiplexer and programmable gain amplifier (Interactive Microware Inc., State College, PA) was used for data aquisition and interpretation (see Figure 1).

GC-MS analyses were performed on a VG Micromass 7070F mass spectrometer (VG Analytical, Altrinchan, U.K.) equipped with a Varian 3700 gas chromatograph. Samples were chromatographed on the fused silica capillary columns described above with the same temperature program. The column was connected directly to the mass spectrometer and inserted to within 2 cm of the electron beam. Electron impact ionization with an electron energy of 70 eV was

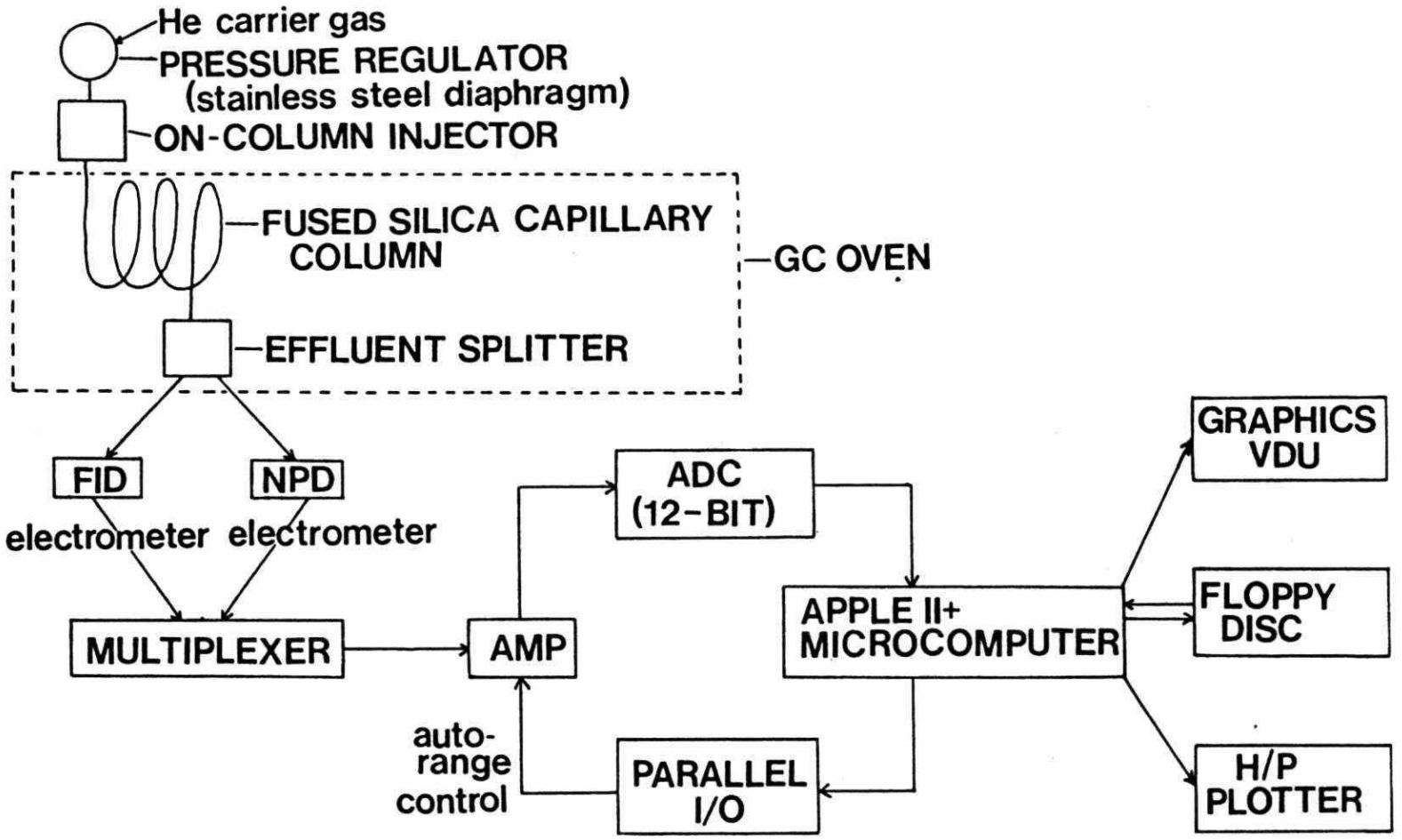


Figure 1: Schematic of capillary column gas chromatography and data acquisition system.

used. Data was acquired with a VG 2035 data system, either by scanning from 400 to 90 amu, at 1 sec/decade, or by performing selected ion monitoring on up to 10 ions with accelerating voltage stepping and a 100 msec sampling interval for each ion.

Microbore reverse phase HPLC was performed on Spectra-Physics 8700 liquid chromatograph (Santa Clara, CA) which was modified with a splitting system that allowed a pump flow rate of 1 mL/min to be split to 30 uL/min flow rate through the microbore column (see Figure 2). Injections were made with a 1 uL injection loop injector (Rheodyne 1710). A Schoeffel 770 variable wavelength UV detector equipped with a 0.5 uL flow cell was used for UV absorption detection. The column was a custom-packed Alltech microbore column (250 x 1 mm, 5 um Vydac 201TP packing). A gradient of 60% acetonitrile/water to 100% acetonitrile over 20 min was used. The column was operated at ambient temperature.

Combined HPLC-MS was performed on a VG7070F mass spectrometer equipped with a polyimide belt transport interface (see Figure 3). Electron-impact ionization and scan conditions were similar to those used for GC-MS.

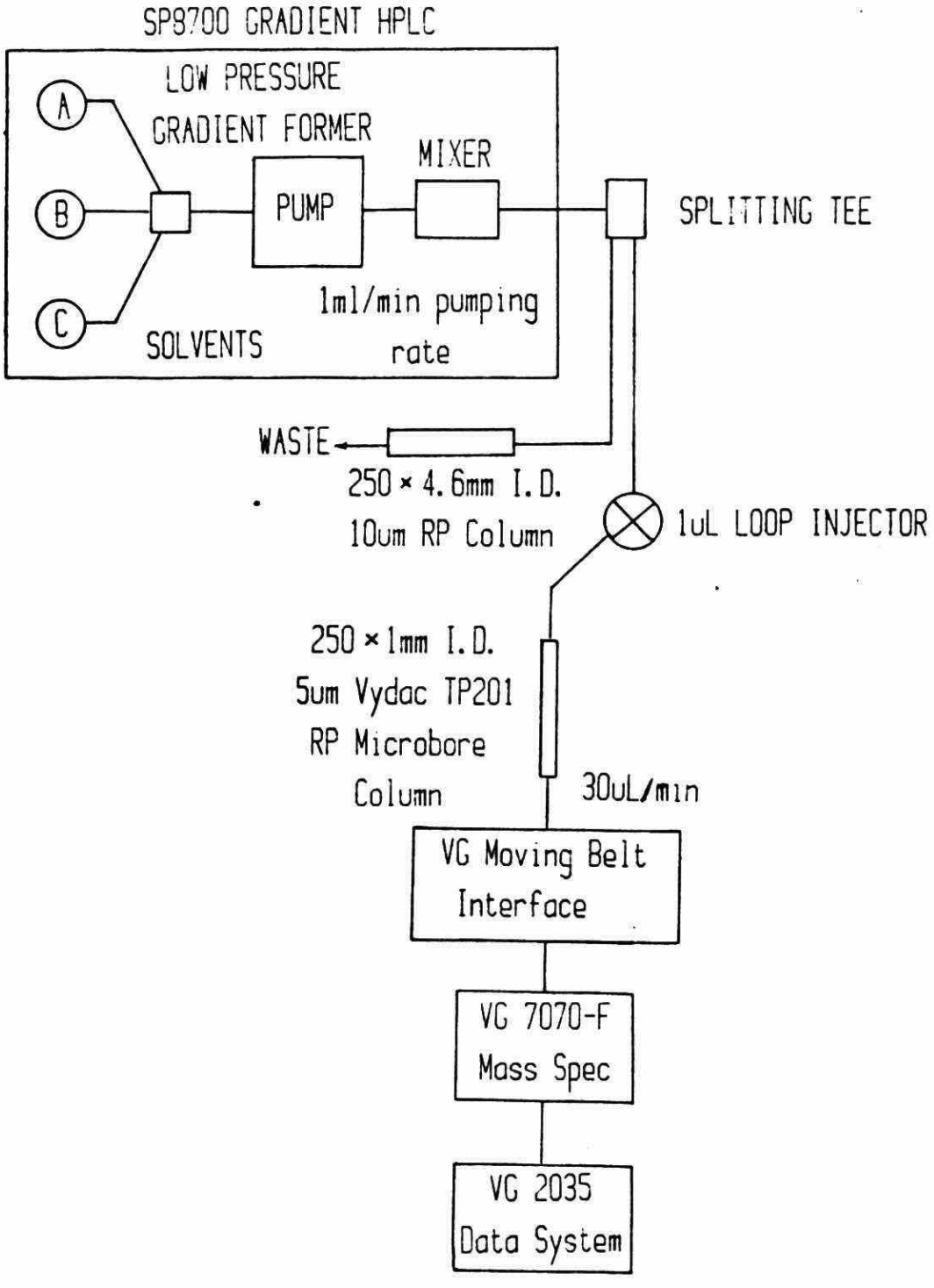


Figure 2: Schematic of microbrore column HPLC-MS system.

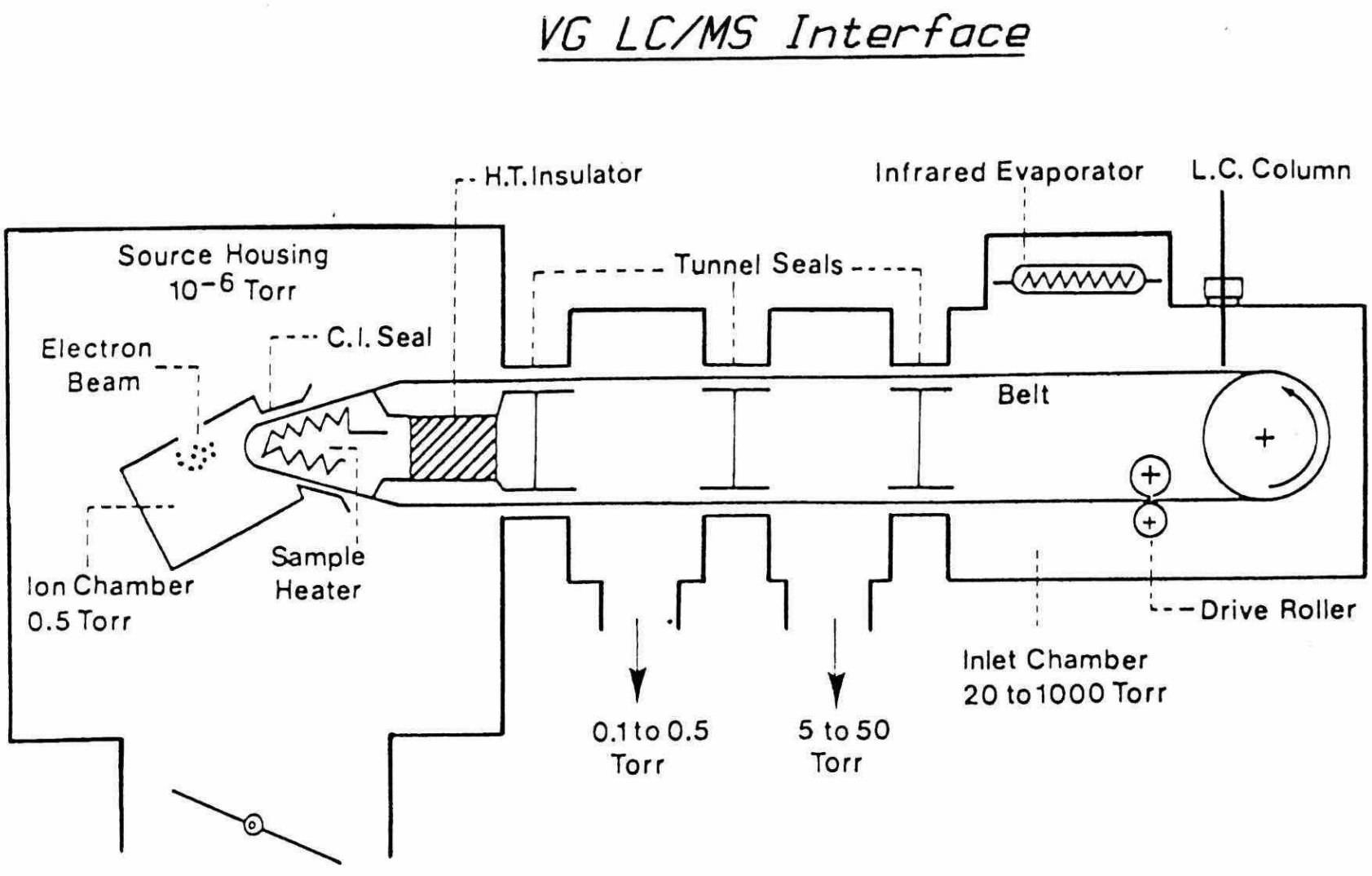


Figure 3: Schematic of LC/MS interface on VG7070F mass spectrometer.

RESULTS AND DISCUSSION

Fractionation Scheme and Profiling

When faced with the analysis of a specific class of compounds present at trace levels in complex environmental samples, one can resort to either highly selective detection methods or high resolution fractionation methods. The use of sophisticated methods of analysis such as MS/MS, while very powerful due to their selectivity, are not readily available to most analysts. An analytical fractionation or clean-up scheme directed towards the isolation of compound classes can dramatically reduce interferences in the final analytical step. Previously, we have developed a specific clean-up scheme to isolate PAHs and nitro-PAHs from diesel exhaust and urban airborne particulate matter (6,7).

Since then, we have modified our fractionation scheme for more general profiling work in order to be able to study artifact formation problems associated with the sampling method used for collecting airborne particulates. Figure 4 illustrates the approach now used in our laboratory. The concept behind the scheme is to separate the sample into fractions corresponding to aliphatics compounds, PAHs, PAH derivatives and highly polar compounds. At present we are interested in examining the levels of PAHs and the derivatives of PAHs, such as nitro-PAHs and oxy-PAHs, that may be formed as artifacts from the reaction of PAHs with reactive gases during sampling. Figures 5 and 6 illustrate capillary column GC-FID/NPD profiles of these two fractions in a typical urban airborne particulate sample. Many of the peaks have been identified by retention indices and GC-MS.

These GC profiling methods and HPLC analyses are now being used to examine

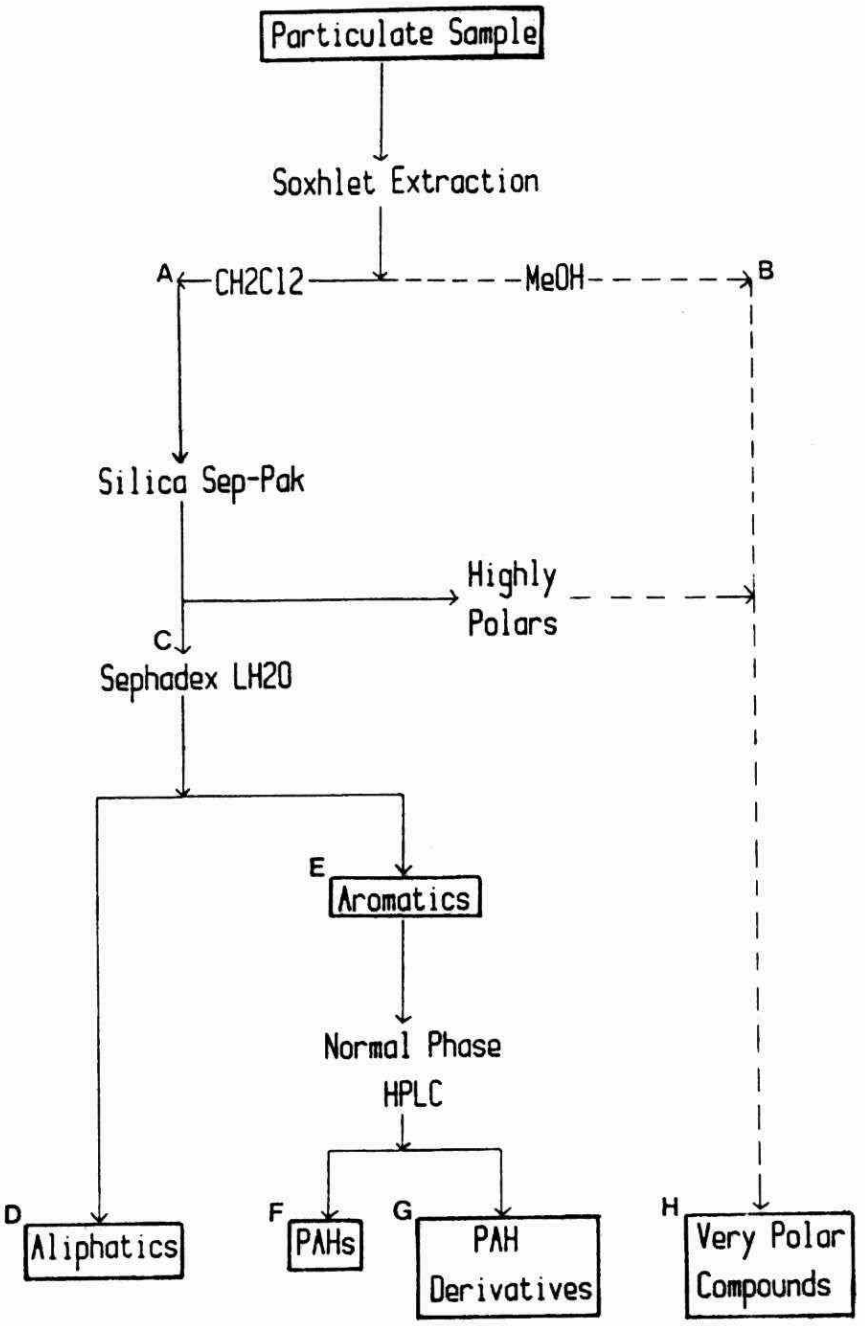


Figure 4: Fractionation scheme used for isolating different compound classes from environmental samples. The dotted line represents work to be done in future studies.

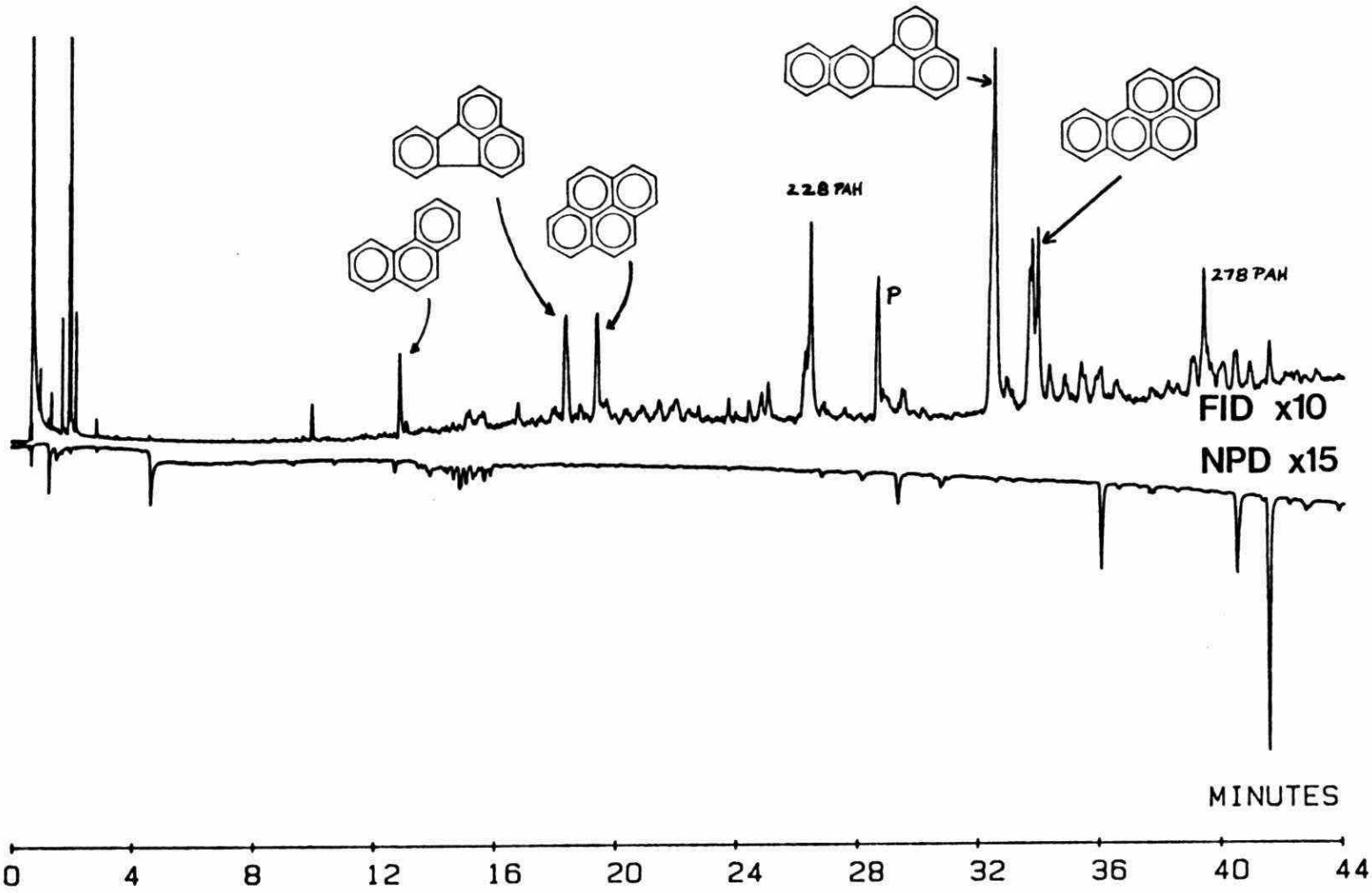


Figure 5: A typical capillary GC-FID/NPD trace for the PAH fraction (F in Figure 4) of a urban airborne particulate sample.

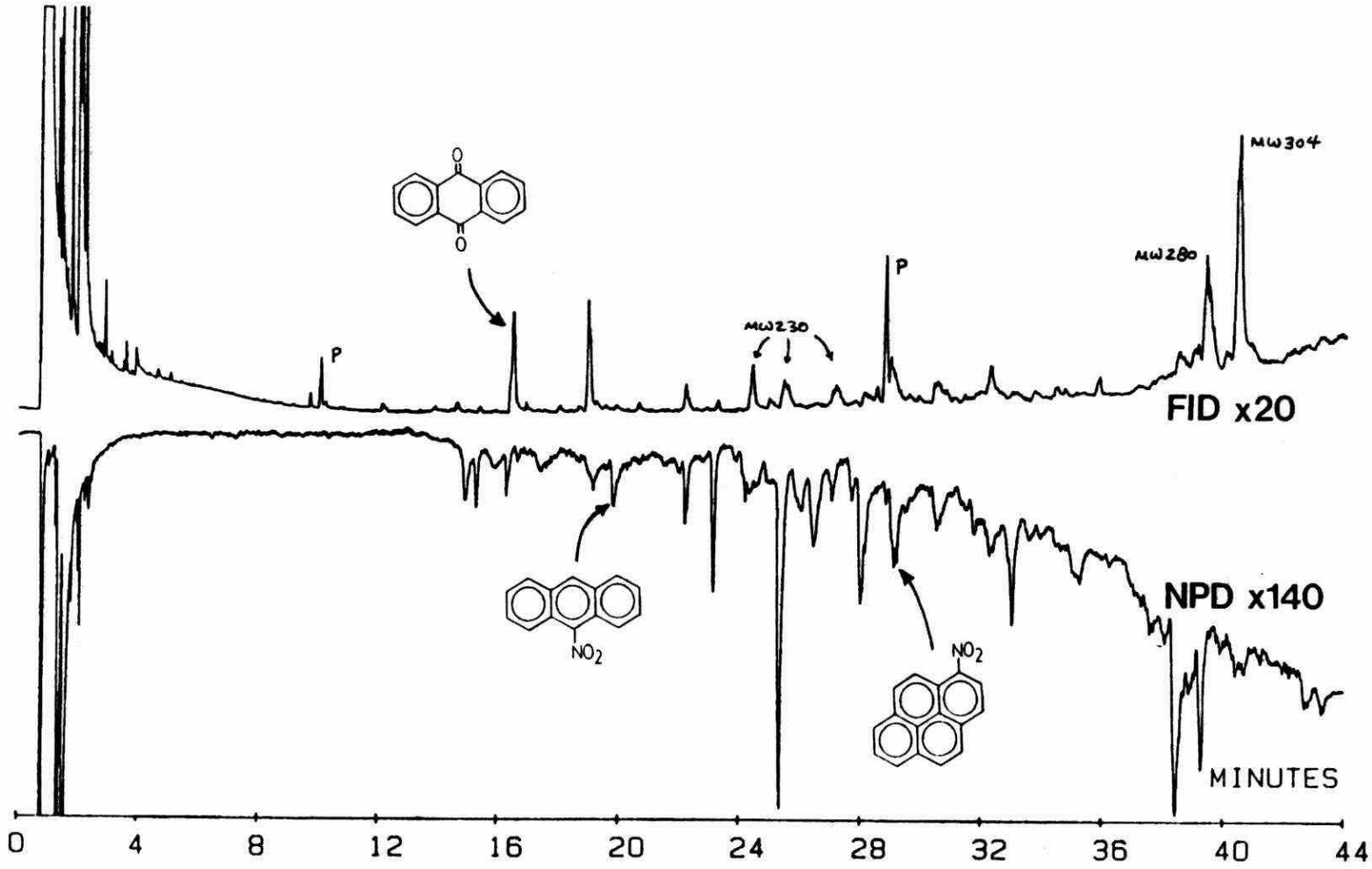


Figure 6: A typical capillary GC-FID/NPD trace for the PAH derivative fraction (G in Figure 4) of an urban airborne particulate sample.

paired samples of airborne particulates that have been acquired with two different types of sampling devices: (a) a conventional hi-vol filter sampler, and (b) a hi-vol sampler equipped with reactive gas denuder system. The latter has been developed by Concorde Scientific (8), who are also doing the field sampling work. The information from these experiments should be useful in determining the efficiency of PAH collection and the degree of artifact formation with the different samplers. In the talk we will present the results for a series of samples for which we are presently doing the analyses.

Microbore HPLC and HPLC-MS

Gas chromatography is the most widely used analytical method in environmental analytical chemistry, mainly because of its high resolving power, the wide selection of general and selective detectors, and the ease of interfacing with mass spectrometry (GC-MS). HPLC, on the other hand, offers many unique advantages such as better quantitation, the ability to analyze low volatility compounds, and the possibility of collecting fractions for mutagenic profiling. For PAHs and PAH derivatives, UV absorption and fluorescence detectors provide very good sensitivity. However, a major weakness is the difficulty in identifying peaks in HPLC chromatograms. HPLC-MS has therefore been of great interest for some time but has never been as succesful as GC-MS. Several different interfacing methods have been developed such as the belt transport system, direct liquid injection, and thermospray. In our laboratory we have a VG7070F mass spectrometer equipped with a belt transport system. It offers the advantage being able to provide both EI and CI mass spectra, the former being very important for structure elucidation. Up until recently, however, we have had difficulty using this HPLC-MS system for trace analysis. The major problem is with gradient reverse phase HPLC and the water in the

mobile phase which is difficult to coat on the belt and to remove in the interface.

In recent years, HPLC microbore columns (1 mm I.D.) have attracted a great deal of interest. The advantages include better solvent economy (only 30 uL/min flow rate) and improved sensitivity with optical detectors. Since the UV absorption detector response is concentration dependent, the low flow rate for microbore columns yields greater sensitivity, as long as the detector cell pathlength is not decreased. Of course, this is somewhat balanced by the fact that smaller injection volumes must be used with microbore columns. Thus, the advantage holds only if there is a small amount of sample, which is usually the case in trace analysis. Microbore columns also offer potentially higher resolving power than conventional columns.

We became interested in microbore HPLC because of the greater ease of interfacing with mass spectrometry. The low flow rate of mobile phase facilitates the use of wide ranging gradients with the belt interface system. Unfortunately, we did not have microbore HPLC equipment. Indeed, it is only very recently that equipment is becoming commercially available for microbore work, particularly gradient operation. We have succeeded in adapting a conventional gradient pumping system, the SP-8700 HPLC, for gradient microbore analyses. This involved using a splitter to split a flow of 1 mL/min from the pump to give approximately 30 uL/min through 1mm I.D. x 25 cm column (see Figure 2). A Rheodyne micro-loop injector (1 uL) was used for injections and a Schoeffel 770 variable wavelength detector was equipped with a micro flow cell. The reproducibility of retention times appeared to be quite good in the short term. However, since the splitting system we have developed uses pressure control, the longer term reproducibility is poorer because of gradual changes

in the pressure drop across the column. Eventually, it will be necessary to invest in a true microbore pumping system.

We have chosen the Vydac 201TP polymeric ODS column packing material for our HPLC-MS studies. The Vydac packing is very popular in the PAH analysis field because of the selectivity that it offers, particularly for the separation of benz[a]anthracene and chrysene. This is very important for HPLC-MS experiments because these compounds have identical mass spectra. We were interested in analyzing samples for a number of target PAHs, given in Table 1. All the target PAHs with the exception of only acenaphthene, 3, and fluorene, 4, are well separated. The poor separation of compounds 3 and 4 is not of great concern for HPLC-MS, however, since they have different molecular weights (154 and 166).

HPLC-MS experiments with the Vydac microbore column proved to very successful. Due to the low flow rates used with the microbore column, there was much less noise in the mass spectrometer due to pressure fluctuations and solvent background than with conventional columns. Some representative chromatograms and spectra for the PAH fraction from a marine sediment reference sample are presented in Figure 7. Due to good retention time reproducibility and good total ion chromatograms, it was possible to match peaks in the UV and mass chromatograms quite easily. The combination of retention times and electron impact spectra allow compounds to be identified quite readily. Scan 616 in Figure 7 illustrates this point very well. From the electron impact spectrum it is easily established that this compound is sulfur (S_8).

We have also performed quantitative analyses with the microbore HPLC-MS system using selected ion monitoring. Figure 8 presents some representative chromatograms from the gradient microbore SIM experiments. Plots of peak height

TABLE 1: PAHs identified and quantitated by HPLC-MS

Cmpd #	MW	Std Soln Conc'n (ng/uL)	Compound Name
1	128	2.3	Naphthalene
2	152	1.9	Acenaphthylene
3	154	2.1	Acenaphthene
4	166	0.49	Fluorene
5	178	0.51	Phenanthrene
6	178	0.33	Anthracene
7	202	0.10	Fluoranthene
8	202	0.98	Pyrene
9	228	0.50	Benz[a]anthracene
10	228	0.47	Chrysene
11	252	0.51	Benzo[b]fluoranthene
12	252	0.50	Benzo[k]fluoranthene
13	252	0.53	Benzo[a]pyrene
14	278	0.37	Dibenz[ah]anthracene
15	276	0.40	Benzo[ghi]perylene
16	276	0.41	Indeno[1,2,3-cd]pyrene

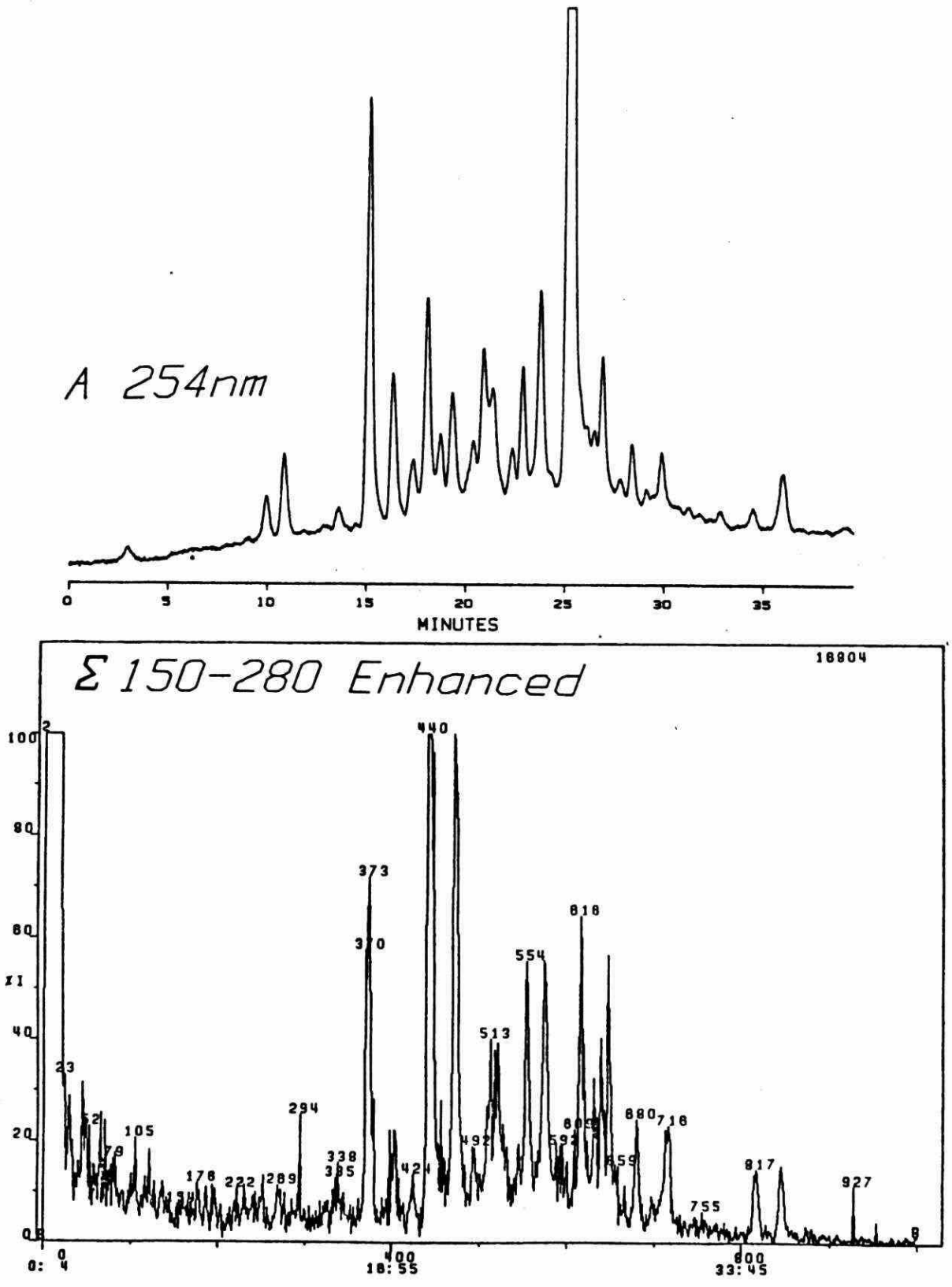


Figure 7: Microbore column HPLC and HPLC-MS chromatograms of the PAH fraction of a marine sediment reference sample.

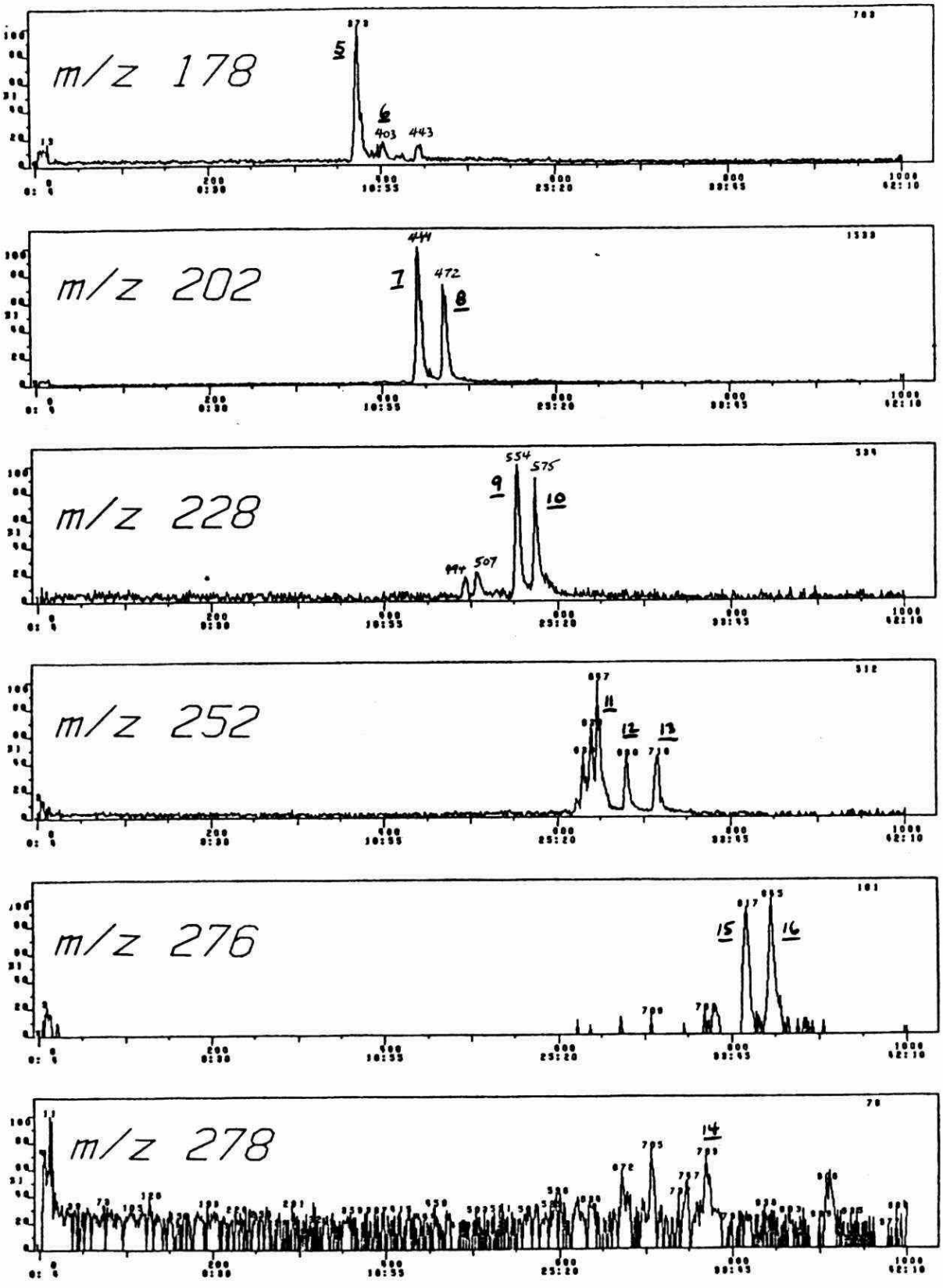


Figure 7 (continued)

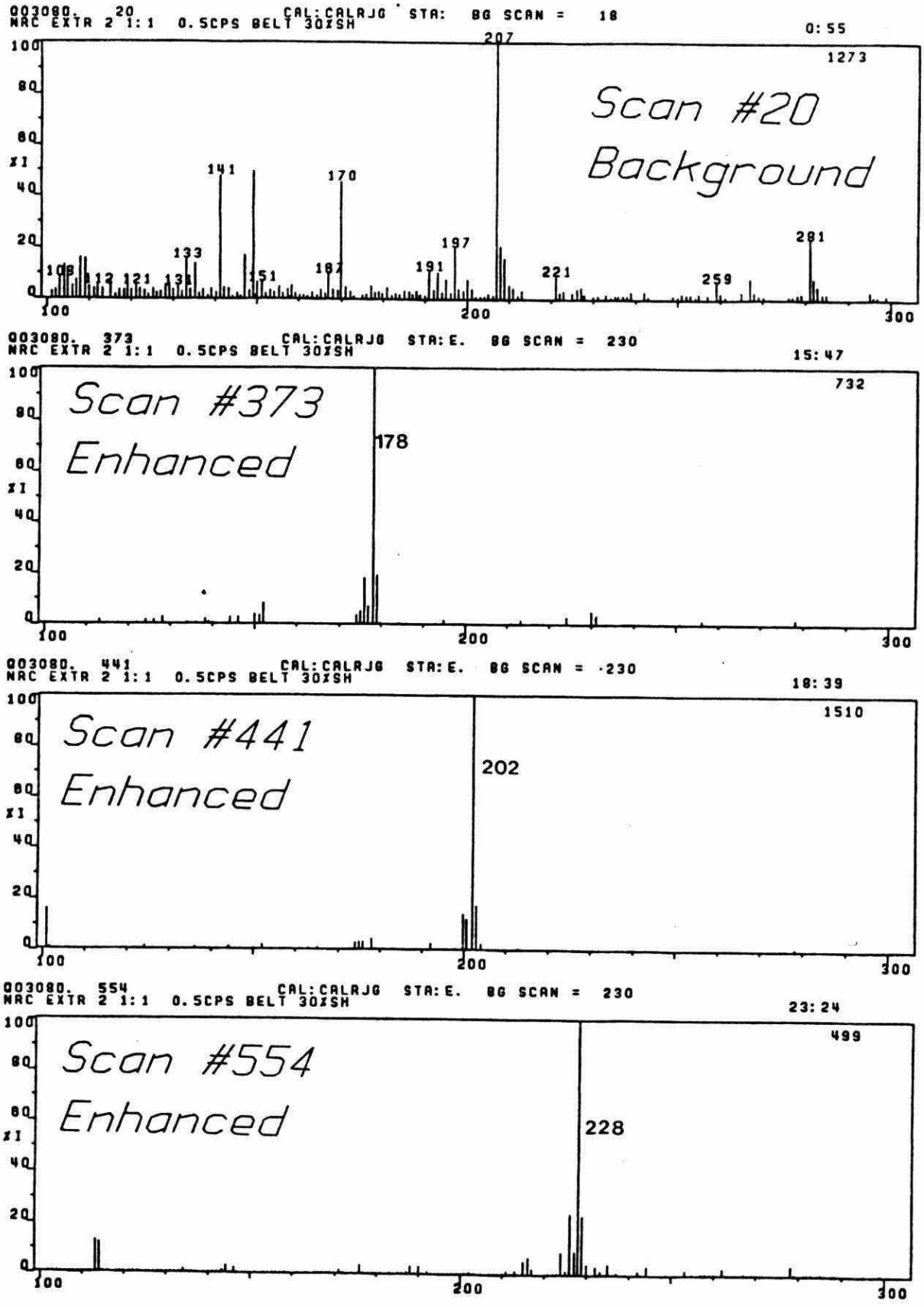


Figure 7 (continued)

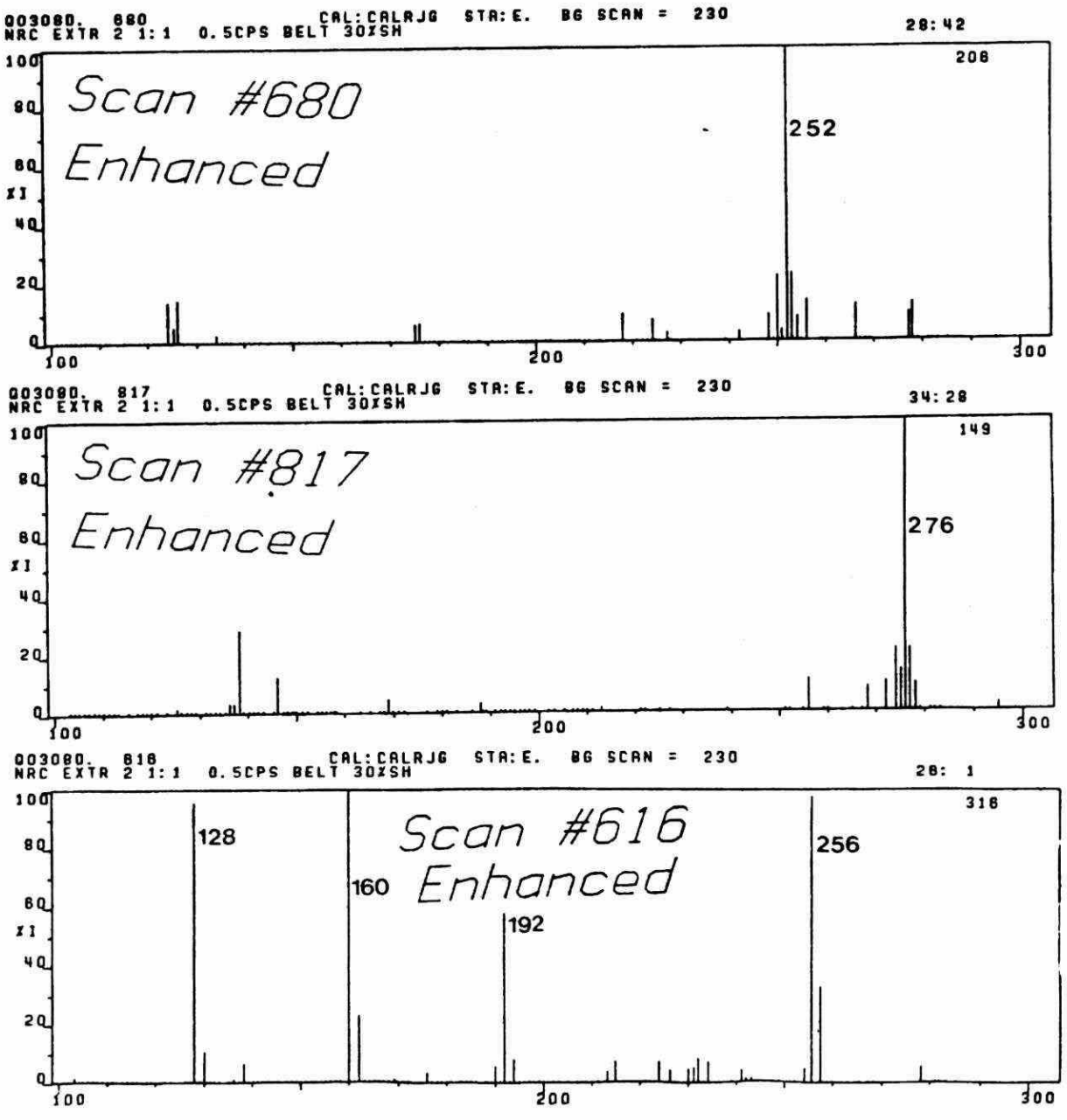


Figure 7 (continued)

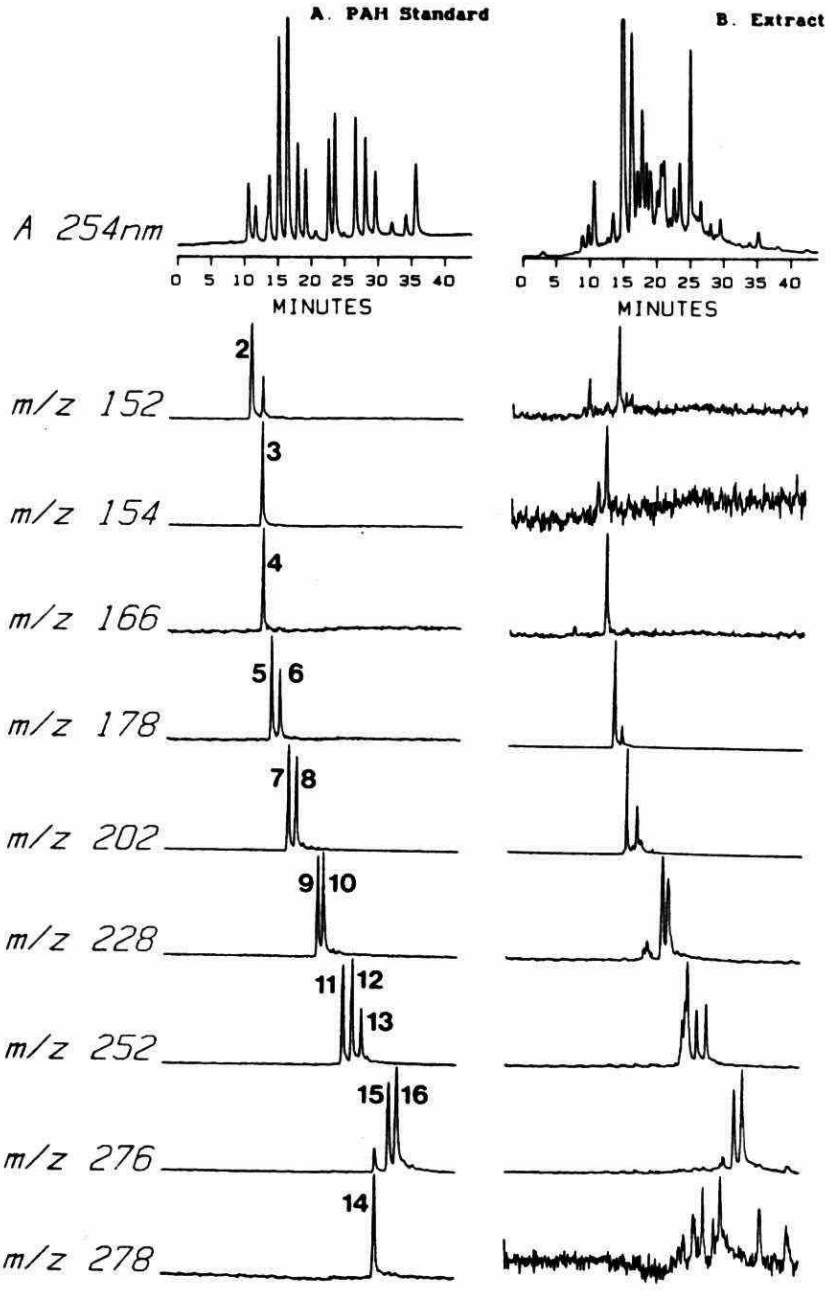


Figure 8: Microbore HPLC-MS selected ion monitoring chromatograms of (a) a PAH standard mixture, and (b) the PAH fraction from an urban airborne particulate sample. Compound numbers are identified in Table 1.

or peak area versus amount injected revealed that there was a linear response with a near zero intercept for most of the compounds. Only one compound, indeno[1,2,3-cd]pyrene, showed an appreciable intercept on the x-axis. This may be due to incomplete evaporation of this very low volatility compound on the first pass of the interface belt through the source. A detection limit of approximately 50 pg (injected) for the higher molecular weight PAHs was estimated. A method detection limit of approximately 10 ppb should therefore be possible if a 350 mg sample was extracted and concentrated to 100 uL.

REFERENCES

1. J.N.Pitts, Jr. et al., Toxicol. Letters 1, 65-70 (1977).

2. B.N.Ames et al., Mutat. Res. 31, 347 (1975).

3. D.Schuetzle et al., Int. J. Environ. Anal. Chem. 9, 93 (1981).

4. T.Nielson et al., Seventh Int. Symp. on PAHs, Columbus, Ohio, Oct. 1982.

5. J.N.Pitts, Jr. et al., Science 202, 515 (1978).

6. M.A.Quilliam et al., 7th Int. Symp. on PAHs, Columbus, Ohio, Oct. 1982.

7. M.A.Quilliam et al., Technology Transfer Conference No. 4, Ontario Ministry of the Environment, Toronto, Nov. 29-30, 1983.

8. R.Caton et al., ibid.

ACKNOWLEDGEMENTS

We gratefully acknowledge funding from the Ontario Ministry of the Environment and thank Steve Guerin and Claude Davis of Concorde Scientific for airborne particulate filter samples.

A MASS SPECTROMETRIC STUDY OF SELECTED AIR POLLUTANTS

Dr. R. E. March and R. J. Hughes

Department of Chemistry,
Trent University,
Peterborough, Ontario.

A MASS SPCTROMETRIC STUDY OF SELECTED AIR POLLUTANTS

R. E. MARCH AND R. J. HUGHES

Trent University, Peterborough

ABSTRACT

Mass spectrometry is an extremely powerful tool not only for identification and quantification of polycyclic aromatic hydrocarbons (PAH), but also for reactivity, structure elucidation and investigation of ion chemistry, energetics and fragmentation behavior.

The results of mass spectrometric studies of reaction products of benzo(a)pyrene and chrysene with NO_2 and $^{15}NO_2$, as well as ion storage studies and reaction of benzo(a)pyrene with O_2 in ultraviolet light are presented.

In addition to conventional electron-impact mass spectra, mass-analyzed ion-kinetic-energy (MIKE) spectra can be obtained using a double-focusing mass-spectrometer in which the magnetic sector precedes the electric sector. Ions of a given species are selected by the magnetic sector and an appropriate fraction of those which are metastable undergo unimolecular dissociation in the second field-free region. The masses and translational energies of the resulting fragment ions are determined from energy spectra obtained by scanning the electric sector.

PAH offer a unique opportunity for the study of multiply-charged species since they readily form doubly- and triply- charged ions. The molecules themselves, and thus their fragments, are composed solely of carbon and hydrogen; charge separation studies of benzo(a)pyrene have led to an estimation of intercharge distances and charge locations within the molecule.

Since 1978 there has been a noticeable increase in the amount of research being performed which relates to Polycyclic Aromatic Hydrocarbons (PAH). This is evidenced by the fact that, since 1982 there have been approximately 1500 publications concerning PAH in general or benzo[a]pyrene (Figure 1(a)) and chrysene (Figure 1(b)) in particular.

A historical and general review of benzo[a]pyrene (B[a]P) is given by Phillips [1]; a review of physical and chemical properties of PAH by Zander [2]; and a biologically oriented review by Zedeck [3].

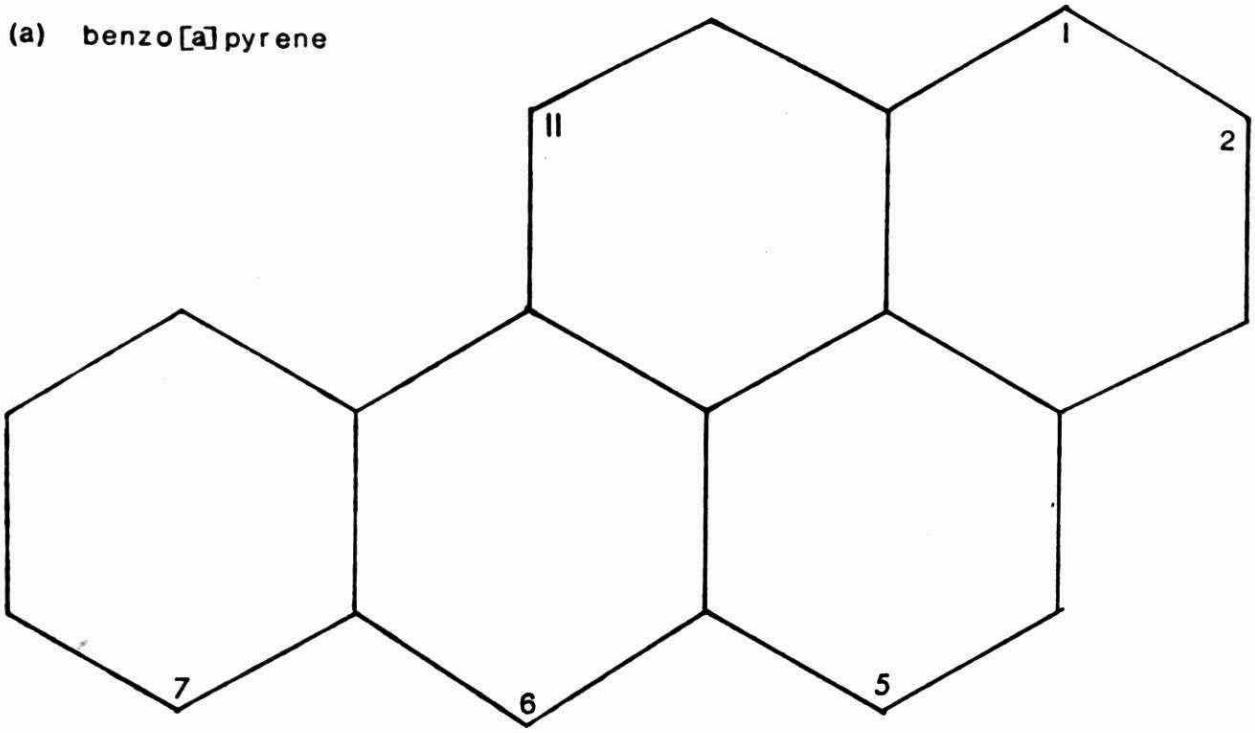
The focus of research conducted on Polycyclic Organic Matter (POM) has been oriented towards the detection, quantification, identification and synthesis of PAH and their metabolities in biological systems. Recent trends have indicated more and more a growing interest in the chemical and physical transformation of PAH and their reaction products both in the atmosphere and on sampling media employed in the collection of particulates. This interest has developed partially because of a desire to use certain PAH or total POM concentrations as indicators of the carcinogenicity and/or extent of pollution of air samples; obviously, transformations which occur during sampling can produce artefacts which will reduce the reliability of any measurements made thereafter. Such artefacts are documented [4-10, for example] although not without controversy [11-15].

Experimental

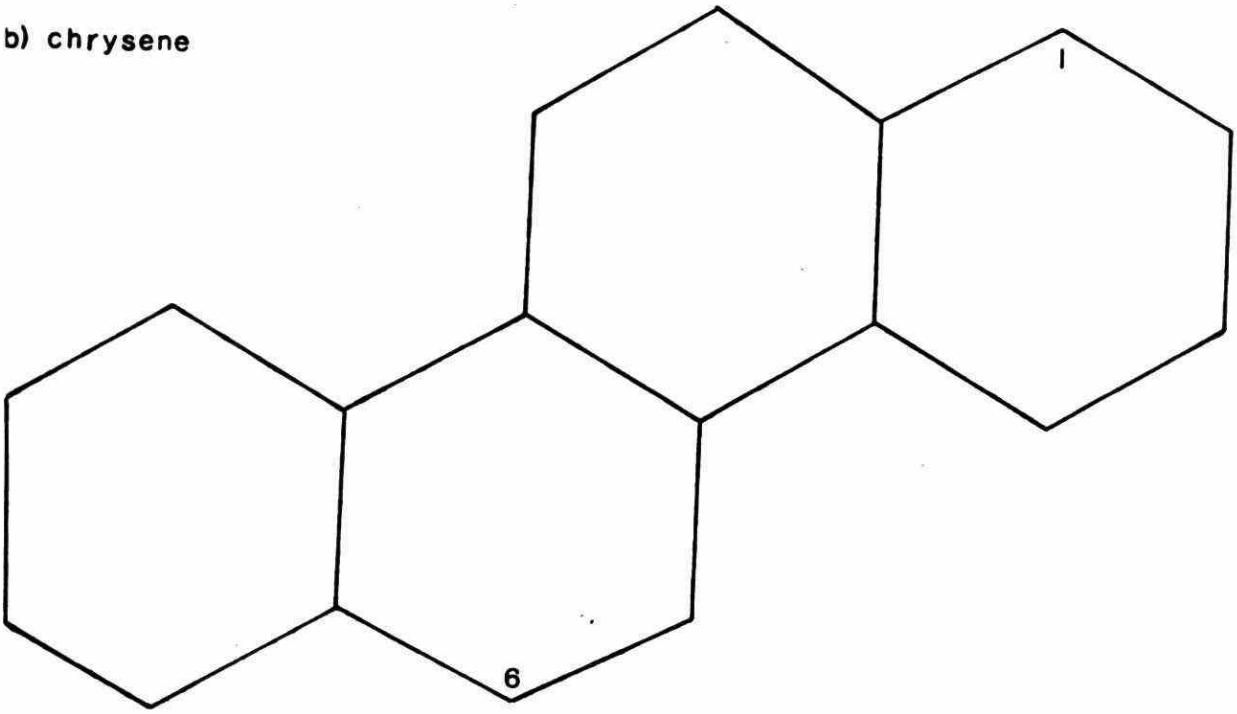
All electron impact (e.i.) spectra were run on either the A.E.I. MS12 or MS30, depending on availability, with an approximate source temperature of 220° C for the PAH and nitrated-PAH studies, and 60° for the $^{14}NO_2$ gas sample. Most of the e.i. spectra were performed at a nominal electron energy of 70eV although some exploratory spectra were run at lower energies. Electron impact

FIGURE 1

(a) benzo[a]pyrene



b) chrysene



spectra of the available $^{14}NO_2$ revealed no detectable impurity peaks above those of the background obtained in the MS12. High-resolution GC/MS spectra were provided by Dr. John Krause of the University of Ottawa. The PAH were obtained from Aldrich and their spectra showed them to be better than 95% pure. The $^{15}NO_2$ was obtained from Stohler Isotope Chemicals of Montreal and was not analyzed. Reactions of PAH with NO_2 were carried out by evacuating 16mm o.d. pyrex test tubes, containing approximately 5 mg PAH, to <.2 Pa, and admitting the proper pressure of NO_2.

RESULTS

Electron Impact (e.i.) Spectra
Benzo[a]pyrene (B[a]P)

Most of the e.i. spectra were performed at a nominal electron energy of 70eV although some exploratory spectra were run at lower energies. The most abundant ion at all ionizing energies employed is the molecular ion at m/z $252(C_{20}H_{12})^{+\cdot}$. The molecular ion gives rise to isotope peaks up to M + 6 and, as the electron energy is increased above 20eV, peaks are observed which correspond to (M-n) for n = 1 to 8, indicating losses of Hydrogen.

The ion at m/z 250 is about 25% the intensity of the molecular ion. It has been suggested that this ion is produced by two successive losses of H atoms; the first resulting in steric relief of the aromatic structure and the second resulting in the breakage of one of the ring systems to an acyclic structure [16]. Peaks due to doubly-charged species are abundant: triply-charged ions are visible at 60eV and quadruply-charged ions have been seen [17]. Extensive rearrangement occurs which results in the loss of CH_3 from the aromatic structure and the presence of $M\text{-}CH_3{}^{2+}$ indicates the processes $252^{2+} \rightarrow 237^{2+} + CH_3$ or $252^{3+} \rightarrow 237^{2+} + CH_3{}^{+}$ also occur in this system.

The remainder of the e.i. spectrum of benzo[a]pyrene may be rationalized as consisting of groups of peaks produced from cleavage and rearrangement/cleavage processes of the type A-C(n)H(n) where A is predominantly M^+ or $(M-2H)^+$, and n ranges from 1 to 7 or 8. The existence of multiple charges on the B[a]P ion enables one to study the interaction of these charges upon the fragments of this ion when they separate. The relative kinetic energy of these fragments will reflect the repulsive forces of these charges on each other and thus the intercharge separation may be calculated. For instance it has been suggested that three positive charges on the benzo[a]pyrene ion will arrange themselves at the corners of an equilateral triangle [17] within the skeleton, at positions 2, 5 and 11 or positions 7, 5 and 11 in fig. 1(a).

Chrysene

As is the case with PAH molecules in general, the mass spectrum of chrysene is dominated by the singly and doubly-charged molecular ion at m/z 228 and 114, respectively. The first major fragmentation observed as the electron energy is raised to about 20 eV is the loss of C_2H_2 accompanied by a metastable peak at 179μ; at 30eV this process is also observed as fragmentation of the doubly-charged ion, with a metastable peak at 89.5μ. Other fragmentation processes observed are similar to benzo[a]pyrene, namely A-C(n)H(n) for n = 1 to 6 and where A is either the molecular ion at m/z 228 ($C_{18}H_{12}^{+\cdot}$) or M-2 at m/z 226 ($C_{18}H_{10}^{+\cdot}$).

Metastable peaks in the spectrum of chrysene indicate successive fragmentations occur such as the initial loss of 39μ (eq. (1)) followed by a subsequent loss of 26. (eq. (2).

(1) $228^{+\cdot} \rightarrow 189^+ + C_3H_3$ m* at m/z 156.7

(2) $189^+ \rightarrow 163^+ + C_2H_2$ m* at m/z 140.5

Reactions with NO_2

The reactions of PAH with NO_2 under conditions normally encountered during air sampling have been fairly well characterized. It has been found by Pitts et al [8-10, 18], Van Cauwenberghe et al [19], Brorstroem et al [4-6], Butler and Crossley [11], and Lindskog [7] that, at ambient temperatures, many PAH produce mononitro derivatives when exposed to 1 ppm. or more NO_2, and that the reaction is catalysed by trace amounts (a few ppb.) of HNO_3. On the other hand, Grosjean has reported a resistance to nitration by NO_2 [15] (HNO_3 had been removed from the reactant NO_2) and has questioned [14] results obtained during simulated sampling experiments.

When nitration does occur, the sites at which it takes place and the relative reactivities correspond to those predicted by Dewar et al [20, 21] in 1956. Although only the mono-nitro derivatives were reported by the various groups above (and chrysene was not nitrated at all in Pitt's experiments) it has been shown [22] that at higher partial pressures of NO_2 and elevated temperatures, dinitro derivatives of B[a]P and chrysene, and trinitro derivatives of B[a]P are produced.

An examination of the nitration of 25 PAH and 4 anthracene derivatives under conditions approximating wet particles in the environment has been carried out by Nielsen [23]. From the results he was able to relate the difference in reactivity to differences in chemical structure. Benzo[a]pyrene and cyclopenteno[cd] pyrene are classified as the most reactive of those carcinogenic PAH that are common in environmental samples. Benzo[b]-and benzo[j]fluoranthene and indeno [1,2,3,-cd]pyrene are classified as the most stable of these. Since the reactions are electrophilic in nature, electron-donating substituents enhance the reactivity of the PAH and electron-attracting substituents diminish it; the effect of methyl substitution was found to be minor.

The relative reactivities of benzo[a]pyrene and chrysene in the gas phase parallel the results above: benzo[a]pyrene begins to react quickly with nitrogen dioxide and visibly darkens at room temperature in a few minutes. At 300°C this PAH is a colorless vapour but in the presence of NO_2 rapidly becomes a black liquid. Mass spectra of products formed indicate ion peaks at m/z values of 252, 297, 342 and 282, which represent the molecules benzo[a]pyrene, mononitro- and dinitro-benzo[a]pyrene and benzo[a]pyrene quinone dimers, respectively, whose structures are shown in Figure 2.

The major ion resulting from the overnight reaction of benzo[a]pyrene and NO_2 where the NO_2 ratio is greater than 5 times that of the PAH has a mass of 300 amu and gives rise to peaks at 256, 228, and 200 along with metastable for the accompanying losses. The mass spectrum and proposed structure are shown in Figure 3. Experiments employing $^{15}NO_2$ were performed which showed that nitrogen was not incorporated into the ring and also that the attached nitro groups preferentially lose nitric oxide (NO) upon electron impact.

Chrysene reacts somewhat more slowly with NO_2 in the gas phase to give at least 5 products whose possible structures are shown in Figure 4: one major product at m/z 230 is at least two isomeric species. High resolution mass spectra have not, as yet, identified the compound. Of the two most likely possibilities, $C_{17}H_{10}O$ and $C_{16}H_8NO$, the high-resolution m/z value favours the nitrogen-containing structure; however, the substitution of ^{15}N for ^{14}N does not increase the m/z value to 231.

Both the starting material m/z 228 and the product m/z 230 add 46($^{14}NO_2$) or 47($^{15}NO_2$) to give peaks at 273/275 or 274/276. However, only the

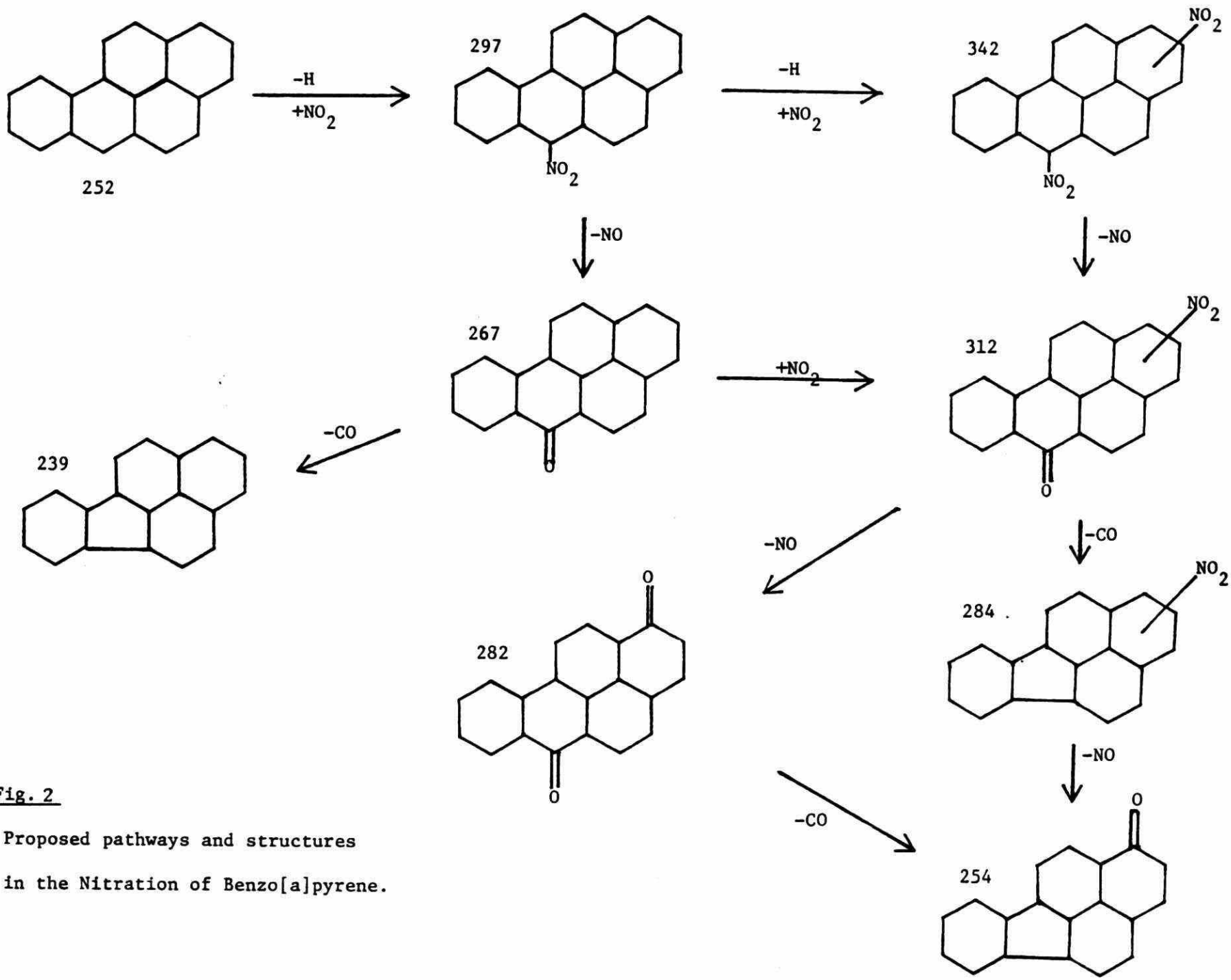
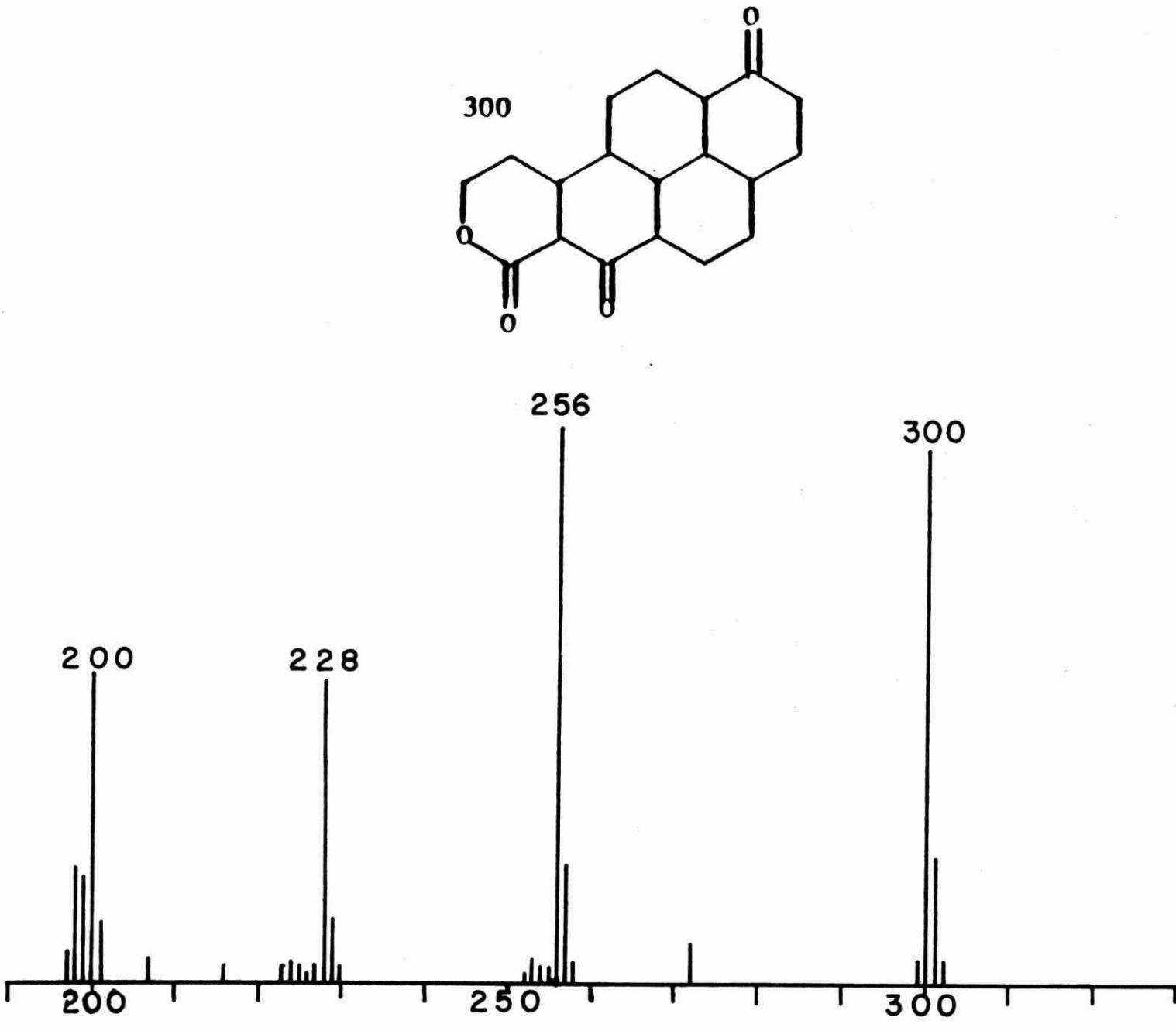


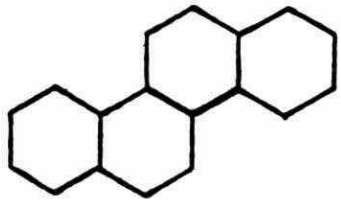
Fig. 2

Proposed pathways and structures in the Nitration of Benzo[a]pyrene.

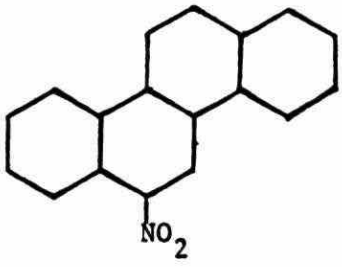
Figure 3

Mass spectrum and possible lactone-quinone structure of nitration product of benzo[a]pyrene.

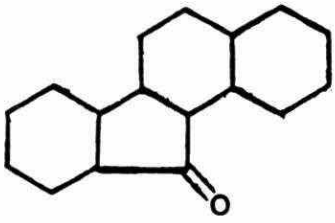




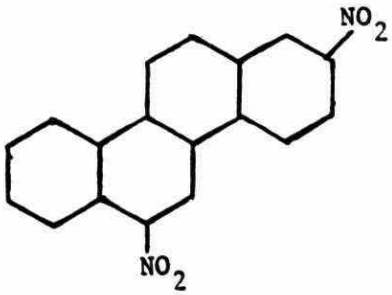
228



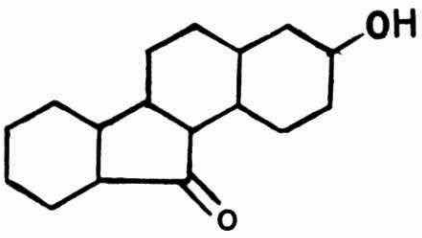
273



230



318



246

Figure 4

$^{m}/_{z}$ values and possible structures of chrysene nitration products

chrysene species at m/z 228 appears to add a second NO_2 group to give peaks at 318($^{14}NO_2$) or 320($^{15}NO_2$). Furthermore, unlike benzo[a]pyrene, these dinitrochrysenes lose 27μ($HC^{14}N$) or 28μ($HC^{15}N$) rather than ^{14}NO or ^{15}NO upon electron impact, as is seen in Figure 5, where the dinitrochrysene at m/z 318 gives rise to a peak at m/z 291 which is larger than the peak at 288 (loss of NO).

A major product of the overnight reaction of chrysene and NO_2 has a molecular ion which occurs at m/z 246. The "best fit" identification of this peak as determined by a library search (EPA/NIH) gives the most probable structure as being octadecahydrochrysene ($C_{18}H_{30}$); however, since there is no source of hydrogen in the reaction vessel, an alternate structure ($C_{17}H_{10}O_2$) has been proposed.

Ion Chemistry of Benzo[a]pyrene and Chrysene

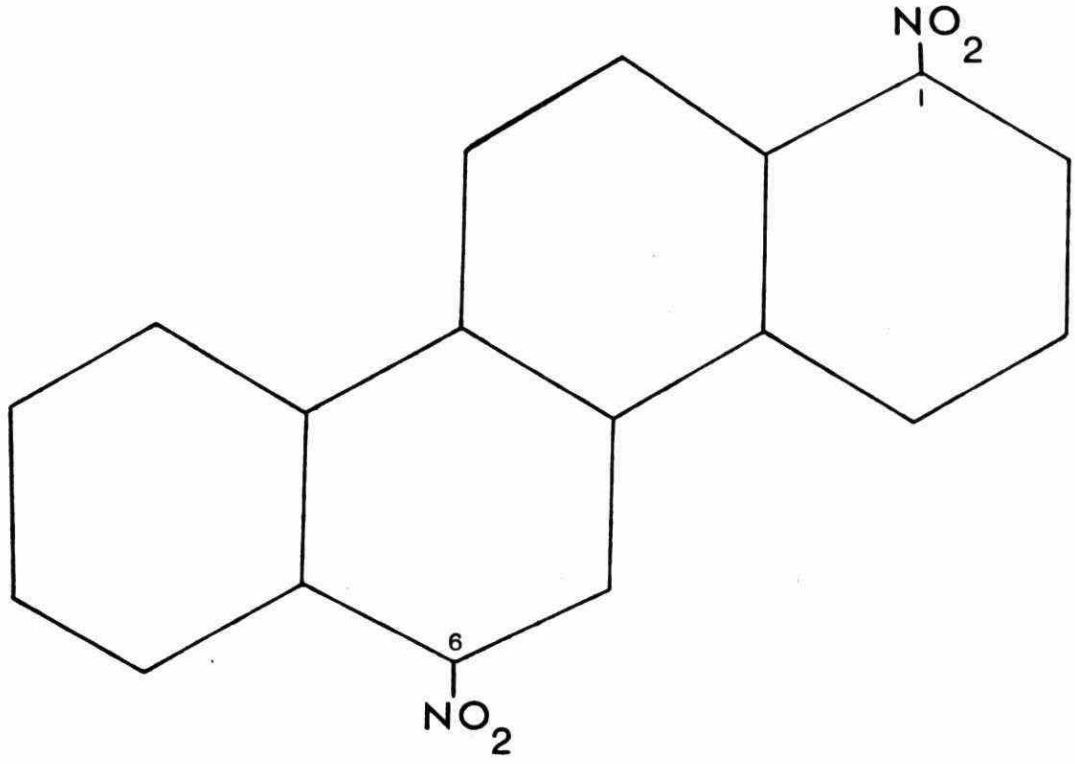
An attempt was made to study the ion/molecule reactions of benzo[a]pyrene and chrysene in the quadrupole ion storage device (QUISTOR) which has been described previously [22, 24 for example].

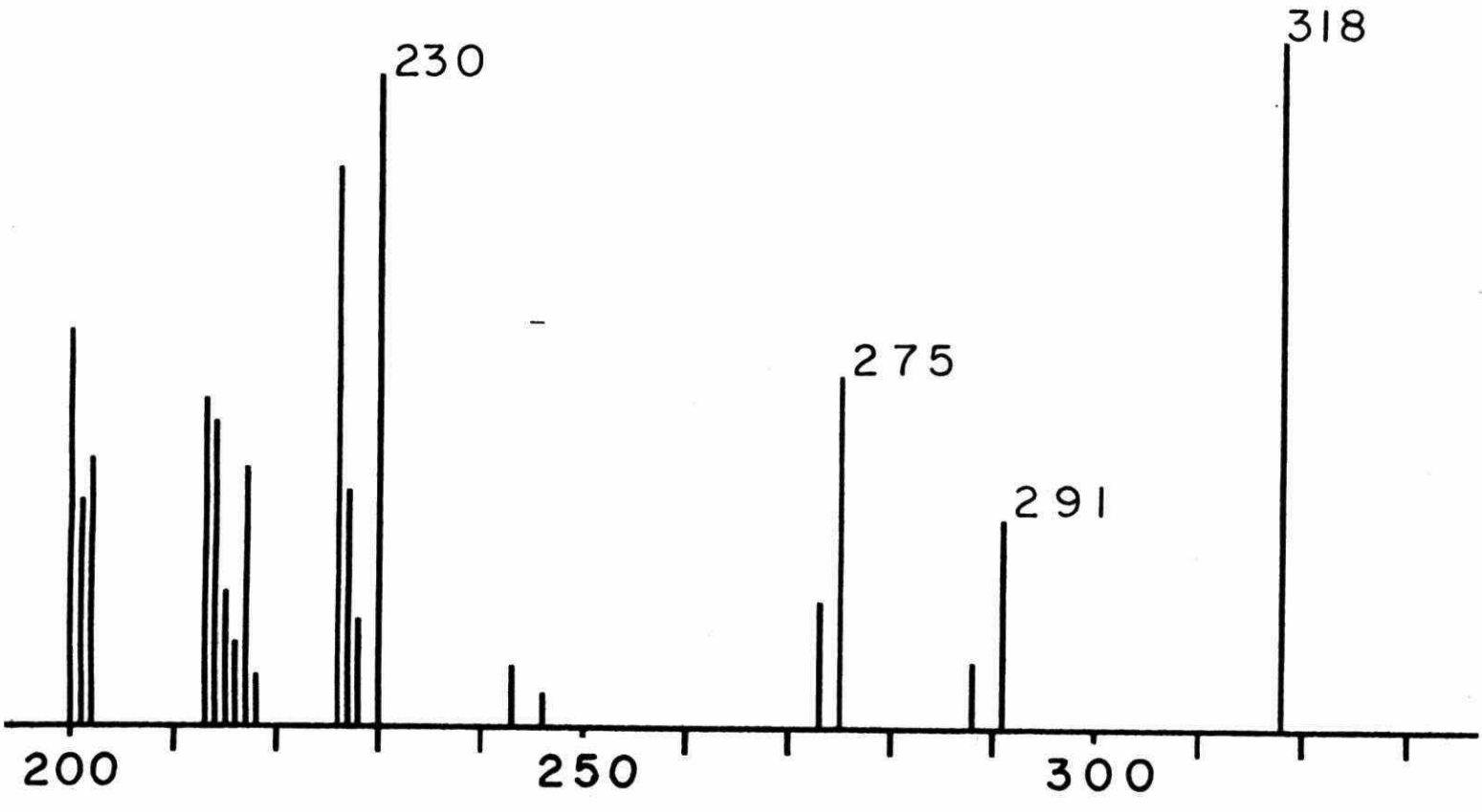
Storage of ions produced by electron impact of the pure compounds benzo[a]-pyrene and chrysene for periods up to 120 ms at pressures up to .5m mPa show very little reaction takes place in these systems. The parent ion accounts for more than 90% of the total ion signal. The smaller peaks are extracted from the background by repeated acquisition using a CYBORG ISAAC 91A digital interface and signal averaging employing an APPLE IIe microcomputer.

Each PAH was subsequently stored in the QUISTOR at about 0.5 mPa and nitrogen dioxide or nitric oxide was admitted to a pressure of 10 mPa. None of the results observed in these systems indicated a significant amount of reactivity of PAH ions under these conditions.

Figure 5

Dinitrochrysene





The lack of reactivity among these PAH ions is understandable on the basis of their aromatic character. The number of rings present in the system delocalize the electronic charge on the ion giving rise to enhanced stability. This stabilization effect is evident in the conventional electron impact spectra which displays an abundance of multiply-charged ions.

Photochemistry and Substrate Material

The extent to which PAH adsorbed on fly ash or other environmental particulate matter are susceptible to photodecomposition is of considerable importance since, if certain PAH have short half-lives in the atmosphere, such compounds cannot serve as reliable air pollution or POM indicators. Also, the ultimate photolysis products of most PAH are carbonyl compounds; these substances, or intermediates in their formation, may be more hazardous than the parent PAH.

The photodecomposition of PAH has been studied extensively by groups such as Katz and Lane [25], Korfmacher et al [26-29], and Grosjean et al [14, 15] to name a few. Generally, photodecomposition tends to occur rapidly on the surface of the adsorbed PAH and then proceed more slowly as the outer layer becomes oxidized. The substrate material has a marked effect on the decomposition: for example, B[a]P alumina underwent 50% decomposition while, by contrast, B[a]P adsorbed onto fly ash underwent only 15% decomposition [27].

Our studies have shown that B[a]P reacts with O_2 at elevated temperatures, without irradiation, and is degraded. Aside from the expected products of carbon dioxide and water, a peak in the mass spectrum at m/z 94 indicated the presence of phenol.

In the presence of ultraviolet light, a peak at m/z 282 indicated that benzopyrene quinones were formed as they were in the oxidation of B[a]P with NO_2. It should be pointed out that our studies employed pure reactants at high concentrations in the gas phase: Grosjean et al [14] have reported a general lack of reactivity of various PAH when present in very low "realistic" concentrations.

Conclusions and Discussion

The study of Polycyclic Aromatic Hydrocarbons has provided much information about the structure and reactivity of these large organic molecules and their ions. Information concerning intercharge separations has been obtained and techniques involving linked scans can be used to differentiate isomeric species [16].

It is obvious that a great deal of chemistry is involved in the nitration of these molecules both on surfaces at ambient temperatures and in the gas phase at elevated temperatures. It is also interesting to note the effect of different starting structures on the ultimate products of reaction with NO_2. With reference to Figure 1, the major difference between the structures of B[a]P and chrysene is the existence of one additional acetylene unit (carbons 4 and 5) in the B[a]P. Since both molecules are nitrated mainly at carbon 6, this difference results in the carbon in the α-position being fused, in B[a]P, to the aromatic ring, whereas in chrysene this carbon is available for reaction. This may explain the production of an apparent 5-membered cyclic ketone (m/z 230) in the case of chrysene indicating the loss of HCNO from the nitrated product (m/z 273): the product from the equivalent 6-nitrobenzo[a]pyrene (m/z 297) appears to be the 6-membered ketone (m/z 267) indicating the loss of NO. Likewise in the e.i. spectra of dinitrochrysene the major loss appears to be HCN as opposed to the loss of NO from nitrobenzo-[a]pyrene.

It is well known that nitro-PAH and PAH ketones, as are formed by ultraviolet irradiation of PAHs in the presence of oxygen, show carcinogenic and mutagenic properties which may be drastically different from the parent hydrocarbon; thus it is important that PAH and their reaction products be

characterized as rapidly and accurately as possible. Commercial glass capillary column gas chromatography/mass spectrometry or GC/MS instruments are becoming more and more widespread in their use for this purpose. Another technique employed successfully in PAH analysis is MS/MS in which one mass spectrometer selects the parent ion of a single PAH from an ionized mixture and the second mass spectrometer analyzes the products of collision of the PAH parent ion with a target gas. The PAH parent may then be identified by its characteristic fragmentation pattern and another PAH parent ion selected and identified.

-REFERENCES-

1. Phillips,D.H. Fifty years of benzo[a]pyrene [Commentary]. Nature; 1983; 303(9 June): 468-72.

2. Zander,M. Physical and Chemical Properties of Polycyclic Aromatic Hydrocarbons. in: Alf Bjoerseth, ed. Handbook of Polycyclic Aromatic Hydrocarbons. New York: Marcel Dekker, Inc.;1983: pp. 1-25.

3. Zedeck,M.S. Polycyclic Aromatic Hydrocarbons:A Review. J. of Environ.Pathol and Toxicol.; 1980; 3:537-67.

4. Brorstroem,E. [and others]. The effect of nitrogen dioxide and ozone on the decomposition of particle-associated PAH during sampling from the atmosphere. Atmos. Environ.; 1983; 17(3): 601-5

5. Broerstrom,E.;Grennfelt,P.;Lindskog,A.;Sjoedin,J.;Nielsen,T. Transformation of Polycyclic Aromatic Hydrocarbons During Sampling in Air by Exposure to Different Oxidized Nitrogen Compounds and Ozone. in: Cooke, M.;Dennis,A.; ed. 7th Int. Symp. Polynuc. Arom. Hydrocarb.,1982. Columbus, Ohio: Battelle Press; 1983: pp 201-210.

6. Broerstrom,E.;Grennfelt,P.;Lindskog,A.;Sjoedin,J.;Nielsen,T. Transformation of Polycyclic Aromatic Hydrocarbons During Sampling in Air by Exposure to Different Oxidized Nitrogen Compounds and Ozone. Tech. Report: Inst. Vatten-Luftvaardsforsch., Goeteborg, Sweden; 1982; IVL B 682; 22 pages; CODEN IVLBDQ.

7. Lindskog,A. Transformation of Polycyclic Aromatic Hydrocarbons During Sampling. EHP, Environ. Health Perspec.; 1983; 47: 81-84.

8. Pitts,J.N. Jr.;Van Cauwenberghe,K.A.;Grosjean,D.;Schmid J.;Fitz,D. Belser,W.;Knudson, G.;Hynds,P. Atmospheric Reactions of Polycyclic Aromatic Hydrocarbons:Facile Formation of Mutagenic Nitro Derivatives. Science; 1978; 202(3 November): 515-519.

9. Pitts,J.N. Jr. Photochemical and biological implications of the atmospheric reactions of amines and benzo[a]pyrene. Phil. Trans. R. Soc. Lond. A; 290; (1979): 551-576.

10. Pitts,J.N. Jr.; Lokensgard,D.M. Photochemical and thermal reactions of combustion-related particulate organic matter: A combined chemical and biological approach. Dept. Energy Res. Contract No. DE-AM03-76FS00034; 1982; Project DE-AT03-79EV0048: 117 pages.

11. Butler,J.D.;Crossley,P. Reactivity of Polycyclic Aromatic Hydrocarbons Adsorbed on Soot Particles. Atmos. Environ.; 1981; 15(1): 91-94.

12. Pitts,J.N. Jr. Reactivity of Polycylic Aromatic Hydrocarbons Adsorbed on Soot Particles: Comments. Atmos. Environ.; 1981; 15(9): 1782-3.

13. Butler,J.D. Reactivity of Polycylic Aromatic Hydrocarbons Adsorbed on Soot Particles: Reply to Comments. Atmos. Environ.; 1981; 15(9): 1783-4.

14. Grosjean,D. The Effect of Nitrogen Dioxide and Ozone on the Decomposition of Particulate-associated Polycylic Aromatic Hydrocarbons During Sampling from the Atmosphere. Atmos. Environ.; 1983; 17(10): 2111-14.

15. Grosjean,D.;Fung,K.;Harrison,J. Interactions of Polycyclic Aromatic Hydrocarbons with Atmospheric Pollutants. Environ. Sci. Tech.; 1983; 17(11): 673-679.

16. Shushan,B.;Boyd,R.K. Unimolecular and Collision Induced Fragmentation of Molecular Ions of Polycyclic Aromatic Hydrocarbons. Org. Mass Spec.; 1980; 15(9): 445-453.

17. March,R.E.;Brenton,G.;Hughes,R.J.;Beynon,J. Charge Separation of Metastable Multiply-charged Ions Derived from Benzo[a]pyrene; (in preparation).

18. Pitts,J.N. Jr. Formation and Fate of Gaseous and Particulate Mutagens and Carcinogens in Real and Simulated Atmospheres. Environ. Health Perspect.; 1983; 47: 115-140.

19. Van Cauwenberghe,K.;Van Vaeck,L.;Pitts,J.N. Jr. Physical and Chemical Transformations of Organic Pollutants During Aerosol Sampling. Proc. Eur. Sym. Phys.-Chem. Behav. Atmos. Poll.; 1979; (pub. 1980): 194-209.

20. Dewar,M.J.S.;Mole,T.;Urch,D.S.;Warford,E.W.T. Electrophilic Substitution. Part IV. The Nitration of Diphenyl, Chrysene, Benzo[a]pyrene, and Anthanthrene. J. Chem. Soc.; 1956; Part III: 3572-75.

21. Dewar,M.J.S. et al. Electrophilic substitution. Part VI. The nitration of aromatic hydrocarbons; Partial rate factors and their interpretation. J. Chem Soc.; 1956; Part III: 3581-6.

22. Hughes,R.J. and March,R.E. A Mass Spectrometric Study of Selected Air Pollutants. Proc. 4th Technology Transfer Conference, Part 2; Toronto, Nov. 29 and 30, 1983; pp 628-643.

23. Nielsen,T. Reactivity of PAH toward nitrating species. Environ. Sci. Tech.; 1984; 18(3): 157-63.

24. Armitage,M.A.,Fulford,J.E.;Hughes,R.J.;March,R.E.;Mather,R.E.;Waldren,R.M.;Todd,J.F.J. Quadrupole Ion Store: Application and Further Characterization in Adv. Mass Spec., Volume 8B, 1983, pp 1754-1763.

25. Lane,D.A.;Katz,M. The photomodification of B[a]P, B[b]fluoranthene, and B[k]fluoranthene under simulated atmospheric conditions. In: I.H.Suffet, Editor. Advances in Environmental Science & Technology; [1980]; volume 8(Part 2-Chemical and Biological Fate of Pollutants in the Environment): pp 137-55.

26. Korfmacher,W.A. [and others]. Nonphotochemical decomposition of fluorene vapor-adsorbed on coal-fly ash. Environ.Sci.Technol.; 1981; 15(11): 1370-5.

27. Korfmacher,W.A. [and others]. Oxidative transformations of PAH adsorbed on coal fly ash. Science; 1980; 207(4432): 763-5.

28. Korfmacher,W.A. [and others]. Resistance to photochemical decomposition of PAH vapor-adsorbed on coal fly ash. Environ.Sci. & Tech.; 1980; 14(9): 1094-9.

29. Korfmacher,W.A. [and others]. Thermal and photochemical decomposition of particulate PAH. in: Jones,P.W.;Leber,P., ed. Polynucl. Aromat. Hydrocarbons, 3rd Int. Symp. Chem. Biol.- Carcinog.Mutagen.; 1978; publ. 1979: 165-70.

Acknowledgements

We thank the Ontario Ministry of the Environment for their support of this work. We also thank Dr. John Krause of the University of Ottawa for providing the GC-high resolution MS of the chrysene compounds.

RETROSPCTIVE CORRELATION SPECTROSCOPY AND ITS APPLICATIONS TO ATMOSPHERIC MONITORING

R.W.NICHOLLS
CENTRE FOR RESEARCH IN EXPERIMENTAL SPACE SCIENCE
YORK UNIVERSITY
4700 Keele St. Downsview, Ontario M3J 1P3

CONTENTS

1: INTRODUCTION
- 1.1: Basic Concepts
- 1.2: Correlation Spectroscopy

2: ANALYSES
- 2.1 Elementary Analyses
- 2.2 More Realistic Analyses
  - 2.2.1 Wavelength Dependence of I_o
  - 2.2.2 Features of unequal strength, unequal half width and unequal spacing
  - 2.2.3 Absorption cross sections represented by other than Gaussian Combs and Masks represented by other than Heaviside Combs
- 2.3 Band Models

3: EXPERIMENTAL STUDIES

4: NON-DISPERSIVE GAS FILTER CORRELATION SPECTROSCOPY USING THE GASCOFIL INSTRUMENT
- 4.1 The GASCOFIL Instrument
- 4.2 Field Measurements with GASCOFIL

5: SUMMARY, CONCLUSIONS AND RECOMMENDATIONS
- 5.1 Summary
- 5.2 Conclusions
- 5.3 Recommendations

REFERENCES

ACKNOWLEDGEMENTS

FIGURES

ABSTRACT

RETROSPECTIVE CORRELATION SPECTROSCOPY AND ITS APPLICATIONS TO ATMOSPHERIC MONITORING.

R.W.NICHOLLS
Centre for Research in Experimental Space Science
York University.

For environmental applications Retrospective Correlation Spectroscopy(RCS) uses the properties of the correlogram of a field spectrum, and a mask function (which represents the pollutant absorption features in the field spectrum) in a diagnostic fashion to infer concentrations and column densities of pollutants.

The work of the past year started with a numerical assessment of correlograms of the infrared spectrum of CO. This showed at once that it was essential to develop an detailed understanding of how the correlogram depends upon the characteristics of the field spectrum and of the mask.

Thus much effort has been devoted during the year to analytical and numerical studies of the properties of correlograms for model spectra and various masks. The model studies are applicable to the sulphur dioxide UV absorption spectrum.

The algebraic form for the correlation function which was developed in this work suggests a direct method for determination of column densities of pollutants.

Experiments are in progress to test this method and are discussed.

1: INTRODUCTION

Correlation spectroscopy, is a powerful diagnostic tool for the determination and monitoring of trace atmospheric contaminants. It involves the quantitative correlative comparision between the features of a field spectrum (often absorption of daylight by contaminant plumes) of the atmospheric region of interest and the features of a "mask" function which is representative of the spectral absorption features of the molecular contaminant species on which diagnoses are to be performed. The degree of correlation between the spectral "finger prints" of the field spectrum, and those of the contaminant spectrum embodied in the mask function is interpreted quantitatively to provide information of concentrations of contaminant species in the atmospheric field of view.

The method was first proposed in 1964 (Barringer et al., 1964,a,b; Bottema et al., 1964a,b; Nicholls 1983 (in which full references are given)),and since then has been extensively used in environmental monitoring. Barringer Research Ltd of Rexdale Ontario has been the pioneer of Correlation Spectroscopy and in the development of its instrumentation. Two principal instrumental approaches have evolved viz: a) correlation spectroscopy of dispersed spectra and b) correlation spectroscopy of non-dispersed spectra.

In the first method, the field spectrum is dispersed along a focal surface at which an analogue mask of alternate transparent and opaque slits, characteristic of the spectral features of the contaminant species is located. The mask is oscillated mechanically in the direction of dispersion, and the signal which is passed through the mask is focussed on a photoelectric detector. The correlation between the field spectrum and the mask function is determined through phase sensitive detection (with respect to the mask oscillation) of the signal detected by the photoelectric detector. After suitable calibration, the correlation signal is interpreted as a quantitative measure of the concentration of contaminant molecules in the light path.

In the second (non-dispersive) method (Ward and Zwick, 1975), the field spectrum is passed through cells containing varying column densities of the contaminant gas, whose absorption spectrum is effectively its own correlation mask. After calibration, a comparison between the signals paasing through the different optical paths can be interpreted in terms of the number density of contaminant molecules in the optical path in front of the instrument.

In both of these instrumental approaches, ANALOGUE concepts have been used in mask design and motion, and in electonic detection. In particular a different analogue mask is needed for each contaminant species to be sensed.

In this paper an examination is made of the potential improvements that can be achieved both in dispersive and in non-disperive correlation spectroscopy through the use of DIGITAL concepts in data reduction and in instrumental design. In the following sections we describe

a) an analytical and experimental investigation of the potential advantages of digital (numerical) mask functions which are used retrospectivly to test databases of digital field spectra for the presence of contaminant species. Instrumentally it is now relatively routine to record field spectra by digital rather than by analogue means to avoid drift and noise problems, and to exploit the advantages of current technology. It is much easier to construct numerical masks characteristic of contaminant spectra of each species than to fabricate analogue masks for each species.

b) the design, construction, and field tests on non-dispersive correlation spectrometers which are run entirely by digital, computer controlled systems.

1.1: Basic Concepts

It is well known that the extinction of a radiation flux $I_o(L)$ in a length x of absorbing medium, can in many cases be written in the Beer's law formulation:

$$I(L) = I_o(L) \exp(-k(L)\, x) \qquad (1a)$$

where L is the wavelength. The phemomenological linear absorption coefficient k(L) can be written variously as:

$$k(L) = N\, \sigma(L) = T(L) / x = 1/ X(L) \qquad (1b)$$

Here, N is the number density of absorbers, $\sigma(L)$ is the absorption cross section per absorber, T(L) is the so-called optical depth, and X(L) is the photon mean free path in its transport through the medium.

When T is somewhat less than unity, equation (1a) can be represented to a high degree of accuracy by the first degree expansion:

$$I(L) = I_o\, (\, 1 - Nx\, \sigma(L)) \qquad (1c)$$

Nx is called the column density of the absorber. In laboratory, atmospheric and astrophysical diagnostic applications of traditional absorption spectroscopy,

equation (1c) is used in various ways to estimate the column density Nx of absorbers from measurements of I/I_o, and literature information on o(L),when available.

In one such application, integration of equation (1c) over the wavelength range of a spectral feature leads to the concept of "equivalent width",$\underline{W}$ through:

$$\int (I_o - I)\, dL = \underline{W} = NX \int \sigma(L)\, dL = \pi e^2\, NX\, f/mc \qquad (1d)$$

where f is the so-called oscillator strength of the feature, e and m are the electron charge and mass, and c is the speed of light

This sort of direct application of equation (1c) presents many practical problems when applied to measurement of low concentration levels of absorbers which imply small equivalent widths and is prone to large errors. It is for just such cases that correlation spectroscopy becomes a powerful tool.

1.2 : Correlation Spectroscopy

The correlation between a field spectrum I(L) detected by a spectrometer and a mask function M(L) displaced by z relative to the field spectrm is:

$$C(z) = \int I(L)\, M(L-z)\, dL \qquad (2a)$$

C(z) is often called the correlogram.

If I(L) is derived from a background daylight spectrum, it contains information on absorption by the contaminant as well as information on the background spectrum of daylight. If I(L) is derived from a laboratory continuum light source, the absorption information which it contains relates solely to the absorption species in the optical path. Equations (1c) and (2a) lead to:

$$C(z) = \int I_o(L)\, (1 - Nx\, \sigma(L))\, M(L-z)\, dL \qquad (2b)$$

In many observational circumstances when $I_o(L)$ is not strongly dependent upon L over the range of integration of L where M(L-z) is non zero, it can be written as the constant I_o. A good approximation to equation (2b) is then

$$C(z) / I_o = \int M(L-z)\, dL - Nx \int \sigma(L)\, M(L-z)\, dL$$

$$= T_1 - Nx\, T_2(z) \qquad (2c)$$

where $T_1 = \int M(L-z)\, dL$ = total mask area = A (2d)

and $T_2(z) = \int \sigma(L)\, M(L-z)\, dL$ (2e)

Thus the correlation equation (2b) is of the general form:

$$C(z) = I_o A - Nx I_o T_2(z) \qquad (2f)$$

Equation (2f) suggests an immediate diagnostic method for the direct determination of the column density Nx of contaminant species without the need for an intermediate calibration.

If the I(L) function is an observational digital data stream, and M(L-z) is a suitably chosen mask function which can also be expressed digitally, then the correlogram function C(z), can be evaluated digitally as a function of z. z is the relative displacement (or lack of registration) between the mask function M(L-z) and the field spectrum function I(L). The mask area A is directly evaluated from knowledge of M(L-z). $T_2(z)$ is also directly evaluated if information on the cross section function $\sigma(L)$ is available from the literature of spectroscopy and/or photochemistry.

It is then clear from equation (2f) that a plot of C(z) vs $T_2(z)$ will be linear, with an intercept on the C(z) axis of $I_o A$. As A is known, I_o can be inferred directly from the intercept. The slope of the plot will be $I_o Nx$ from which the column density is at once determined.

This direct diagnostic application of the correlation equations (2a) and (2f) appears to be a new idea and, as described below, it is currently being followed up from theoretical and from experimental points of view. (Nicholls, 1985) If the simplifying assumption that I_o is quasi-constant be relaxed, and simple, realistic functional forms (linear, exponential, polynomial etc) be adopted for its variation with wavelength over the wavelength segment of importance, the integrals for T_1 and T_2 are somewhat less simple, but the same sort of plot will lead to a direct determination of Nx.

In order to apply this method with confidence to "real world" cases it is first necessary to develop optimum simple forms for the mask functions M(L-z), best suited to the low, medium and high resolution field spectra from various instruments. It is also necessary to establish reasonable forms for $\sigma(L)$ which while based on photochemical data, are straightforward to use, so that changing from one numerical mask to another is a simple procedure. Finally the sensititivity of $T_2(z)$ to the choice of M(L-z) and $\sigma(L)$ also needs to be understood.

In a previous investigation (Cann and Nicholls,1982), a

digital study was made of the shape of the correlogram for a variety of molecular cases. This work showed how sensitive C(z) was to the exact spectrum concerned. It was clear from this work how essential it is to understand the sensitivity of $T_2(z)$ to the spectrum and the mask in general terms, before starting to apply digital correlation spectroscopy to specific spectral features such as the low resolution UV bands of SO_2, the medium resolution visible and red features of I_2, or the high resolution infrared features of CO, all of which have been addressed in the current study.

Thus after the general formulation of the retrospective correlation method summarized by equation (2f), the next task, described below, is to make a model analytical study of the form and systematics of the convolution function $T_2(z)$, and its dependence upon the forms of M(L-x) and $\sigma(L)$ which are adopted This work is outlined in section 2 below. In section 3 a brief description is made of the related experimental and observation work in support of this model study. Finally in section 4 an overview is presented of our instrumental and field studies using non-dispersive correlation instruments.

2:ANALYSES

In this section we outline the model studies on $T_2(z)$

2.1: Elementary Analyses

Low and medium resolution absorption spectra of molecular species of importance in atmospheric contamination problems often exhibit over a limited wavelength range a series of separated, similarly shaped features. The well known SO_2 UV absorption bands and the I_2 visible absorption bands are typical examples of such spectra. Inspection of such band profiles suggests that each spectral feature could be well represented by a simple Gaussian function. Thus the absorption cross section of a number p of adjacent features, which might be adopted as a "finger print" for simulation by a correlation mask function M(L), can be well represented analytically by the Gaussian comb. That is:

$$\sigma(L) = \sum_{n=1}^{p} a_n \exp(-b_n^2 (L-L_n)^2) \qquad (3a)^*$$

Here, a_n is the strength of the n'th feature which has a half-width $W_n = 1/b_n$. In point of fact, the line half-width at ordinate y is $(1/b_n)(-\ln y)/2$. We thus arbitrarily adopt y= 0.3678 in order to identify the half width W with $1/b_n$. L_n is the location of the line centre of the n'th feature. It is then convenient to recast equation (3a) as:

* In the p-term summation of equation 3a, and in other equations of this paper, E is to be read as the capital Greek sigma summation operator.

$$\sigma(L) = \sum_{n=1}^{p} a_n \exp\left(-(L-L_n)/W_n\right)^2 \qquad (3b)$$

Equation (3b) will be equally useful to represent p rotational lines of a band at high resolution as to represent p unresolved bands.

In selecting an appropriate mask function, equation (3b) suggests that it could also be used for M(L). This possibility should not be overlooked. In the entirely numerical study by Cann and Nicholls (1982) this approach was in fact used. For a model study however an algebraically uncomplicated form of $T_2(z)$ is to be preferred. As shown in section 2.2, adoption of equation (3b) for M(L) leads to a rather cumbersome algebraic form for $T_2(x)$.

To simulate the experimental situation of alternating transparent and opaque slits, the Heaviside comb:

$$M(L) = \sum_{m=1}^{p} A_m\left(H(L-(L_m-W_m) - H(L-(L_m+W_m))\right) \qquad 3c)$$

is preferred and adopted. Here, H is the Heaviside unit step function and L_m is the line centre of the m'th feature of half-width W_m

If equations (3b) and (3c) be adopted it is easy to show that T_1 , the mask area of equations (2c and 2d) is:

$$T_1 = \sum_{m=1}^{p} 2A_m W_m \qquad (3d)$$

and $T_2(z)$ of equations (2e and 2f) is:

$$T_2(z) = \sum_{n=1}^{p} \sum_{m=1}^{p} a_n A_m I_{nm} \qquad (3e)$$

where:

$$I_{nm} = \int_0^{\infty} \exp(-((L-L_n)/W_n)^2)(H(L-(L_m+z-W_m))-H(L-(L_m+z+W_m)))dL \qquad (3f)$$

or

$$I_{nm} = \int_{L_m+z-W_m}^{L_m+z+W_m} \exp(-(L-L_n)/W_n)^2)\ dL \qquad (3g)$$

Thus $I_{nm} = (\pi^{1/2} W_m/2)\ (\mathrm{erf}(M_{mn}) - \mathrm{erf}(N_{mn}))$ (3h)

where $M_{mn} = (L_m - L_n + z + W_m)/W_n$ (3i)

and $N_{mn} = (L_m - L_n + z - W_m)/W_n$ (3j)

erf(X) is the error function and it is odd. That is erf(-X) = - erf(X). This property is used in equation (31) below.

In order to make analytic progress in this simple model study it is convenient to make some further reasonable approximations at this point. The first is to assume that all of the feature half widths W_n, and mask half widths W_m are equal to W. The second is that the features are equally spaced, and thus that the mask elements are also equally spaced. For the SO_2 and I_2 spectra, this is not too unrealistic.

That is $F = |L_{n+1} - L_n| = |L_{m+1} - L_m|$ (3k)

The equations can now be cast in non-dimensionalised form with respect to the half-width W. The non-dimensionalisd inter- feature distance is D=F/W. The non-dimensionalized distance between the mask feature m and the spectral feature n is $t_{mn}D = T = |(L_m - L_n)|/W$. The non-dimensionalised mask displacement from zero register is Y = z/W. In terms of these non-dimensionalised variables we can recast equation (3h) as

$$I_{mn} = (\pi^{1/2} W/2)\ (\mathrm{erf}(1 \pm Y \pm T) + \mathrm{erf}(1 \mp Y \mp T)) \qquad (3l)$$

For the purposes of this model calculation we now make the further simplifying assumption that all of the a_n's and A_m's are equal to, say B. Examination of some characteristic spectra (of say SO_2 and I_2) show that this is not too crude an approximation to reveal the general behaviour of $T_2(z)$ under conditions which are not too diferent from those exhibited by actual molecules. The symmetries of the derivation which follows can be somewhat relaxed by actual spectra, the correlograms of which retain the same general forms as those predicted below.

Equation (3e) is then

$$T_2(Y) = B^2 \sum_{n=1}^{p} \sum_{m=1}^{p} I_{nm} \qquad (3m)$$

The summation of I_{mn} over the square array of m and n can conveniently be made over the diagonals m-n= t. That is:

$$T_2(Y) = B^2 \left(\sum_{n=1}^{p} \sum_{m=n+1} (I_{nm}+I_{mn}) + \sum_{n=1}^{p} I_{nn} \right) \qquad (3n)$$

or

$$T_2(Y) = B^2 \left(\sum_{t=1}^{p-1} (p-t)\,(I_{nm}+I_{mn}) + \sum_{n=1}^{p} I_{nn} \right) \qquad (3o)$$

Here t is the diagonal number. There are (p-t) terms on the p'th diagonal. The second summation is over the p terms on the prime diagonal.

For the summations of equation (3o) it is convenient to write from equation (31)

$$I_{nm}+I_{mn}=(W\overline{II}^{1/2}/2)x \\ (erf(1+T+Y)+erf(1+T-Y)+erf(1-T+Y)+erf(1-T-Y)) \qquad (3p)$$

and thus:

$$T_2(Y) = (pB^2W\overline{II}^{1/2}/2)\,(erf(1+Y) + erf(1-Y) + \\ + \sum_{t=1}^{p-1} E((p-t)/p)(erf(1+T+Y)+erf(1+T-Y)+erf(1-T+Y)+erf(1-T-Y))) \qquad (3q)$$

But from equation (2c)

$$C(Y)/I_o\,A = 1 - Nx\,T_2(Y)/A \qquad (3r)$$

where A = mask area = T_1 = p 2W B for a p-element mask, each element of which has an area of 2WB.

Equations (3q) and (3r) therefore lead to:

$$C(Y) / I_o\,A = 1 - Nx\,B((II)^{1/2}/4)\,E(Y) \qquad (3s)^*$$

---

* E(Y) in equation (3s) and on the left hand side of equation (3t) overleaf is the convolution between the absorption cross section and mask functions. The E on the right hand side of equation (3t) is the summation symbol, capital Greek sigma. See footnote on page 6

where the convolvution E(Y), which, apart from a factor is the same as $T_2(Y)$, is

$$E(Y) = (\mathrm{erf}(1+Y) + \mathrm{erf}(1-Y) + \sum_{t=1}^{p-1} E((p-t)/p)(\mathrm{erf}(1+T+Y)+\mathrm{erf}(1+T-Y)+\mathrm{erf}(1-T+Y)+\mathrm{erf}(1-T-Y)) \quad (3t)$$

Equations (3s) and (3t) represent a specific form of equation (2f). The way in which E(Y) depends upon mask and spectral paramters is directly calculable from equation (3t) which is easy to programme for various cases using the rational function approximation for erf(X). Correlograms of real spectral features (eg of SO_2, NO_2, I_2 etc) are thus easily simulated in non- dimensionalized form by use of equation (3t) to the level of the approximations used.

Figure (1) illustrates the form of E(Y) for a specific choice of input parameters. For a spectrum, and associated mask, each with p features E(Y) will have 2p-1 maxima and 2p minima. These 4p-1 points are probably the best ones to use in the plots of C(Y) vs E(Y).

It is clear that E(Y) has a maximum at Y=0 which corresponds to complete registration between the mask and the spectrum. It is also clear that C(Y) has a minimum at the same place. Indeed all maxima of C(Y) are minima of E(Y)

When Y=0, the prime diagonal terms only are taken into account in the summations of equation (3t) and:

$$E(0) = 2\ \mathrm{erf}(1) = 1.67 \quad (3u)$$

$$\text{Thus } C(0) = I_o\ A - 0.42\ Nx\ I_o\ AB\ (\pi)^{1/2} \quad (3v)$$

from which Nx can in principle also be determined. However it is probably most reliably determined from the slope of the plot of C(Y) vs E(Y) for the plot uses more data points from the correlogram.

In a practical application (see section 3 below) C(Y) can be calculated digitally from I(L) and M(L-z), and E(Y) can be evaluated (digitally) from equation (3t). For such spectra as SO_2 and I_2 the approximations of the method, listed below, are not expected to introduce a great error in this application of the simple analysis.

The simple analyses of this section from which much physial insight can be gained on the nature of the correlograms, can be applied to real spectral features which conform fairly well to the the simplifying assumptions used

in the derivation. They are

i) I_o is a constant
ii) All features are of equal strength B
iii) The features and all of equal half- width W
iv) The features are equally spaced
v) The absorption cross sections of individual features are well represented by a Gaussian comb.
vi) The correlation mask is best represented by a Heaviside comb

While some of these assumptions may in the first instance appear to be gross oversimplifications of real world spectra, a little reflection and comparision with selected spectral features of important contaminant molecules confirms their applicability to a number of practical cases. In addition this analysis provides a great deal of general insight into the correlograms and their diagnostic use in practical applications of correlation spectroscopy to atmospheric diagnosis.

2.2 More realistic analyses

Naturally some spectral features cannot be well simulated by a model which incorporates the above simplifying approximations. Thus an investigation is being made of the effects of relaxing these assumptions. A brief narrative account of the results of this work is given here. In the interests of brevity the cumbersome algebraic forms encountered are not reported in detail.

2.2.1: Wavelength dependence of I_o

Three cases are being examined. They are:

a) The general linear variation:

$$I_o(L) = a + b(L) \qquad (3a)$$

b) The general exponential variation

$$I_o(L) = a \exp(bL) \qquad (3b)$$

In each of these equations, a and b can be of either sign

c) The general Planckian variation which has some application to the spectrum of daylight

$$I_o(L) = a\, L^{-5}\, (\exp(b/L)-1)^{-1} \qquad (3c)$$

The somewhat cumbersome algebraic implications of each of these to the equations for C(Y) and E(Y) are being investigated with a view to practical applications for which

specific values of a and b have to be assigned in each case.

2.2.2: Features of unequal strength, unequal half width and unequal spacing

The implications of these assumptions to equations (3e)and (3f) are under investigation. In principle these equations can be numerically and digitally evaluated for each specific case of interest, and the diagnostic use of the plots of equation (2f) is unchanged.

2.2.3:Absorption cross sections represented by other than Gaussian Combs, and Mask represented by other than Heaviside Combs

Investigations are in process of the assumptions:

a) Both the absorption cross section and the mask are indentical gaussian combs.

b) Both the absorption cross section and the mask function are identical Heaviside combs.

c) Absorption cross sections are linear and the mask is a Heaviside comb.

The cumbersome algebraic structures for each of these cases are easy to programme for comparison, when needed, with actual spectra.

2.3 Band Models

A preliminary survey has been made of the applicability of the theory of Band Models of spectral profiles to the form of for $\sigma(L)$

3:EXPERIMENTAL STUDIES

For the past decade we have been building a data base of digitally recorded solar irradiance spectra (spectrum of daylight) from the CRESS Atmospheric Observatory on the main York University Campus. These spectra have been used to infer number densities of NO_2 and number densities and particle sizes of urban aerosols in the optical observation path of the instrument.

It was therefore thought that the spectral data base, and other observations especially made for the purpose could be used to test, and then to use the diagnostic plots of equation (2f) which were propsed in the introduction.

Some time was therefore spent in a "quick look" examination of the data to hand to see if any of it was suitable for SO_2 studies using the UV spectral features in the L= 300nm region. As the cumulative observations of the data base had not been made with this specific application in mind, and the viewing paths had not been optimised for

SO_2 observations, no data appeared to be specifically applicable. However our digital spectrometer system is very applicable to this problem. It should be noted that the SO_2 bands in question are being absorbed against an $I_0(L)$ which rises very rapidly with wavelength from very small values near the ozone cut off.

Some laboratory trials of the graphical method on the SO_2 spectrum have therefore been started using controlled column densities of SO_2, and the digital scanning spectrometer system. This work is still in progress.

The I_2 molecule has an absorption band system in the visible and near infrared which also exhibits a well known set of quasi equally spaced, equal intensity, equal width bands. An experimental system is thus under construction to produce a controlled numnber density and optical depth of I_2 vapour for a similar assessment of the graphical method.

Relevant model calculations of E(Y) for both of these band systems are in progress.

4: NON-DISPERSIVE GAS FILTER CORRELATION SPECTROSCOPY USING THE GASCOFIL INSTRUMENT

Over the past three years two digital non-dispersive correlation spectrometers (GASCOFIL AND GASCOSCAN) have been developed. The work, which is continuing, was supported by an NSERC Strategic Grant which terminated earlier this year. (Nicholls and Morrow 1984). As the instrumental development and preliminary field tests of these instruments are within the scope of the title of this paper, they will be briefly reported upon here, in the spirit of Technology Transfer.

The first task of this project was to convert an analogue multi-channel Barringer GASPEC (Ward and Zwick,1975) gas filter correlation spectrometer (which had been built under contract as a balloon-borne instrument for long path IR remote sensing of stratospheric contaminants in the Atmospheric Environment Service Project Stratprobe) into a single channel tropospheric remote sening instrument. This was done with a large (sixteen times) increase in sensitivity. Laboratory tests showed that 9.2 parts per trillion of NO could be detected over a 10km NO path length. This is 0.092ppm metre. (Morrow and Nicholls 1985)

It was clear from this work, that with the advent of digital opto-electronic technology since GASPEC had been developed nearly a decade ago, it would now be challenging to attempt to develop new Gas Filter Correlation Instruments whose electronics, control, and data processing were entirely digital.

Two instruments, GASCOFIL and GASCOSCAN have evolved from this work. The smaller, hand held gas filter correlation instrument, GASCOFIL, and its supporting system have been designed as a rugged field instrument, built and field tested. This instrument and its performance is reported on below.

The larger, spectral scanning multipurpose instrument GASCOSCAN is still in the last stages of development, and will not be reported on further here.

4.1 The GASCOFIL Instrument

GASCOFIL is small rugged hand held computer-controlled instrument which can easily be mounted in an upward viewing mode by clamping it to the window of an automobile used to make a field survey. The sensor head weighs only 2kg. It is designed to measure the column density of specific moleclar atmospheric contaminants, using the IR, visible or UV regions of the spectrum between 0.3 to 9.5 microns depending upon filters and detectors used.

Figure 2 is an optical diagram in which the components of the instrument are identified. After passing through a protecting quartz window the almost parallel field radiation is collected by a Cassegrain telescope system of primary and secondary mirrors. A small hole in the secondary mirror holds the calibration lamp. The parallel incident radiation is collected by the primary mirror, focused onto the secondary mirror which once again renders it parallel, and of smaller cross section. The radiation passes through a central aperture in the primary mirror onto the gas-cell holder and chopper wheel which is rotated under computer control by a motor. The chopper wheel can hold four gas cell filters. The normal arrangement is to place a blank cell in one holder, no cell (clear) in another and two gas cells in the other two. As explained below, a differencing signal processing system is used

After passing through the filter wheel chopper the light passes through an interferemnce filter, selected to define the principal spectral pass band of the instrument. It is the wavelength range of the spectral feature(s) of interest. The chopped radiation beam is then detected by a photomultiplier or solid state detector.

Primary calibration is carried out by use of a full aperture absorption cell containing a known sample of the target gas placed in front of the telescope. Secondary calibration is carried out continuously by differencing signals from the beam passing through each of the filter

locations. Radiometric calibrations are carried out by measuring the signals from a quartz-iodine lamp mounted in the centre of the secondary mirror.

Figure 3 illustrates the signal handling logic circuits controlled by an Apple II+ computer. Signals from the sensor are amplified by a low noise pre-amplifier and digitized by an Interactive Structures 12 bit high speed analogue to digital converter. Data acquisition is synchronized with the rotation of the gas cell by interrupt signals derived from optical pick-offs on the chopper rim. About 4000 12 bit A/D conversions per second are accumulated in 8 software registers. In contrast to analogue signal processing procedures used in other correlation spectrometers, this digital method allows for signal extraction at each of the 8 sectors seen in one rotation of the chopper. The instrument can thus make concurrent radiometric and correlation measurements. A large number of dedicated software packages have been written to enable the compter to be used as a telemetry system, an oscilloscope, a motor speed controller, a timer process controller, a phase sensitive detector, and least squares data processing and graphical data display.

The recorded signals are differences between the accumulated signals from the sectors. Radiometric signals arise from the difference between clear cell and the blank sector signals. This subtraction of a blank sector compensates for offsets from detector dark current and amplifier properties. Correlations signals arise from differences between clear cell and gas cell signals.

In simple terms the radiometric signal can be written as:

$$RS = awf \int_{Dv} N(v)\ T(v)\ T_c(v)\ dv \qquad (4a)$$

and the correlation signal can be written as:

$$CS = awf \int_{Dv} N(v)\ T(v)\ (T_g(v)-T_c(v))\,dv \qquad (4b)$$

where:
a= aperture of the instrument
w= solid angle
f= electro-optical conversion factor
v= frequency
Dv= bandpass
N(v) = background radiance (watts cm^{-2} sr^{-1}/cm^{-1})
T(v) = spectral transmission of the gas cloud
$T_c(v)$= spectral transmission of the clear cell

and $T_g(v)$= spectral tansmission of the gas cell

With four cell positions in the chopper wheel, the instrument can sense concurrently two species. When sensing only one species two cells are be used for it alone.

4.2: Field Measurements with GASCOFIL

Mobile field tests of a battery operated version of GASCOFIL have been made using the Ontario Hydro Lakeview thermal generating station as a known source of SO_2. Typical distances travelled during such tests are 280km. between Alliston Ont, York University, Lakeview Hydroelectric station and Georgetown Ont and return.

The GASCOLFIL sensor head was clamp-mounted in a vertical viewing configuration on the window of the vehicle, The field of view had a 0.5 degree semi angle. The gas-cell chopper was fitted with two SO_2 cells containing 600 and 1200 ppm of SO_2 repectively. The spectral bandpass of the instrument was determined by the interference filter to be between 295 and 305nm. This includes the stronger of the UV SO_2 bands. The microcomputer, the digital to analogue interface, the monitor and disc drive were mounted inside the vehicle near to the driver and operator. The sensor head communicated with the control electronics through a 2m cable.

Data acquired during the test were stored on a diskette file, although in principle, with software now available they could also be reduced as they are recorded. Primary calibration was carried out before the survey started using the full aperture gas cell in front of the instrument. For the secondary calibrations, the detector viewed the zenith sky under conditions which ranged from clear to 100% cloud cover.

The field survey reported here was divided into three parts In the first part, which covered the trip from Alliston to York University in NW Metro Toronto, correlation data acquisition was achieved under conditions of low atmospheric SO_2 concentrations. The second part was carried out with the very much valued assistance of the operations staff of the Lakeview generating station. It involved mapping and diagnosis of the plumes from the station on service roads north of the station sites and at successively further distances from the station. In this phase fourteen scans were made under the plume from the station site itself and at various locations between the station and Georgetown Ont. It should be emphasised in consideration of the results from this part of the work that the plumes had been sufficiently well treated in the stacks before emission into

the atmosphere that they were INVISIBLE TO THE NAKED EYE. The plume tracking observations, based solely on remote sensing by GASCOFIL of the SO_2 from their residual emissions, correlated very well indeed with the data provided by Ontario Hydro. One stack was inoperative and three were emitting.(see figure 4) The third part of the survey was made between Georgetown and York University and from York University to Alliston. During this part of the survey, which included the region of Pearson International Airport, a large plume of uncertain origin near the airport was detected.

This field test involved continuous operation of GASCOFIL from 0755est to 1553 est under sky conditions which varied from 90% clear to 80% cloud cover (cirro stratus). Winds were from the SE between 195 and 270 degrees.

Some of the results of the field test are illustrated in Figures 4 and 5. Figure 4 shows the near field radiometer channel scan by GASCOFIL across the three Lakeview plumes which were operating at about noon. It is seen that the sensor data is strongly correlated with the output from each stack. Several runs were also made between 1300 and 1400 edt for which Ontario Hydro supplied wind direction and speed. The total SO_2 flux F could then be obtained from our data by the equation

$$F = \int_{x_2}^{x_1} W(x)\, O(x) \cos(a)\, dx \qquad (4c)$$

where F = SO_2 flux in tonnes per hour
W(x) = average windspeed in vertical column (m/hr)
O(x) = Overburden of SO_2 above GASCOFIL (tonnes/m^2)
a = Angle of survey path to plume axis
x_1 and x_2 are start and finish points of survey

Using this approach we estimated an output of 6.57 tonnes per hour of SO_2. Ontario Hydro's estimate of SO_2 flux ,kindly provided to us, was derived from thermochemical calculations of coal consumption. It was 6.95 tonnes per hour. We are naturally skeptical about the use of three significant figures in either calculation!. Nevertheless we are encouraged in the agreement between the two estimates of 6.6 and 7.0 tonnes per hour

Figure 5 illustrates the dispersion of structure in the Lakeview plume at distances between 3.5 and 21.5 km from the source. A number of diagnostic inferences could be drawn from these data if we had access to wind field information at the time of the observations.

The signal to noise performance of the instrument was excellent. It operated very reliably in a very vibration prone environment (bumpy roads and speeds between 40 and 90 km/hr). In the first segment of the test the sky brightness in the sensor bandpass varied over a factor of 6. The correlation algorithm in the signal processing system had no difficulaty in handling this dynamic range.

The observations recorded near the airport revealed the presence of a large plume of unknown origin.

5: SUMMARY, CONCLUSIONS AND RECOMMENDATIONS

5.1 Summary

In this paper a number of instrumental developments, field observations, experimental and theoretical studies in the broad field of correlation spectroscopy and its applications to atmospheric pollution diagnostics are reported. They include:

Model studies on the theory of retrospective correlation spectroscopy

A new diagnostic method is proposed to determine the column density Nx of the contaminant species. A plot is made of the of the correlation function C(z), determined retrospectively from the field spectrum and a numerical mask function, vs the convolution E(z), determined numerically from the absorption cross-section function and the mask function. Its intercept gives information on the incident flux I_o, and its slope gives information on the column density. The algebraic implications of this have been worked out for realistic model spectra. The work is now being extended to include the properties of "real world" spectra.

Laboratory studies

After evaluation of field spectra in our database, laboratory tests of the diagnostic method are being performed using the SO_2 and I_2 absorption spectra, both of which exhibit comb-like "fingerprints" of nearly equally spaced, nearly equal intensity, nearly equal width features.

Development and Field Tests of the GASCOFIL non-dispersive Correlation Spectrometer

The rugged mobile fully digital gas filter correlation spectrometer GASCOFIL has been designed, constructed and field tested within some tens of km of the Ontario Hydro Lakeview Generating Station. The instrument is designed for UV, Visible and Infrared operation. The tests confirmed its excellent performance characteristics. It confirmed SO_2

emission fluxes from the Lakeview stacks within a few percent of Ontario Hydro thermochemical estimates.

A larger more versatile and sophisticated instrument, GASCOSCAN has also been designed and built. It is on the point of laboratory and field testing.

5.2 Conculsions

a) The method of retrospective digital numerical correlation spectroscopy appears to have excellent potential as a diagnostic tool for use with dispersed field spectra to determine column densities of atmospheric contaminants

b) The digital non-dispersive gas filter correlation spectrometer system, GASCOFIL has been shown to be an excellent and reliable tool for the monitoring and diagnosis of contaminant plumes in the atmosphere. It and the larger related digital instrument GASCOSCAN would appear to have real potential for further development and application.

5.3 Recommendations

a) The modelling, experimental and field test programmes of digital retrospective correlation spectroscopy should continue to be vigorously prosecuted for application to selected spectral features of important atmospheric contaminants.

b) The field testing programme of GASCOFIL should be continued and the instrument fully tested in a number of contrasting environmental conditions. The instrument should also be used as a diagnostic tool in pollution and acid rain research problems including studies on SO_2, NO_2 and other target species. The work should be carried out firstly in the Toronto-Hamilton region and then in other environmentally sensitive regions of Ontario.

The performance characteristics of the related instrument GASCOSCAN should be determeined in the laboratory, and a programme of field tests started in its use as a passive an active and an ambient level remote sensor in fixed and moving locations.

References

BARRINGER, A.R. (1964a)
Proc. Third International Symposium on Remote Sensing (Univ. Mich. Press, Ann Arbor, Mich)

BARRINGER, A.R. AND SHOCK, J.P.(1964b)
Proc Fourth International Symposium on Remote Sensing (Univ. Mich. Press, Ann Arbor)

BOTTEMA, M., PLUMMER, W. AND STRONG, J. (1964a)
Astrophysical Journal, **139**, 1021

BOTTEMA, M., PLUMMER, W. AND STRONG, J (1964b)
Astrophysical Journal, **140**, 1640

CANN, M.W.P and NICHOLLS, R.W. (Dec 1982)
"Retrospective Correlation Spectroscopy" (pp21)
Appendix to Final Report to NSERC on PRAI Grant P7908
"Applications of Spectroscopic Field Measurements to the Remote Sensing of Atmospheric Pollutants" by R.W.Nicholls

MORROW, W.H. and NICHOLLS, R.W. (1985)
On point of submission to Applied Optics

NICHOLLS, R.W. (1983)
"Retrospective Correlation Spectroscopy and its applications to atmospheric monitoring"
Proceedings of the 1983 MOE Technology Transfer Conference pp 787-794

NICHOLLS, R.W. (1985)
Submitted to Applied Optics

NICHOLLS, R.W. and MORROW. W.H. (May 1984)
Final Report to NSERC Strategic Grant G0630
"Remote Sensing of Atmospheric Pollutants by Gas Filter Correlation Spectrometer"

WARD, T.V., AND ZWICK H.H. (1975)
Applied Optics **14**, 2896

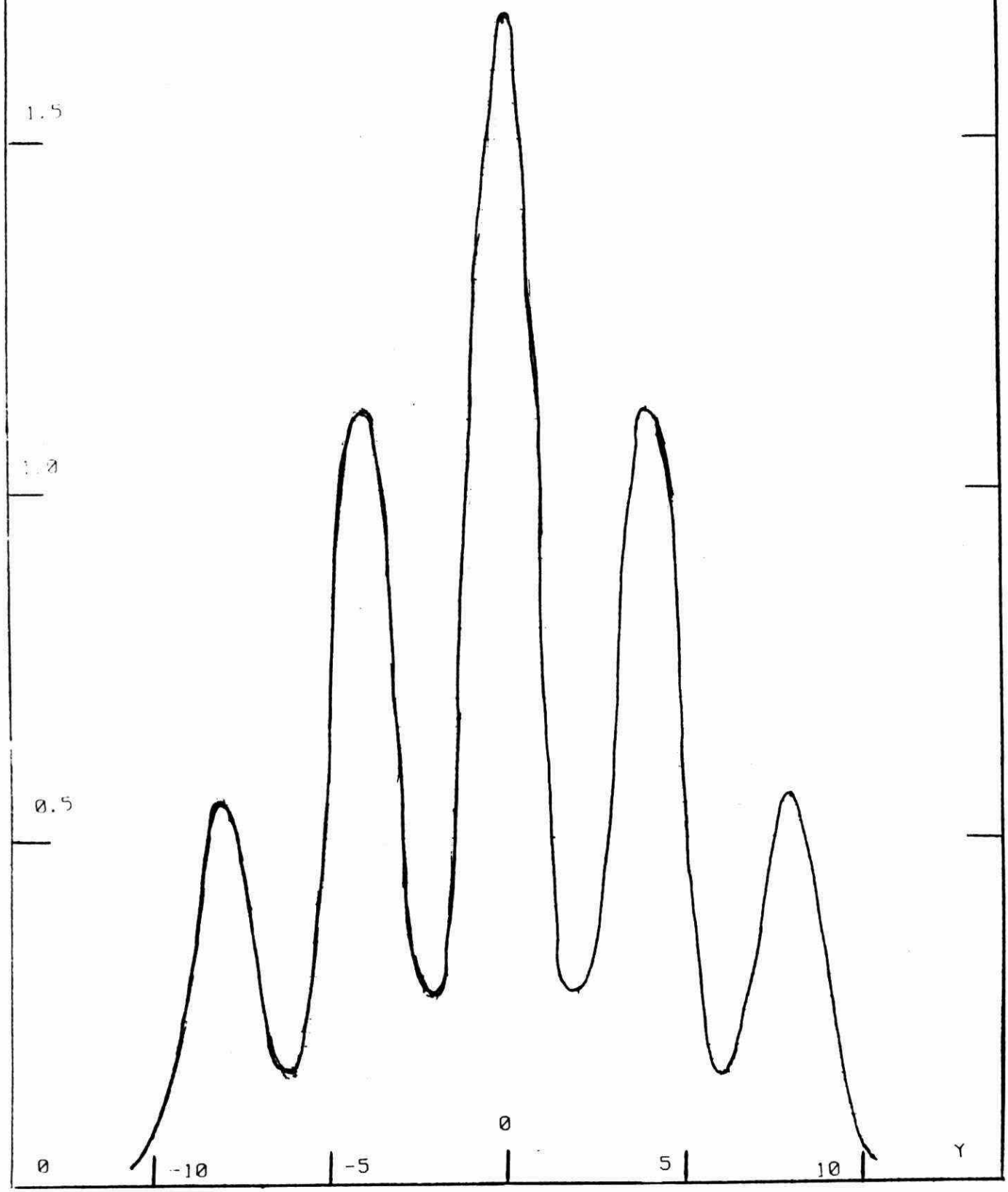
Acknowledgements

This work would not have been possible without the much appreciated support of a research grant from the Ontario,Ministry of the Environment.

I wish to thank Dr. Walter Chan of that Ministry for his advice and encouragement, and for his helpful introduction to Ontario Hydro staff which led to the successful field tests of GASCOFIL. We are most grateful to the Ontario Hydro operations engineering staff at the Lakeview Generating Station for their help and willing cooperation in these field tests of GASCOFIL.

Mr.M.Amani performs the calculations described in section 2.2. Dr.M.Mandelman performs the laboratory and observational work described in section 3. Mr W.H.Morrow has been responsible for most aspcts of the GASCOFIL and GASCOSCAN project described in section 4. Until May 1884 this work was supported by an NSERC strategic grant.

FIGURE 1
THE CONVOLUTION FUNCTION E(Y) VS Y
FOR 3 EQUAL WIDTH SPECTRAL FEATURES
SPACED 4 WIDTH UNITS APART.



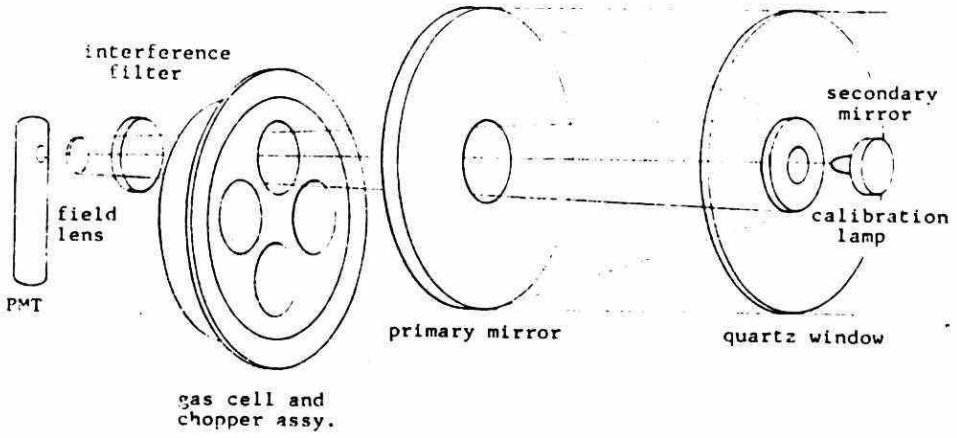


FIGURE 2:

OPTICAL SYSTEM OF GASCOFIL

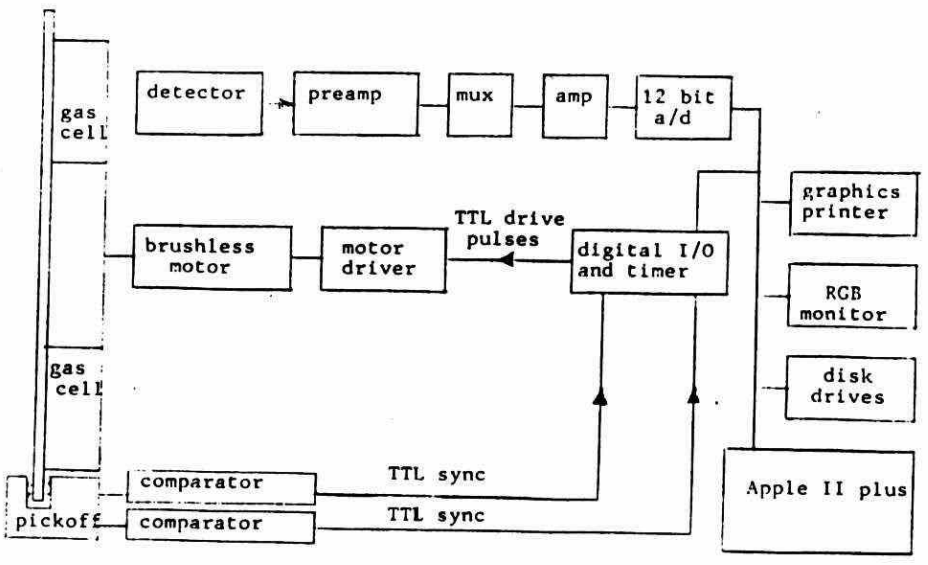


FIGURE 3:

ELECTRONIC SYSTEM OF GASCOFIL

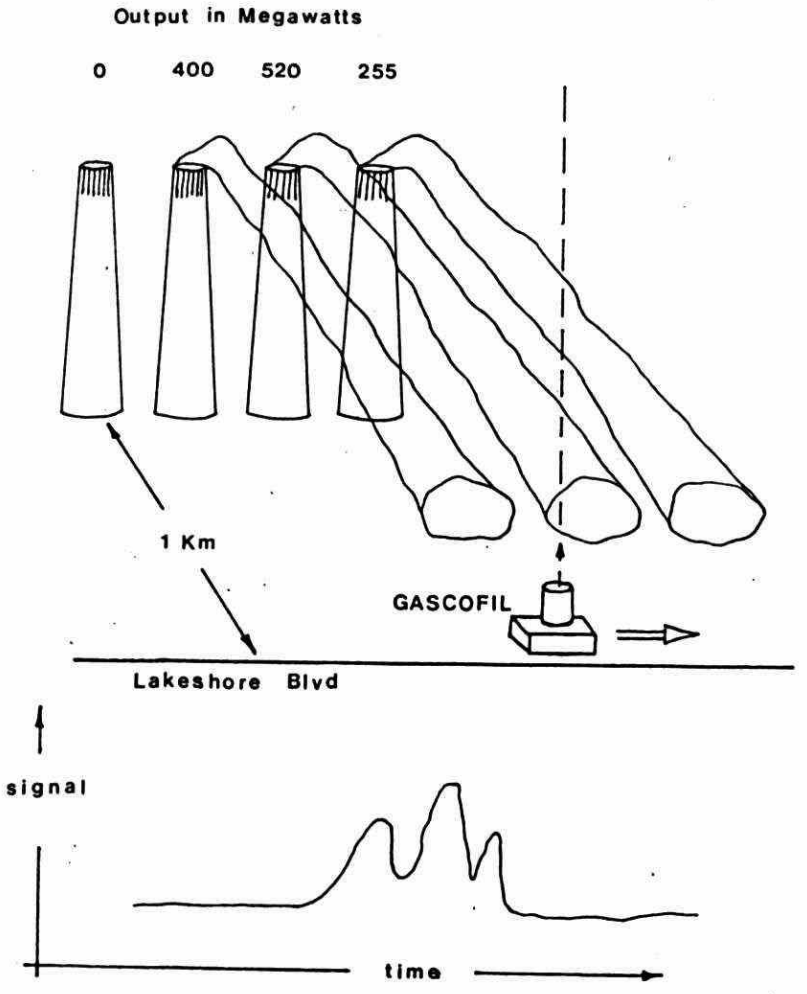


FIGURE 4

GASCOFIL OBSERVATIONS ON SO2 EMISSIONS
FROM THE LAKEVIEW GENERATING STATION
(Note the plumes are not
visible to the naked eye)

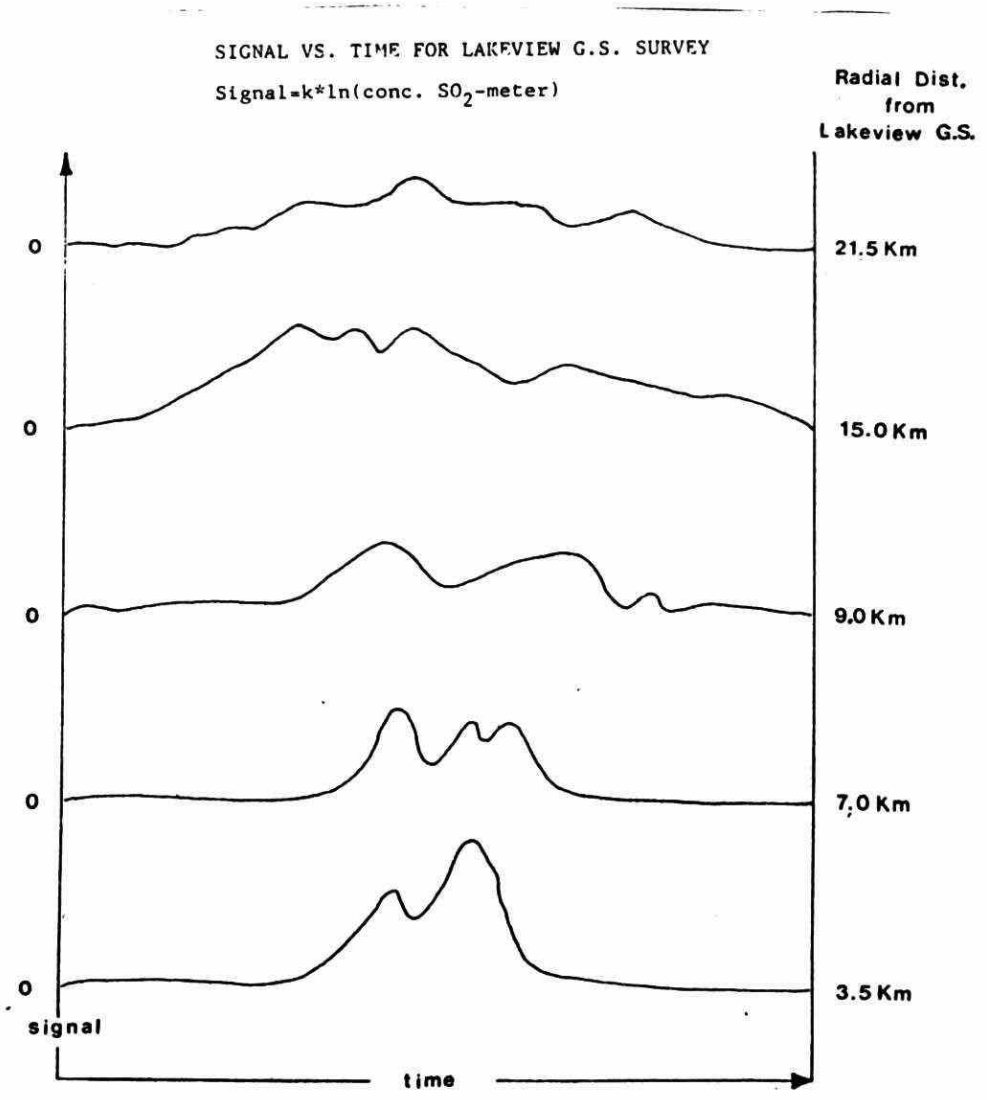


FIGURE 5

DIFFUSION OF LAKEVIEW PLUMES
AS A FUNCTION OF DISTANCE FROM
THE SOURCE
(Note the abscissa time is a measure
of distance travelled by GASCOFIL
at a constant speed perpendicular
to the plumes)

DEVELOPMENT OF A TUNABLE DIODE LASER BASED HYDROGEN PEROXIDE MONITOR

F. Slemr[1], G.W. Harris[2], D.R. Hastie and H.I. Schiff

York University

[1]Present Address: Max-Planck Institute for Chemistry, 65 Mainz, F.R.G.

[2]Present Address: Unisearch Associates Inc., Concord, Ontario L4K 1B5, Canada.

Development of a Tunable Diode Laser Based Hydrogen Peroxide Monitor

F. Slemr, G.W. Harris, D.R. Hastie and H.I. Schiff

Department of Chemistry, York University

ABSTRACT

Atmospheric gaseous hydrogen peroxide is formed mainly by the recombination of HO_2 radicals. Consequently, the measurement of its mixing ratio can be related to the mixing ratio of HO_2 and provide valuable insights into the chemistry of the odd hydrogen compound family in the troposphere. Also, hydrogen peroxide is believed to be the most important oxidant in the aqueous phase conversion of S(IV) to S(VI) in the troposphere.

A method for the real time determination of H_2O_2 in ambient air has been developed. It is based on tunable diode laser absorption spectroscopy in the 7.8 μm region. With a dual beam system and a multireflection cell pathlength of 40 m, 1-2 ppbv of H_2O_2 could be detected by scanning over a single absorption line every min. Spectra averaging over multiple scans and the subtraction of the background spectra improved the detection limits to 0.3-0.6 ppbv for a 15 min measurement time.

A permeation tube based system has been developed for the generation of gaseous calibration mixtures of H_2O_2 ranging from low ppbv to low ppmv mixing ratios. The effects of the transfer line materials and the linearity of the dilution of ppmv H_2O_2 mixtures down to the low ppbv range have been tested extensively.

1. INTRODUCTION

Atmospheric gaseous hydrogen peroxide is formed mainly by the recombination of HO_2 radicals (Logan et al., 1981). Consequently, the measurement of its mixing ratio can be related to the mixing ratio of HO_2 and provide valuable insights into the chemistry of the odd hydrogen compound family in the troposphere (Logan, 1981; Chameides and Tan, 1981). Also, hydrogen peroxide is believed to be the most important oxidant in the aqueous phase conversion of S(IV) to S(VI) in the troposphere (Penkett et al., 1979; Middleton et al., 1980).

Despite its importance, few measurements of the H_2O_2 mixing ratio have been reported. Buffalini et al. (1972) report 40-180 ppbv H_2O_2 during moderate and severe smog episodes at Riverside, California. Kok et al. (1978) reported mid-afternoon values of 10 to 30 ppbv at two locations in the Los Angeles region and mixing ratios of 100 ppbv in the plumes of grass and forest fires. Kelly et al. (1979) found much lower mixing ratios of 0.3-3 ppbv at a rural site near Boulder, Colorado. Their values are close to the 2 ppbv predicted for mid-latitudes in summer (Logan et al. 1981).

For all these measurements ambient air was bubbled through an impinger containing an aqueous solution of some trapping agent. After collecting enough H_2O_2 the trapping solution was analyzed by colorimetric Ti (IV) methods (Pilz and Johann, 1974; Cohen and Purcell, 1967) or by chemiluminescence from luminol oxidation (Kok et al., 1978). However recent studies of aqueous trapping methods have cast doubt on all the measurements. Zika and Saltzman (1982), Heikes et al. (1982) and Heikes (1984) found that considerable amounts of H_2O_2 can be formed by bubbling ambient air through aqueous solutions, most probably by reactions of ozone and its decomposition products with water. Consequently, Zika and Saltzman (1982) question all H_2O_2 measurements that use aqueous traps. Additionally,

aqueous trap methods may suffer from SO_2 interference (Heikes et al., 1982) and from interference by other organic hydroperoxides, which are also expected to be present in the troposphere (Logan et al., 1981). Direct H_2O_2 determination in the gas phase would obviously overcome all these problems. Previous work in our laboratories has demonstrated that tunable diode laser absorption spectroscopy (TDLAS) coupled with a multireflection (White) cell is capable of detecting 0.3, 0.2 and 0.35 ppbv of NO, NO_2 and HNO_3, respectively (Hastie et al., 1983). These detection limits are at least one order of magnitude better than those achieved by long path FTIR spectroscopy (Tuazon et al., 1980; Hanst et al., 1982). The objective of this work was to evaluate the feasibility of using TDLAS to measure H_2O_2.

2. EXPERIMENTAL

Although TDLAS is, in principle, a universal method, application to the quantitative measurement of a particular gas has 3 requirements: 1) Selection of a suitable laser diode; 2) development and quantification of an appropriate calibration source and 3) establishment of sampling procedures.

2.1. The Tunable Diode Laser Absorption Spectrometer (TDLAS)

The dual beam TDLAS illustrated schematically in Figs. 1 and 2 is an improved version of the instrument detailed recently by this group (Hastie et al. 1983) and Hastie & Schiff, 1983). The main improvements are a dual beam setup including a frequency marker channel, the use of a pinhole for more precise alignment and confining of the IR beam, and the inclusion of a computerised data aquisition system to allow the rapid scan, multiple spectra averaging in addition to the analogue scan.

The optical system illustrated in Fig. 1 is similar to that of Mankin et al. (private communication). The TDL beam is focussed by a f/1 germanium lens L1 and directed by the plane mirrors M1 and M2 onto a 1 mm diameter pinhole. Behind the pinhole the diverging beam is refocussed by the spherical mirror SM (f = 250 mm) into a 1 m base pathlength White cell which was usually set for a 40 m pathlength. After passing through the White cell the beam is refocussed by the f/1 germanium lens L3 onto the signal channel detector. A CaF_2 flat plate, 5 mm thick, serving as a beam splitter, BS, diverts a small part of the radiation through a wavelength marker cell and is focussed by f/1 CaF_2 lens L2 onto the marker channel detector. Both detectors are P.C. HgCdTe operated at 77 K (Infrared Associates, New Brunswick, N.J.). The frequency marker cell has a glass body with CaF_2 windows sealed by PTFE gaskets. It contains several cm^3 of liquid, 90% H_2O_2 (FMC Corporation, King of Prusia, Pennsylvania) and is continuously pumped to give about 1 Torr of gaseous H_2O_2. All windows and lenses in the system are tilted to reduce the inadvertent formation of etalons.

A He-Ne laser beam can be directed through the pinhole by swinging the mirror, M4, into the TDL beam. Once the He-Ne beam and the TDL beam are adjusted to the same axis the alignment of the optical components behind the pinhole is easily made and checked.

A schematic diagram of the laser control and the signal processing electronics is shown in Fig. 2. The current driving the laser consists of four components. To the base laser current provided by the current control module (Spectra Physics, Bedford, Mass.) are added a sine wave modulation for the frequency modulation detection and a jitter to filter out the White cell etalons (Reid 1980) both generated by the multifunction generator. The ramp necessary for scanning the laser wavelength over the H_2O_2 absorption line is provided either by

the multifunction generator if analogue spectra recording is used or by the computer in rapid scan multiple spectra averaging.

The detector outputs are amplified by wide band preamplifiers (Infrared Associates) and fed into lock-in-amplifiers (PAR, Princeton, N.J.) operated at twice the modulation frequency (2f detection). The outputs of the lock-in amplifiers, are either displayed on a strip chart recorder or digitized and fed into the computer.

To obtain H_2O_2 mixing ratios the outputs of the lock-in amplifiers are either processed in analogue mode using the recorder trace or in digital mode using the accumulated spectra. In analogue mode the line is scanned every 30 seconds and the H_2O_2 mixing ratio calculated from the peak to peak height of the sample spectral feature relative to that of the calibration feature. In this mode the frequency marker channel only indicates the position of the chosen H_2O_2 absorption line. In the digital mode spectra are scanned at a frequency of 10 Hz. The computer (upgraded PET Commodore) accumulates a preselected number of digitized spectra. It then subtracts a background spectrum obtained in the same way but without H_2O_2 in the White cell. The H_2O_2 mixing ratio is then calculated from the least square fit of of this difference spectrum to the background corrected calibration spectrum.

Selection of the H_2O_2 absorption lines is a compromise between the tunability range of the available lasers, their mode structure, the strength of the H_2O_2 absorption lines, and the absence of the interferences by other absorbing atmospheric species. 2 lasers were selected from the 5 tested. The first supplied by Laser Analytics (Bedford, Mass.) was operated on the lines at 1264.590 and 1264.622 cm^{-1} with integrated line strengths of 0.4 and 1.6 x 10^{-20} cm^2 cm^{-1}, respectively. Most of the work was done with a laser supplied by Frauenhofer

Institute for Physical Measuring Techniques (Freiburg, W. Germany) on the line at 1284.206 cm^{-1}, which has a higher line strength of 3.6×10^{-20} cm^2 cm^{-1}. These lines were assigned by comparing the H_2O_2 absorption spectrum and a simultaneously recorded N_2O spectrum against the AFGL compilation (Rothman et al., 1983a & b). The absence of spectroscopic interference from absorption by other atmospheric species was checked by comparing spectra from the synthetic air against ambient air. Both lasers were run at conditions within their single mode region.

2.2. Sampling, calibration and flow control system

The sampling, calibration, and flow control system is shown schematically in Fig. 3. Ambient air enters the instrument through a PFA needle valve (Galtek Corp., Chaska, Minn.). By means of a solenoid 3-way PTFE valve (Nacom Industries, Tustin, Calif.) the air is then directed to the White cell either directly or through a H_2O_2 scrubber. The scrubber is a 30 mm o.d., glass tube, packed either with 27 g of ferrous sulfate (BDH Chemical Ltd., Poole, England) or with 35 g of 8-10 mesh Hopkalite (MSA, Evans City, Pa.). The flow rate through the White cell is usually adjusted to 5 l(STP) min^{-1} at a pressure of 20 Torr. To account for possible losses of H_2O_2 on the walls of the inlet tubing and the PFA needle valve the calibration gas mixture was added close to the ambient air inlet.

To enable quantitative work stable gaseous calibration mixtures of known low H_2O_2 mixing ratios are necessary. The calibration gas mixture was generated by permeation of H_2O_2 through the wall of a low-density polyethylene tubing (3.18 mm o.d., 1.59 mm i.d., Plastic Sales Inc., Toronto) immersed in stabilized 30% or 50% H_2O_2 solutions (Fisher Scientific, Fair Lawn, N.J.) thermostated to 30°C. Nitrogen was used as a carrier gas and its flow rate was adjusted to 10-50 cm^3 min^{-1}.

The H_2O_2 permeation rate was checked every fortnight by the colorimetric $TiCl_4$ method of Johann and Pilz (1974). A stock solution containing 11.6 cm^3 of $TiCl_4$ (Alfa Products, Danvers, Mass.) dissolved in 50 cm^3 of concentrated HCl (37%, 12 M) is prepared, taking safety precautions detailed by the supplier because of the sensitivity of the $TiCl_4$ to air humidity. The bright yellow stock solution keeps indefinitely, but for use is diluted ten-fold with distilled water to produce a colourless solution which keeps only for a few days. The calibration gas mixture is bubbled through the impinger containing 1 cm^3 of diluted solution in 10 cm^3 of 1.2 M HCl until a slight yellow coloration is observed. The solution is then diluted with water to 50 cm^3 and its absorbance at 415 nm is measured in 10 cm long cuvettes relative to the same solution without H_2O_2. The H_2O_2 concentration is calculated using the absorption coefficient of the Ti-H_2O_2 complex of 735 M^{-1} cm^{-1} given by Pilz and Johann (1974) and by Kok et al. (1978). No production of H_2O_2 was observed when the carrier gas alone was passed through the impinger.

Two permeation tubes were used throughout this work. One with 4 m of the polyethylene tubing immersed in a 50% H_2O_2 solution had a permeation rate of 350 ng H_2O_2 min^{-1} the other with 2 m tubing immersed in a 30% H_2O_2 solution yielded 75 ng H_2O_2 min^{-1}. Both devices were stable within ± 5% over a period of 5 months. To prevent decomposition of H_2O_2 on the tubing the devices were pre-cleaned with a hot mixture of 90% H_2O_2 and concentrated H_2SO_4 (1:1).

Materials were tested in the 1-23 ppmv H_2O_2 level using the the $TiCl_4$ method at flow rates of 10-50 cm^3 (STP) min^{-1}. A 6 mm o.d. glass tube was either internally coated or packed with different materials and its H_2O_2 throughput was calculated from the measured H_2O_2 mixing ratios upstream and downstream of the tube. Material tests were also made at the 2-50 ppbv of H_2O_2 at flow rates of 5 ℓ

(STP) min^{-1} in the same way except the TDLAS was used to measure the H_2O_2.

Glass, PFA and CaF_2 did not influence the H_2O_2 mixing ratio. PTFE tubing 1.5 m long and 6.35 mm o.d., initially destroyed 24% of incoming H_2O_2 but no H_2O_2 destruction was observed after flushing the tubing with H_2O_2 gas mixture overnight. Flushing also removed the initial H_2O_2 destruction on the PFA needle valve. Stainless steel tubing, metal needle valves, and aluminum tubing destroyed H_2O_2 almost completely. The epoxy based glues tested (Scotch Weld, 3 M Co., St. Paul, Minn., 5 min Epoxy, Devcon Corp., Danvers, Mass., Torr Seal, Varian, Palo Alto, California) which are commonly used for glueing the IR windows to the body of the absorption cell used for calibration and frequency marking destroyed H_2O_2 quantitatively and cannot be used. Less H_2O_2 destruction was observed on silicone rubber but an absorption cell built up with silicone rubber gaskets still passed only 42% of the incoming H_2O_2. Absorption cells with glass body and CaF_2 windows sealed by PTFE gaskets or glued by Apiezon Wax passed 95-100% of the incoming H_2O_2.

At mixing ratios of 2-50 ppbv H_2O_2 and a flow rate of 5 ℓ (STP) min^{-1} the H_2O_2 destruction was generally less efficient indicating that with the decreasing contact time the fractional H_2O_2 decomposition decreases. No H_2O_2 losses were observed on 30 m of PTFE tubing (6.35 mm o.d.), PTFE solenoid and PFA needle valves. Scrubbers containing $FeSO_4$ and Hopkalite removed H_2O_2 quantitatively both at atmospheric pressure and at the reduced pressure of approximately 20 Torr used in the sampling line between the needle valve and the White cell.

3. RESULTS

3.1. Dilution-linearity tests and the response time

The ability to successfully dilute the H_2O_2 comming from the permeation tube was tested by the $TiCl_4$ method over the range 1-23 ppmv. This was checked by the TDLAS using a 9.5 cm pathlength cell inserted into the beam. The observation of true linearity showed that no losses of H_2O_2 occurred on dilution and the TDLAS was responding linearly to changes in H_2O_2 concentration. Mixtures in the range 1.7 to 50 ppb were produced and flowed through the White cell. Figure 4 shows that again the dilution and TDLAS response was linear.

It then remained to test the influence of the White cell on the low concentration of H_2O_2. This was done by comparing the optical densities (signal) of the ppm mixtures in the 9.5 cm cell against the ppb mixtures in the 40 m White cell. The average ratio of the measured optical densities in the White cell to those calculated from the dilution, the pathlength ratio and the optical density in the 9.5 cm cell is 1.10 ± 0.14 ($n = 6$). That this is not significantly different from 1.00 shows that the H_2O_2 mixing ratio is not affected by the White cell and that it is possible to dilute low concentrations of H_2O_2. Furthermore we have shown that the entire TDLAS shows a linear response to H_2O_2 mixing ratios.

The time response of the TDLAS measuring 50 ppb H_2O_2 in the White cell is shown in Fig. 5. At time zero 50 ppb H_2O_2 was added to the air entering the White cell and at 5 min it was removed. Both the rising and the falling part of the response indicate a time constant (1/e time) of approximately 0.6 min. At 10 ppbv a time constant of 0.7 ± 0.3 min ($N=8$) was measured indicating that the response time is independent of the mixing ratio, at least in the 10 to 50 ppbv region. This time constant is, however, about 6 times larger than the calculated residence time of the air in the White cell.

3.2. Detection Limits

With the analogue mode the best detection limit achieved was 1.5 ppbv. The minimum detection limit (MDL) was determined both from the definition given by Hastie et al. (1983) and from the reproducibility of H_2O_2 mixing ratio measurements at low ppbv levels on the basis of 95% confidence interval (Parris et al., 1977).

In the rapid scan averaging mode the detection limit was determined by a procedure illustrated in Fig. 6. Two successive background spectra (without H_2O_2, trace C) were subtracted from each other and the detection limit calculated by a least square fit of the residual to the calibration spectrum in trace A. This procedure yielded a detection limit of 0.55 ppbv for the residual spectrum shown in trace C. The single measurement detection limits varied as the background changed with time both in frequency and amplitude. The background structure, of which trace C in Fig. 6 is a typical example, seems to originate from the laser itself since no corresponding etalons could be identified. The best one day average detection limit was 0.56 ± 0.38 ppbv (N = 23) measured over a period of 7 hours and the best hourly average was 0.30 ± 0.12 ppbv (N = 4).

3.3. Measurements of the ambient air

To explore the method ambient air was sampled from the roof of our laboratory building about 20 m above ground. The building is located at the northern border of metropolitan Toronto. During the measuring days northwest to northeast winds prevailed and, therefore, little pollution from the city was expected. Attempts to measure H_2O_2 were made on 15 sunny days between February 29 and June 3, 1984.

To account for the variable detection limits each ambient air

measurement such as the one shown in trace B of Fig. 6, was accompanied by a detection limit determination, such as shown in trace C of Fig. 6. The instrument was run automatically with the computer commanding the switching of the 3-way valve and performing data acquisition and analysis. In the measuring sequence a background spectrum (ambient air through H_2O_2 scrubber) was measured first. Then an ambient air spectrum was accumulated followed by another measurement of background spectra. With an acquisition time of 180 seconds for each spectra and a short waiting period after switching the valve to eliminate time constant effects 4 ambient air measurements were made per hour accompanied by 4 determinations of detection limits. No H_2O_2 was detected during these measurements even with hourly detection limit averages as low as 0.3 ppbv.

The laser was removed from the lab system and placed into the mobile TDLAS system where it was used in the Ontario Ministry of the Environment's Sarnia Oxidants Study in June-July 1984. This is now a two laser system, similar to that described in Hastie and Schiff (1983), which is capable of simultaneously measuring the concentration of two species. For this program we used the TDLAS to measure H_2O_2 and CH_2O, a commercial instrument to measure ozone and a modified chemiluminescence instrument capable of measuring nitric oxide to 50 pptv.

While stationed at the coastguard site outside Sarnia we obtained measurements of all species including the first unambiguous detection of gaseous H_2O_2 in the atmosphere. At the time of preparation of this paper the data is still being collated but we can show some of the preliminary data.

Figure 7 shows the H_2O_2 and ozone data from July 3. The high sensitivity NO monitor was not operational at that time but the OME monitors were showing less than 5 ppbv of NO. We measured H_2O_2 for two periods that day. Between 9 and 11:30 a.m. in excess of 3 ppbv of hydrogen peroxide was observed.

The observation of such high levels of H_2O_2 correlates well qualitatively with the other measurements viz. high ozone, low NO_x and high hydrocarbon. The simultaneously measured detection limit was below 1 ppbv throughout this period. Later in the afternoon the ambient concentration had dropped below the detection limit although the concentrations of other species were similar. The difference in H_2O_2 was due to the occurrence of a thunderstorm during the afternoon which would be expected to washout the gaseous hydrogen peroxide.

Figure 8 shows some simultaneous H_2O_2, CH_2O and ozone data over the period. These are daily averages but only for data obtained truly simultaneously. For the H_2O_2 and CH_2O data the averages were obtained by combining spectroscopic files before analysing for concentration. This procedure lowers the minimum detection limit to 0.1 ppb. There is obviously a strong correlation between H_2O_2 and CH_2O concentrations, as one would expect in an oxidising atmosphere, and a weaker but certainly positive correlation of both these species with ozone.

This data is still being processed and will be presented in its entirety in the Sarnia Oxidants Study Report.

4. DISCUSSION

The detection limit of 0.3 ppbv achieved in this work is about two orders of magnitude better than the detection limit of the kilometer-pathlength FTIR apparatus (Tuazon et al., 1980; Hanst et al., 1982).

A detection limit of 0.4 ppbv for the luminol method using a sampling interval of 15-25 min is claimed by Kok et al. (1978). This detection limit is comparable with 0.3 ppb achieved here for a measurement every 15 min including one ambient air and one detection limit determination. The horseradish peroxidase

(HRP) method (Zika et al., 1982; Zika and Saltzman, 1982) was reported to be more sensitive. However, as long as the formation of H_2O_2 in the aqueous solutions used to collect gaseous H_2O_2 is not prevented (Zika and Saltzman, 1982; Heikes et al., 1982) the validity of results of both the luminol and the HPR method remain questionable. Consequently we believe the TDLAS to be a preferred technique because of its absolute specificity.

The mixing ratios of H_2O_2 measured in this program are ower than the 40-180 and 10-30 ppbv values reported by Buffalini et al. (1972) and Kok et al. (1978), respectively, for populated urban atmospheres. They are however comparable with the 1.2 - 2.6 ppbv measurements of Kok (1980) at the ground and at 3.3 km and with the 0.3 - 3 ppbv range reported by Kelly et al. (1979) in rural air. Model calculations by Logan et al. (1981) predict H_2O_2 mixing ratios in clean air ranging from 0.2 ppbv in winter to 2 ppbv in summer. Our data suggests that for several periods during the Sarnia measurement campaign the H_2O_2 concentration was several times that expected for clean air. The tunable diode laser based hydrogen peroxide monitor we have developed and used is now capable of measuring H_2O_2 in mildly polluted rural airmasses. To use the instrument in clean air requires an improvement in sensitivity.

The sensitivity of the TDLAS can be most easily improved by increasing the present absorption pathlength of 40 m. Depending on the available laser power the pathlength can be increased by increasing the number of the reflections in the White cell or by using a cell with a larger base length or a combination of both. Improved data processing such as combining of several stored spectra and a more sophisticated discrimination against background may lead to lower detection limits. By combination of both approaches the MDL an enhancement by a factor of 4

and perhaps more should be achievable. The resulting MDL would then be sufficient for a real time direct spectroscopic measurement of H_2O_2 mixing ratios as low as 0.1 ppbv.

Acknowledgement

The authors wish to thank the Air Resources Branch of the Ontario Ministry of the Environment for financial assistance.

References

Buffalini J.J., Gay B.W. Jr. and Brubaker K.L. (1972) Hydrogen peroxide formation from formaldehyde photooxidation and its presence in urban atmosphere. Environ. Sci. Technol. 9, 816-821.

Chameides W.L. and Tan A. (1981). The two-dimensional diagnostic model for tropospheric OH: An uncertainty analysis. J. Geophys. Res. 86, 5209-5223.

Hanst P.L., Wong N.W. and Bragin J. (1982). A long-path infra-red study of Los Angeles smog. Atmos. Environ. 16, 969-981.

Hastie D.R., Mackay G.I., Iguchi T., Ridley B.A. and Schiff H.I. (1983). Tunable diode laser systems for measuring trace gases in tropospheric air. Environ. Sci. Technol. 17, 352A-364A; correction Environ. Sci. Technol. 17, 510A.

Hastie D.R. and Schiff H.I. (1983). Development of a method for measuring hydrogen peroxide using a tunable Diode Laser Absorption Spectrometer, Technology Transfer Conference No. 4.

Heikes B.G., Lazrus A.L., Kok G.L., Kimen S.M., Gandrud B.W., Gillin S.N. and Sperry P.D. (1982). Evidence for aqueous phase hydrogen peroxide synthesis in the troposphere. J. Geophys. Res. 87, 3045-3051.

Heikes B.G. (1984). Aqueous H_2O_2 production from O_3 in glass impingers. Atmos. Environ. 18, 1433-1445.

Kelly T.J., Stedman D.H. and Kok G.L. (1979). Measurements of H_2O_2 and HNO_3 in rural air. Geophys. Res. Lett. 6, 375-378.

Kok G.L., Darnall K.R., Winer A.M., Pitts J.N. Jr. and Gay, B.W. (1978a) Ambient air measurements of hydrogen peroxide in the California South Coast air basin. Environ. Sci. Technol. 12, 1077-1080.

Kok G.L., Koller T.P., Lopez M.B., Nachtrieb H.A. and Yuan M. (1978b). Chemiluminescent method for determination of hydrogen peroxide in the ambient atmosphere. Environ. Sci. Technol. 12, 1072-1076.

Kok G.L. (1980). Measurements of hydrogen peroxide in rainwater. Atmos. Environ. 14, 653-656.

Logan J.A., Prather M.J., Wofsy S.C. and McElroy M.B. (1981). Tropospheric chemistry: A global perspective. J. Geophys. Res. 86, 7210-7254.

Middleton P., Kiang C.S. and Mohnen V.A. (1980). Theoretical estimates of the relative importance of various urban sulfate aerosol production mechanisms. Atmos. Environ. 14, 463-472.

References cont'd

Parris G.E., Blair W.R. and Brinckman F.E. (1977). Chemical and physical considerations in the use of atomic absorption detectors coupled with a gas chromatograph for determination of trace organometallic gases. Anal. Chem. 49, 378-386.

Penkett S.A., Jones B.M.R., Bruce K.A. and Eggleton A.E.J. (1979). The importance of atmospheric ozone and hydrogen peroxide in oxidizing sulphur dioxide in cloud and rainwater. Atmos. Environ. 13, 123-137.

Pilz W. and Johann I. (1974). Die Bestimmung kleinster Mengen von Wasserstoffperoxyd in Luft. Intern. J. Environ. Anal. Chem. 3, 257-270.

Reid J., El-Sherbiny M., Garside B.K. and Ballik E.A. (1980). Sensitivity limits of a tunable diode laser spectrometer, with application to the detection of NO_2 at the 100-ppt level. Appl. Optics 19, 3349-3354.

Rothman L.S., Goldman A., Gillis J.R., Gamache R.R., Pickett H.M., Poynter R.L., Husson N., and Chedin A. (1983a). AFGL trace gas compilaton: 1982 version. Appl. Opt. 22, 1616-1627.

Rothman L.S., Gamache R.R., Barke A., Goldman A., Gillis J.R., Brown L., Toth R.A., Flaud J.M., Cany Peyret C., (1983b). AFGL atmospheric absorption line parameters compilation: 1982 version. Appl. Opt. 22, 2247-2256.

Tuazon E.C. Winer A.M., Graham R.A. and Pitts J.N. Jr. (1980). Atmospheric measurements of trace pollutants by kilometer-pathlength FT-IR spectroscopy. In Advances in Environmental Science and Technology, Vol 10 (edited by J.N. Pitts, Jr. and R.L. Metcalf), John Wiley, pp. 259-299.

Zika R.G. and Saltzman E.S. (1982). Interaction of ozone and hydrogen peroxide in water: implications for analysis of H_2O_2 in air. Geophys. Res. Lett. 9, 231-235.

Zika. R.G., Saltzman E.S., Chameides W.L., and Davis D.D. (1982). H_2O_2 levels in rainwater collected in South Florida and the Bahama Islands. J. Geophys. Res. 87, 5015-5017.

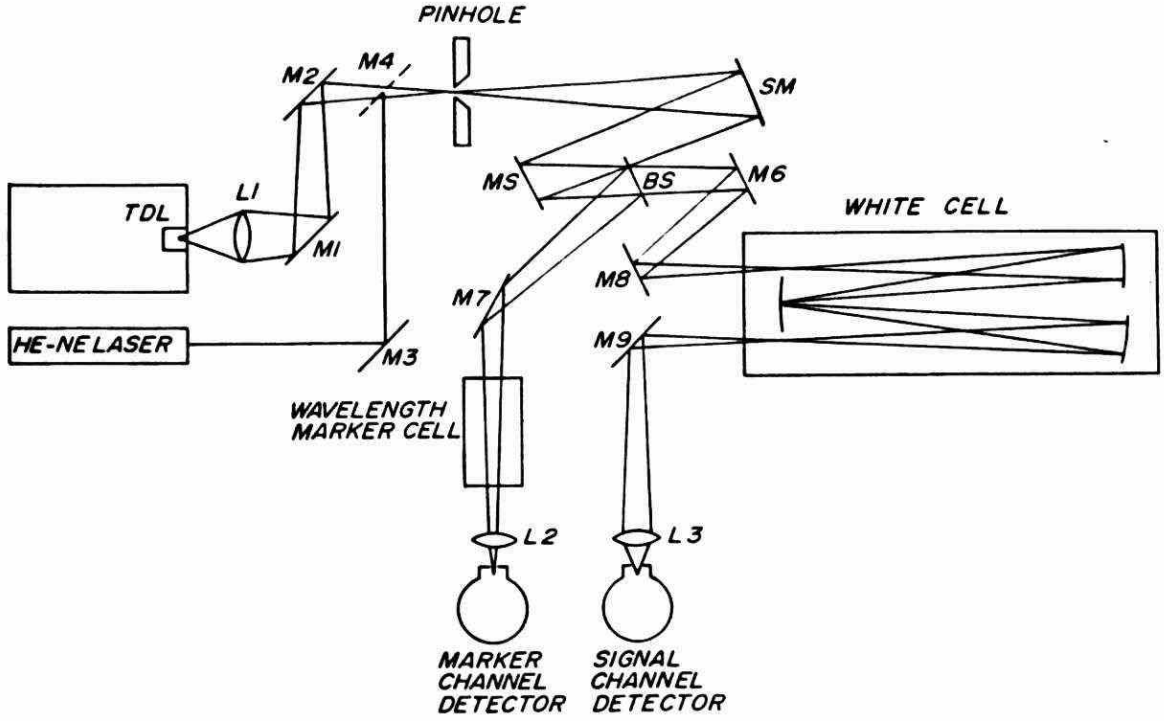


Fig. 1. Optical layout of the double beam tunable diode laser absorption spectrometer (TDLAS).

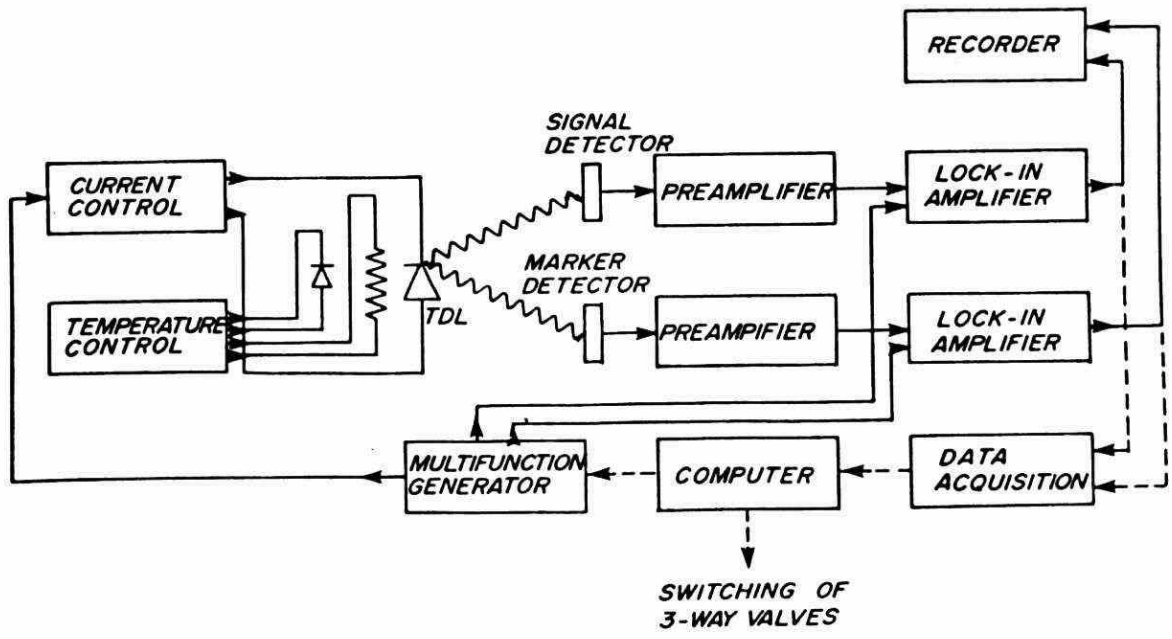


Fig. 2. Electronic block diagram of the TDLAS.

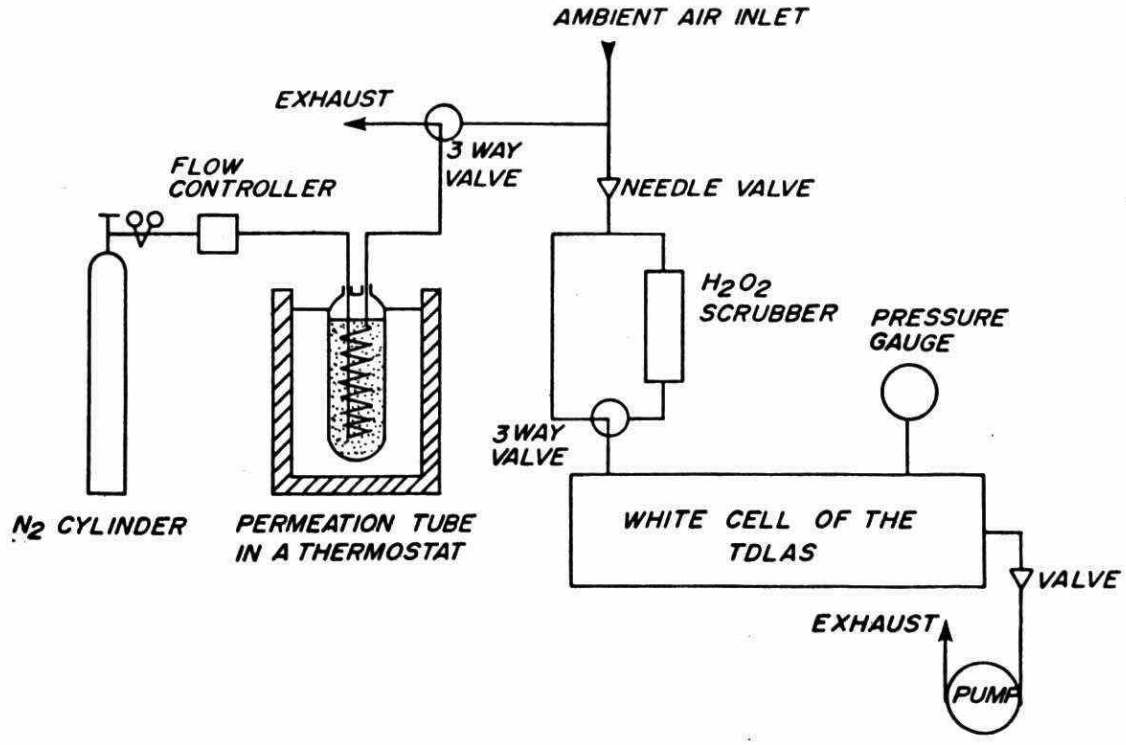


Fig. 3. Sampling, calibration and flow control system.

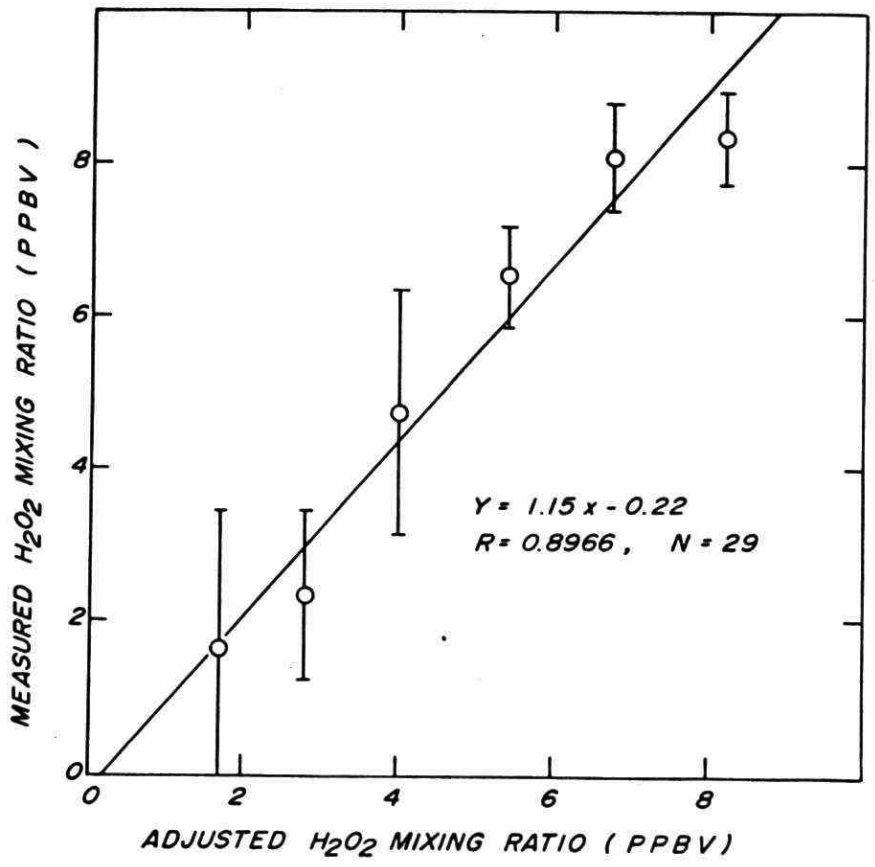


Fig. 4. Linearity of H_2O_2 dilution at low ppbv mixing ratios.

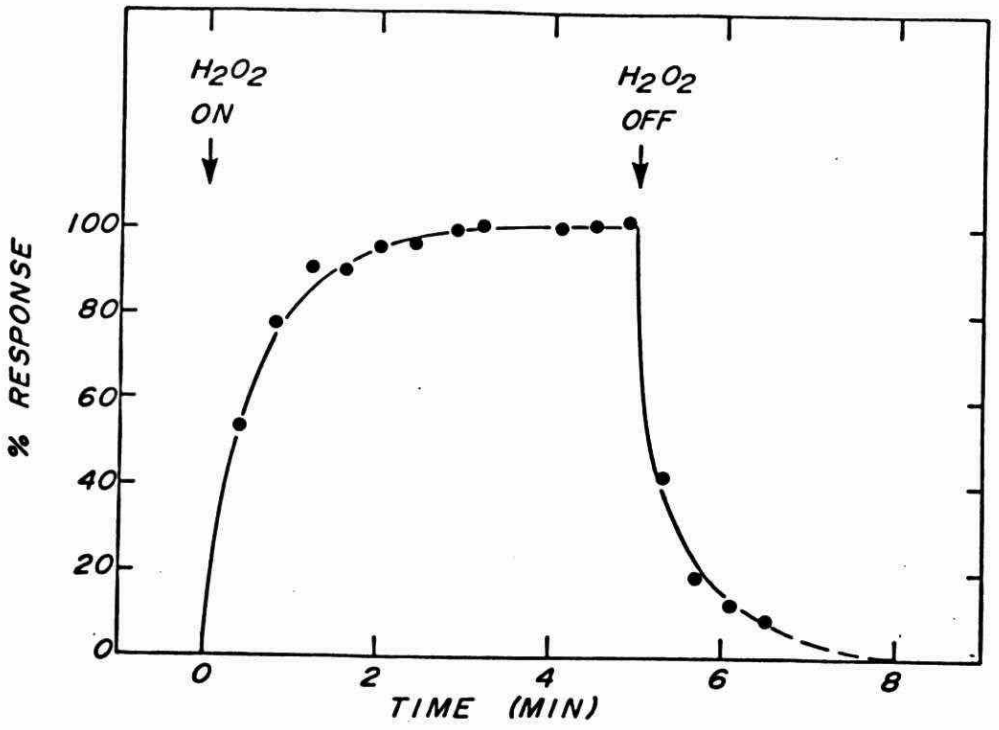


Fig. 5. Time response of the TDLAS measured in analogue mode with 50 ppbv mixing ratio of H_2O_2 and a flow rate of 5 ℓ (STP) m^{-1} through the White cell.

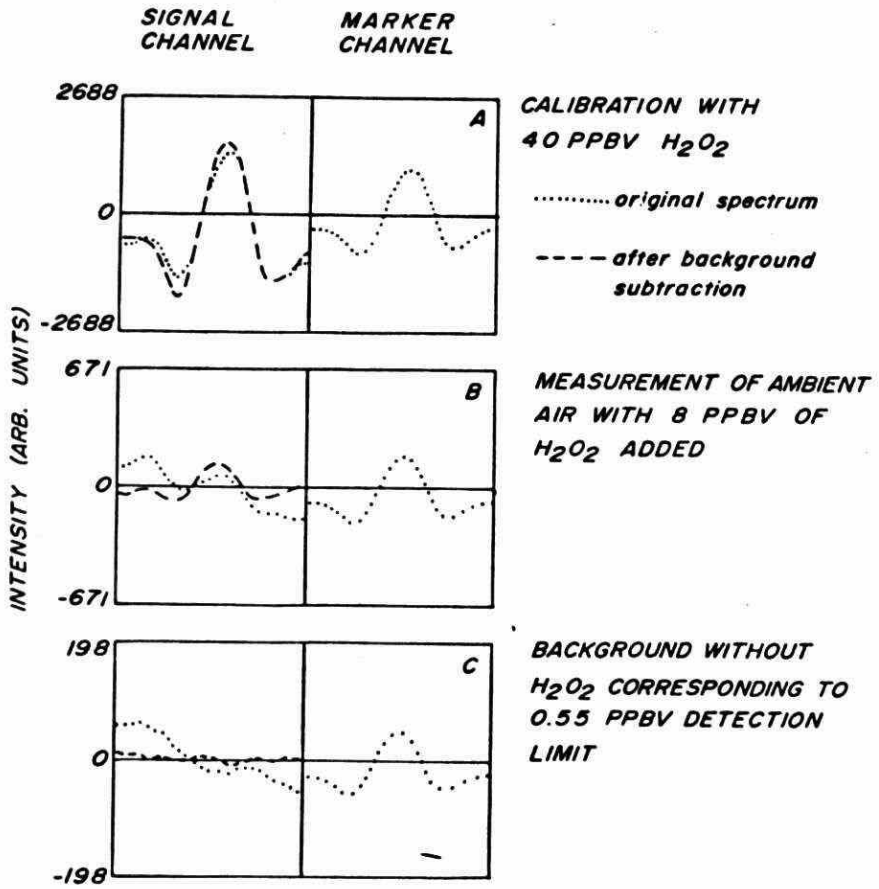


Fig. 6. Typical calibration, measuring, and background spectra before and after the background spectra subtraction as obtained by multiple scan averaging over 120 s acquisition time.

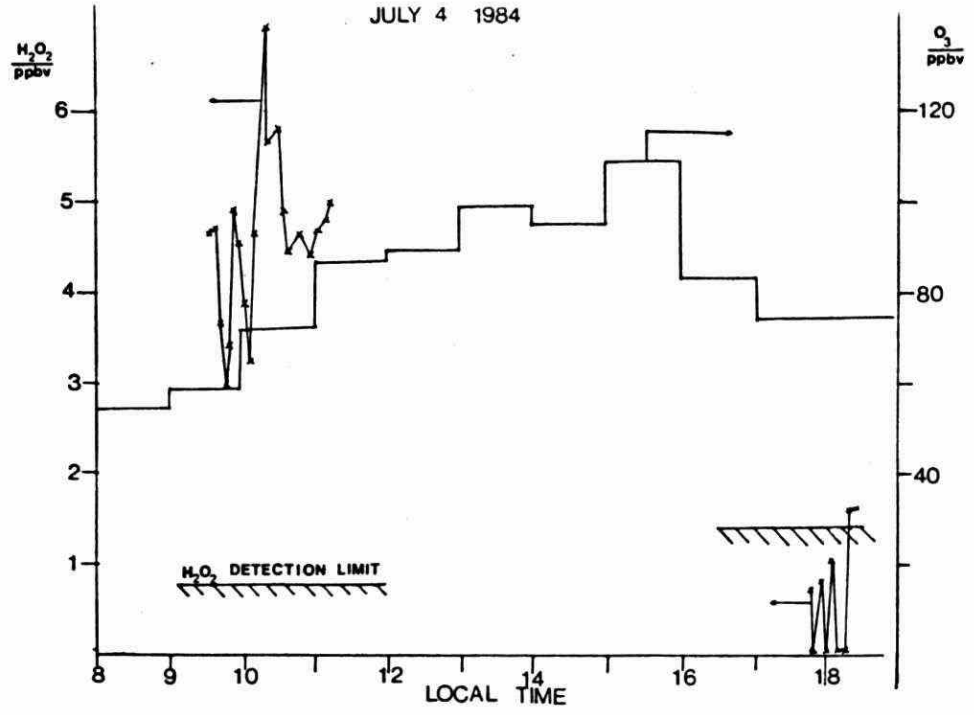


Fig. 7. H_2O_2 and ozone data for July 4, 1984.

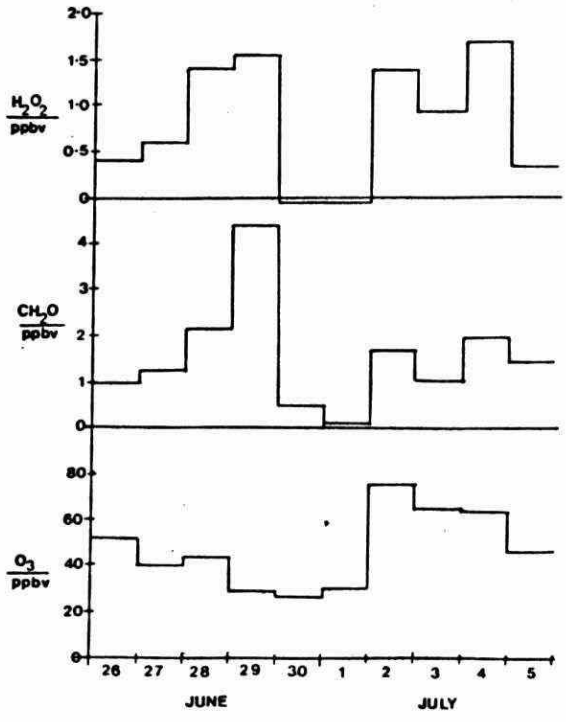


Fig. 8. Daily averages of simultaneous H_2O_2, CH_2O and O_3 data from Sarnia, June - July, 1984.

CHEMICAL SPECIATION OF AIRBORNE PARTICULATES

D.D. Burgess and M. Browne
McMaster University
Hamilton, Ontario

Chemical Speciation of Airborne Particulate Matter

Donald D. Burgess and M. Browne
Department of Chemistry
McMaster University, Hamilton, Ontario

Studies directed towards the determination of the chemical forms of elements present in airborne particulate material will be described. The reactions of vapours of fluorinated derivatives of 2,4-pentanedione with various elements and their compounds are being investigated. These reactions produce volatile metal complexes that can be used to collect the metal for determination. Several elements have been found to react and iron is under intensive study as a model element. Results obtained to date indicate that different compounds of iron react at different temperatures and that it should be possible to distinguish among these compounds on this basis.

Four approaches to trapping the volatilized material have been investigated. This study has shown that it should be possible to achieve separation of elements in the collection step in order to reduce interferences in the determination of the collected material.

As it is intended to employ neutron activation analysis (NAA) for the determination of collected elements, the automatic design of procedures in NAA is also being studied. A computer program based on mathematical modelling and simplex optimization has been created for the calculation of optimum analytical conditions. This technique can be used to formulate general guidelines for the application of NAA to airborne particulates and other materials. The combination of selective volatilization and properly-designed NAA is expected to lead to methods for the multielement speciation of airborne particulates.

Comprehensive multielement analysis of airborne particulate material is a valuable tool for the study of the sources and behaviour of solid substances found in the atmosphere. The accumulation of data concerning the abundance of many elements by the analysis of samples collected over a suitable period of time and geographical area can permit the application of sophisticated statistical analyses and the formulation of useful models of transport processes. The technique of neutron activation analysis (NAA) has been used for such multielement analyses for some time. NAA, however, provides only limited information in that it can determine only total elemental concentrations and therefore does not give the chemical forms of the elements determined. The project described in this paper is chiefly concerned with an attempt to find methods by which NAA, with its high sensitivity and low analytical blank, can be applied to the determination of the chemical species present in airborne solids.

The approach adopted in my research group for this task is based on volatilization. Vapours of organic reagents such as 1,1,1,5,5,5-hexafluoro-2,4-pentanedione (tfa) are used to convert metals and their compounds to volatile complexes that can then be removed and collected for determination. Direct reactions of these reagents with solids have been reported previously for liquid-solid reactions (1,2) but not for gas-solid reactions. If the formation of volatile complexes can be made to occur under different conditions for different chemical forms of the reacting metal, selective extraction and hence speciation should be possible. Our studies to date have focussed on testing this proposition. The extraction of trace elements as volatile complexes could be useful in other areas such as atomic absorption and inductively coupled plasma methods as well as in NAA.

Experimental Methods

Ligands are vapourised in a stream of nitrogen gas and passed to a pyrex reaction tube containing a pyrex cup that holds powdered sample material labelled with a radioisotope of the element of interest. The reaction tube is heated by a heating tape controlled by circuitry that produces a linear increase in temperature with time. As the experiment progresses, the radioactivity of the sample is monitored by a Na(Tl) scintillation detector connected to a multichannel analyser operated in the multiscaling mode. The sample temperature is monitored by a thermocouple thermometer linked to a microcomputer that also controls the heating and multiscaling rates. This apparatus can be operated to temperatures of about 500° C. The experimental configuration has been described previously (3).

Several arrangements for trapping the volatilised metals were tested. A water-cooled probe of pyrex was employed for condensation of vapours and a pyrex probe containing a heating cartridge was used with a temperature controller for reduction with hydrogen and deposition of metals as sulphides by reaction with hydrogen sulphide. A narrow tube placed at the exit from the reaction tube was used to test collection by ion exchange, reaction with sodium sulphide and reaction with phosphoric acid solution placed on glass wool. A pyrex capillary tube entering the exit zone was used to deliver gasses for testing deposition by reaction with gasses such as hydrogen chloride and hydrogen sulphide.

Results and Discussion

We have previously reported the volatilization of iron and chromium by 1,1,1-trifluoro-2,4-pentanedione (tfa) (3). Since that time, we have also observed volatilization of copper by tfa. Trials with hfa have demonstrated the volatilization of copper, iron, nickel and chromium and have shown that hfa is a more efficient volatilization reagent than tfa. We have selected iron as a model element for detailed study because of its versatile chemistry, environmental significance and convenient radiochemistry.

Radiotracer experiments with iron have yielded well-defined activity versus time/temperature data. Figure I shows an example and Table 1. gives the reaction threshold temperatures for several chemical forms of iron. These data indicate that these iron species do indeed begin to react at different temperatures. The data for Fe_3O_4 are puzzling in that only one step is seen in the radiothermogram whereas two steps would be expected, one for the ferric component and one for the ferrous component. This step, however, overlaps the step for Fe_2O_3 at the heating rate used. Experiments with FeO and with reduced heating rates are now in progress to determine whether Fe_3O_4 does indeed behave as a single compound. Experiments in which the compound of interest is synthesised from radioactive iron are also planned to confirm these results. The change in threshold temperatures found when the ligand is changed indicates that reagent programming as well as temperature programming can provide selectivity in these extractions. Trials with thio analogs of the pentanedione compounds discussed above will be undertaken in the near future to examine the effect of this modification of the ligand.

Before experiments with radioactive tracers could be performed safely, it was necessary to find an effective means of trapping the volatilized metal and since the ligands used are moderately expensive, ligand recycling is desirable. Simple condensation of the vapours exiting the reaction tube was found to be unsatisfactory as the complexes condense at roughly the same temperature as the ligands. Attempts to effect deposition by reduction with hydrogen at a heated surface was successful only for copper. Attempts to reduce iron complexes with sulphur dioxide and hydrazine also failed. Solid sodium sulphide was ineffective in trapping iron from its complexes and a trap packed with a sulphonic acid ion exchange resin had too little capacity for the ligand-complex mixture to be useful. Satisfactory retention of complexes may be possible using other chromatographic packings.

Protonation of the ligand component of complexes by means of strong acids has proved to be a satisfactory approach to trapping metals from volatile complexes. Hydrogen chloride gas was found to deposit metals from the complexes, but the location of the deposit is difficult to control. This problem could be solved by careful design of the apparatus used to mix the gases and collect the solid chloride salts. Similar experiments with hydrogen sulphide showed that heat is required for deposition of metals as sulphides and that chromium could not be collected in this way. A simpler protonation method in which the gas stream is passed through a tube packed with glass wool wetted with phosphoric acid solution has proved the most satisfactory and is in routine use. If the tube is maintained at 150° C, the metals are deposited on the glass wool and the ligand is carried through the packing for recovery and recycling.

Our experiments with reduction by hydrogen have suggested a potentially

useful method for the separation and concentration of copper. This would be useful in NAA as the otherwise most convenient radioisotope of copper is subject to numerous interferences due to overlapping gamma-ray peaks in strictly instrumental NAA. The possibility of selectively transporting copper from solid samples to a heated surface in the presence of hfa and hydrogen is now being tested. This would allow post-irradiation separation of copper using a single vessel and minimal manual manipulation and would allow the radioactive copper to be counted without further handling. If suitable deposition reactions can be found, it may be possible to collect other elements in a similar fashion.

Auxiliary Studies

NAA is most advantageously applied in multielement analysis. The design of procedures, however, is complicated by the large amount of information that must be taken into account. Half-lives, reaction cross sections, isotopic abundances etc must be considered for all elements expected to be present in a sample. We are currently carrying out research aimed at the development of computational tools for this method design task.

The method being developed, called Simplex Optimization by Advance Prediction, uses mathematical models of neutron activation and gamma-ray spectrometry to predict the gamma-ray spectrum that would be observed for a specified sample composition under given conditions such as sample size and irradiation, decay and counting times. This predicted spectrum is then used for the computation of a quantity (response) that expresses the merit of a determination carried out under the given conditions. Prediction of response values is used instead of actual experiments in simplex optimization of the analytical conditions for NAA.

We have previously reported the optimization of single-element NAA (3,4) by the method described above. Over the past year, the method has been extended to multielement NAA (5) and a new method for predicting dead time in counting experiments has been developed. Data sets for airborne particulate analysis have been and are being developed and will be used to obtain general guidelines for the application of NAA to atmospheric analysis once the activation model has been adjusted to account for certain nuclear interference phenomena.

A critical element in optimization studies is the response function used. This is especially true for multielement determinations where satisfactory responses are difficult to formulate. In this work we have concentrated on detection limits and analytical precision as measures of method performance.

For a single-element determination, the detection limit (6) can be expressed as

$$L_D = \frac{(2.7 + 4.65\ B^{0.5})\ C\ W}{A} \qquad (1)$$

where L_D is the detection limit, B is the baseline area under a peak, A is the net peak area, C is the concentration of the corresponding element and W is the sample size. The measurement uncertainty can be expressed as

$$RSD = \frac{(A + 2B)^{0.5}}{A} \qquad (2)$$

where RSD is the relative standard deviation of the measured net peak area.

When multielement determination is contemplated, definition of a response depends on the goal of the experiment. In this work, the goal has been defined as the determination of a set of elements with each element having a roughly equal chance of satisfactory determination. Possible response functions are simple sums, LM and RSDM, of the detection limits or peak area precisions found for the individual elements. These functions, however, cause the optimization to concentrate on the most difficult elements, often at the expense of others. A more satisfactory solution has been found in weighted averages of individual responses with the reciprocal of the response found for each element in single-element optimization used as its weighting factor.

$$LMW = \frac{\sum_{i=1}^{n} \left(\frac{1}{L_{Dsi}}\right) L_{Di}}{\sum_{i=1}^{n} \left(\frac{1}{L_{Dsi}}\right)} \qquad (3)$$

$$RSDMW = \frac{\sum_{i=1}^{n} \left(\frac{1}{RSD_{si}}\right) RSD_i}{\sum_{i=1}^{n} \left(\frac{1}{RSD_{si}}\right)} \qquad (4)$$

where LMW and RSDMW are the weighted average multielement responses, n is the number of elements determined and an s subscript refers to a response obtained in single-element optimization. Table 2 demonstrates the effect of weighting the responses. This method of obtaining a multielement response function could very probably be employed with other analytical techniques such as atomic emission and chromatography.

Future work in method design will include nuclear interferences, dynamic selection of gamma-ray lines and sets of elements for simultaneous determination and epithermal neutron activation analysis.

References

1) W.D. Ross and R.E. Sievers, Anal. Chem. 41 1109 (1969)
2) M.S. Black and R.F. Browner, Anal. Chem. 53 249 (1981)
3) D.D. Burgess, Proceedings, Technology Transfer Conference No. 4, Ontario Ministry of the Environment, 1983, pg 854
4) D.D. Burgess and P. Hayumbu, Anal. Chem. 56 1440 (1984)
5) D.D. Burgess and P. Hayumbu, Proceedings of the 5th International Conference on Nuclear Methods in Environmental and Energy Research, 1984
6) L.A. Currie, Anal. Chem. 40 586 (1968)

TABLE 1.

Volatilization Reactions of Iron

Compound	Threshold Temperature °C	
	hfa	tfa
Fe metal	225	137
$FeCl_3$	125	130
$FeCl_2 \times H_2O$	---	124
Fe_2O_3	335	> 233
Fe_3O_4	260	---

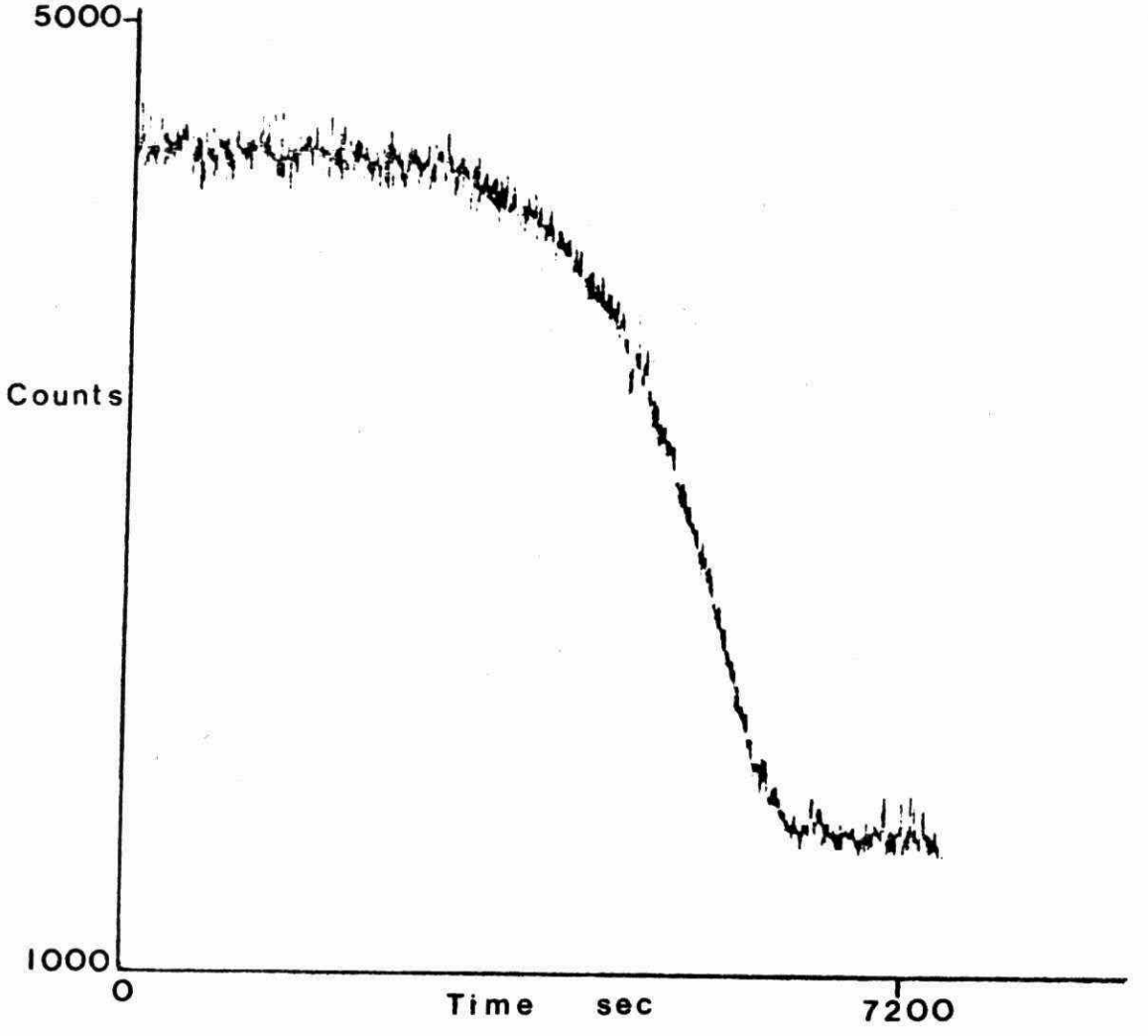
TABLE 2

Effects of Weighting and Half-life on Optimization of Detection Limits: Times are in minutes. Sample: urban particulate.

* minimum allowed value, L_D detection limit

	unweighted				weighted			
element	L_D	(L_D/L_{Ds})	L_D	(L_D/L_{Ds})	L_D	(L_D/L_{Ds})	L_D	(L_D/L_{Ds})
	μg		μg		μg		μg	
Mg	48.4	(1.13)	--------		195	(4.54)	--------	
I	0.0664	(1.00)	--------		0.147	(2.21)	--------	
Mn	0.00825	(1.93)	0.0596	(13.9)	0.0043	(1.01)	0.00870	(2.03)
Cu	0.893	(5.82)	0.157	(1.02)	0.290	(1.88)	0.176	(1.14)
Zn	24.7	(6.85)	3.60	(1.00)	9.44	(2.62)	5.15	(1.43)
As	3.71	(12.6)	0.388	(1.31)	1.25	(4.24)	0.701	(2.37)

Figure I
Radiothermogram: Fe_3O_4, reaction with tfa



TD
172.5
.O57
1984
part 2

Proceedings : technology
transfer conference no. 5
76017